SYNTHESIS OF ORGANO-FLUORINE COMPOUNDS BY METAL COMPLEX-MEDIATED AND -CATALYZED TRANSFORMATIONS OF FLUORO-ALKENES AND FLUORO-ARENES

By

Nicholas Orlando Andrella

Thesis submitted in partial fulfillment of the requirements for the

Doctorate in Philosophy degree in Chemistry

Ottawa-Carleton Chemistry Institute

Faculty of Science

University of Ottawa

Abstract

The prevalence of fluorine in natural products is scarce. There are but a handful of compounds that have been discovered to date. This could be largely attributable to the occurrence of fluorine in nature as fluoride (F^-). — One might recognize such nomenclature from the ingredients list on a toothpaste tube — In fact, naturally occurring fluoride is most commonly found as fluorite (CaF_2) or cryolite (Na_3AlF_6). As such, the introduction of fluorine via biological pathways has been limited to use of aqueous F^- (a very poor nucleophile). This fact — coupled with its naturally low concentration in water — has created the ripe conditions for this shortage. In a way this has proven fertile for synthetic chemists because nature has not yet evolved a method for the deconstruction of partially or fully fluorinated compounds.

Considering the above, as synthetic methodologies for the construction of carbon-fluorine bonds became available, so too did the discovery of their valuable properties. So beneficial are these properties that C-F bond-containing compounds have become commonplace in many households throughout the world. For example, practically every home relies on these compounds for use in their refrigerators. Other examples of useful fluorinated materials include blowing agents, non-stick coatings, pharmaceuticals, agrochemicals, liquid crystals, and lubricants.

With all these applications and seemingly easy availability of these compounds, it is interesting to learn that original synthetic methods are still being employed today. As such, the objective of this Thesis is to develop ‘greener’ routes for the synthesis of fluorocarbons. We hypothesized that by studying transition metal-fluoroalkyl complex-mediated reactions, a more efficient catalytic system could be developed. A foreseen complication arises from the

thermodynamic stability of C-F, transition metal-F and transition metal-C_{RF} bonds. Improvements to overcome these caveats include the use of first-row late transition metal complexes. Presented herein are additions to this body of knowledge by expanding on the reactivity of nickel, copper and silver fluoroalkyl complexes.

The approach applied in this work, in line with 'green' chemistry principles, was to source readily available fluorinated reagents, i.e. fluoroalkenes and fluoroarenes, to reduce the number of steps for the synthesis of new fluorinated compounds. Chapter 2 builds on the well-established oxidative cyclization of C_2 fluoroalkenes to nickel (0), which yields new C_4 units. The use of a bulky N-heterocyclic carbene ligand was found to enhance reactivity by reducing the coordination number at nickel. Examples of room temperature Cα-F and Ni-C^F bond activation and functionalization reactions are presented. Chapters 3, 4 and 5 re-examine the insertion of fluoroalkenes into silver and copper fluorides and hydrides. Building on precedent of addition reactions to hexafluoropropene, this fluoroalkene was examined first. In so doing, a versatile and inexpensive copper heptafluoroisopropyl reagent was developed (Cu-F addition to $(CF_3)CF=CF_2$. With easy access to new heptafluoroisopropyl complexes, they were systemically studied for their applications in catalysis. This revealed key features, particularly the lability of the M-hfip bond, which could be detrimental to catalytic reactions. As such, a nickel complex-mediated carbonylative heptafluoroisopropylation reaction and copper complex-mediated nucleophilic addition to electrophiles were developed. When a copper hydride was used instead, the *in situ* generated fluoroalkyl [Cu-H addition to $(CF_3)CF=CF_2$] was susceptible to β-fluoride elimination. Chapter 4 expands this methodology to achieve the catalytic consecutive hydrodefluorination of fluoroalkenes, demonstrating the scope and limitations of this system. Furthermore, the critical role of the phosphine ligand in accessing an L_3Cu-H addition and

unusual β-fluoride elimination mechanism is highlighted. However, tetrafluoroethylene proved resistant to this reaction because the fluoroalkyl resting state of this alkene, Cu-CF_2CF_2H, is unusually robust. Chapter 5 investigates the utility of this fragment and others in C(sp^2)-R^F cross-coupling and nucleophilic substitutions. With focus on new routes for late stage fluorination and examples of nickel (0) complex-catalyzed selective C-F bond functionalization reactions, Chapter 5, continues studies for low-temperature and DMAP-assisted conditions for aryl-F cross-coupling reactions with boronic acid esters.

Lastly, Chapter 6 reviews the advances presented in this *Thesis*, provides a link to the expected lasting impacts and attempts to provide guidance to future research on transition-metal complexes in the synthesis of C-F or C-R^F containing compounds. Moreover, with the introduction of a new hydrodefluorination technology, previously scarce fluoroalkenes (e.g. 1,2-difluoroethylene) can now be used more freely, potentially leading to the development of new refrigerants or materials applications.

Acknowledgements

The opportunity to continue my passion in organometallic chemistry, after my undergraduate studies, would not have been possible without the support and guidance from my family and colleagues. They are the crucial pillars to my foundation without which I could not have pursued my studies with zealot-like ferocity. My appetite for learning is huge and my attention span borders on zilch when I am absorbed in my work. I can only imagine what you all must have tolerated from me over these last few years. For this, I am eternally grateful.

Prof. Tom Baker, thank you for recognizing my potential and being an exemplar of great leadership. Your open-door policy, your willingness to listen, and your positive and constructive criticism are always valued. Your patience in teaching me to own my work and moulding my writing style will be carried with me for the rest of my career.

Finally, I will have the pleasure of joining the prestigious group of Baker alumni. Obtaining this status has also come with the pleasure of meeting so many from this community who also call themselves the same or will call themselves such soon. To Kaitie, Christian, Matthew, Graham, Mehdi, Uttam, Alex Daniels and Yahya. Writing this has reminded me of the support I got from you all. From hours helping me prepare presentations through to discussions about advances and direction for my research; my accomplishments are only as great as they are because of your backing. To Alex Sicard and Hassan, on top of all this you guys willingly took-up a desk next to me. Not only did we share lab space, we also shared a desk space where we were forced to listen to each other, if we liked it or not… for the whole day. I know that I can talk a lot so thank you for having the stamina and keeping up with me. I think, because of this, our friendship goes beyond the usual definition. Thanks also to Nancy and Karen, the two best

undergraduate students I could have worked with. With your hard work and determination, together we probed the frontiers of organometallic space. But most of all, “Thank you for making my time in the Baker lab memorable.” To Andrea, its unfortunate you spent such a short time here, we made quite the Italian trio. Thank you, for showing my wife and me around Bologna. Wherever our careers lead, I know we will stay in touch.

To my family and friends, unbeknownst to you, you all helped carry me to the end. To Andrew, Marc, Matt, Ryan, Jordan, Hebert, Bianca and Michel; I don’t think I could have foreseen myself completing this body of work without our timeless friendships. The intermittent distractions that you guys brought to my ceaseless thinking on chemistry helped restore my calm; like the feeling of listening to waves break on a sandy beach or maybe a bit more like the relief of anxiety after booting up your PC from a crash and seeing the login screen again.

To my Japanese colleagues, thank you for being such wonderful hosts. You were all so generous and hospitable, and I’m so grateful I had the opportunity to do research in your labs. To Fujimoto-san, thank you so much for all your help, I will never forget the delicious cake you made for my wife and me. To Ogoshi Sensei, your mentorship during my stay was invaluable. Your passion for chemistry is inspiring and it was truly an honour to work with you. To Ohashi Sensei, thank you for all the help in mounting my crystal and solving the structures… Oh and for the delicious natto.

To Mike and Pam, it has been 29 years (25 years) that we have helped each other get to where we were going. You guys are the best and I wouldn’t wish for better siblings. I don’t think I can thank you enough… because you guys have put up with more things than I could ever write or am allowed to say here.

To Mom and Dad, without you I could not have made it this far. You have taught me far more then what I could have ever learned through my studies. I am only an astute learner because Dad taught me patience and attentiveness. I am only a good presenter because Mom taught me to be uncompromisingly honest and authentic. I am only a good teacher because you both taught me confidence and passion. I am who I am because you provided me with the opportunity to be hard-headed, a trait you couldn't have known would be fit for a chemist. Thank you, thank you, thank you.

Most importantly, I have carried out the work in this *Thesis* on the back of a most special woman, my wife. Tania, every second that I have put towards my *Thesis* would not have existed if I could not have shared it with you. Thank you for staving off my anxiety and listening to my grumblings, I could not have crossed this finish line without you. You have been the keystone of my arch. Your can-do attitude and strong character have continuously been a source for my inspiration. I love you.

Table of Contents

List of Figures

List of Schemes

List of Tables

List of Abbreviations

Ar	aryl
Ar^F	fluoro-aryl
atm	atmosphere
BDE	bond dissociation energy
bipy	2, 2’-bipyridine
BTB	1,3-bis(trifluoromethyl)benzene
BuLi	butyl lithium
Cp	cyclopentadienyl
cod	1,5-cyclooctadiene
CPME	cyclopentyl methyl ether
CTFE	chlorotrifluoroethylene
DiCTFE	1,2-dichlorodifluoroethylene
Cy	cyclohexyl
dcpe	1,2-bis(dicyclohexylphosphino)ethane
DFT	density functional theory
dipp	2,6-di-isopropylphenyl
DMAc	dimethylacetamide

DMAP	N,N-dimethylaminopyridine
dmeda	N,N’-dimethylethylenediamine
DMF	dimethylformamide
dmphen	2,9-dimethyl-1,10-phenanthroline
DMPU	N,N’-dimethylpropyleneurea
DMSO	dimethylsulfoxide
dppp	1,3-bis(diphenylphosphino)propane
dppf	1,1’-bis(diphenylphosphino)ferrocene
dtbpy	4,4’-di-tert-butyl-2,2’-dipyridyl
EPR	electron paramagnetic resonance
Et	ethyl
FA	fluoroalkene
HAT	halogen atom transfer
HDF	hydrodefluorination
HFA-1225ye	1,2,3,3,3-pentafluoropropene
hfip	heptafluoroisopropyl
HFP	hexafluoropropene
HOMO	highest occupied molecular orbital

IAd	N,N’-diadamantyl-imidazol-2-ylidene
IPr	N,N’-bis(2,6-diiso-propylphenyl)-imidazol-2-ylidene
IPr^{*}	1,3-bis(2,6-bis(diphenylmethyl)-4-methylphenyl)imidazol-2-ylidene
^{i}Pr	iso-propyl
$^{i}Pr_2Im$	N,N’-diiso-propyl-imidazol-2-ylidene
ItBu	N,N’-di-tert-butyl-imidazol-2-ylidene
L	ligand
LUMO	lowest unoccupied molecular orbital
Me	methyl
MeCN	acetonitrile
mes	mesityl
MesDAD	N,N’-(2,4,6-trimethylphenyl)-1,4-diaza-1,3,diene
MPA	Mulliken population analysis
neop	neopentyl glycolato
NHC	N-heterocyclic carbene
NMR	nuclear magnetic resonance
NMP	N-methyl-2-pyrrolidone
Nor	norbornyl

Nu	nucleophile
OAc	acetate
ORTEP	Oak Ridge thermal-ellipsoid plot program
O^{t}Bu	tert-butoxide
OTf	triflate
PFCB	perfluorocyclobutene
PFCP	perfluorometallacyclopentanes
PFP	pentafluoropropene
Ph	phenyl
phen	1,10-phenanthroline
pin	pinacolato
PMHS	polymethylhydrosiloxane
Pr	propyl
PTFE	poly(tetrafluoroethylene)
Py	pyridine
R^F	fluoroalkyl
R-134a	1,1,1,2-tetrafluoroethane
R-245fa	1,1,1,3,3-pentafluoropropane

R-410a	azeotropic mixture of difluoromethane and pentafluoroethane
R-1234yf	2,3,3,3-tetrafluoropropene
rt	room temperature
SET	single electron transfer
SI	supporting information
SIMes	1,3-bis(2,4,6-trimethylphenyl)imidazolidin-2-ylidene
SIPr	1,3-bis(2,6-di-iso-propylphenyl)imidazolidin-2-ylidene
SOMO	singly occupied molecular orbital
tbuXphos	2-di-tert-butylphosphino-2',4',6'-triisopropylbiphenyl
Tc	thiophene carboxylate
TES	triethylsilane
TFA	trifluoroacetic acid
TFE	tetrafluoroethylene
THF	tetrahydrofuran
TMDS	1,1,3,3-tetramethyldisiloxane
TMP	2,2,6,6-tetramethylpiperidine
TMS	trimethylsilyl
Tol	toluene

ToN	Turnover number
TrFE	trifluoroethylene
TS	transition state
UV-vis	ultraviolet-visible spectroscopy
Umemoto's	5-(trifluoromethyl)dibenzothiophenium trifluoromethanesulfonate
VdF	vinylidene difluoride
Xantphos	4,5-bis(diphenylphosphino)-9,9-dimethylxanthene
xyl	2,6-dimethylphenyl

Chapter 1

1. Introduction

1.1. The Relevance of Fluorine

The synthesis of carbon fluorine (C-F) bonds has brought with it the discovery of applications in numerous fields. These fields of applications include refrigerants, surfactants, blowing agents, polymers, liquid crystalline materials, pharmaceuticals and agrochemicals (Scheme 1.1).[1-41] At a glance, because of the breadth and scope of these applications, the valuable properties within each group appear seemingly unrelated. However, given the large body of knowledge available today, generalities can be made. These commonalities arise because of the low polarizability and strength of the C-F bond.[42-49] For example, this low polarizability is one of the attributes considered in the suppression of boiling points of C-F containing products vs their C-H bond-containing analogues and, at the same time, it allows for the modulation of the lipophilicity of biologically active molecules.

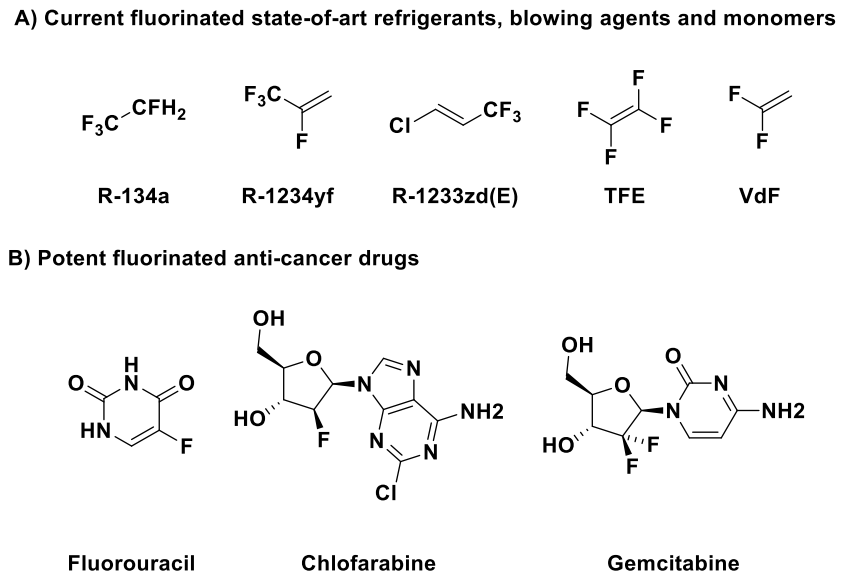

Scheme 1.1 Examples of prevalent fluorinated compounds

This improved understanding of the properties of fluorinated compounds has reciprocally led to continued interest and research on these compounds. Yet the industrial strategies to access these compounds, especially partially fluorinated ones, remain limited. For instance, the industrial synthesis of some of these compounds still relies on Swarts fluorination strategies developed in the 1890s.[50] Some impediments to the development of these strategies arise from: the low nucleophilicity of fluoride in media in which it is soluble, the strength of the C-F bond and the oxidation potential of F_2. (Scheme 1.2) Consequently, these strategies require caustic or highly reducing or oxidizing conditions or high temperatures.[51-63]

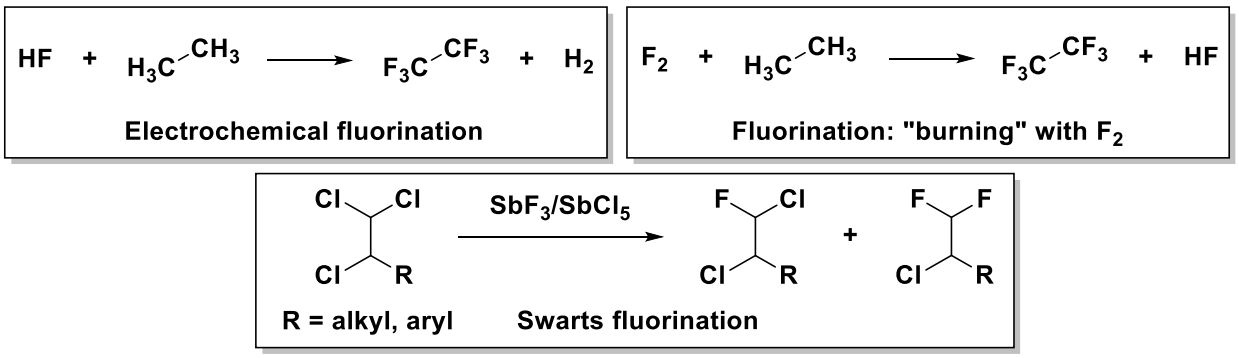

Scheme 1.2. Early methods used for the formation of C-F bonds

Methods to circumvent these fundamental limitations are the focus of this *Thesis*. In general, the highlighted synthetic approaches are convenable when handling simple small fluorinated molecules with few or no functional groups [albeit, with some safety concerns]. Many C_2 and C_3 fluorocarbons are successfully generated on huge industrially relevant scales employing these strategies. Some popular fluorinated monomers, tetrafluoroethylene, and hexafluoropropene, are synthesized by pyrolysis of chlorodifluoromethane at ~500 °C (Scheme 1.3, Top).[77-81] Likewise, a new generation refrigerant, 1,1,1,2-tetrafluoropropene, is synthesized stepwise by hydrogenation of a fluoroalkene precursor followed by dehydrofluorination [loss of HF] at elevated temperature. (Scheme 1.3, Bottom).[82-87] As a

result, it is not currently feasible to supplant these syntheses with “greener” ones. Instead, because of the relative ease of synthesis and bulk quantities of some fluorocarbons, there are potential benefits if they could be used in the development of new fluorinated compounds. To this end, two methodologies have been considered herein for value-added greener routes to fluorocarbons. The first method is their application to the construction of C-C bonds and the second is selective C-F bond activation.

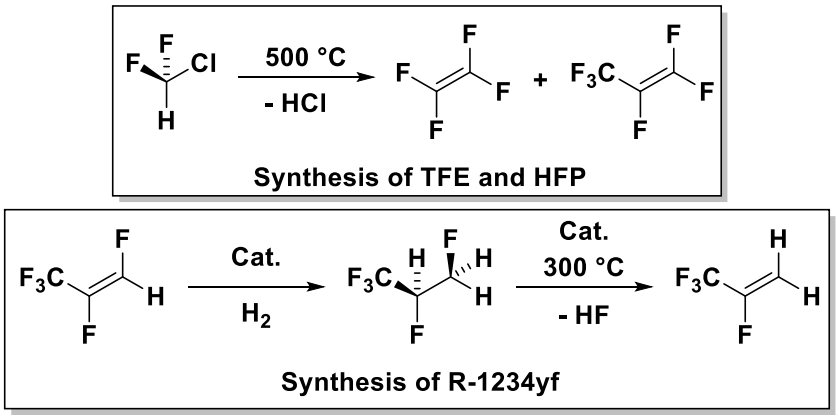

Scheme 1.3. The modern synthesis of some common C_2 and C_3 fluorocarbons.

1.2. Considerations for Transition Metals in Greener Routes to Fluorocarbons

Considerable advances have been made in the development of applications of small fluorocarbons in the synthesis of new compounds. In no small part, the use of transition metals has led to these innovations. With the now well-established use of transition metals in applications involving non-fluorinated congeners, it is no surprise they should find their way into this field.[88-91] Notably, initial studies highlighted drawbacks in the use of early transition metals and, thus, research in the use of late transition metals has become more prominent. For example, zirconium alkyl catalyzed ethylene polymerization is an industrially applied process, but no such equivalent exists for tetrafluoroethylene polymerization.[91] In fact, a current research focus has been in developing transition metal-catalyzed routes to fluorocarbons,

stemming from advances gathered from research on transition metal-mediated hydrocarbon reactions. The list of reagents being developed is continuously expanding and various organometallic complexes containing fluorinated moieties, M-R^F, have been synthesized. Members of this group include, but are not limited to, tetrafluoroethyl, pentafluoroethyl, *n*-heptafluoropropyl, heptafluoroisopropyl, octafluorobutyl, fluoroarenes, difluorocarbene, =CF(CF_3), =C(CF_3)$_2$, pentafluorosulfanyl, trifluoromethoxide, trifluoromethyl thiolate, difluoromethyl, trifluoromethyl.

Although many synthetic challenges exist in developing such compounds (discussed below), these have not prevented the use of synthetic strategies generally applied to their hydrocarbon congeners. It is sometimes the inherent stability of the carbon-fluorine bond that has permitted the synthesis and isolation of these compounds. But the trend is clear - early transition metal fluoroalkyl complexes remain scarce, while late transition metal complexes are far and away more studied. This is likely related to the stability of the metal fluoride (M-F) bond in comparison to the C-F bond. As such, when M-F > C-F spontaneous α- or β-fluoride eliminations can occur.[92, 93] For this reason, we also observe a shortage of first-row transition metal organofluorine complexes in the literature.

1.3. Strategies for the Synthesis of M-R^F Complexes

1.3.1. Synthesis of M-CF_3

Of the fluoroalkyl chains, the most popular remains the trifluoromethyl (CF_3) group. The CF_3 group has retained its popularity likely because its precursors are abundant, and it has, time and again, demonstrated utility in pharmaceutical and agro-chemical applications (Scheme 1.4). These factors, coupled with a push for “late-stage” reactions, have instigated a renaissance in

transition metal-mediated and -catalyzed fluoroalkylation reactions. As such, M-CF_3 complexes continue as the most studied of this group to date.

A discussion on the strategies used for the synthesis of M-CF_3 complexes will also provide an evaluation on most of those used to make other fluoroalkyl complexes. Within the context of this *Thesis*, impediments to extending some procedures to other fluoroalkyl groups will be highlighted. Furthermore, unique strategies which do not apply to C_1 units will be discussed separately.

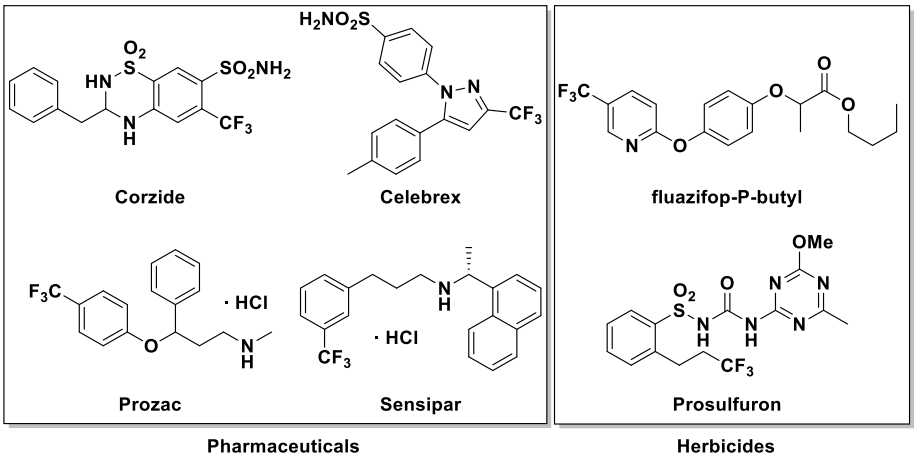

Scheme 1.4. Commercially available trifluoromethyl-containing bio-active compounds.

1.3.1.1. Using Iodofluoroalkanes

One of the earliest approaches to synthesize transition metal fluoroalkyls was *via* oxidative addition of iodotrifluoromethane which reacts with elemental metals or low-valent molecular complexes to yield the corresponding M-CF_3 complexes. This method was first studied by Emeleus *et al.* where, by reacting Hg and ICF_3, $HgI(CF_3)$ could be produced. [95-96] However, this reaction does not occur spontaneously and conditions favoring the generation of CF_3 radicals were necessary to obtain good yields of the desired product. These early experiments suggested that the ethane series, e.g. iodopentafluoroethane, would not yield any

useful products. It was later shown that the choice of solvent is crucial for the preparation of these compounds. For example, Zn readily reacts with ICF_2CF_3 in DMF to produce $ZnI(CF_2CF_3)$.[96] This work was extended some years later to reactions of molecular complexes. Since the first report by Stone *et al.*, this route has since been applied with various other transition metals (Scheme 1.5). [94-104] This method has not obtained widespread use, however, because of its propensity to generate fluoroalkyl radicals, rendering it somewhat unreliable. Nonetheless, many elegant applications stemming from the generation of these fluoroalkyl radicals have been subsequently developed and their importance in synthetic organic applications should not be understated. [105-112]

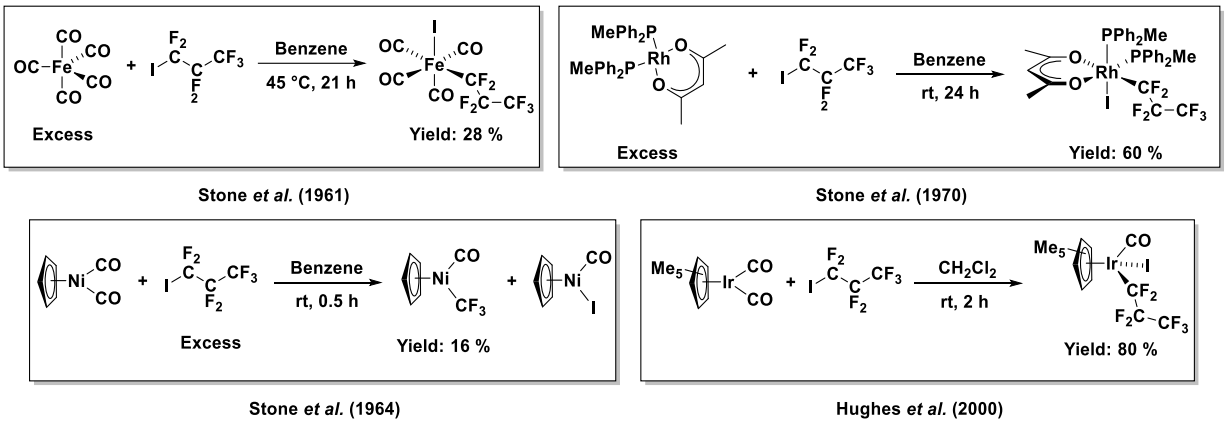

Scheme 1.5. Use of iodofluoroalkanes in the synthesis of transition metal fluoroalkyl complexes.

Given that these oxidative addition reactions yielded mixed results, other routes using these inexpensive fluoroalkyl precursors were sought (Scheme 1.6). Therefore, metalation of I-R^F compounds was explored, and, in 1984, Naumann *et al.* successfully prepared the first $(L)Zn(CF_3)_2$ from $ZnEt_2$.[113] They also demonstrated their synthetic strategy's utility in the synthesis of various other zinc fluoroalkyls. Given the affordability of $ZnEt_2$, it is no surprise that others have explored this route to generate more Zn organofluorine complexes for use in metal-mediated reactions. Recently, this route was employed by Vicic *et al.* [114] to synthesize an

(L)Zn(μ-C_4F_8)$_2$Zn(L) complex and, again, by Mikami *et al.* [115] to synthesize (DMPU)$_2$Zn(CF_3)$_2$. Both these groups endeavoured to developed practical reagents for the synthesis of organofluorine compounds.

These examples highlight some complexities when employing Zn fluoroalkyl complexes as synthons. Primarily, except for a few sparse examples, these reagents do not readily react as nucleophiles for the transfer of CF_3 to organics. Instead, there must first be a transmetalation step (*vide infra*), generally to Cu, to achieve any desirable products. Beyond Zn, the use of this methodology in the synthesis of transition metal fluoroalkyls is underutilized.

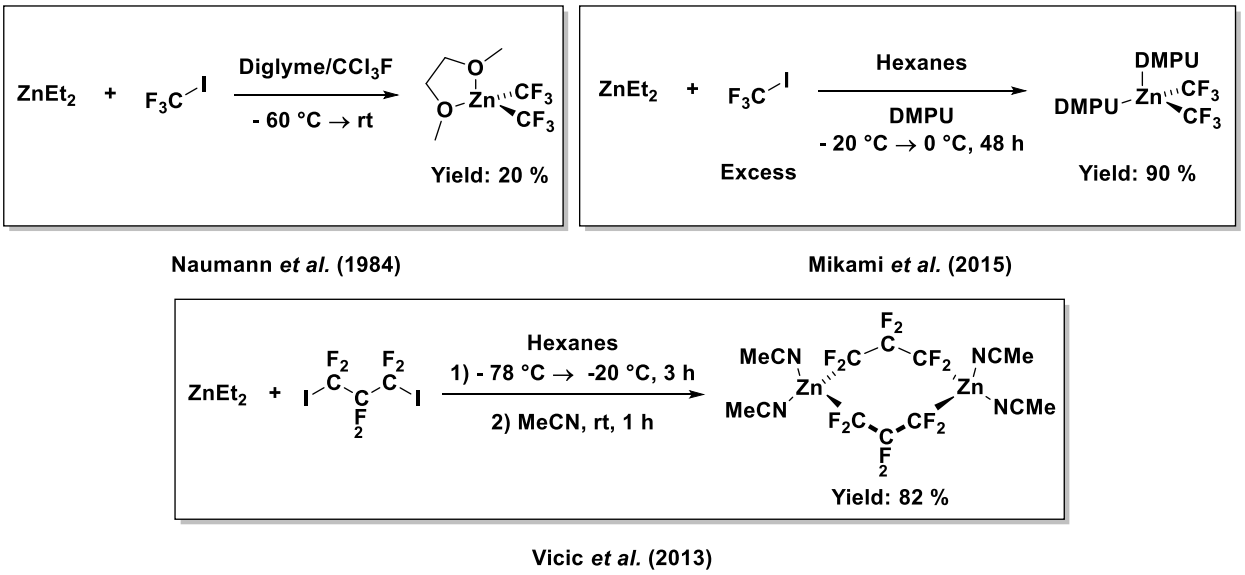

Scheme 1.6. Metalation of iodofluoroalkanes in the synthesis of transition metal fluoroalkyl complexes.

Some examples have used Turbo Grignard® to generate Mg fluoroalkyl reagents using the same approach, suggesting a more adaptable procedure than the oxidative addition route (Scheme 1.7).[116]

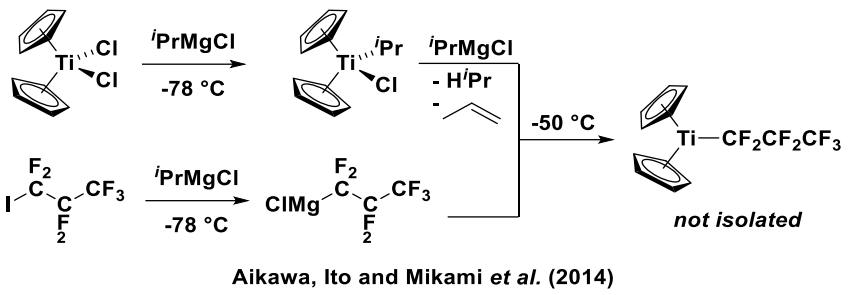

Scheme 1.7. Metalation of iodo-perfluoropropyl with Turbo Grignard, in the synthesis of a suspected Ti^{III}-R^F complex

1.3.1.2. Using Trifluoroacetic Acid and its Derivatives

Consistent with using commercially available sources of CF_3, derivatives of trifluoroacetic acid have also proven timeless in their use as synthons. If either an acid chloride or anhydride is employed under common substitution or oxidative addition conditions, an M-$C(O)CF_3$ or XM-$C(O)CF_3$ complex can be synthesized and readily decarbonylated to yield M-CF_3, although both routes necessarily require a two-electron process (Scheme 1.8). As such, the generality of this approach is limited to transition metals with either significant nucleophilic character, e.g. Mn^- and Co^-, or reduction potential, e.g. Ni^0 and Pd^0. [117-127] Another route starting from sodium trifluoroacetate, a more easily handled reagent, has also been garnering significant attention. In this case, an M-$OC(O)CF_3$ complex, is prepared and subsequently heated in an appropriate solvent to generate "M-CF_3" *in situ*.[128-129] So far, these conditions have been used successfully to synthesize various CF_3 containing substrates from a mixture of $XOC(O)CF_3$ and CuI. Additionally, Vicic *et al.* used an isolable (SI^iPr)Cu[$OC(O)CF_3$] complex to generate a Cu-CF_3 complex but found that it did not outperform the $XOC(O)CF_3$/CuI mixture in DMAc.[131] A caveat of this route is that these complexes often require temperatures ≥130 °C to initiate decarboxylation and the stability of M-CF_3 is questionable under these conditions.

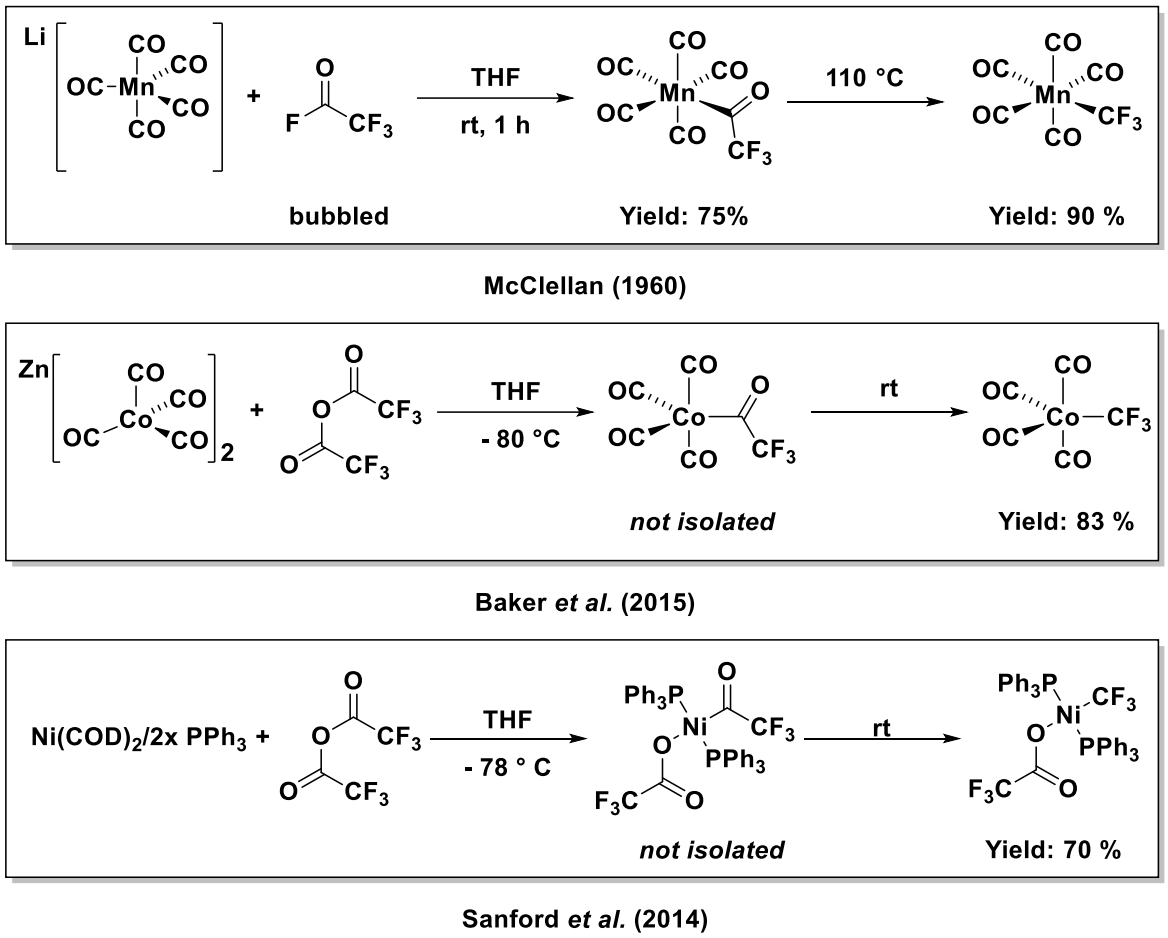

Scheme 1.8. Decarbonylation strategies for the synthesis of metal trifluoromethyl complexes

1.3.1.3. Using Ruppert-Prakash Reagent

In 1984, Ruppert *et al.* introduced the trimethylsilyltrifluoromethane reagent which is prepared using inexpensive and commercially available starting materials.[132] Comparatively, however, $TMSCF_3$ is three times more expensive than CF_3I and one hundred times more expensive than trifluoroacetic acid. The reagent has nonetheless gained wide popularity since its inception because of ease of handling and its facile generation of the $(CF_3)^-$ anion.[133-141] For example, $LiCF_3$ is unstable even at low temperature and decomposes swiftly to LiF and $:CF_2$.[142-143] Given this anionic character, one could expect $TMSCF_3$ to be used in transmetalation reactions, like a step in the Hiyama cross-coupling reaction (Scheme 1.9).

Following this revelation, $TMSCF_3$ has been used extensively in the preparation of various M-CF_3 complexes. Tyrra reported a straightforward preparation of $AgCF_3$ by mixing AgF and $TMSCF_3$ in a sufficiently polar solvent, prior to which it was difficult to prepare as $AgCF_3$ is susceptible to decomposition.[144-146] Vicic *et al.* and Grushin *et al.* adapted this approach for copper in which $[(SI^iPr)Cu(O^tBu)]_2$ or $(PPh_3)_3CuF$ was mixed with $TMSCF_3$ to generate gram quantities of $(SI^iPr)CuCF_3$ or $(PPh_3)_3CuCF_3$ respectively. [147,148]

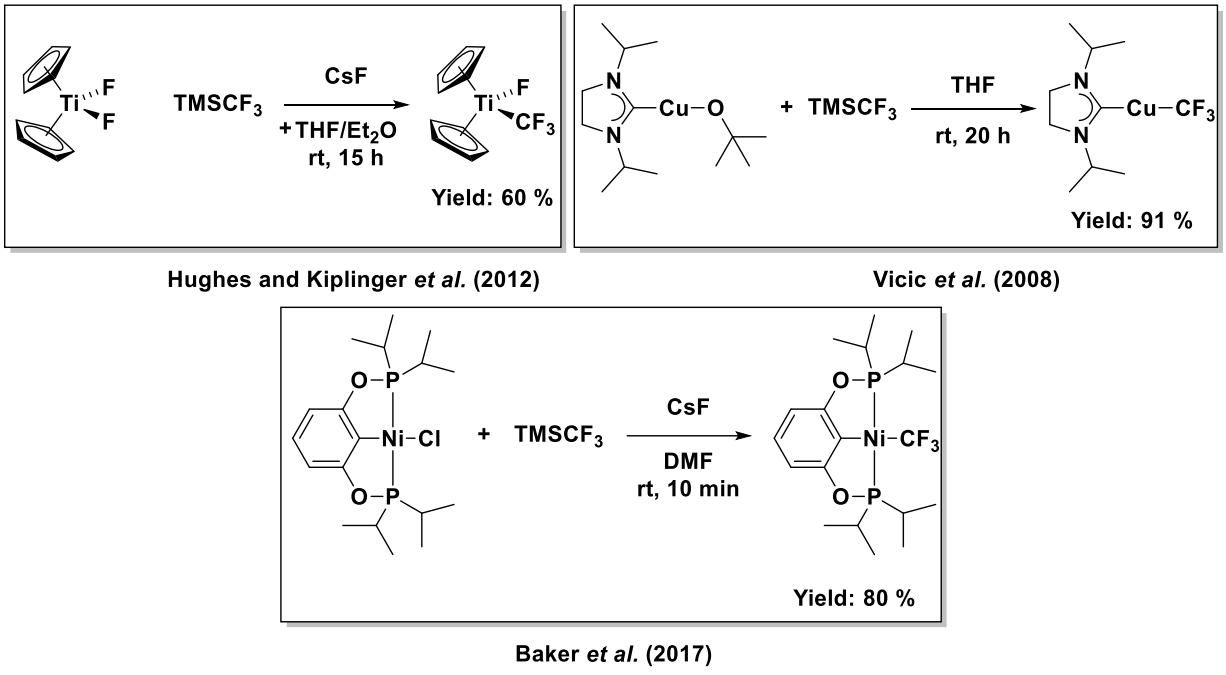

Scheme 1.9. Transmetalation of M-X with $TMSCF_3$

Various other groups have modified these procedures for other metals, including Pd, Ni and Co [149-159]. Most importantly, this is one of the few procedures that can be employed in the synthesis of early transition metal M-CF_3 complexes (cf. preparation of $Cp_2Ti(OTf)CF_3$ using $TMSCF_3$ by Kiplinger *et al.*).[150]

1.3.1.4. Using Fluoroalkanes

The value-add proposition for using fluoroalkanes to prepare metal fluoroalkyls is quite enticing. The former have a long history of use as refrigerants, propellants and blowing agents while others are industrial waste products, e.g. fluoroform, CHF_3. It is no surprise then that these products are manufactured on huge scales and their prices remain quite low. However, it wasn't until 2011 that procedures were developed for the use of fluoroform in the synthesis of Cu-CF_3.[160-166] Daugulis *et al.* used a bis(tetramethylpiperidinide) zinc complex as a base to generate ZnR^F_2 complexes, which could then transmetalate CuCl *in situ*.[160] Importantly, their methodology could be used with a wide variety of linear fluoroalkanes. In contrast, the success of the conditions employed by Grushin *et al.* hinged on the use of 2 equivalents of KOtBu with 1 equivalent of CuCl to generate K(DMF)[Cu(O^tBu)$_2$] as the base in the reaction media (Scheme 1.10).[161] The same authors later reported the same procedure for the synthesis of Cu-CF_2CF_3 from HCF_2CF_3. Of all the fluoroalkanes tested using this method, e.g. heptafluoropropane, iso-heptafluoropropane, etc., only fluoroform and pentafluoropropane gave the desired Cu complexes.[162]

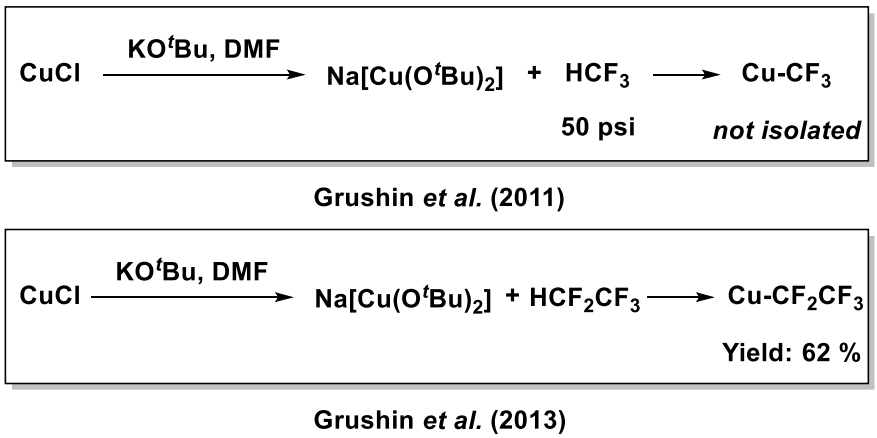

Scheme 1.10. Metalation of fluoroalkanes

1.3.1.5. Using M-CF_3 in Transmetalation Reactions

M-CF_3 compounds are the most widely used synthons for the preparation of transition metal CF_3 complexes, since fluoroalkyls of Zn, Hg and Cd are some of the earliest studied compounds. Although the use of Hg and Cd has continued to wane because of their associated toxicity (Scheme 1.11), [167-178] they have proven invaluable in the synthesis of various organometallic complexes, which could not otherwise be made using previously described methods (*vide supra*). Lately, the focus has been on the use of Ag, Zn and Mg to synthesize new M-R^F complexes.[179-184] Of these, Zn continues to be most widely researched. Not only are these reagents generally stable at room temperature and easy to prepare but a wide array of fluoroalkyl zinc complexes are available. Furthermore, ZnR^F complexes have been used successfully for transmetalation in cross-coupling catalysis. Mikami *et al.* and Vicic *et al.* concurrently reported the use of $(DMPU)_2Zn(CF_2H)_2$ in the presence of either Cu or Ni, respectively, for the preparation of Ar-CF_2H compounds. [179,181]

1.3.2. Synthesis of M-$(CF_2)_n$-X

With respect to the -CF_3 group, applications in the organic synthesis of longer chain fluoroalkyl complexes have remained somewhat overshadowed. However, several routes to these complexes, not derived from C_1 procedures, do exist. One exciting avenue is the preparation of metallacyclopentanes, which generates a C_4 unit starting from two C_2 units, e.g. fluoroalkenes, a process which has been exploited in the preparation of 1,4-dihydrooctafluorobutane.[185] Several other interesting routes which capitalize on the reactivity of fluoroalkenes have been developed and will be discussed herein.

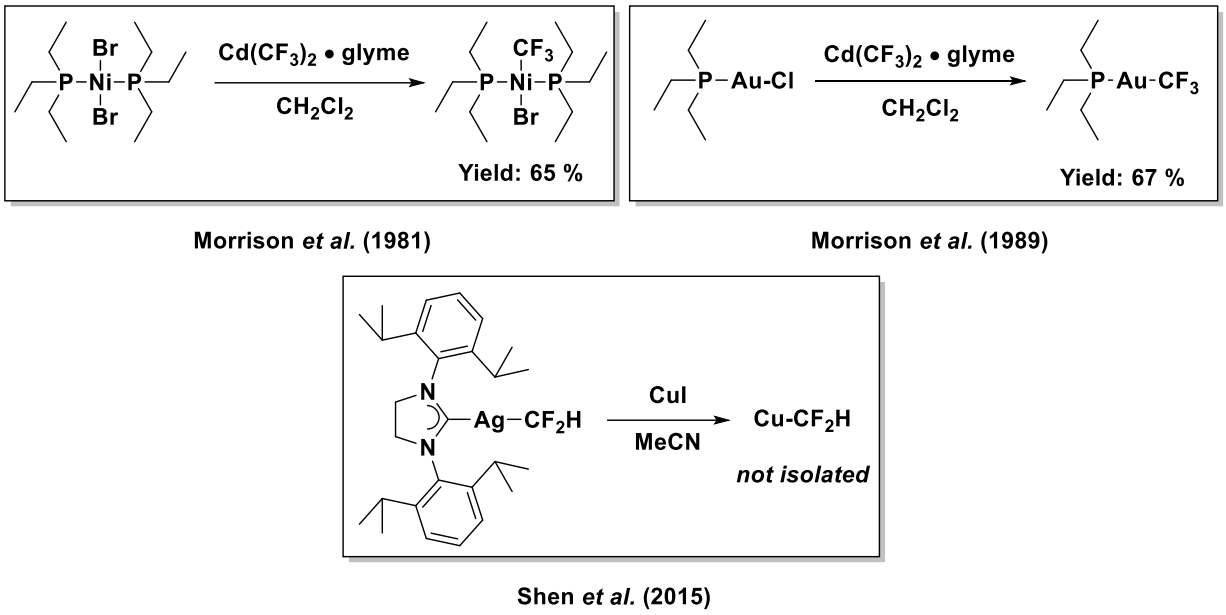

Scheme 1.11. Transmetalation strategies for the synthesis of M-R^F

1.3.2.1. Using Fluoroalkenes for C-C Bond Formation

The synthesis of fluorometallacycles has been explored since pioneering studies by Stone *et al.* The paradigm established the use of low-valent, electron-rich metal complexes in reactions with fluoroalkenes to generate metallacyclic products, either fluorometallacyclopropanes or fluorometallacyclopentanes.[185-207] There is a delicate balance between the formation of either these 3- or 5-membered metallacycles (Scheme 1.12). This balance is dictated by the steric bulk and electronic parameters of the fluoroalkene and ancillary ligands. (cf. it has been demonstrated that (bipy)Ni(C_2F_4) does not form (bipy)Ni(C_4F_8) even upon exposure to excess C_2F_4 under high pressure and temperature, by Pörschke *et al.*[208,209]).

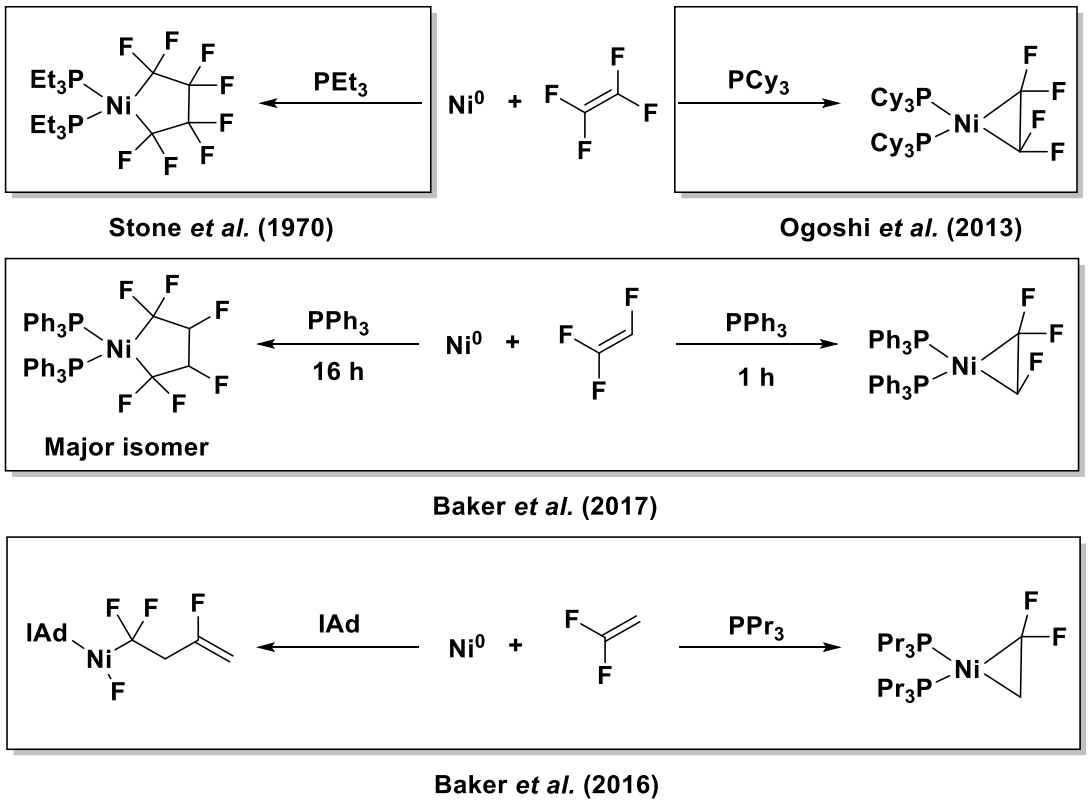

Scheme 1.12. Synthesis of Ni-R^F complexes

It should be noted that most, if not all the following precedents are extrapolated from reactivity observed with nickel and precious metal (Ru, Rh, Pd, Pt) complexes. Only a few examples exist for other metals, such as Fe and Co, and corollaries are being drawn. Overall, both nickelacyclopropanes and nickelcyclopentanes have been characterized. As such, bulky groups have been found to lead to the formation of nickelacyclopropanes. For example, the reaction using PCy_3 and tetrafluoroethylene (TFE) affords $(PCy_3)_2Ni(C_2F_4)$ while the slightly less bulky ligand, P(O-*o*-tolyl)$_3$, gives, under the same reaction conditions, $[P(O\text{-}o\text{-tolyl})_3]_2Ni(C_4F_8)$. Similar reactivity has been reported for trifluoroethylene (TrFE).[207] In stark contrast to the TFE reaction, hexafluoropropene (HFP), a considerably bulkier fluoroalkene, only yields $L_2Ni(C_3F_6)$ even with less bulky ancillary ligands.[199] Moreover, the propensity to generate a 5-membered ring is less for the heavier 5d metals. The reaction of $Pt(COD)_2$ with TFE,

for example, gives a diplatinacyclohexane, while that with HFP leads to a μ-$C(CF_3)_2$ alkylidene complex via a 1,2-fluoride shift, Scheme 1.13.[201]

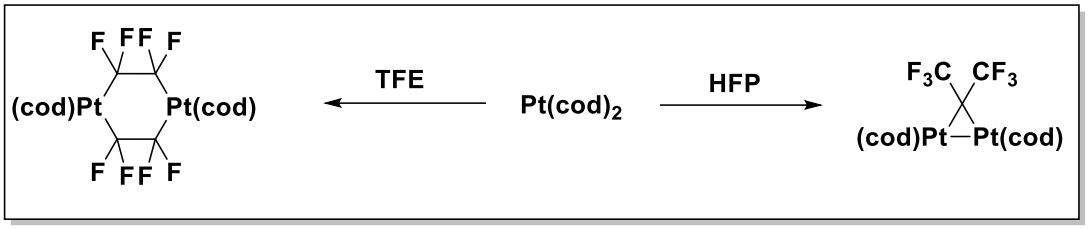

Stone *et al.* (1977)

Scheme 1.13. Synthesis of Pt-R^F complexes from TFE and HFP.

Another class of these compounds is those prepared from mixed constituents, i.e. two types of fluoroalkenes or a fluoroalkene and non-fluorinated alkene. These fluorometallacycles can be generated in a similar fashion to those mentioned above**.** Ogoshi *et al.* used this approach in various ways for the synthesis of new fluorocarbons. In one example, the nickel complex intermediate was isolated from the reaction mixture. The authors found that when mixing Ni^0/PCy_3 with TFE and ethylene a 7-membered metallacycle was produced, which consisted of at least one Ni-C_{RF} bond. [210]

1.3.2.2. Using Fluoroalkenes: C-F bond Activation

In parallel to this work, the reactivity of fluorometallacyclopropanes was also being explored. It was found that addition of a Lewis acid to abstract a fluoride anion leads to the synthesis of new fluoroalkenyl complexes. The prevalence of this reaction is now well established in organometallic chemistry. Several Lewis acids can be used to initiate this transformation. The addition of LiI or MgBr or $BF_3{\cdot}Et_2O$ to $L_2Ni(C_2F_4)$ or $L_2Pd(C_2F_4)$ always leads to the formation of $L_2NiX\text{-}CF{=}CF_2$ or $L_2PdX\text{-}CF{=}CF_2$. Under thermal conditions, these low-valent metal complexes can undergo C-F bond oxidative addition to provide another route,

without additives, to fluorovinyl complexes. This reactivity is not limited to TFE complexes, but also applicable to HFP complexes. Under Lewis acid addition conditions $(PCy_3)_2Pd(C_3F_6)$ rearranges to $(PCy_3)_2Pd[-CF=CF(CF_3)]BF_4$, $(PMe_3)_3Ni(C_3F_6)$ to $(PMe_3)_2NiCl[-C(CF_3)=CF_2]$ and, (dppe)Pt(C_3F_6) to (dppe)PtCl$[-CF=CF(CF_3)]$.[211-216] Beyond these oxidative addition routes, C-F bonds can also be activated using carbonylmetallates. An early study by Stone *et al.*, treated $[CpFe(CO)_2]^-$ with TFE to make the stable Fp-$CF=CF_2$ complex.[217,218] On top of this, trifluorovinyl lithium can be synthesized at low temperature upon treatment of 1,1,1,2-tetrafluoroethane with BuLi. If this reagent is mixed with $[CpFeI(CO)_2]$ at low temperatures, Fp-$CF=CF_2$ can be isolated in 50 % yield (Scheme 1.13). [219,220] A less direct metalation reaction was also proposed by Clark and Tsang *et al.* They noted that reaction of a [Pt]-H complex with TFE at 120 °C afforded a [Pt]-$CF=CF_2$ complex rather than the expected insertion product, [Pt]-CF_2CF_2H. Similar [Pt]-H reactions with TrFE and perfluorocyclobutene generated [Pt]-CF=CFH and [Pt]-(η^1-C_4F_5) respectively. [221,222]

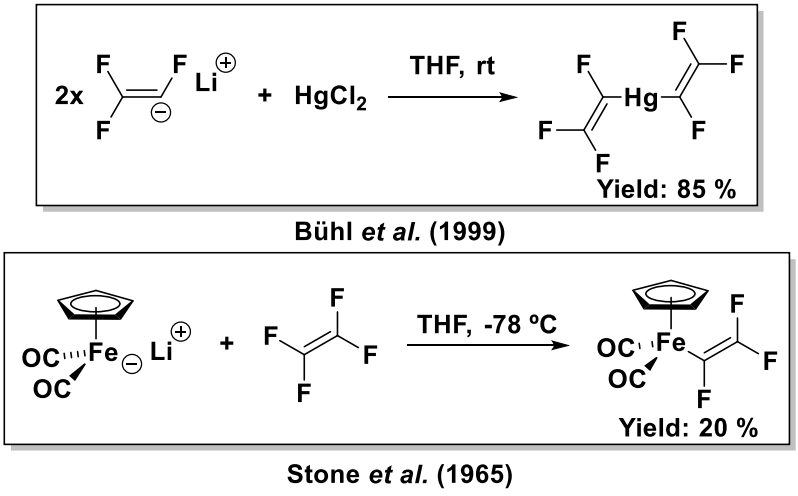

Scheme 1.14. Synthesis of fluorovinyl complexes**.**

1.3.2.3. Using Fluoroalkenes: Insertion into M-X

In the work by Clark and Tsang *et al.* they demonstrated that the initial product formed in the reaction of Pt-H with TFE was Pt-CF_2CF_2H, but this readily loses HF to yield the Pt-$CF{=}CF_2$ mentioned above.[221,222] Original reports on this type of reactivity where first produced by Stone *et al.* In this report, $(CO)_5$Mn-H was demonstrated to readily insert TFE, CTFE and DiCTFE yielding the corresponding Mn-R^F complex.[223,225] It was later demonstrated that this reaction protocol was not limited to M-H complexes (Scheme 1.14). For example, Burnard *et al*. showed that metal fluorides also readily insert fluoroalkenes. By mixing AgF with HFP, the insertion product $AgCF(CF_3)_2$, can be prepared on a gram scale.[226] While Stone also demonstrated TFE insertion into the Mn-Me bond[224], Ogoshi *et al.* extended this protocol to include the Cu-arene bond. They found that (phen)Cu-Ar, generated *in situ*, reacts with TFE to provide a scalable route to Cu-CF_2CF_2Ar complexes.[227,228] More recently, J. Hu *et al.* proposed that TFE would react with other Cu complexes to mediate some cross-coupling reactions. They were the first to report the use of a Cu-CF_2CF_3 complex (not isolated) synthesized by insertion of TFE into Cu-F. Later, Ogoshi *et al*. demonstrated that (phen)Cu-CF_2CF_3 could be prepared and isolated using a similar route.[229,230]

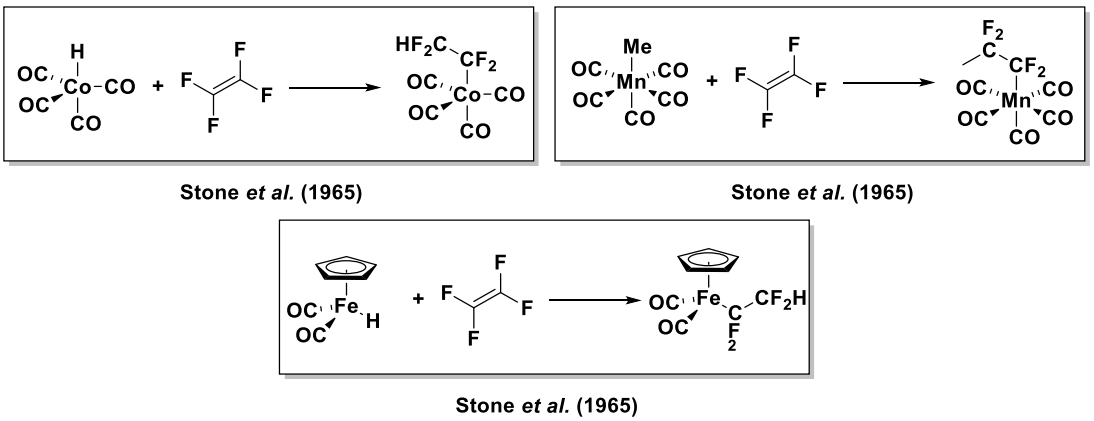

Scheme 1.15. Selected examples of fluoroalkene insertion into M-H/Me bonds

1.4. Properties of M-R^F Complexes

Given the plethora of methods now available for their synthesis (vide supra 1.2.1) it is a purview of this *Thesis* to summarize here a non-exhaustive list of M-R^F complexes to correlate structural parameters to observed reactivity.

1.4.1. Theoretical Considerations of the C-F bond

The C-F bond is highly polarized towards the fluorine. One should also consider that the orbital configurations of fluorine and carbon are very similar. Essentially, we would expect 2p to 2p orbital overlap between these elements or, according to valence bond theory, some hybridized sp orbital, and as such we would expect a significantly strengthened bond.[231] An interesting empirical observation is that upon increasing the number of fluorine substituents on carbon we notice a significant increase in the C-F bond strength (i.e. from 104 kcal/mol in CH_3F to 116 kcal/mol in CF_4) as well as non-negligible shortening of bonds.[49] The current theory for this observation is that bond shortening is caused by the increased electropositive nature of the carbon, thereby increasing the electrostatic C-F interaction, accounting for the shorter bond. To correct for this effect in valence bond theory the hybridized carbon orbital must then decrease from sp^3 to $sp^{2.4}$ for every consecutive fluorine substitution. However, as described by Banks *et al*, while this would account for the C-C bond lengthening in perfluoroethane *vs* ethane, it does not account for the significant increase in C-C BDE of 107 kcal/mol *vs* 100 kcal/mol respectively.[21] While the above discussion provides a qualitative model, some discrepancies remain for explaining certain empirical values.

It is clear from this example that any substituents next to a C-F bond have a profound effect on both bond dissociation energy and length. So, it stands to reason that one might expect a form of C-F bond "activation" by sharing this bonding carbon atom with a metal. Simply by

forming an M-C_{RF} bond, thus modulating the orbital character and electrostatic charge of the carbon, the C-F bond can be strengthened or weakened without necessarily invoking further orbital interaction.

1.4.2. Known M-R^F Complexes: M-C and C-F Bond Lengths

Since the synthesis of the first M-R^F complexes, one intrigue has always been their disparate reactivity at the M-C or C-F bond vs. their hydrocarbon congeners. A few notable examples highlight this comparison. In the first, the reactivity of $Mn(CH_3)(CO)_5$ with CO is compared with the CF_3 analog shown in Figure 1.15.[202,232,233] Under pressure of CO, the CH_3 migrates to a coordinated CO ligand affording the acetyl product, $Mn[C(O)CH_3](CO)_5$ whereas no reaction is observed for the CF_3 analog. In fact, the reverse reaction (decarbonylation) is the thermodynamically preferred pathway for the perfluoroacyl complex prepared independently (*vide supra*). This observation suggests that the insertion pathway for M-R^F complexes encounters high activation energies and M-R^F complexes are thermodynamically more stable.

Another example highlighting this disparity compares the stability of nickelacyclopentanes with their fluorinated counterparts. It was shown that nickelacyclopentanes readily undergo various transformations and need to be kept cold during their preparation.[234] Upon warming to just 9 °C, they can decompose to yield ethylene, cyclobutane and butene isomers, depending on the coordination mode (Scheme 1.16). In comparison, perfluoronickelacyclopentanes are outstandingly robust and withstand decomposition even at elevated temperatures (~100 °C).

These observations are a testament to the thermodynamic stability of the M-C_{RF} bond in these systems. Furthermore, these complexes do not insert either CO or TFE into the M-C_{RF}

bond, to yield expanded ring nickelacycles.[232] However, if the complex allows for coordination of H_2, the Ni-C_{RF} bonds can be cleaved to generate Ni^0 and $HCF_2CF_2CF_2CF_2H$.[185] These results suggest, like the Mn complexes, that the Ni-R^F complexes are kinetically and thermodynamically inert to insertions generating other Ni-C bonds. They also suggest that the Ni- C_{RF} bond energy is in the range of H-C_{RF} bonds.

Although the M-C_{RF} bonds have demonstrated unique stability, the same cannot be said for C-F bonds in proximity, be it alpha or beta, to a metal although the fundamental properties which lead to this somewhat enhanced reactivity are still not fully understood.[150,236-240]

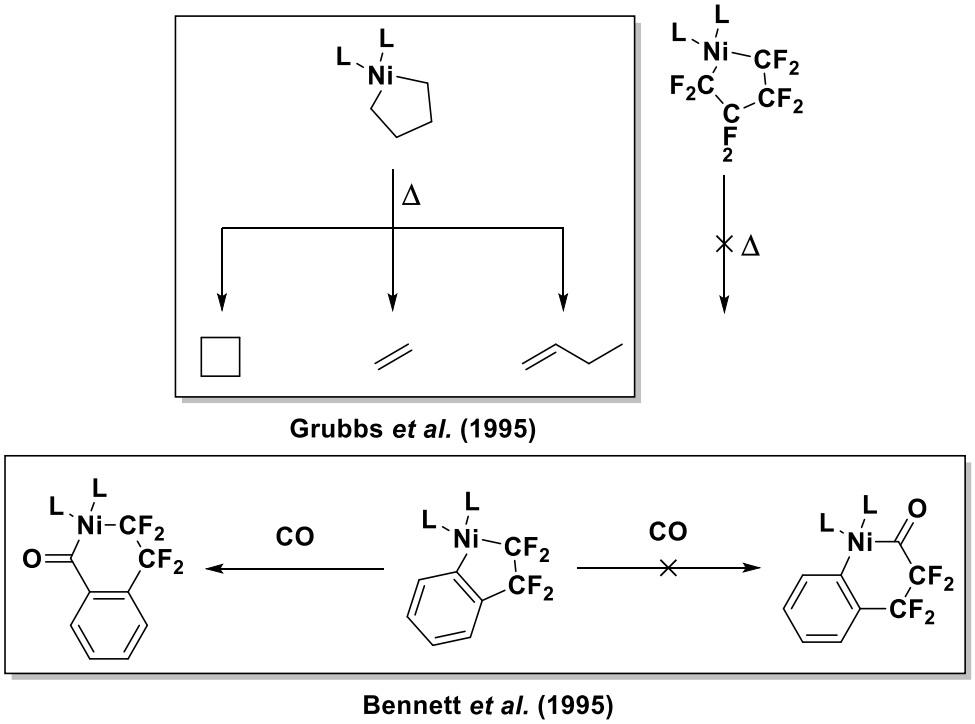

Scheme 1.16. Comparison in the reactivity of M-R vs M-R^F

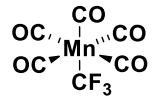

d^6

M-C: 2.056(5) Å
C-F: 1.370 Å

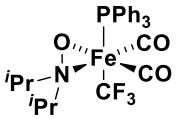

d^6

M-C: 1.986(3) Å
C-F: 1.353 Å

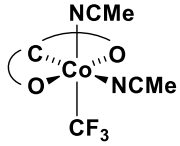

d^6

M-C: 1.9189(14) Å
C-F: 1.3603 Å

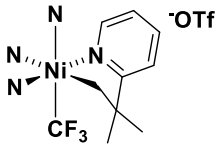

d^6

M-C: 1.956(2) Å
C-F: 1.358 Å

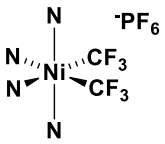

d^6

M-C: 1.910Å
C-F: 1.370 Å

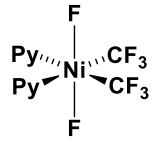

d^6

M-C: 1.965 Å
C-F: 1.321 Å

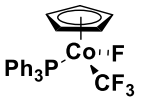

d^6

M-C: 1.936(5) Å
C-F: 1.361 Å

d^0

M-C: 2.221(3) Å
C-F: 1.363 Å

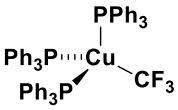

d^{10}

M-C: 2.029 Å
C-F: 1.40 Å

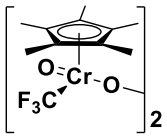

d^2

M-C: 2.096(11) Å
C-F: 1.359 Å

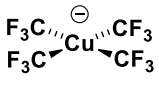

d^8

M-C: 1.966 Å
C-F: 1.35 Å

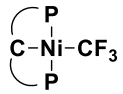

d^8

M-C: 1.9296 Å
C-F: 1.3668 Å

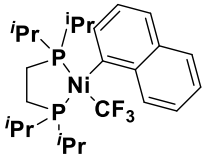

d^8

M-C: 1.9312(14) Å
C-F: 1.357 Å

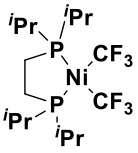

d^8

M-C: 1.927 Å
C-F: 1.378 Å

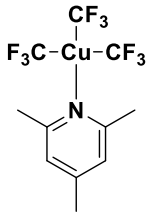

d^8

M-C: 1.981 Å (trans to CF_3)
C-F: 1.337 Å
M-C: 1.959 Å
C-F: 1.305 Å

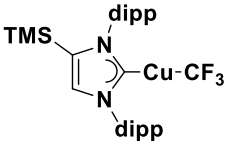

d^{10}

M-C: 1.967(6) Å
C-F: 1.338 Å

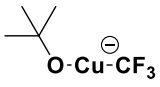

d^{10}

M-C: 1.888 Å
C-F: 1.38 Å

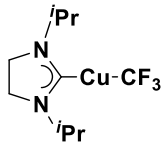

d^{10}

M-C: 2.072(3) Å
C-F: 1.302 Å

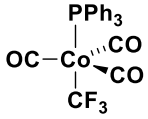

d^8

M-C: 1.953(6) Å
C-F: 1.356 Å

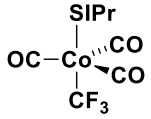

d^8

M-C: 1.964(2) Å
C-F: 1.363Å

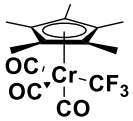

d^4

M-C: 2.072(3) Å
C-F: 1.302 Å

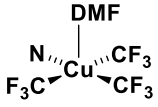

d^8

M-C: 1.957 Å (trans to CF_3)
C-F: 1.321 Å
M-C: 1.924 Å
C-F: 1.341 Å

Scheme 1.17. Some metal trifluoromethyl complexes

In this case, “enhanced” or “activated” implies that addition of non-reducing exogenous reagents (e.g. Lewis acids) leads to reactivity at the C-F bond, in cases where that same reagent would not react with the respective perfluoroalkane or fluoroalkane. For example, H-CF_3 does not readily react with TMSOTf but most M-CF_3 complexes do (as discussed below). Scheme 1.17 shows the structures of a variety of M-CF_3 complexes which have been fully characterized, including by X-ray crystallography.[241-271] It highlights the difficulty in defining any form of an empirical trend with respect to bond lengths (M-C or C-F) and so-called “activation”. A rudimentary analysis suggests that structure and the position occupied by the CF_3 ligand are the greatest factors in determining this C-F bond elongation or contraction, and each complex has been binned accordingly. Several attempts have been made to interrogate these complexes with DFT in determining a rationale for the observed M-C_{R^F} inertness and C-F enhanced reactivity. These studies suggest that multiple factors are responsible for these effects; primarily, the enhanced s character of the carbon with a minor contribution from back-donation of a filled metal d orbital into a C-F σ* orbital. [150,240]

Counter to the above arguments, it is well known that the trifluoromethyl anion rapidly decomposes to difluorocarbene and fluoride ion.[141,142] Therefore, it could also be argued that M-CF_3 complexes allow for a unique stabilization of the R^F ligand. That is to say that they could be characterized as concealed CF_3 anions. This Cα-F stabilization trend is less clear for greater chain-length R^F groups because, in such cases, the thermodynamic product results from Cβ-F elimination to yield M-F and a fluoroalkene. This is supported by reactivity trends in which carbenium ions generated from Cα-F fluoride abstraction from longer chain R^F’s are quite unstable and do not usually form stable M=C_{R^F} complexes. [240]

A noteworthy example of these trends in stability was recently highlighted by J. Hu and colleagues using copper fluoroalkyl complexes. Upon mixing CuCl, KF, and $TMSCF_3$ in DMF, a $Cu\text{-}CF_3$ complex could be generated in the first 30 minutes. If the reaction is left to sit for 24 hours, nearly complete conversion to $Cu\text{-}CF_2CF_3$ is achieved and only small amounts of $Cu\text{-}CF_2CF_2CF_3$ are observed as a co-product (Scheme 1.17). [272]

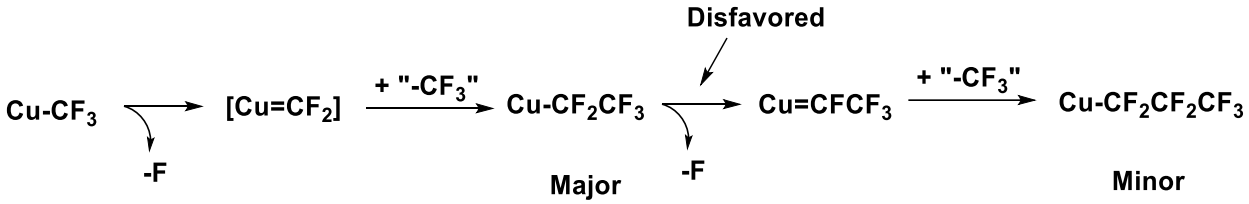

Scheme 1.18. Stability of $Cu\text{-}R^F$ towards spontaneous C-F bond activation

1.5. Reactivity of M-R^F Complexes: Metal-Mediated or -Catalyzed

The stability of $M\text{-}R^F$-complexes has not undermined their use in organic transformations although it has significantly hindered the development of *catalytic* routes. This is particularly true for the synthesis of $Ar\text{-}R^F$ using Ni- or Pd-catalyzed routes (popular catalysts for the synthesis of Ar-R). The diverse mechanisms of these reactions should be analyzed separately as each one has unique caveats. As such, the methods will be considered as two categories: $\text{-}R^F$ synthesis and C-F bond activation.

1.5.1. M-R^F in cross-coupling reactions

Due to the importance of the CF_3 group in pharmaceutical and agrochemical industries, significant effort has been applied to catalytic reactions involving this functionality. A catalytic system had long eluded chemists, though several key metal-mediated reactions have been identified such as the stoichiometric trifluoromethylation of aryl halides using Cu, first disclosed by Fuchikami *et al.* [274] However, no discreet metal complex was used in the reaction.

Naturally, catalytic systems followed and Amii *et al.* successfully coupled Ar-I and TES-CF_3 using a KF/CuI/1,10-phenanthroline mixture.[275] Following these results, Cu has emerged as the metal of choice for R^F cross-coupling reactions (Scheme 1.19)[273-284] although some Ni-mediated and Pd-catalyzed variants have been reported. [285-289]

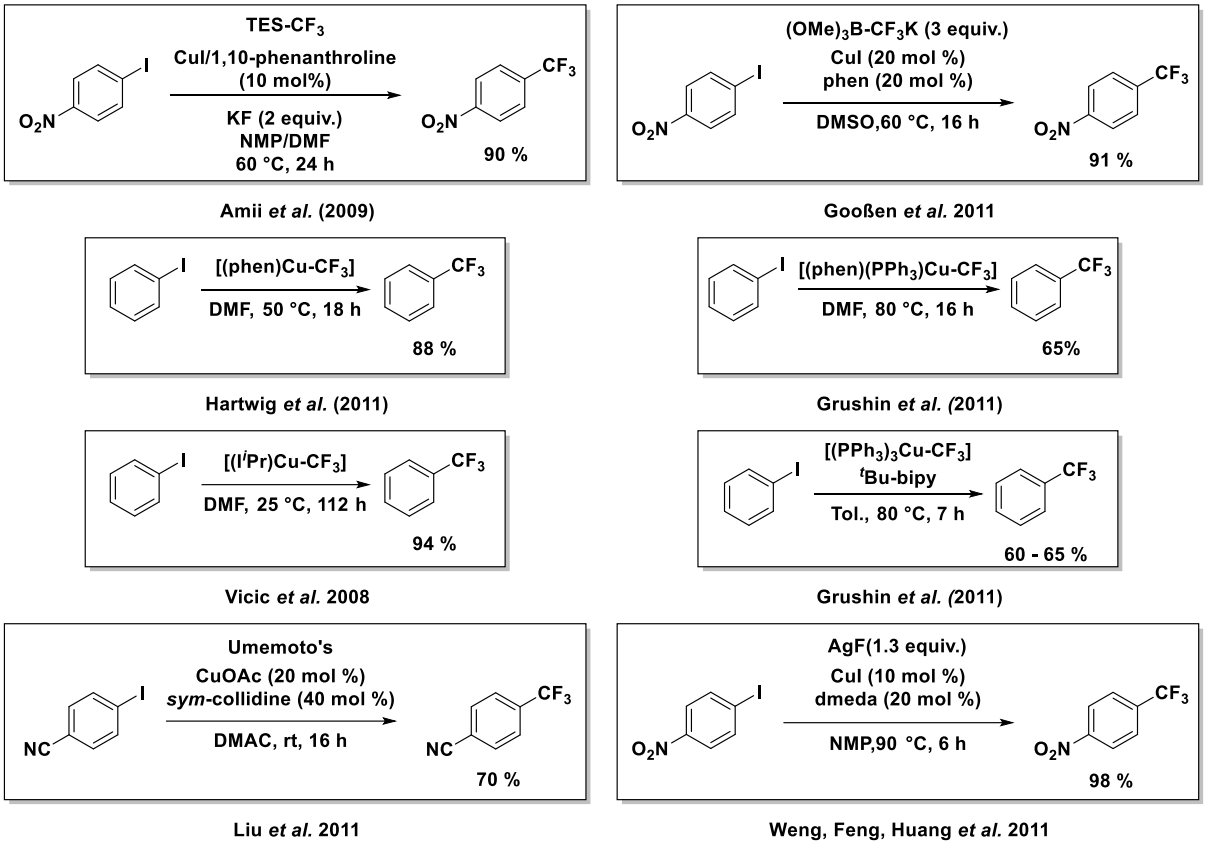

Scheme 1.19. Protocols for the synthesis of Ar-CF_3 compounds

These reactions are of use in the design of methodologies for the installation of other fluoroalkyl chains in the framework of this *Thesis*. Furthermore, the mechanistic details of these reactions could provide useful insight into this design. In 2014, Grushin *et al.* carried out a comprehensive mechanistic study on the DMF-solvated copper trifluoromethylation of aryl iodides.[290] This seminal work provided support for the generally accepted oxidative addition pathway (Cu^I/Cu^{III}) (Scheme 1.20), all but ruling out SET or HAT mechanisms. Li *et al.* built on

these calculations for his study of the (I^iPr)Cu-CF_3 system. Their studies revealed similar trends, with oxidative addition to (I^iPr)$CuCF_3$ proving to be the rate limiting step and the lowest energy pathway.[291] However, computational details for the phen/$CuCF_3$ reaction with aryl halides are not yet available.

Far fewer examples of longer chain perfluoroalkylation reactions exist today. Hartwig and coworkers were able to extend the conditions they employed in the copper-catalyzed

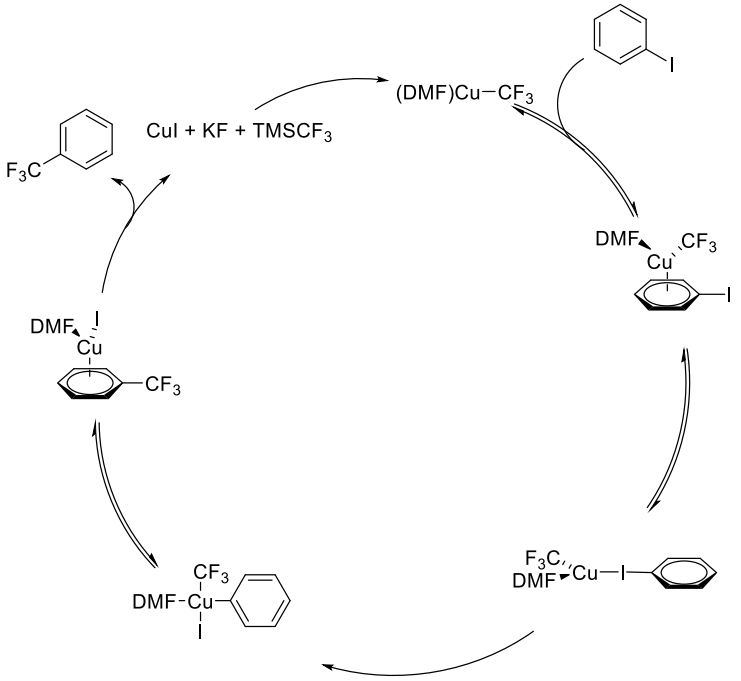

Scheme 1.20. The mechanism for the cross-coupling of Ar-I with Cu-CF_3.

trifluoromethylation reaction to n-heptafluoropropyl trimethylsilane.[281] Using an isolated [(phen)$CuCF_2CF_2CF_3$] complex, n-heptafluoropropyl benzene analogues could be prepared. Daugulis and coworkers (drawing inspiration from C-H bond activation of pentafluorobenzene) prepared similar products.[160] With the same catalytic mixture used in trifluoromethylation reactions, CuI/phen ~10 mol%, and a strong base, $Zn(TMP)_2$, in a polar aprotic solvent, a series of fluoroalkanes (HCF_3, HC_2F_5, HCF_2CF_3, etc.) were shown to react with aryl iodides. As

described above (**Section 1.2.1.1.4**), this reaction likely generates first a fluoroalkyl zinc reagent which serves to transmetallate the Cu(I). This *in situ* generated Cu-R^F then reacts with the Ar-I. Later, Grushin *et al.* showed that DMF-solvated Cu-CF_2CF_3 could be mixed with aryl bromides to yield a series of Ar-CF_2CF_3 complexes.[162] This work was unique in that it did not require the use of a ligand to obtain good yields, more closely resembling the original Ullman-type reaction conditions.

The pentafluoroethyl group has gained a somewhat more popular status then others and a few more examples have appeared in recent years. The groups of J. Hu and Ogoshi simultaneously developed similar protocols, again relying on either CuI/phen in catalytic amounts or a discreet [(phen)CuCF_2CF_3] complex to achieve cross-coupling.[229,230] More recently, J. Hu and coworkers extended the use of $TMSCF_3$ to generate DMF/Py-solvated $CuCF_2CF_3$ which, when heated to 80 °C, could pentafluoroethylate various Ar-I substrates.[272] To date, a few reports have applied similar procedures (CuI/phen and DMF/CuI) for the introduction of various other fluoroalkyl chains such as -CF_2CF_2Ar and -CF_2CF_2OR.[227,230,292]

Most examples of metal-assisted Ar-CF_3 synthesis involve the coupling of M-CF_3 with Ar-I. In line with this paradigm, most syntheses of R-C(O)-R^F involve the coupling of M-CF_3 with R-C(O)-Cl although some novel carbonylation reactions have been developed. For example, Perutz *et al.* showed that Ni^{II}(-C_5NF_4)Me does not reductively eliminate C_5NF_4-Me but will readily eliminate C_5NF_4-C(O)Me when exposed to CO.[293] In 2016, Yang, Xhou and Wu *et al.* also showed that Pd^{II}(-C(O)Ph)CF_3 can be used to synthesize Ar(CO)CF_3. Strangely, a comparable Pd^{II}(Ph)CF_3 complex does not insert CO and thus does not generate Ar(CO)CF_3. Therefore, it was rationalized that a Pd acyl complex must first be generated by insertion of CO

into $Pd^{II}(Ph)I$ prior to transmetallation with $CuCF_3$.[294] Mixed constituent metallacycles are also known to undergo these types of reactions. For example, Bennett *et al.* showed that a mixed constituent metallacyle, where one Ni-C bond exists, readily inserts CO and reductively eliminate fluoro-ketones.[235]

Since that early report of reactivity on mixed constituent metallacycles, Ogoshi *et al.* have made considerable contributions to this field (Scheme 1.20).[295,298] They have since expanded the insertion of $Ni(C_4F_4H_4)$ to include ethylene, aldehydes, acetylenes, and styrenes. A key feature of this catalytic system is the generation of a 7-membered metallacycle, e.g. $Ni(C_6F_4H_8)$, which can readily β-hydride eliminate, forming a $Ni^{II}H(R^F)$ intermediate which quickly reductively eliminates to yield Ni^0 and H-R^F. In fact, this work nicely supports earlier findings by Baker *et al* who found that $Ni^{II}(C_4F_8)$ complexes --- which are for the most part inert to insertion reactions --- can undergo hydrogenolysis, leading to Ni^0 and H-R^F-H.[185]

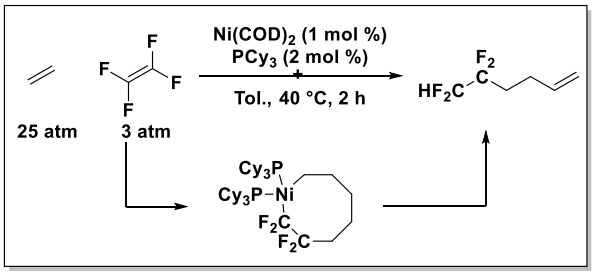

Ogoshi *et al.* (2015)

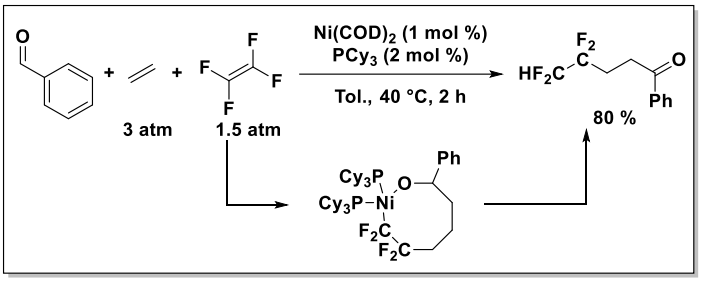

Ogoshi *et al.* (2015)

Scheme 1.21. Examples of catalytic C-C bond forming reaction where there is at least one M-R^F bond**.**

1.5.2. Metal-Mediated/Catalyzed C-F bond activation

C-F bond activation has long attracted attention because of the ability to obtain regiocontrol in a multifluorinated system. This allows for further derivatization of the fluoro-organic fragment without necessarily sacrificing fluorine content. A prominent example of this type of reactivity is the C-F bond activation of fluoroarenes, which will be detailed further in *Chapter 6*.

This exemplar involves oxidative addition of a C-F bond to a metal center. An analogy can be drawn with this type of reaction and the synthesis of M-R^F_{vinyl} complexes and their use in cross-coupling reactions. Although not necessarily involving oxidative addition of a C-F bond, the Cα-F bond activation product of 3-membered metallacycles are the same as the oxidative addition product of the respective alkene. As such, various groups have used this reactivity to synthesize R-R^F_{vinyl} compounds. As a first example, Ichikawa and Minami *et al.* reacted fluorovinyl ethers with zirconocene.[299] They found that the resulting 3-membered metallacycle was unstable and re-arranged to Cp_2ZrF(-CF=CH(OR)). When this complex was mixed with ZnI_2 (4 equiv)/Pd_2dba_3 (2 mol%) and an aryl iodide in THF, the corresponding α-fluoro-β-alkoxystyrenes were generated. Ogoshi *et al. then* successfully used tetrafluoroethylene in a cross-coupling reaction with diaryl zinc, alkyl zinc, or allyl Grignard reagents to synthesize Ar-$CF=CF_2$, Et-$CF=CF_2$, and allyl-$CF=CF_2$.[216] However, the reaction only produced appreciable yields when LiI or LiCl was added to the reaction mixture. The suspected role of the LiI/LiCl was to a) act as a Lewis acid and b) generate diaryl zincates. The first role was supported by a stoichiometric reaction in which an isolated Pd(C_2F_4) complexes was stirred with LiI, producing I-Pd-$CF=CF_2$. These authors followed up this research, later showing that heating (~100 °C) both Ni and Pd 3-membered metallacycles leads to formation of a vinyl complex

without the use of an additive.[205] They found that these F-M-CF_2=CF_2 complexes react with aryl boronic acid esters at high temperatures, yielding fluorostyrenes. Interestingly, use of the iodo complexes did not produce the desired product under the same reaction conditions. These base-free Suzuki type cross-coupling reaction conditions employed could also be used for Hiyama type cross-coupling reactions if aryl silanes were used instead of aryl boronic acid esters.[300]

Other somewhat related approaches, taking advantage of facile C-F bond elimination, are those which first generate a new C-X bond, then undergo fluoride elimination to yield the organic fragment. These types of reactions can be divided into two classes. One class involves the generation of a 5- or 4-membered metallacycle that then undergoes F-elimination. The second involves the addition of a metal-X bond to a fluoroalkene, followed by β-fluoride elimination from the respective M-R^F complex.

Using the oxidative cyclization route, a nickel-catalyzed route for the synthesis of fluoro-benzenes and nickel-mediated route for the synthesis of perfluorocyclobutene and difluorophenyl butadienes have been achieved.[298] These routes use the well established α-fluoride elimination of fluoronickelacycles to achieve novel reactivity. In 2014, Ichikawa *et al.* reported an example of an uncommon β-fluoride elimination and successfully synthesized a series of fluorocyclopentadienes starting from trifluoropropene derivatives and an alkyne (Scheme 1.22). The *in situ* generated 5-membered nickelacycle was unstable, and quickly β-fluoride eliminates. Insertion of the resulting alkene into the Ni-$C_{alkenyl}$ bond followed by a second β-fluoride elimination generates the observed diene.[302,303,304] Although this system is unique because it has a β-fluoride in proximity to metal, it is related to work carried out by our group.

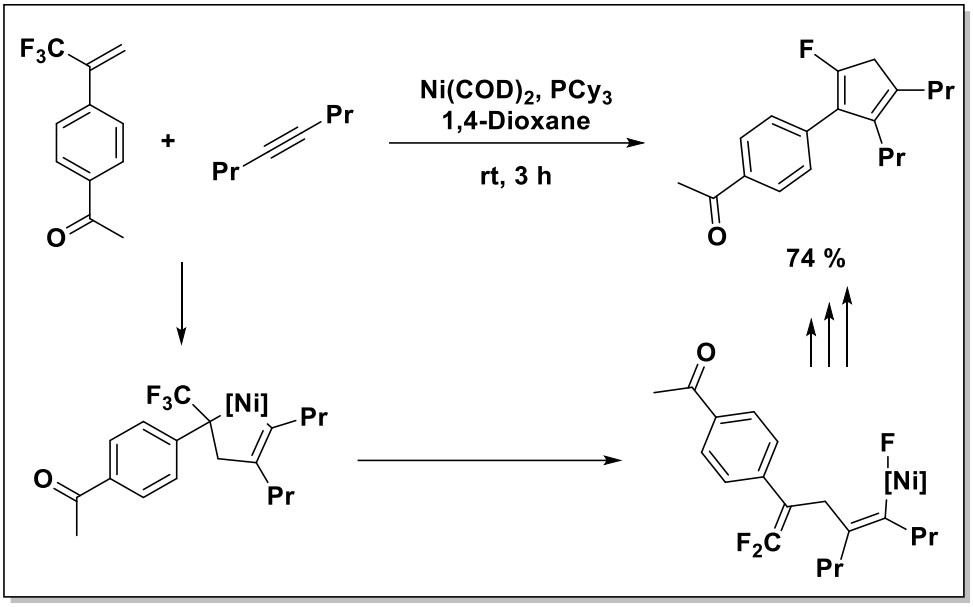

Ichikawa *et al.* (2014)

Scheme 1.22. Example of coupling reactions involving C-F bond activation.

Similarly, to the work described in *Chapter 2*, Dr. Kaitlin Giffin and Mr. Alexandre Sicard discovered that the stability of nickelacyclopentanes is linked to the degree of fluorination. The synthesis of these classes of fluoronickelacycle led to new routes to fluorobutenes. The fluoronickelacycles generated from the head-to-tail reaction of 2x TrFE with Ni^0, although stable at rt, underwent a novel dual-α and dual-β fluoride elimination in the presence of a Lewis acid, producing tetrafluorobutadienes.[207] With one less degree of fluorination, using VdF, the presumed *in situ* generated nickelacycle undergoes spontaneous β-fluoride elimination, as Ni-$CF_2CH_2CF{=}CH_2$ is isolated as the only product. Furthermore, these complexes were found to catalyze the hydrodefluorodimerization of VdF using silanes.[206] In another example by our group, 4-membered cobaltacycles, made from the 2+2 cycloaddition of $Co{=}CF_2$ and TFE, also underwent β-fluoride elimination in the presence of a Lewis or Bronsted acid, affording alkenyl complexes or ring contraction to cobaltacyclopropanes.[305]

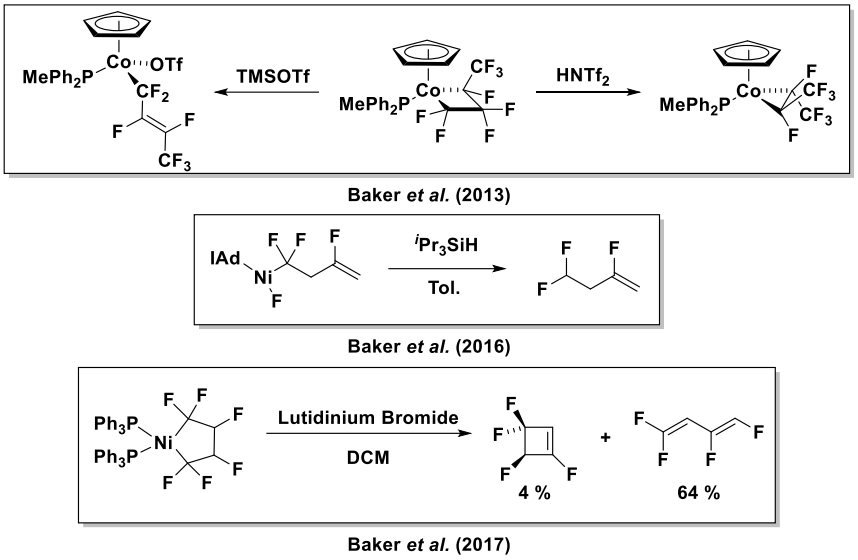

Scheme 1.23. Examples of C_β-F bond activation.

Using the M-X addition or Heck-like route, Heitz *et al.* synthesized α-fluorostyrenes from Ar-I and VdF. The reaction likely proceeds *via* insertion of VdF into the Pd-Ar bond. Interestingly, VdF always inserts to give Pd-CH_2CF_2Ar. The Pd-R^F then undergoes β-fluoride elimination, producing $Pd^{II}F$ and H_2C=CF-Ar. The purpose of the addition of triethylamine to the reaction mixture is not clear since no PdHF is generated and the regeneration of Pd^0 remains ambiguous.[306] Sometime later, the groups of Murakami and Ogoshi reported Rh- and Cu-catalyzed coupling of aryl boronic acid esters and α-trifluoromethylstyrenes, involving a similar Ar addition/elimination pathway.[307] To date, several other Cu catalyzed processes have been disclosed, including but not limited to Cu-B, Cu-Si, and Cu-H.[308-310]

1.6. Summary and Thesis Outline

Fluorinated compounds have dramatically impacted the quality of life around the globe. Such compounds have become invaluable in our efforts to develop new pharmaceuticals, agro-chemicals, non-toxic refrigerants, and anesthetics, to name a few. Although their preparation on industrial scales remains viable, they have a rather large carbon footprint. Issues with the current

procedures have been introduced and transition metal-catalyzed routes are recommended as feasible alternatives. As such, this work develops "greener" routes for the synthesis of fluoro-carbons using coinage metals (e.g. Ni, Ag, Cu).

The synthesis of metal fluoroalkyl complexes was discussed above to initiate those who are not familiar with the art. The synthetic strategies generally employ fundamental organometallic concepts and are not necessarily "novel", but they highlight the difficulties in the preparation of these compounds. The strategies were separated into classes of fluorinated precursors used as starting materials. When possible, these reagents were discussed based on cost, yields of products and generality of use. For example, $TMSCF_3$ has a wide scope of application and provides good yields but is considerably more expensive then other $-CF_3$ delivery reagents. To appreciate the complications in their manipulations, the properties of the C-F bond and M-R^F bond were discussed. This allows the reader to understand the current paradigm and limitations for the applications of M-R^F complexes in synthetic organic chemistry. It establishes the acceptance for the use of metal-mediated routes and the push to discover catalyzed ones. For instance, 2011 saw a resurgence in research for the catalytic introduction of the $-CF_3$ group using copper. Lastly, to establish the worth of these complexes and the inspirations for the work of this *Thesis*, applications pertaining to the advances herein were introduced. These applications were divided into C-C bond formation and C-F bond activation methodologies.

As indicated, this *Thesis* builds on the body of knowledge of M-R^F complexes to establish new synthetic strategies for the synthesis of small fluorinated molecules. In chapters 2 and 5, we present the advantages offered by low-coordination numbers enabled by a bulky N-heterocyclic carbene ligand. In the first instance, the low-coordinate fluorometallacycle complex, C-F bond, and Ni-R^F bond activation strategies are explored. This work helps to further clarify the exciting

differences between hydrocarbon-based and fluorinated metallacycles and illustrates some of the potentially useful reactivity of the latter. The chemistry of the oxidation product is also explored, especially with respect to reductive elimination and insertion reactions. This work further highlights the disparities between the hydrocarbon analogues and shows the potential in developing a catalytic cycle for the synthesis of R^F-R^F compounds based on a $Ni^{II/IV}$ cycle. In the second instance, the use of a Ni^0 complex bearing a bulky-NHC was explored in a base-free Suzuki cross-coupling reaction. This strategy allowed for the facile oxidative addition of C_{Ar}-F bonds. Upon treatment with DMAP, the isolated dimers could be easily fragmented and when mixed with excess aryl boronic acid ester could effectively promote the coupling of Ar-F and neopB-Ph. In chapter 3, we investigated the synthesis of metal-hfip complexes using HFP to expand on their reactivity; Ag-, Ni- and Cu-hfip complexes were presented. This contribution opens the door for the eventual development of catalyzed transfer of the hfip fragment using inexpensive HFP gas. In chapters 4 and 5, we present the advantages of using a commercially available copper-hydride complex, in a comprehensive study of its reactions with fluoroalkenes. In a full ligand screen, we established a selective and consecutive hydrodefluorination reaction, with a dependence on ligand size and without the use of additives. A scope of various fluoroalkenes is established to demonstrate the robustness of our strategy, except for TFE, which instead produces a stable Cu-CF_2CF_2H complex. This is the first synthesis of a Cu-CF_2CF_2H complex, that allows for the use of easily and safely handled TFE Safe Supply®. This could provide a facile route for the study of tetrafluoroethyl-containing pharmaceuticals and agro-chemicals. Chapter 6 is a summary of this *Thesis* and provides a discussion on potential future work stemming from it.

Chapter 2

2. Published Contributions

A T-shaped Ni[κ^2-$(CF_2)_4$–] NHC complex: unusual C_{sp3}–F and M–C^F bond functionalization reactions

N. O. Andrella, A. J. Sicard, S. I. Gorelsky, I. Korobkov, and R. T. Baker *Chem. Sci* **2015**, *6*, 6392-6397.

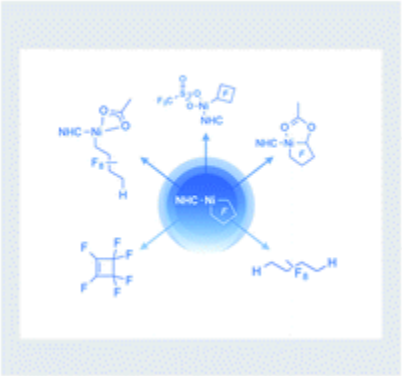

Andrella and Baker wrote the manuscript. Andrella performed most of the experiments, Sicard was responsible for the synthesis of starting material.

Gorelsky was responsible for Computational Studies

Korobkov was responsible for X-ray diffraction data collection and refinement.

2.1. Abstract

A T-shaped octafluoronickelacyclopentane–NHC complex is prepared and characterized. While the solid-state structure includes a weak isopropyl-CH_3 agostic interaction, the reactivity of this complex with Lewis- and Brønsted acids is clearly enhanced by its low coordination number. Reaction with Me_3SiOTf, for example, yielded a rare metal–heptafluorocyclobutyl

complex whereas carboxylic acids gave substitution at the α-carbon and/or Ni–C^F bond protonolysis to afford thermally robust 4H-octafluorobutyl Ni complexes.

2.2.Introduction

Fluorocarbons and their derivatives are valuable as refrigerants, agrochemicals, unique solvents/surfactants and fluoropharmaceuticals, with annual sales of the latter alone in the billions of dollars.[1,2,34, 311] As the demand for fluorinated chemicals has increased, so too have synthetic methods for introducing fluorine and fluorocarbon groups.[92, 147, 261, 281, 285, 312-316] Despite recent advances, transition metal-mediated/-catalyzed routes are rare in comparison to the well-developed organometallic chemistry of hydrocarbons.[317, 318] The challenge rests in the stability of metal–perfluoroalkyl (M–R^F) bonds, relative to metal–alkyl bonds.[94, 119, 150, 233] M–C^F bonds are typically inert to processes such as insertion/alkyl migration reactions, vital to metal-mediated catalytic cycles.[319] Moreover, C–F bonds are stronger than C–H bonds,[1, 2] posing another obstacle to metal-based approaches. We are investigating perfluoronickelacyclopentane complexes (PNCPs) as platforms for functionalized fluorocarbons with an initial focus on fundamental stoichiometric reactions. PNCPs have been synthesized previously by reaction of tetrafluoroethylene (TFE, CF_2=CF_2) with Ni^0 complexes. The displacement of P ligands by bidentate ligands has also been reported (Scheme 2.1).[167, 191, 192, 197, 200, 320]

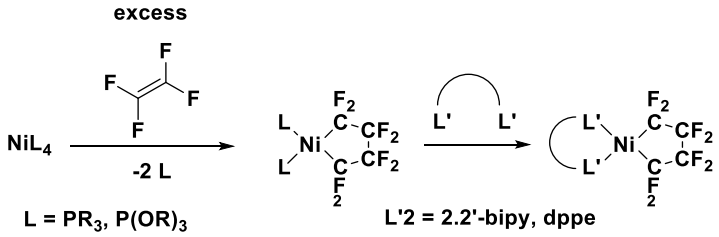

Scheme 2.1. Synthesis of perfluoronickelayclopentanes.

To date, reports concerning the reactivity of PNCPs are sparse: Burch and co-workers found that Lewis acidic BF_3 effects fluoride abstraction from Cα and phosphine migration to the activated carbon (Scheme 2.2a).[321] Extending this reaction to the unsymmetrical P^S chelate, we showed that treatment with excess isonitrile effected cleavage of the Ni–C^F bond (Scheme 2.2b).[203] With phosphite co-ligands, a remarkable hydrogenolysis reaction enables the selective catalytic hydrodimerization of TFE (Scheme 2.2c).[185, 187] As far as we know, this reaction is the only example of a perfluoro-metallacyclopentane participating in a catalytic cycle.[215]

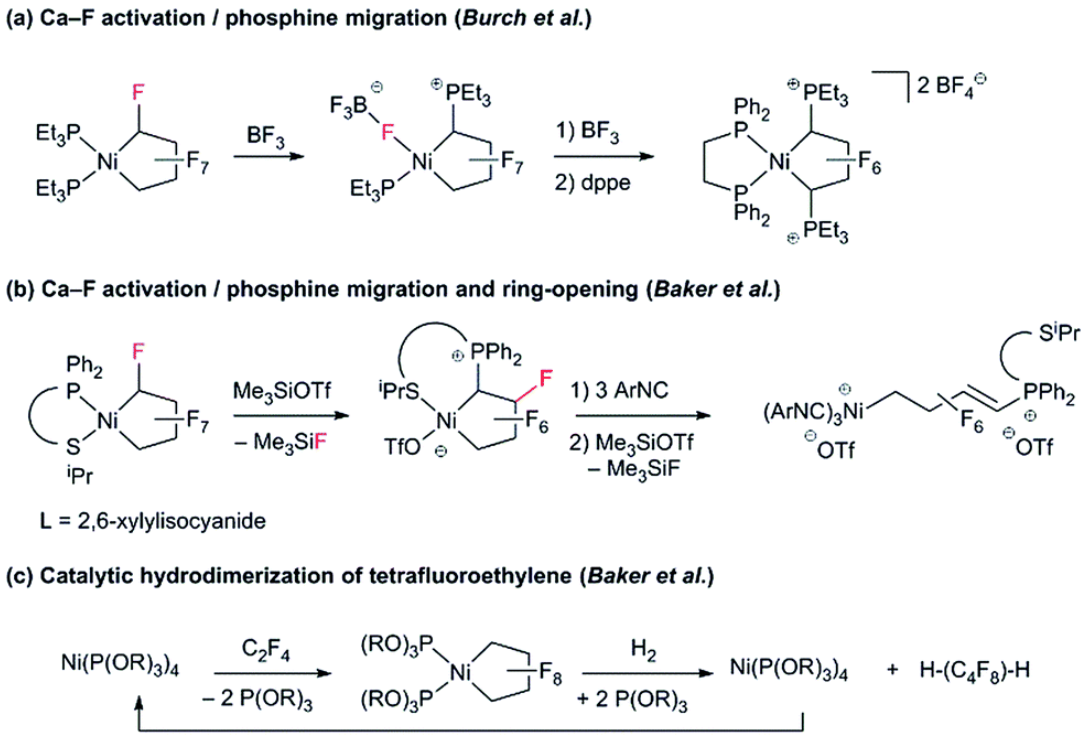

Scheme 2.2. Previously reported reactivty of perfluoronickelacyclopentanes.

Our approach to metallacycle functionalization hinges on the reactivity of metal-activated Cα–F bonds[322-328] wherein we replace a C–F bond by C–Nu vs. the current paradigm C–L (Nu = nucleophile, L = ligand). Using N-heterocyclic carbenes (NHCs),[329, 330] we aimed to

access low-coordinate PNCPs wherein the strong M–C_{NHC} bond may also prevent ligand migration to Cα. There is a considerable precedent for such an approach to low-coordinate metal complexes.[331] Hillhouse and coworkers prepared a two-coordinate nickel–imido complex bearing the exceptionally bulky IPr* ligand (analog of IPr with 2,6-bis(diphenyl-methyl)phenyl groups instead of 2,6-diisopropylphenyl).[332] Similarly, Miyazaki and coworkers synthesized a T-shaped three-coordinate nickel(I) chloride species [Ni(IPr)$_2$Cl] by treatment of two-coordinate [Ni(IPr)$_2$] with aryl chlorides.[333] Also, Hartwig et al. synthesized low-valent, three-coordinate palladium(II) norbornyl species [Pd(SIPr)(NHAr)(Nor)], which underwent facile C–N bond reductive elimination when heated.[334] In this report, we show that low-coordinate NHC Ni perfluorometallacycles undergo facile Csp^3–F and M–C^F bond cleavage as well as Cα-F functionalization. We also demonstrate the first migration of a fluoroalkyl to a reactive carbon center. This is significantly different from the reactivity previously observed for phosphine Ni perfluorometallacycle complexes. [321]

2.3 Results and discussion

Starting from bis(phosphite) PNCPs[203] (**2.1a** and **b**) we were able to cleanly synthesize coordinatively-saturated or -unsaturated nickel perfluorometallacycles. Thus, **2.1a** reacts smoothly with 1 equiv. of ItBu (ItBu = 1,3-di-tert-butylimidazol-2-ylidene) to afford the NHC/phosphite product **2.2** (Scheme 2.3, top; X-ray structural characterization presented in ESI†).[335] Significantly, the reaction between the larger SIPr ligand [SIPr = 1,3-bis(2,6-diisopropylphenyl)imidazolin-2-ylidene] and a nickel metallacycle with sterically-demanding co-ligands (**2.1b**) results in displacement of both phosphite ligands, yielding the pseudo-three-coordinate/14e$^-$Ni(II) metallacycle **2.3** (Scheme 2.3, bottom).

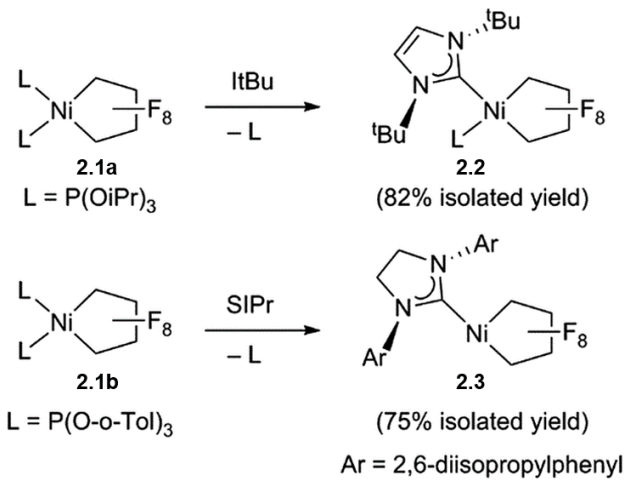

Scheme 2.3. Synthesis of NHC perfluoronickelacyclopentane complexes.

The molecular structure of complex **2.3**, as determined by single crystal X-ray diffraction, exhibits a T-shaped coordination about the Ni and features a weak agostic interaction with the isopropyl methyl group (Ni–C = 2.757(1) Å; compare Ni–C^F bond distance trans to the NHC (1.934(1) Å) with that trans to the agostic interaction (1.875(1) Å) (Figure 2.1a). The ^{19}F NMR spectrum of **2.3** in C_6D_6 is consistent with ideal C_{2v} symmetry at room temperature, with only two distinct singlet resonances at 101.9 (Fα) and 138.6 ppm (Fβ). While these resonances both broaden significantly at 213 K, it is apparent that the T-flip interconversion encounters only a small energy barrier.[336] To confirm this, we carried out DFT calculations (at the B3LYP/ TZVP level with and without the empirical dispersion correction of Grimme).[337] Intriguingly, the calculations reveal two spin singlet structures with a very small energy difference (DG298 K = 0.0–1.5 kcal mol^{-1}). The first computed structure coincides well with the observed solid-state structure of **2.3**; the 3-center bond order index between the Ni and the corresponding C–H bond of 0.05 is much less than 8/27 (0.3), the maximum possible value for a 3-center 2-electron bond. As a result, the Mayer valence index for Ni in structure 3 is only 3.09. The second structure (**2.3**) features a weak η^3 interaction between the aryl group of the NHC ligand at the 4th coordination

site of the Ni atom (Figure 2.1b). Mayer bond orders for the corresponding three Ni–C interactions are in the 0.02–0.05 range, with a total bond order of 0.09. This suggests a semi-bidentate binding mode for the class of NHC ligands possessing pendant aryl groups. From calculations with the dispersion correction, structure **2.3** has the same Gibbs free energy as **2.3**. Without the dispersion correction, structure **2.3** is actually 1.5 kcal mol^{-1} lower in energy than **2.3**. The 3-coordinate structure with trigonal coordination around Ni and symmetric binding of the C_4F_8 ligand is a transition state with a low energy ($\Delta G^{\ddagger}$ 298 K = 2.1 kcal mol^{-1} relative to **2.3**). Thus, it is clear that cleavage of the weak agostic and/or η^3 -aryl bond is facile and allows for rapid reorientation of the ligands around the Ni center. Attempts to obtain evidence for structure **2.3** by low temperature NMR were frustrated by dynamic processes associated with the T-flip and hindered rotations about the M–C and perhaps N–C bonds.

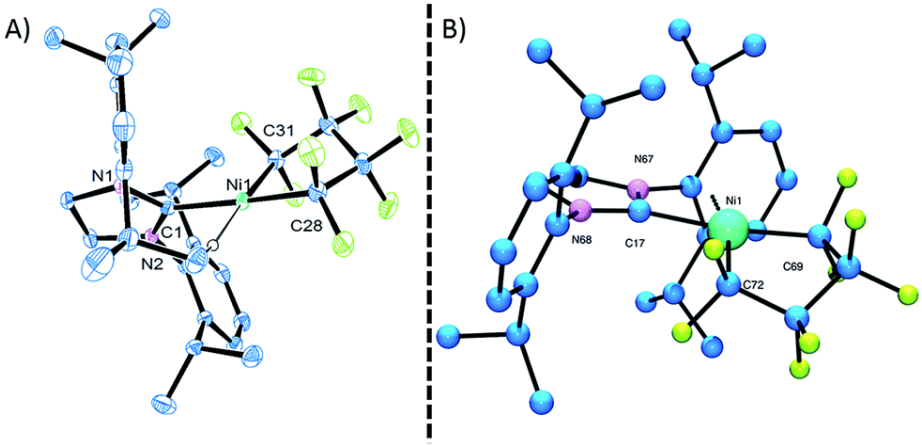

Figure 2.1. A) ORTEP representation of the molecular structure of **2.3**. Thermal-ellipsoid probabilities are set to 35% with hydrogen atoms omitted for clarity. The Ni-C(1) distance is 1.854(2) Å. (B) Optimized structure of low energy Ni-aryl isomer **2.3'**; Ni-C_{aryl} distance are = 2.818, 3.329, 3.379, 4.166, 4.204, 4.543 Å. The Ni-C(17) distance is 1.989 Å.

The HOMO of **2.3** (ε = 6.01 eV; Figure 2.2, left) is localized on the Ni (87%), primarily from a dz^2 orbital contribution (71%). Lower-lying orbitals display interactions between metal dxz, dyz orbitals and the δ-system of the aryl group.[338] The LUMO (ε = 1.96 eV; Figure 2.2, right) is

an anti-bonding combination of the metal dx^2-y^2 orbital (total Ni character of 45%) with the π-donor orbitals of the NHC and C_4F_8 ligands. Thus, the reactivity of the M–C bond is likely under orbital control and arises from an interaction with the HOMO of **2.3**. In contrast, C–F bond activation is likely a combination of orbital and charge control with a slant towards the latter as the hardness of the Lewis acid increases.[339]

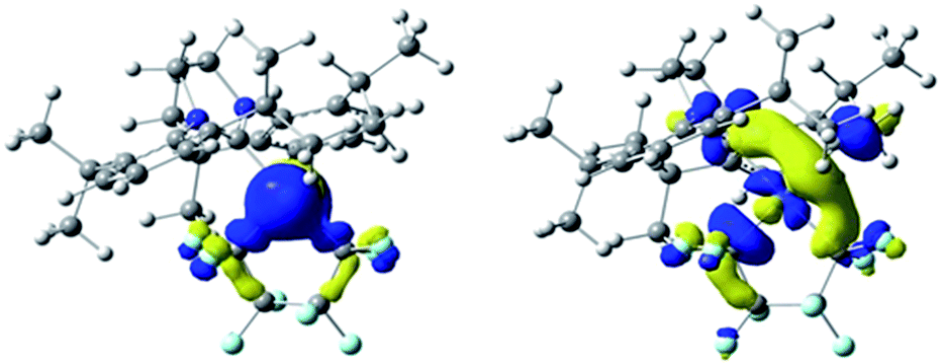

Figure 2.2. The HOMO (left) and LUMO (right) of 3. Isosurface values of 0.04 au are used.

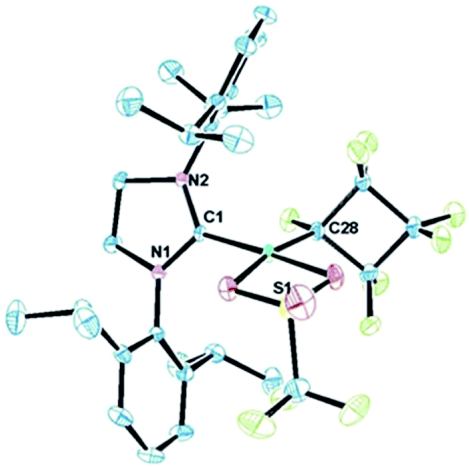

Figure 2.3. ORTEP representation of the molecular structure of **2.4a** with thermal ellipsoid probabilities set to 30% and hydrogen atoms omitted for clarity. The Ni-C(1) distance is 1.854(2) Å.

Initial studies on the C–F bond activation reactions of **2.3** are promising in the context of synthesizing functionalized fluorocarbons by metal-mediated approaches. Firstly, when **2.3** is treated with the Lewis acid TMSOTf (TMS = Me_3Si, OTf = SO_3CF_3), α-fluoride-abstraction,

accompanied by Ni–C^F bond cleavage and C^F–C^F bond formation, furnishes a rare perfluorocyclobutyl complex **2.4a** (Figure 2.3, 75% isolated yield).[340, 341] The driving force behind this transformation is likely related to the triflate leaving group ability and the formation of a strong C–C bond.[342] Importantly, the NHC remains bound to the nickel atom (i.e., does not migrate to Cα), potentially opening new pathways to functionalized fluorocarbon derivatives. Upon heating complex **2.4a** (80 °C in C_6D_6, 24 h), perfluorocyclobutene is produced, presumably via a β-fluoride elimination mechanism, although the metal-containing co-product(s) have not yet been identified.[307, 343] Interestingly, a single OTf containing product can be discerned by ^{19}F NMR (93.37 ppm) but a Ni–F signal could not be located. The ^{1}H NMR shows that the NHC remains intact. Upon addition of PPh_3 to the reaction mixture, PPh_3F_2 was identified as a major product, suggesting the formation of a Ni– F thermolysis co-product.

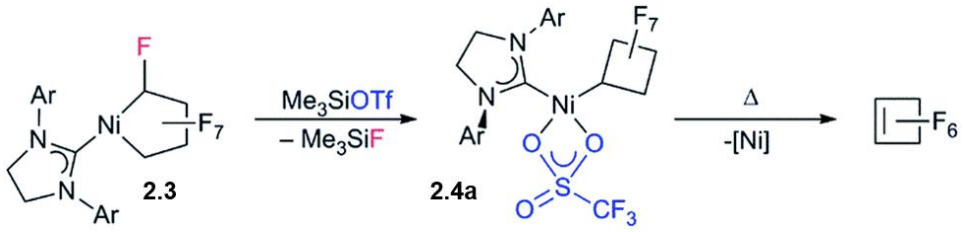

Scheme 2.4. Synthesis and decomposition of **2.4a**.

The distorted square planar structure of complex **2.4a** (Figure 2.3) features a bidentate triflate ligand which can also likely access the κ^1 -mode in solution as evidenced by the simple ^{19}F NMR spectrum[344] and observed tendency to eliminate. The perfluorocyclobutyl ring is nearly planar, the Ni–C bond is short [1.890(2) Å] due to the weak σ-trans influence ligand, and the Cα–F bond distance (1.384(3) Å) is considerably longer than the other C–F bonds (average of 1.33 Å). The reactivity enhancement offered by low-coordinate **2.3** is evidenced by the sluggish reaction of 4-coordinate complex **2.2** with TMSOTf to give a mixture of unidentified

products. Indeed, monitoring the reaction of **2.3** and TMSOTf at 25 °C allowed for the identification of a Ni–C_4F_7 intermediate **2.5a** apparently containing a Cα–OTf linkage (triflate CF_3 ^{19}F NMR resonance is coupled to Cα–F: $^5J_{FF}$ = 11 Hz). This is in contrast to previous suggestions of a metal fluorocarbene intermediate (Scheme 2.5).[321]

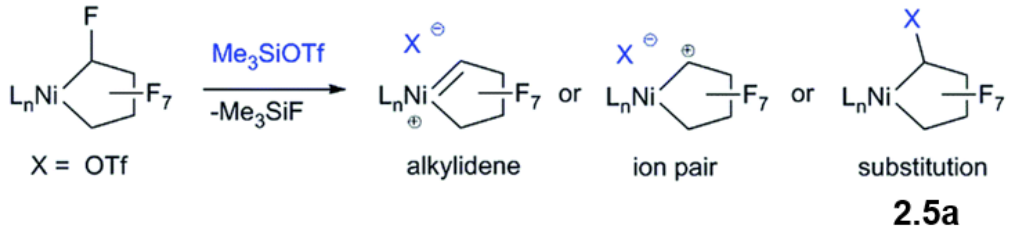

Scheme 2.5. Possible intermediates in the reaction of **2.3** with TMSOTf.

Having established that the NHC ligand remains bound to the metal upon fluoride-abstraction from **2.3**, we shifted our focus to C–F bond functionalization using *Brønsted* acids. Treatment of **2.3** with trifluoroacetic acid [TFA; pKa = 3.4 (DMSO)][345] gives HF and the more stable (vs. **2.5a**) trifluoroacetate-substituted metallacycle **2.5b** that could be characterized spectroscopically at room temperature (Scheme 2.6). Nonetheless, accompanying formation of perfluorocyclobutene, presumably formed via an analogous structure to **2.4a**, led us to move to weaker Brønsted acids. Remarkably, the reaction of **2.3** with acetic acid [pKa = 12 (DMSO)][346] (Scheme 2.6, bottom) yielded the stable ester metallacycle **2.5c** (30% isolated yield) as well as the Ni–C^F bond cleavage product **2.6a** in a 1 : 1 ratio. At a similar acidity [pKa = 11 (DMSO)][347] but increased steric bulk, 2,4,6-trimethyl-benzoic acid gave a 10 : 1 mixture favouring the ring cleavage product, **2.6b**.

The molecular structure of **2.5c** features similar Ni–C bond distances (1.895(7) vs. 1.896(6) Å) and a distorted square planar coordination (Figure 2.4). The functionalized heptafluoro-metallacyclopentane ring is puckered with the smallest C–C bond distance being

C(32)α–C(39)β [1.49(1) Å]. The carbonyl oxygen completes the nickel coordination sphere (Ni–O1 =1.969(4) Å).

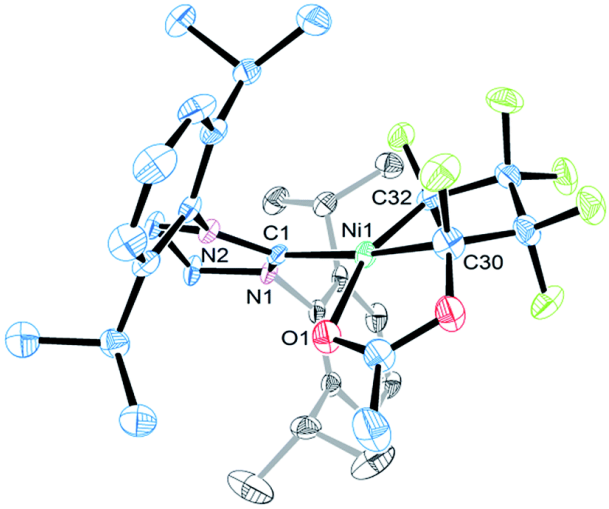

Figure 2.4. ORTEP representation of the molecular structure of **2.5c** with thermal ellipsoids probabilities set to 30% and hydrogen atoms omitted for clarity. The Ni-C(1) distance is 1.928(2) Å

The ^{19}F NMR spectra of **2.5a–d** are very similar and support our original proposal for the low temperature intermediate **2.5a** in the reaction of **2.3** with TMSOTf. The Cα–F ^{19}F chemical shifts of the functionalized carbon, (117.2 and 119.2 ppm) can be compared with those of the phosphonium analogs (115.6 and 117.8 ppm) shown in Scheme 2.2. As expected, the ring-opened products **2.6a** and **b** display nearly identical ^{19}F NMR chemical shift patterns with the Cγ– and Cδ–F resonances distinguished by F–H coupling of 6 and 52 Hz, respectively. These unique complexes have been identified as their potassium cation adducts using ESI-MS (747.2 g mol^{-1} and 851.4 g mol^{-1} respectively) and are surprisingly inert to thermolysis at 80 °C in C_6D_6 for 20 h. Considering the importance of esters as synthons in organic transformations[348] this C–O bond-forming reaction **2.3 / 2.5** is very appealing from the standpoint of synthesizing functionalized fluorocarbons. As such, understanding competing pathways for M–C vs. C–F bond cleavage would be valuable.[349] Viable reaction pathways can be considered as

proceeding via either 5- or 6-membered transition states (Scheme 2.7). The selective HF elimination observed for TFA is eroded as Ni–C bond protonolysis (orbital control) competes using acids of intermediate acidity (e.g. pKa 11).[350] With the bulkier trimethylbenzoic acid, kinetic acidity factors in the tighter 5-membered ring transition state could severely limit HF elimination.[199]

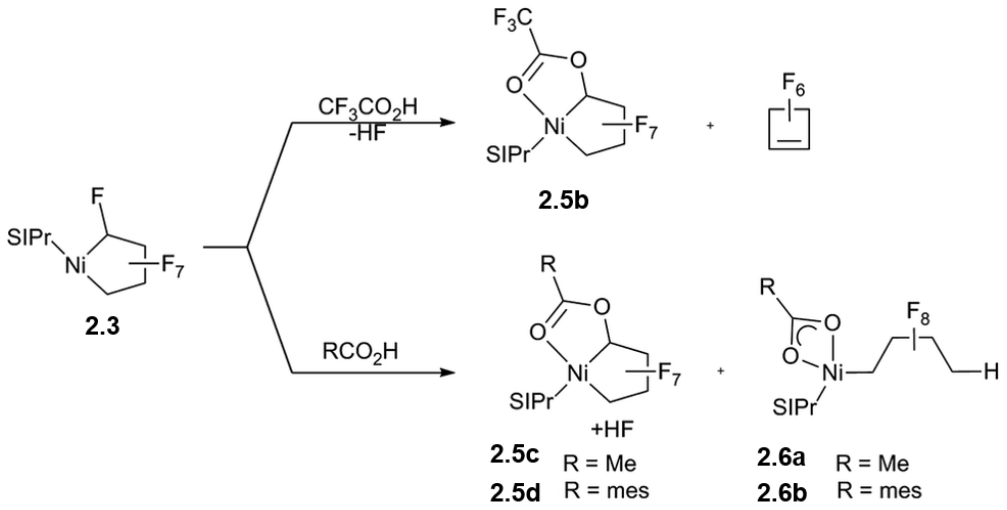

Scheme 2.6. The reaction of **2.3** with trifluoroacetic, acetic and 2,4,6-trimethylbenzoic acids.

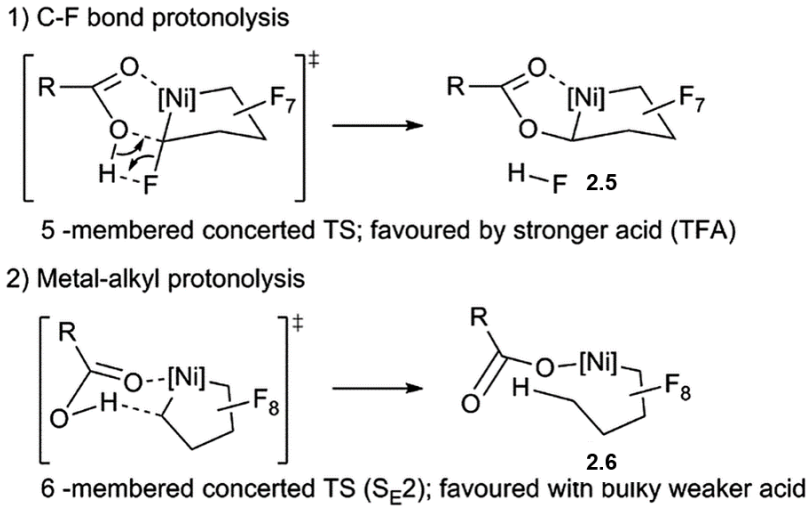

Scheme 2.7. Proposed reaction pathways for C-F activation *vs.* Ni-R^F protonolysis.

2.3. Continued Work

2.3.1. Oxidation Chemistry

Previous work in the Baker group showed that (N-N)Ni(C_4F_8) complexes could be oxidized with diacetoxy iodobenzene [PhI($OAc)_2$] to give stable 19e$^-$ pseudo-octahedral complexes, (N-N)Ni(C_4F_8)(κ^2-O_2CMe) (N-N = 2,2' bipyridine, 1,10-phenanthroline.[351] Interestingly, these complexes also showed reversible oxidation to the 18e$^-$ Ni(IV) complex, although attempts to cleanly generate these complexes were unsuccessful. The preference of these high-valent Ni complexes for 6-coordination was further confirmed by reaction of the acetate complexes with Me_3SiCl which afforded the 19e$^-$ Cl-bridged dimer. As all attempts to isolate high-valent complexes with phosphine co-ligands were also unsuccessful, we were keen to investigate the oxidation of **2.3**.

Upoon exposure of **2.3** to 1 equiv. of [PhI($OAc)_2$] in dichloromethane, an instantaneous colour change was observed, signalling the formation of a five-coordinate, 17e$^-$ Ni^{III} metallacycle (SIPr)Ni(C_4F_8)(κ^2-O_2CMe) **2.7**.

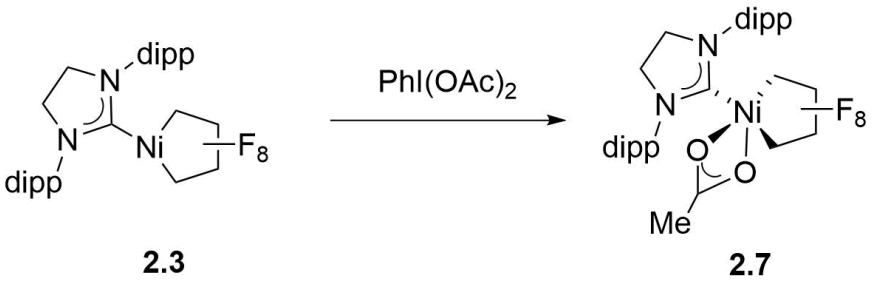

2.3 **2.7**

Scheme 2.8. Synthesis of Ni^{III} complex, **2.7**

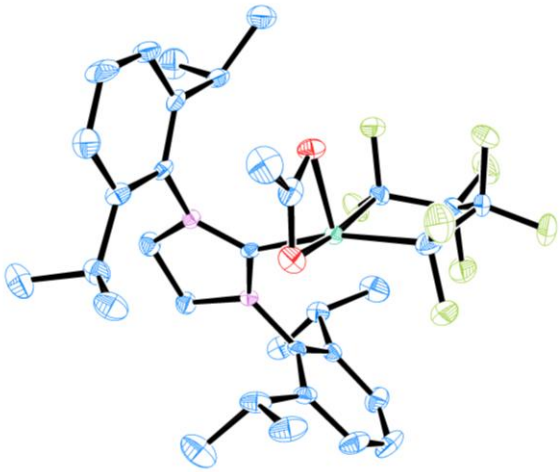

Figure 2.5. ORTEP representation of the molecular structure of **2.7** with thermal ellipsoid probabilities set to 30% and hydrogen atoms omitted for clarity. The Ni-C(1) distance is 1.928(2) Å.

The molecular structure of **2.7**, as determined by single crystal X-ray diffraction, exhibits a distorted square pyramidal coordination about the Ni. The Ni-C_{NHC} and Ni-C_F (trans to NHC) lie roughly 7 ° below the plane and the Ni-O_{axial} bond is roughly 23 ° off axis. Interestingly, the change in oxidation state does not bring about a significant change in the Ni-C^F bond lengths and are like previously reported complexes. The Ni-C bond length most affected by this change in oxidation state is the Ni-C_{NHC} bond going from 1.941 Å (Ni^{II}) to 1.987 Å (Ni^{III}). Similarly, the stability of **2.7** can also be attributed to the bulk of SIPr as it shields the orbital (dz^2) in which the unpaired electron lies, as supported by DFT calculations (See SI). Remarkably, the complex is sufficiently stable that it does not decompose upon contact with air. To be exact, the ^{1}H NMR and ^{19}F NMR do not vary when exposed to air. As well, the IR spectra upon immediate exposure to air and after 1 day of exposure, in the solid state, show no new bands. Importantly, an IR was acquired in the presence of hexanes, which shows bands in line with those of complex **2.7**. However, when a drop of isopropanol is added, immediate evolution of gas was observed, and the IR no longer demonstrates the characteristics bands of **2.7**. (See Figure B1-3)

To better support, the Ni^{III} identity of complex **2.7**, EPR and NMR data were collected. Room temperature EPR revealed 2 overlapping singlet signals (306.3 mT (0.5 mT broad) and 308.8 mT). This has been corroborated by EPR simulation. Although, this distinctly indicates a single unpaired electron on nickel, as supported by DFT; it raises concerns over the identity of the species in solution. The ^{19}F NMR shows two very broad features centered at -176 and -195 ppm in acetone-d_6. This is consistent with the paramagnetic nature of **2.7**. Although the ^{1}H NMR suffers from similar broadening, characteristic SIPr signals are identifiable, allowing for characterization of the ligand.

Interestingly, complex **2.7** showed a chemically accessible and reversible oxidation to, presumably, a Ni^{IV} complex. As such, the chemical oxidation to access this species was attempted. As expected, the reaction of **2.7** with XeF_2, leads to an immediate colour change. The so formed product was unstable at room temperature and only lasted one hour. When the reaction is left to sit, the ^{19}F NMR signals of the Ni^{IV} product (**2.8'**) have vanished and are replaced by a single resonance due to perfluorocyclobutane. This represents a rare example of C-C reductive elimination from a bis-fluoroalkyl nickel complex generating an R^F-R^F bond.

2.4. Conclusions

In summary, we have prepared the first NHC–perfluorometallacyclopentane complexes and exploited the bulky SIPr ligand to stabilize a pseudo-three-coordinate nickelacycle, **2.3**. Importantly, **2.3** undergoes Cα–F abstraction reactions without migration of the NHC ligand. Instead, we see an unprecedented migration of the fluoroalkyl to the reactive carbon center, giving rise to the novel perfluorocyclobutyl complex via Ni–C^F bond cleavage. More importantly, the low-coordinate nature of **2.3** allows for ring functionalization. Strong acids favor selective Cα functionalization, but the resulting products are unstable with respect to competion with

metallacycle ring contraction and elimination of perfluorocyclobutene. With less acidic reagents stable ring-functionalized products are formed but a competing Ni–C^F bond cleavage pathway comes into play and dominates for bulkier carboxylic acids. These are the first examples of selective functionalization of a PNCP and synthesis of thermally stable Ni–C_4F_8H complexes. These results are encouraging in the context of developing metallacycle-based routes to functionalized fluorocarbons. Ongoing work is focused on (a) expanding the scope of ring functionalization substrates suitable for reactions with **2.3** and (b) reductive (see Scheme 2, above) and oxidative approaches for removing the functionalized fluorocarbon fragments from the metal. Preliminary results of the hydrogenolysis of compound **2.3** indicate enhanced reactivity towards H_2 (i.e., at 7 psig and 25 C) vs. reported 4-coordinate phosphite variants. However, the loss of selectivity[352] is observed with the synthesis of two distinct products. Full details of these results will be published in due time.

2.5.Experimental Section

2.5.1. General Procedures.

Experiments were conducted under nitrogen, using Schlenk techniques or an MBraun glove box. All solvents were deoxygenated by purging with nitrogen. Toluene, hexanes, diethyl ether (DEE) and tetrahydrofuran (THF) were dried on columns of activated alumina using a J. C. Meyer (formerly Glass Contour®) solvent purification system. Benzene-d6 (C_6D_6) was dried by stirring over activated alumina (ca. 10 wt. %) overnight, followed by filtration. Acetonitrile-d_3 (CD_3CN) was dried by refluxing over calcium hydride under nitrogen. After distillation, CD_3CN was further dried by stirring over activated alumina (ca. 5 wt. %) overnight, followed by filtration. All solvents were stored over activated (heated at ca. 250 °C for >10 h under vacuum) 4 Å molecular sieves. Glassware was oven-dried at 120 °C for >2 h. The following chemicals were

obtained commercially, as indicated: trimethylsilyl trifluoromethanesulfonate (Me_3SiOTf, Aldrich, 99%), bis(1,5- cyclooctadiene)nickel (0) ($Ni(cod)_2$, Strem, 98+%), triisopropyl phosphite ($P(OiPr)_3$, Aldrich, 95%), tri-ortho-tolyl phosphite ($P(O\text{-}o\text{-}tolyl)_3$), Alfa Aesar, 97%), 1,3-bis(2,6-diisopropylphenyl)imidazolidin-2-ylidene (SIPr, SigmaAldrich) and 1,3-di-tert-butylimidazol-2-ylidene (ItBu, Sigma-Aldrich). Tetrafluoroethylene (TFE) was purchased from ABCR (99%) or made by pyrolysis of polytetrafluoroethylene (Scientific Polymer Products, powdered) under vacuum, using a slightly modified literature procedure [10-20 mTorr, 650 °C, 30 g scale, product stabilized with R(+)-limonene (Aldrich, 97%), giving TFE of ca. 97% purity]. Compound $Ni[P(OiPr)_3]_2(C_4F_8)$ was made by oxidative addition of tetrafluoroethylene to $Ni[P(OiPr)_3]_4$ using slightly modified literature procedures. $Ni[P(OiPr)_3]_4$ complex was prepared from $Ni(cod)_2$ following reported methods. Metallacycle $Ni(C_4F_8)[P(O\text{-}o\text{-}tolyl)_3]_2$ was prepared by addition of TFE to $Ni[P(O\text{-}o\text{-}tolyl)_3]_3$ using slightly modified literature procedures. $Ni[P(OiPr)_3]_4$ complex was prepared from $Ni(cod)_2$ following reported methods. ^1H, ^{19}F, $^{31}P\{^1H\}$, and $^{13}C\{^1H\}$ NMR spectra were recorded on a 300 MHz Bruker Avance instrument at room-temperature (21-23 °C) unless stated otherwise. ^1H NMR spectra were referenced to residual proton peaks associated with the deuterated solvents (C_6D_6: 7.16 ppm; CD_3CN: 1.94 ppm). ^{19}F NMR spectra were referenced to internal 1,3-bis(trifluoromethyl)benzene (BTB) [unless stated otherwise] (Aldrich, 99%, deoxygenated by purging with nitrogen, stored over activated 4 Å molecular sieves), set to –63.5 ppm. $^{31}P\{^1H\}$ NMR data were referenced to external H_3PO_4 (85 % aqueous solution), set to 0.0 ppm. Electrospray ionization mass spectral data were collected using an Applied Biosystem API2000 triple quadrupole mass spectrometer. UV-vis spectra were recorded on a Cary 100 instrument, using sealable quartz cuvettes (1.0 cm pathlength). Elemental analyses were performed by Laboratoire d'analyse élémentaire,

Université de Montréal. (Montreal, Quebec, Canada). Note that the NMR spectra (^{1}H, ^{19}F, $^{19}F\{^{1}H\}$, and $^{31}P\{^{1}H\}$ for the title compounds are displayed at the end of the Supporting Information (http://www.rsc.org/suppdata/c5/sc/c5sc01886b/c5sc01886b1.pdf).

2.5.2. Computational Methods

Density Functional Theory (DFT) calculations were performed for each structure using the Gaussian 09 package. Geometry optimization at the B3LYP/TZVP level of theory (with and without the empirical dispersion correction GD3 of Grimme) was performed using the molecular structure of **2.3** from the X-ray diffraction experiment as a starting point. Harmonic frequency calculations were used to characterize the stationary points obtained during the geometry optimization. Tight SCF convergence was used in each calculation. Mulliken population analysis (MPA)-compositions of molecular orbitals, and 2- and 3-center Mayer bond orders were calculated using the AOMix package (www.sg-chem.net). Optimized structure coordinates are presented in SI.

2.5.3. Experimental.

Synthesis of Ni[κ^2-$(CF_2)_4$-](ItBu)[$P(OiPr)_3$] (2.2). Yellow complex Ni[κ^2-$(CF_2)_4$-][$P(OiPr)_3]_2$ (**2.1a**) (0.100 g, 0.15 mmol) was placed in a 15 mL scintillation vial and dissolved in ~7 mL of toluene. Colorless [ItBu] (29 mg, 0.16 mmol) was then added to the mixture and left to sit at 25 °C for ~24 hours. Large yellow block crystals suitable for X-ray analysis formed. They were filtered off (30 mL medium pore fritted funnel), washed with pre-cooled hexanes (4 °C, 3 x 3 mL), and dried in vacuo to yield 85 mg of 2 (0.13 mmol, 89 % based on Ni[κ^2-$(CF_2)_4$-][$P(OiPr)_3]_2$). The isolated material was stored at room temperature under nitrogen. UV-vis (1.0 mM in THF): λmax(ε) = 322(341). ^{1}H NMR (300 MHz, CD_3CN) δ 1.19 (d, J ≈ 6 Hz, 18H, MeiPr) 1.94 (s, 18H, MetBu), 4.65 (sept, m, J ≈ 6 Hz, 3H, iPr H) 7.34 (s, 2H, CHIm). ^{19}F NMR

(282 MHz, CD_3CN) δ -100.50 (d 'quint', $^3J_{FP}$ = 31, $^3J_{FF} \approx {}^4J_{FF}$ = 6 Hz, 2Fα), -102.93 (d 'quint', $^3J_{FP}$ = 33, $^3J_{FF} \approx {}^4J_{FF}$ = 4 Hz, 2Fα), -137.03, -138.54 (mult, 2Fβ). $^{31}P\{1H\}$ NMR (121 MHz, CD_3CN) 115.8 ppm ('quint' 'tr', $^3J_{PF} \approx 32$, $^4J_{PF} \approx 7$ Hz). Anal. Calc. for $C_{24}H_{41}F_8N_2NiO_3P$: C, 44.54, H, 6.39, N, 4.33. Found: C, 44.54, H, 6.53, N, 4.28. See Figures S7-9 for ^1H, ^{19}F, $^{31}P\{^1H\}$ NMR spectra.

Synthesis of Ni[κ^2-(CF$_2$)$_4$-](SIPr) (2.3). Yellow complex Ni[κ^2-(CF$_2$)$_4$-][P((O-*o*-tol)]$_3$]$_2$ (**2.1b**) (1.00 g, 1.04 mmol) was placed in a 20 mL scintillation vial and dissolved in ~ 10 mL of benzene. Colorless [SIPr] (446 mg, 1.14 mmol) was then added to the stirred mixture and the mixture heated at 35 °C for ~24 hours. The resulting deep red solution was concentrated in vacuo to a thick paste with some red precipitate. Hexanes (15 mL) were then added to precipitate the product which was subsequently filtered (30 mL medium pore fritted funnel), washed with pre-cooled hexanes (4 °C, 3 x 5 mL), and dried in vacuo, affording **2.3** as a light red powder. Yield: 506 mg (0.78 mmol, 75 % based on Ni[κ^2-(CF$_2$)$_4$-][P(O-o-tol)$_3$]$_2$. The isolated material was stored at room temperature under nitrogen. UV-vis (1.5 mM in benzene): λmax(ε) = 486(461). ^1H NMR (300 MHz, C_6D_6) δ 1.09 (d, J ≈ 6 Hz, 12H, 4 Me), 1.68 (d, J ≈ 6 Hz, 12H, 4 Me), 3.04 (sept, J ≈ 6 Hz, 4H, 4 iPr H), 3.13 (s, 4H, 2 CH2Im), 7.00-7.30 (mult, 6H, 6 Ar-H). $^{13}C\{^1H\}$ NMR (75 MHz, C_6D_6) δ 24.78, 24.96, 29.40, 53.50, 125.63, 127-129, 129.57, 131.26, 147.67. ^{19}F NMR (282 MHz, C_6D_6, 25 °C) δ -101.90 (s, 4Fα), -138.63 (s, 4Fβ). ^{19}F NMR (282 MHz, CD_2Cl_2, -50 °C) δ -99.32 (s, 2F'α), -103.07 (br s, 4Fα), -119.17 (s, 2F'α), -138.37 (s, 2F'β), -139.64 (br s, 4Fβ), -141.21 (s, 2F'β). Anal. Calc. for $C_{31}H_{38}F_8N_2Ni$: C, 57.34, H, 5.90, N, 4.31. Found: C, 56.22, H, 6.18, N, 4.17 (These values reflect those expected for the water adduct **2.3•H$_2$O** Anal. Calc. for $C_{31}H_{40}F_8N_2NiO$: C, 55.79, H, 6.04, N, 4.20. See Figure S34, Table S11-12) See Figures S10-12 for the ^1H, $^{13}C\{^1H\}$, and ^{19}F NMR spectra.

Synthesis of Ni[κ^1-(cyclo-C$_4$F$_7$)](SIPr)(OTf) (2.4a). Red complex Ni[κ^2-(CF$_2$)$_4$-](SIPr) (**2.3**) (0.100 g, 0.15 mmol) was placed in a 15 mL scintillation vial and dissolved in ~ 7 mL of benzene. Me_3SiOTf (42 μL, 0.23 mmol) was added to the stirred mixture and left to stir at room temperature for ~24 hours. (N.B. Product **2.4a** is unstable under these reaction conditions for prolonged periods of time, reaction times longer than 24 hours will lead to the formation of perfluorocyclobutene in the reaction medium). The deep pink solution was concentrated in vacuo and the resulting pink powder **2.4a** was washed with pre-cooled hexanes (4 °C, 3 x 5 mL) and dried in vacuo. Yield: 0.108 g, 0.14 mmol, 90 % based on Ni[κ2-(CF2)4-](SIPr). The isolated material was stored at room temperature under nitrogen. UV-vis (1.0 mM in benzene): λmax(ε) = 503(218), 332(312). ^{1}H NMR (300 MHz, C_6D_6) δ 1.04 (d, J = 7 Hz, 12H, 4 Me), 1.60 (br d, J ≈ 5 Hz, 6H, 2 Me), 1.71 (br, 6H, 2 Me) 3.2 (br ov mult, 6H, 4 iPr H + 2 CH2Im), 3.4 (br mult, 2H, CH2Im), 6.5-7.8 (mult, 6H, 6 Ar-H). ^{13}C{^{1}H} NMR (75 MHz, C_6D_6) δ 24.78, 24.96, 28.53, 28.87, 53.37, 124.3-125, 130.02, 133.96, 146.89.^{19}F NMR (282 MHz, C_6D_6) δ -77.60 (s, CF_3), -110.01 (br d, $^2J_{FF}$ ≈ 228 Hz, 2Fβ), -123.75 (d, $^2J_{FF}$ = 229 Hz, 1Fβ), -123.79 (d, $^2J_{FF}$ = 229 Hz, 1Fβ) -129.80 (d mult, $^2J_{FF}$ = 222 Hz, Fγ), -131.59 (d, $^2J_{FF}$ = 222 Hz, Fγ), -197.74 (br s, Fα). ^{19}F NMR (282 MHz, CD_2Cl_2, -50 °C) δ -78.93 (s, CF_3), -109.27 (d mult, $^2J_{FF}$ ≈ 227 Hz, 1Fβ), -112.22 (d mult, $^2J_{FF}$ ≈ 231 Hz, 1Fβ), -124.18 (d, $^2J_{FF}$ = 227 Hz, 1Fβ), -124.26 (d, $^2J_{FF}$ = 231 Hz, 1Fβ) -129.80 (d mult, $^2J_{FF}$ = 222 Hz, Fγ), -131.59 (d, $^2J_{FF}$ = 222 Hz, Fγ), -197.74 (br s, Fα). Anal. Calc. for $C_{32}H_{38}F_{10}N_2NiO_3S$: C, 49.31, H, 4.91, N, 3.59, S, 4.11. (These values reflect those expected for the water adduct Anal. Calc. for $C_{32}H_{40}F_{10}N_2NiO_4S$: C, 48.20, H, 5.06, N, 3.51, S, 4.02.) Found: C, 47.53, H, 5.05, N, 2.76, S, 4.21. See Figures S13-15 for the ^{1}H, ^{13}C{ ^{1}H} and ^{19}F NMR spectra.

^{19}F NMR spectrum of intermediate leading to 2.4a. Ni[κ^3-(CF$_2$)$_3$CF(OTf)-](SIPr) (2.5a): ^{19}F NMR (282 MHz, Tol-d8, -35 °C) δ -73.27(d, $^5J_{FF}$ = 11 Hz, CF$_3$[OTf]), -83.98 (d mult, $^2J_{FF}$ = 225 Hz, Fα), -99.73 (d mult, $^2J_{FF}$ = 225 Hz, Fα), -106.29 (br mult, Fα), -127.11 (d mult, $^2J^{FF}$ = 246 Hz, Fβ), -129.23 (d mult, $^2J_{FF}$ = 246, Fβ), -137.07 (d mult, $^2J_{FF}$ = 246 Hz, Fβ), -144.71 (d mult, $^2J_{FF}$ = 246, Fβ).

Synthesis of Ni[κ^3-(CF$_2$)$_3$CF(O$_2$CCF$_3$)-](SIPr) (2.5b). Red complex Ni[κ^2-(CF$_2$)$_4$-](SIPr) (**2.3**) (50 mg, 0.08 mmol) was placed in a 20 mL scintillation vial and dissolved in ~ 7 mL of benzene. Trifluoroacetic acid (7 μL, 0.085 mmol) was added to the stirred mixture (reaction should not be attempted in toluene) and left to stir at 25 °C for 10 minutes. The fluorescent yellow solution was concentrated in vacuo until a thick paste with some light yellow precipitate was remaining. Cold hexanes (4 °C, 3 x 5 mL) were added and decanted off to wash. The resulting product was dried in vacuo, affording **2.5b** as a light yellow powder. Yield: 47 mg (0.06 mmol, 82 % based on Ni[κ^2- (CF$_2$)$_4$-](SIPr). The isolated material was stored at room temperature under nitrogen. UV-vis (1.5 mM in benzene): λmax(ε) = 486(461). ^{1}H NMR (300 MHz, C$_6$D$_6$) δ 1.05 (ov d, J ≈ 6 Hz, 12H, 4 Me), 1.36 (d, J ≈ 6 Hz, 6H, 2 Me), 1.47 (br, 6H, 2 Me), 3.19 (br, ov mult, 3H, 3 iPr H), 3.37 (br, ov mult, 5H, i-Pr H + 2 CH$_2$Im), 6.80-7.06 (mult, 6H, 6 Ar-H). ^{13}C{ ^{1}H} NMR (75 MHz, C$_6$D$_6$) δ 22.66, 22.82, 26.17, 26.28, 28.41, 53.89, 124.20, 124.39, 127-129, 129.33, 146.57. ^{19}F NMR (282 MHz, C$_6$D$_6$, 25 °C) δ -72.97 (s, CF$_3$), -90.06 (d mult, $^3J_{FF}$ = 245 Hz, 1Fα), -99.09 (d mult, $^3J_{FF}$ = 245 Hz, 1Fα), -116.17 (dd, $^3J_{FF}$ = 22, 11 Hz, 1Fα), -126.14 (d mult, $^3J_{FF}$ = 248 Hz, 1F, 1 CβF$_2$), -130.76 (d d mult, $^3J_{FF}$ = 248, 22 Hz, 1Fβ), -134.17 (d mult, $^3J_{FF}$ = 248 Hz, 1Fβ), -142.71 (d d mult, $^3J_{FF}$ = 248, 11 Hz, 1Fβ). Anal. Calc. for C$_{33}$H$_{38}$F$_{10}$N$_2$NiO$_2$: C, 53.32, H, 5.15, N, 3.77. Found: C, 53.15, H, 6.01, N, 3.87. See Figures S16-18 for the ^{1}H, ^{13}C{ ^{1}H} and ^{19}F NMR spectra

Synthesis of Ni[κ^3-(CF$_2$)$_3$CF(O$_2$CCH$_3$)-](SIPr) (2.5c). Red complex Ni[κ^2-(CF$_2$)$_4$-](SIPr) (**2.3**) (50 mg, 0.08 mmol) was placed in a 20 mL scintillation vial and dissolved in ~ 7 mL of toluene. Acetic acid (5 μL, 0.085 mmol) was added to the stirred mixture and left to stir at 25 °C for 24 hours. The deep yellow solution was concentrated in vacuo (~ 1 mL). 5 mL of hexanes was added and the product was crystallized (-20 °C). The supernatant was decanted and the yellow crystals of **2.5c** were washed with hexanes (2 x 5 mL) and dried in vacuo. Yield: 20 mg, 0.063 mmol, 38 % based on Ni[κ^2-(CF$_2$)$_4$-](SIPr). The isolated material was stored at room temperature under nitrogen. UV-vis (1.0 mM in benzene): λmax(ε) = 632 (361); 103 (485). ^{1}H NMR (300 MHz, C$_6$D$_6$) δ 1.05 (ov d, J ≈ 6 Hz, 12H, 4 Me), 1.36 (d, J ≈ 6 Hz, 6H, 2 Me), 1.47 (br, 6H, 2 Me), 3.19 (br, 4H, 4 iPr H), 3.37 (br, 4H, 2 CH2Im), 6.80-7.06 (m, 6H, 6 Ar-H). ^{13}C{^{1}H} NMR (75 MHz, C$_6$D$_6$) δ 22.66, 22.82, 26.17, 26.28, 28.41, 53.89, 124.20, 124.39, 27-129, 129.33, 146.57. ^{19}F NMR (282 MHz, C$_6$D$_6$, 25 °C) δ -91.23(d mult, $^2J_{FF}$ = 253 Hz, Fα) , -101.86 (d mult, $^2J_{FF}$ = 253 Hz, Fα), -119.78 (d d, $^3J_{FF}$ = 17, 15 Hz, Fα), -126.35 (d mult, $^2J_{FF}$ = 247 Hz, Fβ), -130.90 (d d mult, $^2J_{FF}$ = 247, $^3J_{FF}$ = 15 Hz, Fβ), -135.10 (d mult, $^2J_{FF}$ = 248 Hz, Fβ), -143.33 (d d, $^2J_{FF}$ = 248, $^3J_{FF}$ = 17 Hz, Fβ), Anal. Calc. for C$_{34}$H$_{43}$F$_7$N$_2$NiO$_2$: C, 57.49, H, 6.16, N, 3.98. Found: C, 57.05, H, 6.21, N, 4.11. See Figures S19-21 for the ^{1}H, ^{13}C{ ^{1}H} and ^{19}F NMR spectra.

Synthesis of Ni[κ^1-(C$_4$F$_8$H)](SIPr)(OAc) (2.6a). Red complex Ni[κ^2-(CF$_2$)$_4$-](SIPr) (**2.3**) (50 mg, 0.08 mmol) was placed in a 20 mL scintillation vial and dissolved in ~ 7 mL of toluene. Acetic acid (5 μL, 0.085 mmol) was added to the mixture and left to stir at 25 °C for 24 hours. The deep yellow solution was concentrated in vacuo to ca. 1 mL, 5 mL of hexanes were added and the product allowed to crystallize at -20 °C. The supernatant was decanted, concentrated and filtered through a short silica column (eluent: benzene), the first yellow band was collected. The volatiles were removed in vacuo. Yield of **2.6c**: 25 mg (0.035 mmol, 45 % based on Ni[κ^2-

$(CF_2)_4$-](SIPr). UV-vis (1.0 mM in benzene): λmax(ε) = 296(343) ;427(494). ^{1}H NMR (300 MHz, C_6D_6) δ 1.01 (s, 3H, 1 Me), 1.05 (d, J ≈ 7 Hz, 6H, 2 Me), 1.07 (d, J ≈ 7 Hz, 6H, 2 Me), 1.55 (d, J ≈ 7 Hz, 6H, 2 Me), 1.55 (d, J ≈ 7Hz, 6H, 2 Me), 3.13 (sept, J ≈ 7 Hz, 1H, 1 iPr H), 3.20 (sept, J ≈ 7 Hz, 1H, 1 iPr H), 3.21 (s, 2H, 1 CH_2Im), 3.42 (sept, J ≈ 7 Hz, 1H, 1 iPr H), 3.45 (sept, J ≈ 7 Hz, 1H, iPr H), 3.48 (s, 2H, 1 CH_2Im), 5.65 (tr tr, $^2J_{FH}$ = 53 Hz, $^3J_{FH}$ = 6 Hz, 1H, CF_2H), 6.90-7.75 (mult, 6H, 6 Ar-H). $^{13}C\{^1H\}$ NMR (75 MHz, C_6D_6) δ 21.73, 22.73, 23.04, 26.43, 26.66, 28.33, 28.63, 53.57, 124.22, 124.64, 129.53, 135.29, 147.06, 147.56, 191.30; ^{19}F NMR (282 MHz, C_6D_6) δ -95.90 (br tr, $^3J_{FF}$ = 9 Hz, Fα), -120.47 (br tr, $^3J_{FF}$ = 7 Hz, 2Fβ), -130.98 (br d mult, $^3J_{FH}$ = 6 Hz, 2Fγ), -137.99 (br d mult, $^2J_{FH}$ = 52 Hz, 2Fδ); m/z calcd for {Ni[κ^1-(C_4F_7H)](SIPr)(OAc)]}K+ (% intensity), 747.2 (100), 748.2 (36), 749.2 (46), 749.2(6.8) 751.2 (20), 752.2(3), 753.2 (2); m/z found, 747.3 (100), 748.3 (36), 749.2 (50), 751.2 (19), 752.2(3), 753.2 (1); See Figures S22- 24 for the ^{1}H, $^{13}C\{^1H\}$ and ^{19}F NMR spectra.

Synthesis of Ni[κ^1-(C_4F_8H)](SIPr)(O_2Cmes)] (2.6b). Red complex Ni[κ^2-$(CF_2)_4$-](SIPr) (**2.3**) (50 mg, 0.08 mmol) was placed in a 20 mL scintillation vial and dissolved in ~ 7 mL of toluene. 2,4,6-trimethylbenzoic acid (14 mg, 0.085 mmol) was added to the stirred mixture and left to stir at 25 °C for 24 hours. The deep yellow solution was concentrated in vacuo to 1 mL, 5 mL of hexanes were added and the product allowed to crystallize at -20 °C. The supernatant was decanted and the crystals were washed with hexanes (2 x 5 mL). Yield of **2.6d**: 48 mg (0.06 mmol, 77 % based on Ni[κ^2-$(CF_2)_4$-](SIPr). UV-vis (1.5 mM in benzene): λmax(ε) = 486(461). ^{1}H NMR (300 MHz, C_6D_6) δ 0.95 (d, J ≈ 7 Hz, 6H, 2Me), 1.04 (d, J ≈ 7 Hz, 6H, 2 Me), 1.07 (d, J ≈ 7 Hz, 6H, 2 Me), 1.51 (d, J ≈ 7Hz, 6H, 2 Me), 1.56 (d, J ≈ 7 Hz, 6H, 2 Me), 1.78 (s, 3H, MeAr), 1.94 (s, 6H, 2 MeAr), 3.09 (s, 2H, CH_2Im), 3.12 (sept, J ≈ 7 Hz, 2H, 1 iPr H), 3. (sept, J ≈ 7 Hz, 1H, iPr H), 3.40 (s, 2H, 1 CH_2Im), 3.54 (sept, J ≈ 7 Hz, 1H, 1 iPr H), 5.65 (tr tr, $^2J_{FH}$ ≈ 52 Hz,

$^{3}J_{FH}$ ≈ 6 Hz, 1H, CF2H), 6.34 (mult, 2H, Ar H), 7-7.20 (mult, 6H, 6 Ar-H). $^{13}C\{^{1}H\}$ NMR (75 MHz, C_6D_6) δ 19.52, 20.62, 23.05, 23.44, 26.15, 26.56, 28.39, 28.80, 53.85, 124.52, 124.70, 129.38, 134.94, 135.62, 138.55, 146.61, 147.46, 189.86. ^{19}F NMR (282 MHz, C_6D_6) δ -95.90 (br tr, $^{3}J_{FF}$ = 8 Hz, 2Fα), -120.80 (br tr, $^{3}J_{FF}$ = 8 Hz, 2Fβ), -130.99 (d mult, $^{3}J_{FH}$ = 6 Hz, 2Fγ), -138.68 (br mult, $^{2}J_{FH}$ ≈ 52 Hz, 2Fδ); m/z calcd for{[Ni[κ^{1}- (C_4F_7H)](SIPr)(OAr)]}K+ (% intensity), 851.3 (100), 852.3 (45), 853.3 (46), 853.3(10), 854.3(22), 855.3 (9), 856.3(4), 857.3 (2); m/z found, 851.4 (100), 852.3 (46), 853.4(49), 854.3 (22), 855.41(10), 856.3 (4), 857.3 (2); See Figures S25-27 for the 1H, 13C{ 1H} and 19F NMR spectra. ^{19}F NMR spectrum of minor product, Ni[κ^{3}-$(CF_2)_3CF(O_2Cmes)$-](SIPr) (**2.5d**): ^{19}F NMR (282 MHz, C_6D_6, 25 °C) δ -91.22 (d mult, $^{2}J_{FF}$ = 254 Hz, Fα), -101.86 (d mult, $^{2}J_{FF}$ = 254 Hz, Fα), -119.74 (d d, $^{3}J_{FF}$ = 17, 15 Hz, Fα), -126.25 (d mult, $^{2}J_{FF}$ = 245 Hz, Fβ), -130.80 (d d mult, $^{2}J_{FF}$ = 245, $^{3}J_{FF}$ = 17 Hz, Fβ), -135.05 (d mult, $^{2}J_{FF}$ = 248 Hz, Fβ), - 143.27 (d d, $^{2}J_{FF}$ = 248, $^{3}J_{FF}$ = 15 Hz, Fβ).

Variable-temperature ^{19}F NMR spectra of reaction intermediates leading to 2.4a: Red complex Ni[κ^{2} -$(CF_2)_4$-](SIPr) (**2.3**) (10 mg, 0.015 mmol) was dissolved in 0.5 mL of CD_2Cl_2 in a screw cap NMR tube. The solution was precooled to 193 K and then placed in the NMR probe cooled to 223 K and a ^{19}F NMR spectrum was obtained (Figure S3) after 5 minutes to allow for temperature equilibration. The low temperature ^{19}F NMR clearly indicates no de-coalescence of signals associated with **2.3**, this indicates the presence of low energy processes which are consistent with our calculations. However, four new signals develop at this temperature, which may indicate interference and the formation of a new product possibly involving trace water coordination. The sample was removed from the probe and re-cooled to 193K. A pre-prepared solution of TMSOTf (4 μL, 0.023 mmol) in 0.5 mL of CD_2Cl_2 was injected into the NMR tube. The NMR tube was then placed in the NMR probe. The probe was cooled to 223 K and the ^{19}F

NMR spectrum was obtained (Figure S1) after 5 minutes to allow for temperature equilibration. The sample was warmed to 253 K and low temperature ^{19}F NMR spectra were acquired at 30 min, 2 hours and 3 hours corresponding to Figures S1 a-d respectively. It is noted that a distinct intermediate possessing ^{19}F NMR signals similar to those observed for **2.5b**, **c** is present in solution already after 5 minutes. However, the intermediate quickly dissipates even at low temperature after only 2 hours. After warming to room temperature, the intermediate is no longer present.

Synthesis of Ni[κ^2-$(CF_2)_4$-](SIPr)(OAc) (2.7). Red complex Ni[κ^2-$(CF_2)_4$-](SIPr) (**2.3**) (100 mg, 0.154 mmol) was placed in a 20 mL scintillation vial and dissolved in ~ 5 mL of DCM. Colorless [$PhI(OAc)_2$] (50 mg, 0.154 mmol) was then added to the stirred mixture. The resulting bright yellow solution was concentrated *in vacuo* to a thick paste with some yellow precipitate. Hexanes (10 mL) were then added to precipitate the product which was subsequently filtered (30 mL medium pore fritted funnel), washed with hexanes (3 x 2 mL), and dried *in vacuo*, affording **2.7** as a yellow powder. Yield: 82 mg (0.12 mmol, 75 % based on Ni[κ^2-$(CF_2)_4$-](SIPr). The isolated material was stored at room temperature under nitrogen. UV-vis (1.5 mM in DCM): λmax = 313.29 and 430.24. ^1H NMR (300 MHz, $(CD_3)_2CO$) δ 1.28 (d, J $\approx$ 5 Hz, 12H, 4 Me), 1.40 (d, J $\approx$ 5 Hz, 12H, 4 Me), 2.72 (H_2O), 3.3 (br, 4H, 4 iPr H), 4.03 (br , 4H, 2 CH_2Im), 7.40-7.70 (mult, 6H, 6 Ar-H). ^{19}F NMR (282 MHz, $(CD_3)_2CO$) δ -176 (br), -195 (br). See Figure B.5-6 for the ^1H and ^{19}F NMR spectra.

Chapter 3

3. Published Contributions

Metal Heptafluoroisopropyl (M-hfip) Complexes for use as hfip Transfer Agents

N. O. Andrella, K. Liu, B. M. Gabidullin, M. Vasiliu, D. A. Dixon and R. T. Baker *Organometallics* **2018**, *37*, 422-432

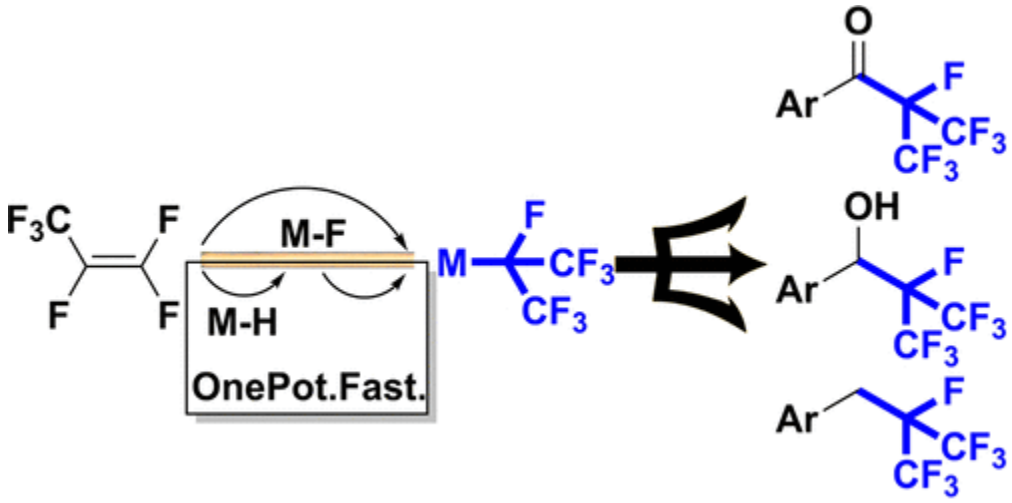

Andrella and Baker wrote the manuscript. Andrella performed most of the experiments, Liu was responsible for scope screening

Vasiliu and Dixon were responsible for Computational Studies

Gabidullin was responsible for X-ray diffraction resolution.

3.1. Abstract

New coinage metal heptafluoroisopropyl (L_nM-hfip) complexes are synthesized from the metal fluoride and inexpensive hexafluoropropene [M = Ag, Cu; L = PPh_3, 2,2,6,6-tetramethylpiperidine (Htmp)]. The reaction of the silver Htmp complex with a Ni dibromide

complex led to an efficient hfip transfer to afford $L_2NiBr(hfip)$ [L = 2-ethylpyridine]. Treatment of the Ni-hfip complex with $ZnPh_2$ gave the corresponding $L_2NiPh(hfip)$ complexes that were investigated for reductive elimination of $PhCF(CF_3)_2$. Although the desired reductive elimination proved unsuccessful, the addition of carbon monoxide to $L_2NiPh(hfip)$ achieved an efficient heptafluoroisopropyl carbonylative cross-coupling. Further, while the silver complex does not undergo hfip transfer to organic electrophiles, the copper complex [$(phen)(PPh_3)Cu(hfip)$; **3.3b**] effectively transfers the hfip unit to various substrates. We investigated the scope of **3.3b** with acid chlorides toward the synthesis of perfluoroisopropyl aryl ketones. Additionally, reaction conditions for hfip transfer to *p*-fluorobenzyl bromide and *p*-fluorobenzaldehyde were identified. As a bonus, **3.3b** was easily generated on a gram scale using commercially available copper hydride by taking advantage of a rapid hydrodefluorination to generate "Cu-F" *in situ*. Aspects of the observed reactivity are supported by DFT calculations.

3.2. Introduction

Fluorinated carbon fragments, i.e. fluoroalkyls and -aryls, have become quite common in many applications.[353,354] In the pharmaceutical industry,[311,355] for example, many household drugs now contain these functional groups[15] which offer benefits in metabolic stability, solubility, lipophilicity, and bioavailability. Many of these fluoroalkyl-containing drugs have become 'block-busters', such as Celebrex®, Prevacid®, and Pantoprazole®.

While many such fragments can be envisioned, only a few are currently readily accessible. For example, trifluoromethylation reactions have seen a period of rapid growth spurred by unique biological applications.[356-360] However, installation of other fluoroalkyl fragments such as $-CF_2H$,[180,361-363] C_2F_5,[229,364,365] OCF_3,[366-368] and SCF_3[135,369] remains challenging. There has also been a huge investment in identifying new biologically

active agents for use in both the agro-chemical and pharmaceutical industries. For example, the heptafluoroisopropyl (hfip) group has recently been incorporated into insecticides (Figure 3.1)[370-374] prompting our current study of its synthesis, coordination chemistry and transfer to organic electrophiles.

The success and application of fluoroalkylation routes generally hinge on the stability and ease of access to the critical reagent.

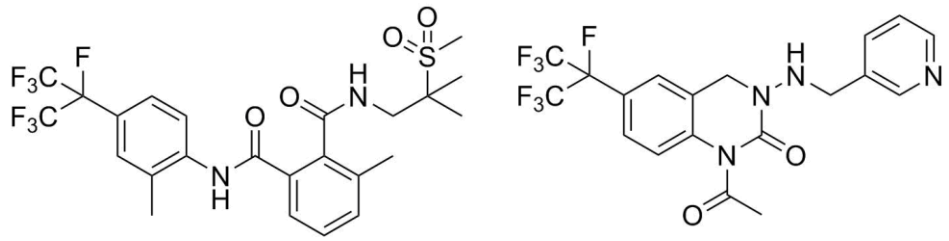

Figure 3.1. Biologically active compounds containing the hfip group.

The Ruppert-Prakash reagent, $Me_3Si\text{-}CF_3$, for example, has seen widespread adoption primarily because of its moderate cost and ready availability.[375] Recently, Grushin *et al.* successfully prepared a series of $[Cu]CF_2CF_3$ complexes generated from pentafluoroethane[162] and Vicic *et al.* developed a zinc reagent of the type $[Zn]CF_2H$.[181] In both cases, the cost of preparation for these reagents remains low by using base metals and readily available hydrofluoroalkanes. The reactivity of these reagents depends heavily on the choice of ancillary ligand, with 1,10-phenanthroline (phen) giving rise to increased reactivity — like the $(phen)Cu(CF_3)$ Trifluoromethylator®.[281] In this report, we find that changes in the coordination chemistry of copper lead to the improved transfer of the hfip fragment to organic electrophiles.

To date, methodologies for the introduction of the hfip group to organic molecules remain scarce. One can generate the hfip nucleophile as the hfip anion, $[CF(CF_3)_2]^-$, (Figure 3.2A)[376,377] or a metal complex [M]-hfip (Figure 3.2B).[177,378-385] In these procedures, two reagents provide a foundation to

access the hfip moiety. The more obvious of the two is 2-iodohepta-fluoropropane, which has been successfully metallated to yield hfip complexes (Scheme 3.1A)[386,387] Alternatively, one can generate similar compounds from hexafluoropropene (HFP) and a source of fluoride (Scheme 3.1B).[226,340] This route benefits from the significantly less expensive starting material [23.7 (HFP) vs 192 $/mol (Ihfip)] and HFP can be generated selectively from waste polytetrafluoroethylene (PTFE).[388,389]

In reports that explore such reactivity, four reagents stand out: the hfip anion and hfip complexes of cadmium, silver, and copper (Scheme 3.2).[390-392] Evidently, each system comprises their own drawbacks which could possibly be remediated with the development of new hfip organometallic reagents. Herein, we report the synthesis and characterization of new Cu, Ni and Ag hfip complexes. The reactivity of each compound is then tested with simple organic electrophiles to determine their nucleophilicity.

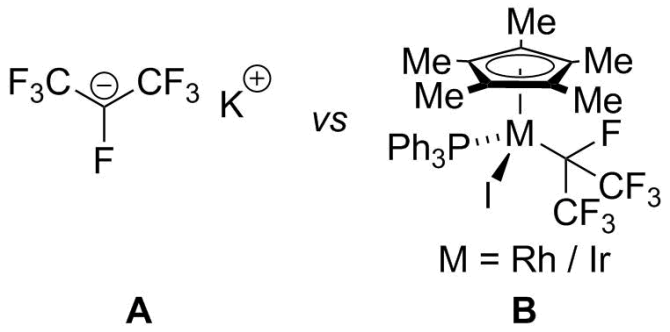

Figure 3.2. Heptafluoroisopropyl anion *vs* M-hfip complex

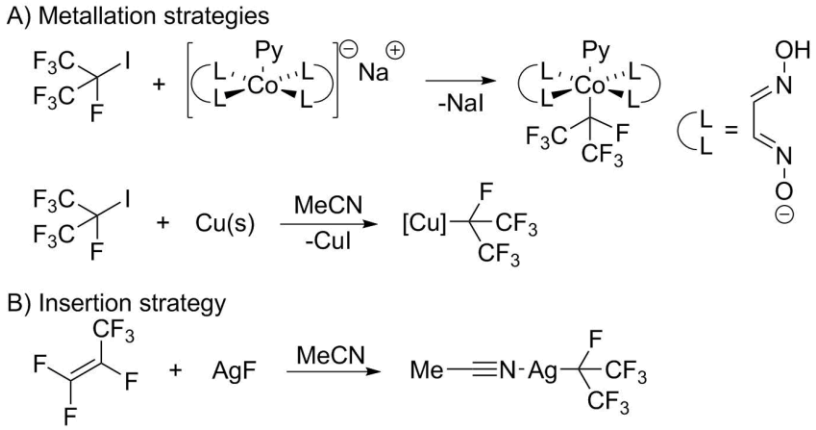

Scheme 3.1. (A) Metallation of heptafluoro-2-iodopropane and (B) Addition of M^0-F to hexafluoropropene

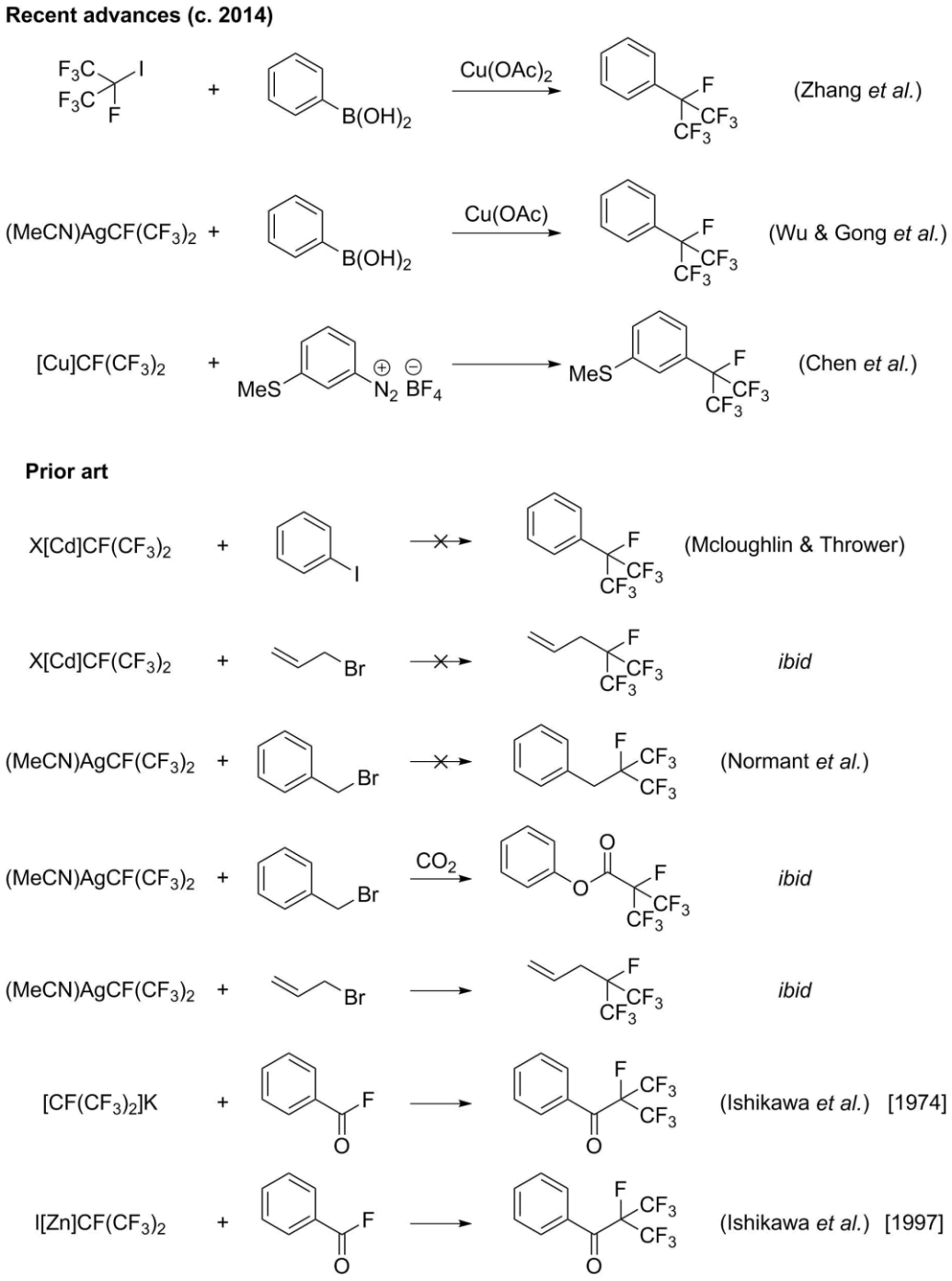

Scheme 3.2. Reported Reactions of hfip compounds

3.3. Results and Discussion

Synthesis and Characterization of a Silver hfip Complex. Following a modified literature procedure,[226] the new silver hfip complex **3.1** was prepared directly from HFP and silver

fluoride in the presence of 2,2,6,6-tetramethylpiperidine (Htmp) (Scheme 3.3). As is typical for such reactions, only a single isomer is observed. The metal fluoride inserts HFP such that the less sterically hindered and the more δ+ carbon (=CF_2) is oriented towards the fluoride. This choice of the ligand was inspired by previous work with $AgCF_3$ complexes,[393] to target the neutral compound (*vs* $[Ag(CF_3)_2]^-$). The colorless powder **3.1** is slightly unstable at room temperature, becoming progressively grayer over time. However, this did not preclude the collection of single-crystal X-ray diffraction data (Figure 3.3).

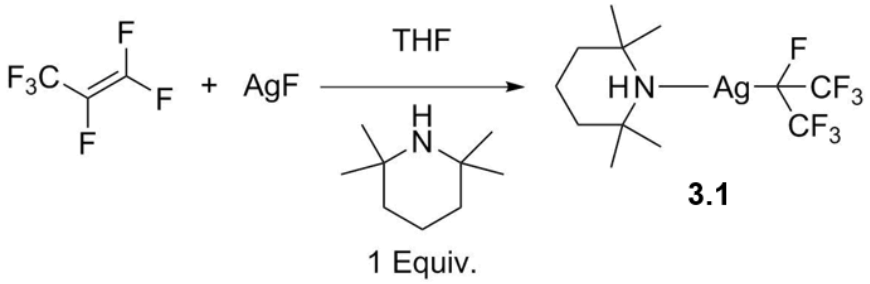

Scheme 3.3. Synthesis of compound **3.1**.

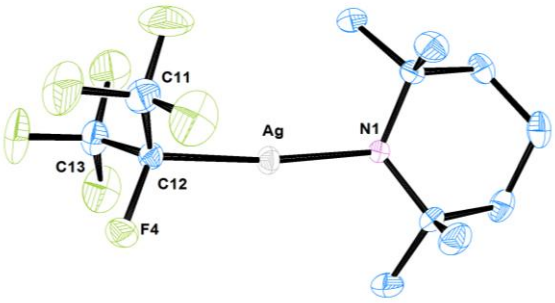

Figure 3.3. ORTEP representation of the molecular structure of **3.1**. Thermal-ellipsoid probabilities are set to 35% with hydrogen atoms omitted for clarity.

The molecular structure of complex **3.1** exhibits linear coordination about Ag and features a hydrogen bond interaction (N—H--F) between the isopropyl fluoride (F4) and the tetramethylpiperidine amine (N1—H1') from the neighboring complex in the crystal lattice (See

Figure S40 in Supporting Information). There is a slight distortion from linearity with the shortest angle between C12—Ag—N1 being 173°.

The ^{19}F NMR spectrum of **3.1** in C_6D_6 is consistent with the structure determined in the solid state. Whereas the trifluoromethyl group displays a chemical shift difference for the ^{106}Ag and ^{107}Ag isotopomers, the iPr fluoride does not and neither resonance displays Ag—F coupling. Consistent with previous reports, on dissolution in more polar and coordinating solvents an equilibrium between (Htmp)Ag[$CF(CF_3)_2$] and $Ag^+[Ag\{CF(CF_3)_2\}_2]^-$ is evident with the neutral complex being favored.[177]

Synthesis and Characterization of Nickel hfip Complexes. With the stable Ag complex **3.1** in hand, we proceeded to transmetallate the hfip fragment to other transition metal halides.[252] Generally, the reaction with transition metal halides led to decomposition of **3.1** by the formation of HFP (β-fluoride elimination) or 2-H-heptafluoropropane. Reaction with bis(2-ethylpyridine) nickel dibromide in benzene, however, yielded the singly transmetallated product, **3.2a** (Scheme 3.4) Even when using an excess of **3.1**, only **3.2a** was observed.

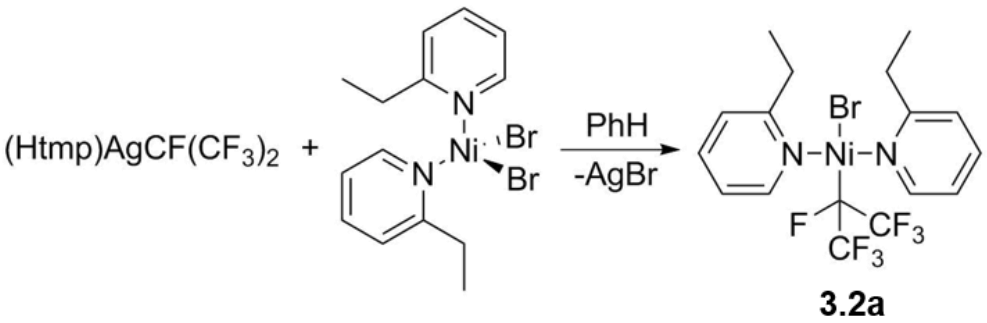

Scheme 3.4. Synthesis of Compound **3.2a**

The nickel atom of complex **3.2a** adopts a square planar geometry with the hfip and bromide trans to each other (Figure 3.4). While the C_α-F bond appears to be significantly

longer[127,152,322-325,327,328,395] than that in **3.1** [1.59 Å (average) vs 1.420(2) Å in **3.1**], this is likely an artifact of the disorder in the crystal structure as the calculated value is in line with other complexes (Table 3.1).

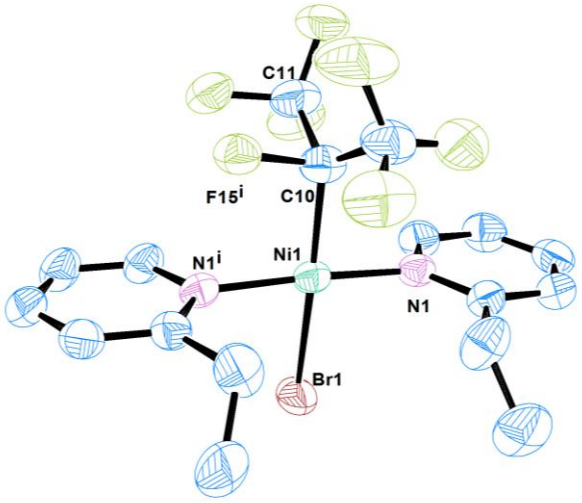

Figure 3.4. ORTEP representation of the disordered molecular structure of **3.2a** (ethyl groups can be syn, anti or anti, anti to hfip). Thermal-ellipsoid probabilities are set to 35% with hydrogen atoms omitted for clarity.

The ^{1}H NMR spectrum of **3.2a** has three broad signals centered at δ 4.5, 5.2 and 9.4 respectively. These are assigned to the CH_2Et and CHpy fragments which reside closest to the metal center. The dynamic process that contributes to these broad resonances is most evident in the variable-temperature ^{19}F NMR spectrum that exhibits the expected doublet and septet resonances only at elevated temperature (Figure S8). At room temperature, the inequivalent CF_3 resonances are likely due to hindered rotation about the Ni-C and Ni-N bonds in the two rotamers observed in the solid-state structure.

Seeing as **3.2a** can be considered as the oxidative addition product of Br-$CF(CF_3)_2$ to nickel(0), it may serve as a potential platform to study the cross-coupling synthesis of Ar-$CF(CF_3)_2$. To model such a reaction, we selected diphenyl zinc as a potential coupling partner.

Immediately upon addition of the zinc reagent to a solution of **3.2a** in THF, a reaction was observed to form complex **3.2b**. This new complex [not isolated] was then treated *in situ* with bis(phosphines) to give stable products: 1,2-bis(dicyclohexylphosphino)ethane [dcpe; **3.2c**], 1,1'-bis(diphenylphosphino)ferrocene [dppf; **3.2d** (not isolated)] and xantphos (multiple products).

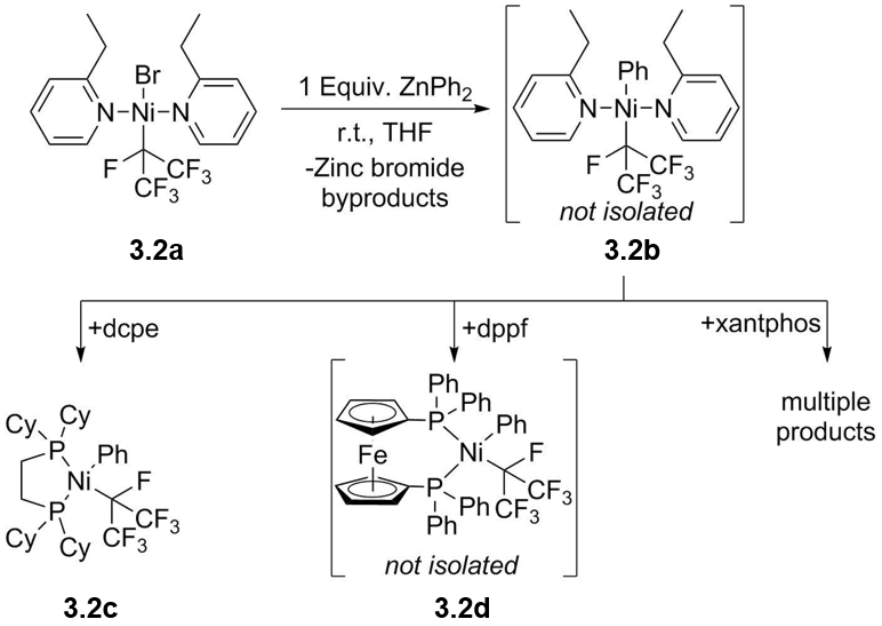

Scheme 3.5. Synthesis of phenyl Ni-hfip Complexes **3.2b**, **3.2c** and **3.2d**.

Complex **3.2c** was isolated as a bright yellow powder and crystallized from acetonitrile. The molecular structure of **3.2c** shows a distorted square planar Ni center with the hfip and the phenyl *cis* to each other (See Figure S1 in Supporting Information). The C_{α}-F bond distance [1.437 Å] is now closer in length to complex **1**.

Synthesis and Characterization of Copper hfip Complexes. The reaction of **3.1** with copper chloride in benzene produces the solvated Cu-hfip complex disclosed previously[380] and used extensively in aryl boronic acid cross-coupling reactions[390] and others.[387,390-392] Looking to avoid the use of the costlier silver fluoride starting material [928 $/mol], we endeavored to

synthesize the Cu complex from commercially available copper fluoride dihydrate [43 $/mol] and triphenylphosphine [45 $/3 mol]. The choice of copper fluorides is limited since only a few have been reported and/or isolated,[396,397] with $(PPh_3)_3CuF$ being successfully used as a source of nucleophilic fluoride. In one example, Szabó *et al.* demonstrated the substitution of allylic C-X bonds [X = Br, Cl, OTf] using said reagent to synthesize allylic C-F compounds.[398]Similarly, Grushin *et al.* employed this complex to easily generate $CuCF_3$ from Me_3SiCF_3.[148] In this regard, we expected the coinage metal fluoride to yield a net addition of Cu-F across the HFP double bond, as seen with AgF.

The copper(I) fluoride complex, $CuF(PPh_3)_3$, was synthesized as previously reported[322] and treatment with HFP in Et_2O over a 24-hour period afforded the hfip complex **3.3a** in high yield (80%) and excellent purity [>90%, Scheme 3.6]. Solvents of higher polarity yielded impurities that are not trivially separated from **3.3a**. Moreover, the use of dichloromethane or *N*,*N*-dimethylformamide [DMF] yielded no product and only HFP oligomers. Like the previously reported pentafluoroethyl copper complex,[399] the molecular structure of **3.3a** features a hfip group and two PPh_3 ligands in a trigonal planar array about the copper [Figure 3.5(left)]. As expected, the Cu-C bond [2.003(3) Å] is shorter than the Ag-C bond [2.114(2) Å] but like those in the $Cu\text{-}CF_2CF_3$ [1.99 Å] and $Cu\text{-}CF_3$ [2.025(7) Å] analogs. On this note, the Cα-F bond distance gets progressively smaller with decreasing fluoroalkyl size [1.44 Å for **3.3a** *vs* 1.4 and 1.39 Å for CF_2CF_3 and CF_3 respectively].

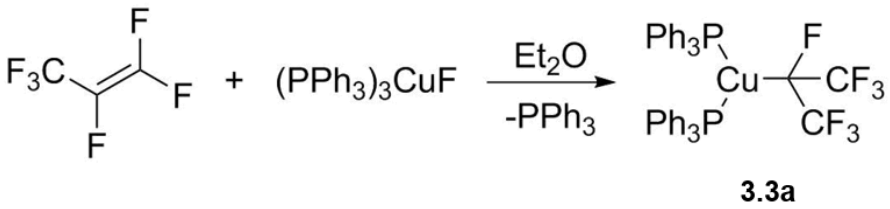

Scheme 3.6. Synthesis of **3.3a** from HFP and copper(I) fluoride

As the reaction to form **3.3a** was slow — likely related to the limited solubility of $[(PPh_3)_3CuF]$ in Et_2O — we sought an alternate Cu-X precursor that upon rapid insertion of HFP would undergo β-fluoride elimination to Cu-F followed by subsequent addition of HFP to yield **3.3a**. For example, Ogoshi *et al*. have taken advantage of β-fluoride elimination of a copper complex to generate fluorostyrenes.[228,292] To avoid side reactions, we selected X such that the produced fluoroalkene would be a gas at room temperature. We thus turned to commercially available $[(PPh_3)CuH]_6$ (Stryker's reagent). Although copper hydride has been used for hydrodefluorination of Ar^F compounds,[400] it has never been used with fluoroalkenes. When $[(PPh_3)CuH]_6$ with 1 additional equiv. of PPh_3 per Cu is exposed to HFP in benzene, it reacts in < 2 h to give **3.3a** in excellent yield (81% based on $[(PPh_3)CuH]_6$, Scheme 3.7). Moreover, the addition of phen to **3.3a** in Et_2O gave [(phen)(PPh_3)Cu(hfip)], **3.3b**, in high yield (> 80% based on $(PPh_3)_2$Cu(hfip)) as a bright orange powder. This change in coordination number and ligand did not have a profound effect on the Cu-C or Cα-F bond lengths [Figure 3.5(right), Table 3.1].

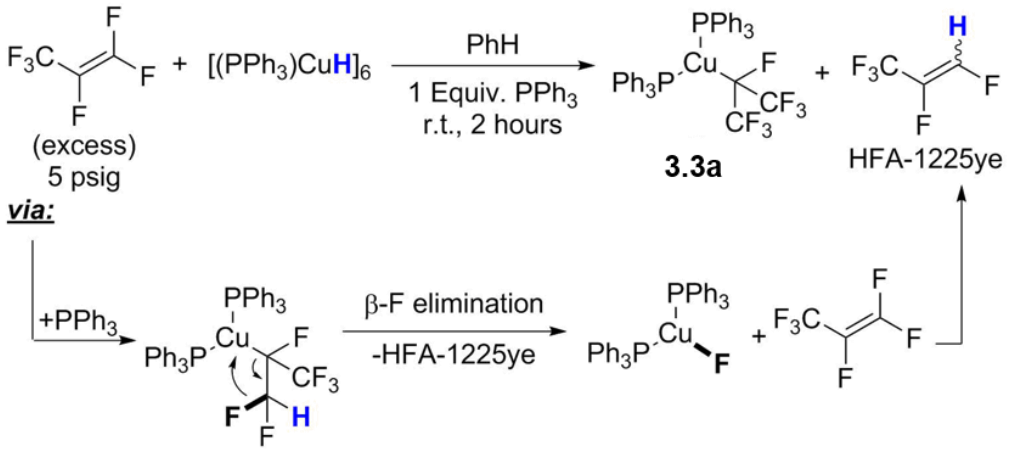

Scheme 3.7. Synthesis of 3a from HFP and Stryker's reagent.

The ^{19}F NMR spectrum of **3.3a** in C_6D_6 shows an unusually broad resonance for Cα-F indicating some fluxional behavior. This is supported by a broad signal in the ^{31}P NMR spectrum at -5 ppm for both PPh_3 ligands. While **3.3b** in C_6D_6 reveals a similar trend in the ^{31}P NMR spectrum (broad resonance at -5 ppm), the ^{19}F NMR spectrum now consists of sharp resonances with the typical $^3J_{FF}$ coupling constant [FC-CF_3] being quite apparent although no J_{PF} could be identified. The ^1H NMR spectrum also shows broadening of the signal assigned to phen-H lying closest to the metal center, resulting presumably from fast cleavage and reformation of the Cu-PPh_3 bond.

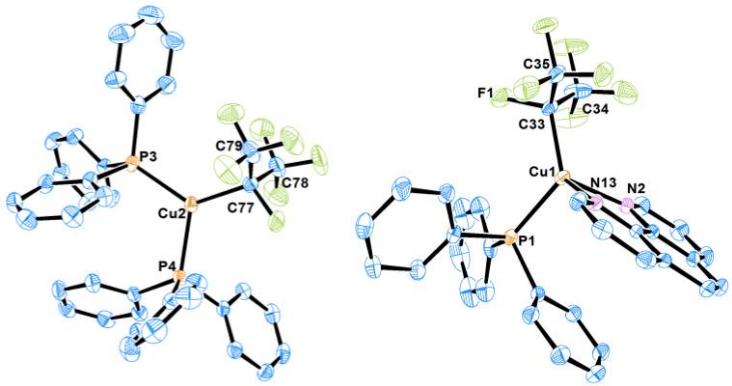

Figure 3.5. ORTEP representation of the molecular structure of (left) **3.3a** and (right) **3.3b**. Thermal-ellipsoid probabilities are set to 35% with hydrogen atoms omitted for clarity.

Table 3.1. Selected Bond Lengths[a]

Complex	**3.1**	**3.2a**	**3.2c**	**3.3a**	**3.3b**
M-C	2.11/2.14	2.00/2.04	2.00	2.00/2.04	2.00/2.04
Cα-F	1.42/1.42	1.60[c]/1.42	1.44	1.43/1.43	1.44/1.43
Cβ-F[b]	1.32/1.36	1.35/1.36	1.35	1.35/1.37	1.34/1.37

[a] All values are rounded and in Å: expt/calc. [b] Average for calculated values at the DFT/B3LYP level. [c] Accuracy likely affected by the disorder.

Reactivity of M-hfip Complexes with Aroyl Chlorides. Having these four new M-hfip complexes in hand, we proceeded to test their reactivity with benzoyl chloride to determine which one may be a suitable platform for further nucleophilic studies. First, when **3.1** was mixed with benzoyl chloride in many solvents no reaction was observed. This is in line with previously described reactivity for the analogous compound (MeCN)Ag[CF(CF_3)$_2$].[384] Second, when **3.2a** was mixed with benzoyl chloride, immediate formation of HCF(CF_3)$_2$ [Hhfip] was observed. In contrast, when **3.3a** or **3.3b** were mixed with benzoyl chloride in DMF, both produced fluorinated ketone **3.4a** in moderate (50%) and high (75%) yields, respectively. In the case of **3.3a,** the reagent is unstable under the reaction conditions and produces an equivalent amount of benzoyl fluoride, arising presumably from β-fluoride elimination with concomitant formation of HFP. Optimizing the reaction of **3.3b** with benzoyl chloride, we found that DMF was required; all other solvents tested yielded no product and gave exclusively Hhfip. The reaction proceeds readily at room temperature over 24 h.

Existing methods for the synthesis of these compounds have been limited either by a) generation of the [CF(CF_3)$_2$]$^-$ anion and accompanying HFP oligomers[376] or b) the use of acid

fluorides, generated from acid chlorides.[385,401] The reaction can be applied to a wide range of acid chlorides bearing various functional groups including, halide (**3.4e-g**), CN (**3.4i**), ether (**3.4k**), alkyl (**3.4c**), nitro (**3.4j**,**k**), naphthyl (**3.4l**) and thiophene (**3.4n**; Table 3.2). Some steric effects could be observed. For example, the ortho derivatives gave lower yields [**3.4d** and **3.4k**]. The extent of this effect is better measured using the 2,4,6-chloro substituted benzoyl chloride that does not react with **3.3b**. In general, the electron-rich aroyl chlorides always gave lower yields, presumably due to reversibility under the reaction conditions. This is more evident in the case of 3,4,5-trimethoxy benzoyl chloride, for which the yield drops off as the reaction progresses. Similarly, this highlights the inherent difficulty in isolating these products as the hfip group is readily substituted and therefore demands rigorously dry conditions. To compound this issue, all the products are volatile and could not be easily separated from DMF. However, they can be collected as the distillate with DMF.[402] Noticeably, phenyl acetyl chloride, the only alkyl acid chloride, does not react with **3.3b**.

Reactivity of Cu-hfip Complexes with Other Electrophiles. Reactions of **3.3b** with several other electrophiles generally required ~1.5 equiv. of **3.3b** due to competing formation of Hhfip.[403] The reaction of **3.3b** with 4-fluorobenzyl bromide (Scheme 3.8**,** Top) gave an unusually low yield and produced several unidentifiable products when heated to 50 °C. To compound the issue, the product **3.5a** was unstable under regular work-up conditions. In one attempt at isolation of **3.5a** by column chromatography, no product was collected. Although we expected the formation of benzyl fluoride to arise from a β-fluoride transfer, we did not observe the concomitant formation of HFP under the reaction conditions.

Table 3.2. Perfluoroisopropylation of Aroyl Chlorides

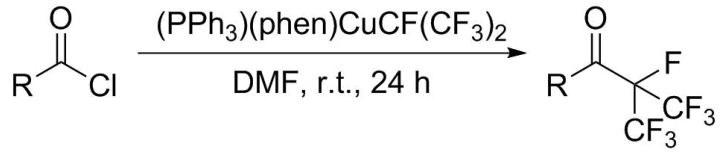

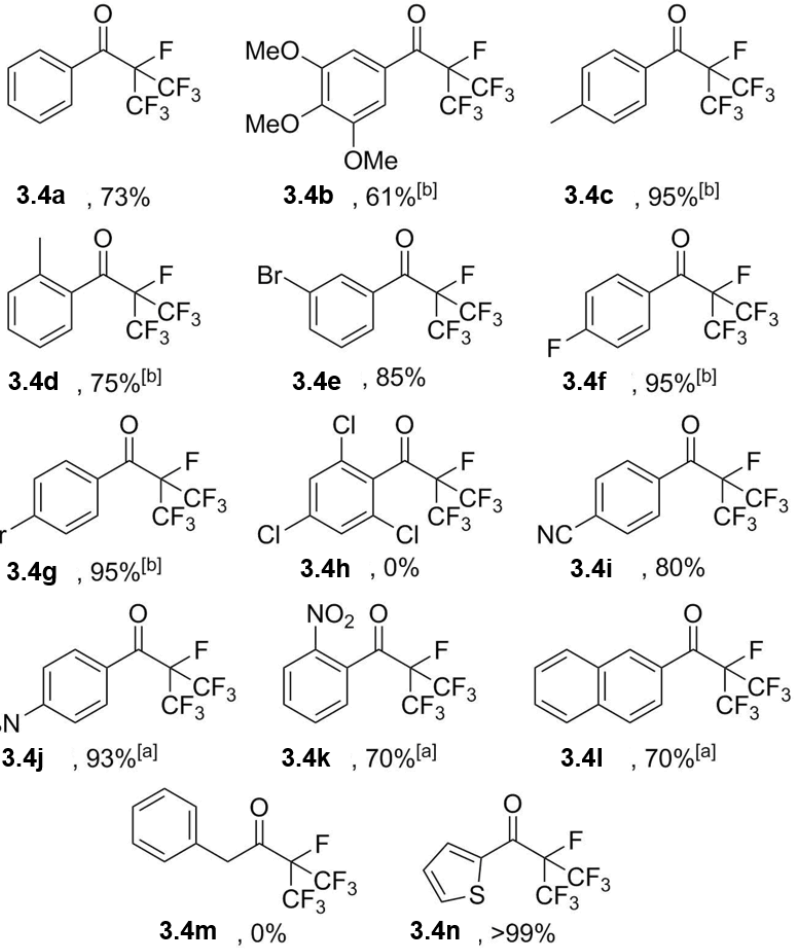

Reaction Conditions: (0.074 mmol) of Cu, (0.049 mmol) acid chloride and (0.027 mmol of internal standard) in 0.5 mL DMF at RT for 24 h. The reactions were performed in an NMR tube sealed with a plastic cap and wrapped with parafilm without stirring. The yields were determined by 19F NMR spectroscopy with hexafluorobenzene as an internal standard *vs* moles of electrophile. For details see the Supporting Information. [a] 1 equiv. of **3.3b**. [b] 4 h at RT.

We suspect that the benzyl fluoride arises from α-fluoride transfer (Scheme 3.9, **route B**) from an intermediate copper (III) complex (**3.3b'**) and is in competition with product formation, corroborating the 30% yield. On the trend of alkyl halides, we found that those vicinal to a

ketone do not react with **3.3a** [e.g. bromoacetophenone]. We also found that bulkier benzhydryl halides do not substitute readily. Unfortunately, **3.5c** was not stable under the reaction conditions and slowly decomposed, precluding its isolation. Lastly, aldehydes could be substituted by employing a weak Lewis acid as an additive. While **3.3b** does not react readily with 4-fluorobenzaldehyde, the addition of a strong Lewis acid also does not produce the desired product. **3.3b** itself reacts with both trimethylsilyl trifluoromethanesulfonate [TMSOTf] and trifluoroborane etherate [$BF_3 \cdot Et_2O$]. However, the addition of triphenylborane gave the desired product **3.5b** in 91% yield.

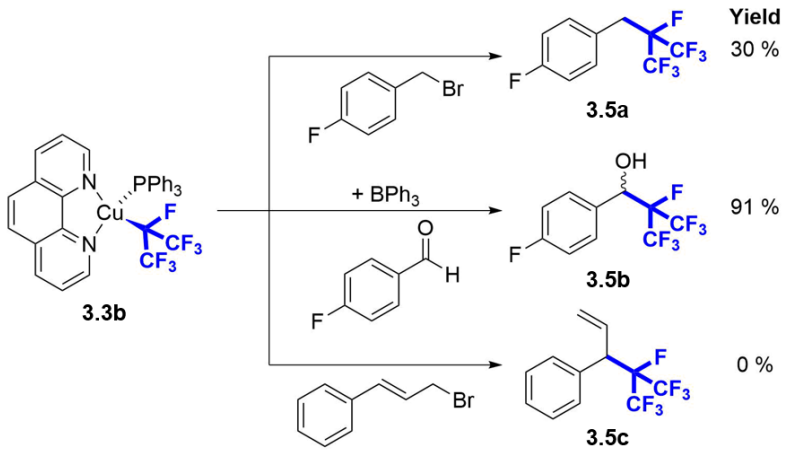

Scheme 3.8. Reactions of **3.3b** with other electrophiles.

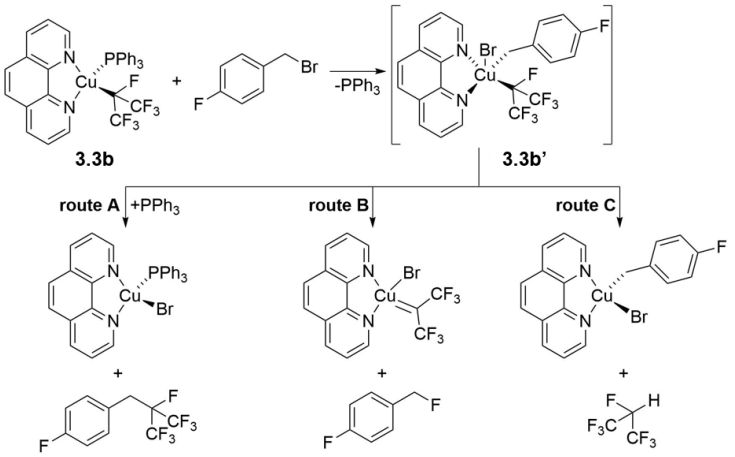

Scheme 3.9. The reaction of **3.3b** with benzyl bromide and suspected decomposition pathways of **3.3b'**.

Reactivity of Ni(Ph)hfip (3.2b) Towards Reductive Elimination. Upon heating complexes **3.2b-d** to 66 °C either (a) no reaction [**3.2c**], (b) decomposition to Hhfip [**3.2b**] or (c) a mixture of unknown products [**3.2d**] was observed. With the stable complex **3.2c** in hand, we attempted to effect the associatively-induced reductive elimination by addition of excess triethylphosphite, 2,6-dimethylphenyl isocyanide or CO gas. Although the addition of triethylphosphite had no effect, the isocyanide reacted immediately to give a mixture of unidentified products. Addition of CO (3 atm) to **3.2c** [in either THF or benzene-d_6] at 50 °C instead produced the ketone in 90% yield (Scheme 3.10) with some Hhfip produced in a side reaction.

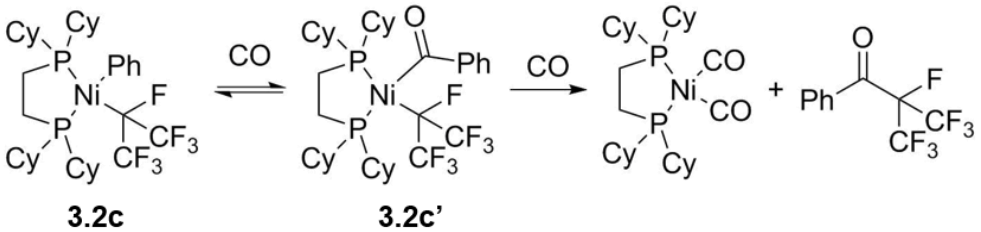

3.2c **3.2c'**

Scheme 3.10. Carbonylation and reductive elimination of the hfip group

This suggests that catalytic perfluoroalkyl-carbonylation[293,294] using nickel could be possible and will be explored further in due course.

Computational chemistry. To provide insight into these reactivity trends, we carried out DFT calculations (at the B3LYP/DZVP2/aug-cc-pvdz-pp(M) level; Table 3.3). The calculated bond distances are in good agreement with experiment (Table 3.1). The calculated ^{31}P gas phase NMR chemical shifts are within about 12 ppm of the experiment while those for ^{19}F differ by ~ 20-30 ppm for the $CF_3{}^{i}Pr^{F}$ and the $CF^{i}Pr^{F}$ (See Supporting Information). This is typical of the usual errors in calculated chemical shifts for these nuclei.

There are two types of bond dissociation energies (BDEs) to consider for this system, homolytic with the formation of a metal-centered radical and the perfluoro-isopropyl radical and heterolytic with the formation of a metal-centered cation and the perfluoro-isopropyl anion. In the gas phase, homolytic cleavage always requires less energy than heterolytic cleavage. However, in solution, heterolytic cleavage can become favored due to solvation of the ions. In the gas phase, **1** and **3.3a** have significantly higher homolytic BDEs than do **3.2a** and **3.3b** with **3.2a** having the lowest homolytic BDE. In DMF solution **3.3a** is predicted to have a heterolytic BDE close to 0 kcal/mol and **3.2a** is predicted to have a heterolytic BDE just above 10 kcal/mol. In contrast, **3.1** and **3.3b** have heterolytic BDEs slightly greater than 30 kcal/mol in solution. The difference between the heterolytic BDEs in **3.3a** and **3.3b** arises from the bulky cation generated from **3b** which is not as well solvated as is the smaller cation generated from **3.3a**. Furthermore, the perfluoro-isopropyl anion can release fluoride to generate $CF_3(F)C{=}CF_2$. The fluoride affinity of perfluoropropene is ΔH_{298K} = 46.3 kcal/mol and ΔG_{298K} = 37.2 kcal/mol in the gas phase at the G3MP2 level[404] (see Supporting information). The inclusion of a solvent effect leads to the result that it is exothermic to release F^- from the $^{i}Pr^{F}$ anion by -6.3 kcal/mol.

The lack of reactivity observed for **3.1** is consistent with the calculated BDEs. The instability of **3.3a** is also consistent with the low energy for heterolytic cleavage and should be very

sensitive to reaction conditions, especially as F- can be generated from the perfluoro-isopropyl anion. The BDEs for **3.2a** suggest that both heterolytic and homolytic cleavage could occur.

Table 3.3. Bond dissociation energies (BDE, $\Delta H_{0K,}$ and ΔG_{298K} at the B3LYP/DZVP2/aug-cc-pvdz-pp(M) level in kcal/mol) and charge distribution of some reported complexes ([a]Ni cation has a triplet ground state).

Complex	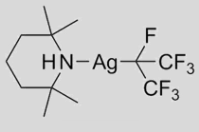 3.1	 3.2a	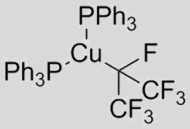 3.3a	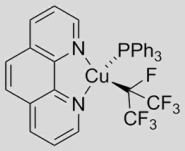 3.3b
Homolytic BDE ΔH_{0K} /ΔG_{298K} ΔG_{298K}(DMF)	71.1/57.3/62.9	46.4/28.4/22.2	80.7/64.1/66.6	55.1/40.0/44.1
Heterolytic BDE ΔH_{0K} /ΔG_{298K}/ ΔG_{298K}(DMF)	133.9/122.1/33.8	116.4/98.0/12.6[a]	90.3/74.3/1.8	86.4/72.6/32.4
Charge (NBO NPA)	M(0.555), C-$^{i}Pr^{F}$(-0.186)	M(0.716), C-$^{i}Pr^{F}$(-0.097)	M(0.598), C-$^{i}Pr^{F}$(-0.275)	M(0.748), C-$^{i}Pr^{F}$(-0.260)

3.4. Conclusions

In summary, we have prepared a series of stable M-hfip complexes and investigated their reactivity. Isolation of the first stable Ni-hfip complexes demonstrates their potential for new

cross-coupling reactions. The synthesis of **3.2a** was enabled by the underexploited salt metathesis reaction between Ag-R^F and transition metal halides, whereby previous attempts had yielded ionic species such as $[Rh]^+[Ag(R^F)_2]^-$,[383] the prior paradigm being that only copper complexes could be synthesized.[379,390] Further, this may enable access to metals in low oxidation states without the need for reduction. However, as demonstrated herein, judicious choice of transition metal starting material and the ligand are necessary for the success of these transfers.

Although the aforementioned reaction does yield the copper complex, we have discovered a new convenient synthesis of Cu-hfip complexes **3.3a,b**. An easily prepared, air-stable copper fluoride can be used to synthesize new Cu-hfip complexes, thus by-passing the need for silver. We have optimized these conditions to prevent side reactions, such as HFP oligomerization, which we found can occur in media other than Et_2O. Still, we wished to improve the reaction efficiency by decreasing the reaction time [likely limited by poor solubility of the Cu-F complex] and increasing the atom efficiency [Cu-F synthesis < 50%]. We have thus shown that a commercially available copper-hydride can readily hydrodefluorinate HFP, generating Cu-F in situ which reacts rapidly with HFP to give the Cu-hfip complex.

On evaluating the reactivity of all new M-hfip complexes towards electrophiles we showed that Cu complexes **3.3a,b**, readily transfer the hfip fragment to benzoyl chloride. These findings have been supported by DFT calculations which yielded parameters against which to compare for suspected reactivity /stability trends. It may serve as a preliminary screening mechanism to identify successful candidates to further expand the scope of hfip transfers.

The trend in BDE explains quite readily the propensity for the formation of Hhfip or HFP over the course of the reaction. Especially, in the case of **3.3b** where, without the judicious

choice of solvent (e.g. DMF), the desired reaction does not occur, although a balance must be struck between M-C BDE (**3.3b**<<**3.3a**) and desired reactivity. As a bonus **3.3b** also possesses a greater positive charge at Cu that could be beneficial for reactivity with less activated substrates.

Ongoing work is focused on (a) expanding the range of electrophiles that can undergo substitution with **3.3b** and (b) exploring conditions for *catalytic* cross-coupling for both **3.2c** and **3.3b** or analogs thereof. Preliminary results of the stoichiometric substitution reactions with **3.3b** are encouraging and indicate an enhanced reactivity of said reagent. Full details of these results will be published in due course.

3.5. Experimental Section

3.5.1. General Procedures.

Experiments were conducted under nitrogen, using Schlenk techniques or an MBraun glove box. All solvents were deoxygenated by purging with nitrogen. Hexanes, diethyl ether (Et_2O), 1,2-dimethoxyethane (DME) and tetrahydrofuran (THF) were dried on columns of activated alumina using a J. C. Meyer (formerly Glass Contour®) solvent purification system. Benzene-d_6 (C_6D_6) was dried by stirring over activated alumina (ca. 10 wt. %) overnight, followed by filtration. All solvents were stored over activated (heated at ca. 250 °C for >10 h under vacuum) 4 Å molecular sieves and glassware was oven dried at 120 °C for >2 h. The following chemicals were obtained commercially, as indicated: silver fluoride (AgF, Alfa, 99%), hexafluoropropene (HFP, Synquest, 99 %), triphenylphosphine (PPh_3, Oakwood Chemical, 99%), copper (II) fluoride dihydrate (CuF_2•$2H_2O$, Alfa), diphenyl zinc ($ZnPh_2$, Strem Chemicals, 99 %), all acid chlorides (Sigma-Aldrich, 99%), 4-fluorobenzylbromide (Oakwood Chemicals, 99%), 4-fluorobenzaldehyde (Oakwood Chemicals, 99%), 3-bromo-1-phenyl-1-propene (cinnamyl bromide, Sigma-Aldrich, 97%), 2,2,6,6-tetramethylpiperidine (Htmp, Sigma-Aldrich, 99%), 1,10-phenanthroline ,

anhydrous (phen, Alfa, 99%), 4,5-bis(diphenylphosphino)-9,9-dimethylxanthene (xantphos, Accela, 97%), 1,1'-bis(diphenyl-phosphino)ferrocene (dppf, Accela, 95%), 1,2-bis(dicyclo-hexylphosphino)ethane (dcpe, Strem, 98%), triethylphosphite ($P(OEt)_3$, Sigma-Aldrich, 99%) and 2,6-dimethylphenyl isocyanide (XylCN, Sigma-Aldrich, 96%). ^{1}H, ^{19}F, $^{31}P\{^{1}H\}$, and $^{13}C\{^{1}H\}$ NMR spectra were recorded on a 300 MHz Bruker Avance instrument at room temperature (21-23°C) unless stated otherwise. ^{1}H NMR spectra were referenced to residual proton peaks associated with the deuterated solvents (C_6D_6: 7.16 ppm). ^{19}F NMR spectra were referenced to internal standard hexafluorobenzene (C_6F_6, Oakwood, 99%) unless stated otherwise, set to -164.5 ppm. $^{13}C\{^{1}H\}$ NMR data were referenced to carbon peaks associated with the solvent (C_6D_6: 128.39 ppm, THF: 67.57 ppm). $^{31}P\{^{1}H\}$ NMR data were referenced to external H_3PO_4 (85% aqueous solution), set to 0.0 ppm. Electrospray ionization mass spectral data were collected using an Applied Biosystem API2000 triple quadrupole mass spectrometer. UV-vis spectra were recorded on a Cary 100 instrument, using sealable quartz cuvettes (1.0 cm path length). IR data were obtained on a Nicolet Nexus 6700 FT-IR spectrometer. For **3.3a**, the sample was prepared by allowing a benzene solution of **3.3a** to evaporate on a NaCl plate under a stream of nitrogen. Elemental analyses were performed by Laboratoire d'analyse élémentaire, Université de Montréal. (Montreal, Quebec, Canada). Note that the NMR spectra (^{1}H, ^{19}F, $^{19}F\{^{1}H\}$, $^{31}P\{^{1}H\}$, and $^{13}C\{^{1}H\}$ for the title compounds are displayed at the end of the Supporting Information (https://pubs.acs.org/doi/suppl/10.1021/acs.organomet.7b00837).

Synthesis of [(Htmp)Ag(hfip)] (3.1). AgF (500 mg, 3.94 mmol) was placed in a 100 mL ampoule and mixed with 15 mL of THF. Colorless Htmp (612 mg, 4.34 mmol) was then added to the slurry. The reaction vessel was attached via a three-way-valve to a HFP canister with a regulator and a Schlenk line. The solution was degassed using regular freeze/pump/thaw method.

The HFP was added to the degassed solution with the regulator set to 5 psi. The reaction was left to stir at 25 °C for ~24 hours and wrapped in tinfoil. The solid became dark green after a few hours. As the reaction progressed, the solution became progressively clear with a slight silver mirror forming. The solution was filtered through a Celite pad (15 mL medium pore fritted funnel), and the remaining solvent was removed *in vacuo* to yield a colorless powder. 10 mL of hexanes were added and the solid was collected (30 mL medium pore fritted funnel), washed with hexanes (4 °C, 3 x 5mL), and dried *in vacuo* to yield 1.44 g of **3.1** (3.55 mmol, 90% based on AgF). The isolated material was stored in a fridge under nitrogen in an amber container. ^{1}H NMR (300 MHz, C_6D_6) δ 1.17 (br, 2H, CH_2), 1.06 (m, J_{HH} = 6 Hz, 4H, CH_2), 0.76 (br, 12H, Me). ^{19}F NMR (282 MHz, C_6D_6) δ -68.45 (d, $^{3}J_{FF}$ = 13 Hz, 6F, CF_3), -68.50 (d, $^{3}J_{FF}$ = 13 Hz, 6F, CF_3), -211.03 (d 'hept', $^{3}J_{FF}$ = 13 Hz, $^{2}J_{AgF}$ = 2 Hz, 1F, $CF^{i}Pr^{F}$), -211.12 (d 'hept', $^{3}J_{FF}$ = 13 Hz, $^{2}J_{AgF}$ = 2 Hz, 1F, $CF^{i}Pr^{F}$). ^{13}C{^{1}H} NMR (75 MHz, C_6D_6) δ 17.3 (Htmp), 32.0 (br, Htmp), 37.3 (Htmp), 54.0 (Htmp), 104.1 ('multiplet', $CF^{i}Pr^{F}$), 127.1 (qdqd, $^{1}J_{CF}$ = 273 Hz, $^{2}J_{CF}$ = 24 Hz, $^{3}J_{CF}$ = $^{2}J_{AgC}$ = 5 Hz). IR: 3262(w), 2948(w, br), 1452(m, br), 1394(s), 1351(s), 1098(w), 932(s), 734(s), 692(s) cm^{-1}. ESI-MS: m/z(%) 562.15 (100), 563.16 (20), 564.15 (95), 566.15 (15) [M^{+}-H + 2THF], 142.16 [L^{+}-H]. See figures S2-4 for ^{1}H, ^{19}F, ^{13}C{^{1}H} NMR spectra.

Synthesis of [(PyEt)$_2$NiBr(hfip)] (3.2a). Purple complex [(PyEt)$_2$NiBr$_2$][431] (1.000 g, 2.31 mmol) was placed in a 100 mL round bottom flask and mixed with 30 mL of benzene. A 10 mL colorless solution of **3.1** in benzene (990 mg, 2.37 mmol) was then added to the slurry. The reaction was left to stir at 25 °C for 24 hours. The solution became progressively pink as the reaction progressed. The deep pink solution with light yellow precipitate (AgBr) was filtered through a Celite pad (15 mL medium pore fritted funnel), and the remaining solvent was removed *in vacuo* to yield a light pink powder. Roughly 5 mL of hexanes were added and the

solid was collected (30 mL medium pore fritted funnel), washed with hexanes (4 °C, 3 x 5mL), and dried *in vacuo* to yield 1.05 g of **3.2a** (2.00 mmol, 87% based on [$(PyEt)_2NiBr_2$]). The isolated material was stored at room temperature under nitrogen. UV-vis (1.0 mM in THF): λmax(ε) = 495(407). ^{1}H NMR (300 MHz, C_6D_6) δ 1.38 (t, $^3J_{HH}$ = 7 Hz, 6H, MeEt), 4.56 (br, 2H, CH_2Et), 5.19 (br, 2H, CH_2Et), 6.23 (td, $^3J_{HH}$ = 7Hz, $^4J_{HH}$ = 1 Hz, 2H, CHPy), 6.36 (d, $^3J_{HH}$ = 7Hz, 2H, CHPy), 6.54 (td, $^3J_{HH}$ = 7Hz, $^4J_{HH}$ = 1 Hz, 2H, CHPy), 9.37 (br, 2H, CHPy). ^{19}F NMR (282 MHz, C_6D_6) δ -68.24 (br, $CF_3{}^iPr^F$), -68.68 (br, $CF_3{}^i$PrF), -70.11 (br, $CF_3{}^iPr^F$), -204.65 (br, CF^iPr^F). ^{1}H NMR (300 MHz, C_6D_6, 50 °C) δ 1.45 (td, $^3J_{HH}$ = 7 Hz, $^4J_{HH}$ = 2 Hz, 6H, MeEt), 4.87 (br, 4H, CH_2Et), 6.34 (t'multiplet', $^3J_{HH}$ = 7Hz, 2H, CHPy), 6.50 (d, $^3J_{HH}$ = 7 Hz, 2H, CHPy), 6.67 (t'multiplet', $^3J_{HH}$ = 7Hz, 2H, CHPy), 9.49 (br, 2H, CHPy). ^{19}F NMR (282 MHz, C_6D_6, 50 °C) δ -68.56 (br, $CF_3{}^iPr^F$), -206.10 (br, CF^iPr^F). Anal. Calc. for $C_{17}H_{18}BrF_7N_2Ni$: C, 39.12, H, 3.48, N, 5.37. Found: C, 38.37, H, 3.71, N, 5.16. See figures S5-6 for ^{1}H, ^{19}F NMR spectra. See figures S7-8 for ^{1}H, ^{19}F NMR spectra at 50 °C.

In situ synthesis of [$(PyEt)_2$Ni(Ph)(hfip)] (3.2b). Pink complex [$(PyEt)_2$NiBr(hfip)] (20 mg, 0.04 mmol) was placed in a 5 mL round bottom flask and mixed with 1 mL of THF. A 1 mL colorless solution of Ph_2Zn in THF (9 mg, 0.04 mmol) was then added to the solution affording a yellow/brown solution after 10 minutes that was used as is. ^{19}F NMR (282 MHz, C_6D_6) δ -66.70 (br, $CF_3{}^iPr^F$(2b')), -67.39 ('quint', $^3J_{FF}$ = $^4J_{FF}$ = 9 Hz, $CF_3{}^iPr^F$(2b''), -68.00 (d, $^3J_{FF}$ = 10 Hz, $CF_3{}^iPr^F$(2b''')), -68.01 (br, CF^iPr^F(2b')), -69.14 ('quint', $^3J_{FF}$ = $^4J_{FF}$ = 9 Hz, $CF_3{}^iPr^F$(2b'')), -197.33 (br, CF^iPr^F(2b')), -214.80 (sept, $^3J_{FF}$ = 9 Hz, CF^iPr^F(2b'')), -215.26 (sept, $^3J_{FF}$ = 10 Hz, CF^iPr^F(2b''')). See figure S9 for ^{19}F NMR spectra.

Synthesis of [(dcpe)Ni(Ph)(hfip)] (3.2c). To a 5 mL solution of complex **3.2b** in THF (100 mg, 0.19 mmol) *vide supra* was added solid dcpe (89 mg, 0.21 mmol). Stirring at 25 °C over 1 hour,

the solution became progressively lighter yellow with concomitant formation of a black precipitate. The light-yellow solution was filtered through a Celite pad (15 mL medium pore fritted funnel), and the remaining solvent was removed *in vacuo* to yield a light-yellow powder. Roughly, 5 mL of acetonitrile were added and the solid was collected (15 mL medium pore fritted funnel), washed with Et_2O (4 °C, 3 x 3 mL), and dried *in vacuo* to yield 105 mg of **3.2c** (0.14 mmol, 75% based on $(PyEt)_2NiBr_2$). UV-vis (1.5mM in THF): λmax(ε) = 373(882), 307(2348). ^{1}H NMR (300 MHz, C_6D_6) δ 7.89 (m, 2H, Ar), 7.05 (m, 2H, Ar), 6.91 (m, 1H, Ar), 2.5 – 0.5 (overlap, 48H, Cy and CH_2Et). ^{19}F NMR (282 MHz, THF) δ -65.19 (dd, $^4J_{FP}$ = 5 Hz, $^3J_{FF}$ = 13 Hz, $CF_3{}^iPr^F$), -169.28 (dsept, $^4J_{FP}$ = 96 Hz, $^4J_{FF}$ = 13 Hz, CF^iPr^F). ^{13}C{^{1}H} NMR (75 MHz, THF) δ 153.1 (dd, $^2J_{PC}$ = 76 Hz, $^2J_{PC}$ = 43 Hz, CαAr), 137.9 (CAr), 124.9 (CAr), 121.1 (CAr), 36.2 (‘multiplet’, dcpe), 34.5 (‘multiplet’, dcpe), 29.9 – 24 (overlap(THF), dcpe), 20.0 (‘multiplet’, dcpe). ^{31}P{^{1}H} NMR (121 MHz, THF) δ 57.81 (dd, $^3J_{PF}$ = 96 Hz, $^2J_{PP}$ = 31 Hz, P*trans*-hfip), 47.75 (dsept, $^2J_{PP}$ = 31 Hz, $^4J_{PF}$ = 6 Hz, P*cis*-hfip). Compound **2c** proved to be quite hygroscopic and sensitive to air and moisture. Collection of elemental analysis returned a value closest to $[(Cy_2PCH_2CH_2P(O)Cy_2)Ni(Ph)(hfip)\cdot 2H_2O]$: Anal. Calc. for $C_{35}H_{57}F_7NiO_3P_2$: C, 53.93; H, 7.37. Found: C, 53.98; H, 7.28. See figures S10-13 for ^{1}H, ^{19}F, ^{13}C{^{1}H}, ^{31}P[^{1}H] NMR spectra.

[In situ synthesis of [(dcpe)NiC(O)-Ph(hfip)] (3.2c'). A J. Young NMR tube containing a 0.6 mL solution of complex **2c** in C_6D_6 or THF (20 mg, 0.028 mmol) was degassed and CO (1 atm) was added. The tube was heated for 2 hours at 50 °C to produce a mixture [6:7:1] of **3.2c**, **3.2c'** and **3.4a** respectively. ^{19}F NMR (282 MHz, C_6D_6) δ -66.24 ('quint', $^3J_{FF}$ = $^4J_{FF}$ = 9 Hz, $CF_3{}^iPr^F$), -67.22 ('quint', $^3J_{FF}$ = $^4J_{FF}$ = 9 Hz, $CF_3{}^iPr^F$), -167.619 (m, $^3J_{FF}$ = $^4J_{FF}$ = 9 Hz, $^3J_{FP}$ = 26 Hz, $^3J_{FP}$ = 120 Hz, CF^iPr^F). ^{31}P{^{1}H} NMR (121 MHz, C_6D_6) δ 45.15 (m, $^3J_{FP}$ = 120 Hz), 39.48 (m, $^3J_{FP}$ = 26

Hz). *N.B. For the reaction to go to completion (yield: 90%) 3 atm of CO should be employed.* See Figure S21-24 for ^{19}F, $^{31}P\{^{1}H\}$ NMR spectra of the reaction carried out at 1 atm: 30 % yield.

In situ synthesis of [(dppf)Ni(Ph)(hfip)] (3.2d). To a J. Young NMR tube containing a 0.6 mL solution of complex **3.2b** in THF (20 mg, 0.04 mmol) was added solid dppf (21 mg, 0.04 mmol). The solution becomes deep orange colored and was used as is. ^{19}F NMR (282 MHz, C_6D_6) δ -65.16 (d, $^{3}J_{FF}$ = 9 Hz, $CF_3{}^{i}Pr^{F}$ (2d)), -66.30 ('quint', $^{3}J_{FF}$ = $^{4}J_{FF}$ = 9 Hz, $CF_3{}^{i}Pr^{F}$ (2d')), -67.96 ('quint', $^{3}J_{FF}$ = $^{4}J_{FF}$ = 9 Hz, $CF_3{}^{i}Pr^{F}$ (2d')), -166.99 (br m, $^{3}J_{FF}$ = $^{4}J_{FF}$ = 9 Hz, $^{3}J_{FP}$ = 150 Hz, $CF^{i}Pr^{F}$ (2d)), -200.42 (sext, $^{3}J_{FP}$ = $^{3}J_{FF}$ = $^{4}J_{FF}$ = 9 Hz, $CF^{i}Pr^{F}$ (2d')). See figure S14 for ^{19}F NMR spectrum.

Synthesis of [PPh_3Cu(hfip)] (3.3a). *Method A:* The colorless complex [$(PPh_3)_3CuF$] (500 mg, 0.56 mmol) was placed in a 100 mL ampoule and mixed with 30 mL of Et_2O. The reaction vessel was attached via a three-way valve to an HFP canister with a regulator and a Schlenk line. The solution was degassed using a regular freeze/pump/thaw method. The HFP was added to the degassed solution with the regulator set to 5 psi. The reaction was left to stir at 25 °C for ~24 hours. A colorless precipitate remained over the course of the reaction. The solvent was removed *in vacuo*, 10 mL of DME was added and filtered through a Celite pad (15 mL medium pore fritted funnel) to remove unreacted Cu-F. The volatiles were removed *in vacuo* and roughly 10 mL of hexanes was added. The solid was collected (15 mL medium pore fritted funnel), triturated with hexanes (3 x 10 mL) and dried *in vacuo* to yield 391 mg of **3.3a** (0.52 mmol, 90 % based on $(PPh_3)_3CuF$). The isolated material was stored at room temperature under nitrogen. *Method B:* The red complex $[(PPh_3)CuH]_6$ (5.23 g, 16 mmol based on the monomeric unit) and PPh_3 (5.03 g, 19.2 mmol) were placed in a 1L Schlenk round bottom flask and mixed with 100 mL of benzene. The reaction vessel was attached via a three-way valve to an HFP canister with a regulator and a Schlenk line. The solution was degassed using a regular

freeze/pump/thaw method. The HFP was added to the degassed solution with the regulator set to 5 psi and the reaction left to stir at 25 °C for ~ 2 hours. The solution became a light-yellow color. The solvent was removed *in vacuo* leaving a buff powder. The powder was dissolved in DME (100 mL) and stirred vigorously. The solution was then filtered (15 mL medium pore fritted funnel) and the solvent removed *in vacuo*. The solid was collected (30 mL medium pore fritted funnel), triturated with cold Et_2O (-35 °C, 3 x 20 mL) and dried *in vacuo* to yield 9.81 g of **3.3a** (12.96 mmol, 81% based on $((PPh_3)CuH)_6$). IR: 3053(m,br), 1480(m), 1434(s,sh), 1292(w), 1231(w), 1146(w), 1116(w), 1094(w), 741(s,sh), 639(s,sh) cm^{-1}. ^1H NMR (300 MHz, C_6D_6) δ 6.88 (m, 18H, Ar), 7.31 (m, 12H, Ar). ^{19}F NMR (282 MHz, C_6D_6) δ -68.93 (br, $CF_3{}^iPr^F$), -207.98 (br, CF^iPr^F). $^{31}P\{^1H\}$ NMR (121 MHz, C_6D_6) δ -4.66 (s, PPh_3). Anal. Calc. for $C_{39}H_{30}CuF_7P_2$: C, 61.87, H, 3.99. Found: C, 63.47, H, 4.12. See figures S15-17 for ^1H, ^{19}F, $^{31}P\{^1H\}$ NMR spectra.

Synthesis of (PPh_3)(phen)Cu(hfip) (3.3b). Colorless complex $[(PPh_3)_2Cu(hfip)]$ (500 mg, 0.66 mmol) was placed in a 20 mL scintillation vial and mixed with 10 mL of Et_2O. Phen (130 mg, 0.73 mmol) was then added slowly while the solution was vigorously stirred. The reaction was left to stir for 1 hour as it changed from clear to deep orange with a significant amount of orange precipitate. Roughly 10 mL of hexanes were added and the solid was collected (15 mL medium pore fritted funnel). The solid was dissolved in 10 mL of DME, filtered through a Celite padded frit (15 mL medium pore fritted funnel), 50 mL of hexanes was added and the solid was collected, washed with hexanes (3 x 10 mL) and dried *in vacuo* to yield 356 mg of **3.3b** (0.53 mmol, 80% based on **3.3a**). The isolated material was stored at room temperature under nitrogen. A second crop of the product could be collected by crystallizing from the remaining solution at -35 °C. UV-vis (1.0 mM in benzene): λmax(ε) = 395(1276). ^1H NMR (300 MHz, C_6D_6) δ 8.88 (br, 2H, phen), 7.49 (m, 6H, PPh_3), 7.28 (m, 2H, phen), 6.99 (s, 2H, phen), 6.90 (m, 9H, PPh_3), 6.72 (m,

2H, phen). ^{19}F NMR (282 MHz, C_6D_6) δ -67.39 (d, $^3J_{FF}$ = 10 Hz, $CF_3{}^iPr^F$), -209.05 (sept, $^3J_{FF}$ = 10 Hz, CF^iPr^F). $^{31}P\{^1H\}$ NMR (121 MHz, C_6D_6) δ -4.95 (br, PPh_3). Anal. Calc. for $C_{33}H_{23}CuF_7N_2P$: C, 58.71, H, 3.43, N, 4.15. Found: C, 58.18, H, 3.51, N, 4.15. See figures S18-20 for ^{1}H, ^{19}F, $^{31}P\{^1H\}$ NMR spectra.

Perfluoro-isopropylation of Acid Chlorides, General Procedure. The copper complex, **3.3b**, (50 mg, 0.07 mmol) was loaded into an NMR tube and mixed with DMF. The benzoyl chloride (A mg, 0.05 mmol) was then added to the solution. The reaction was left to sit at room temperature for 24 hours. The reaction changed from deep orange/red to light orange with a significant amount of orange precipitate being formed. See figures S25-36 for ^{19}F NMR spectra.

PhC(O)(hfip) (3.4a). ^{19}F NMR (282 MHz, DMF) δ -73.95 (d, $^3J_{FF}$ = 7 Hz, $CF_3{}^iPrF$), -179.17 (m, $^3J_{FF}$ = 7 Hz, CF^iPr^F). GC-MS (retention time: 3.91 min.): Expected: 274.1. Found: 274.1

3,4,5-(OMe)$_3$-PhC(O)(hfip) (3.4b). ^{19}F NMR (282 MHz, DMF) δ -73.93 (d, $^3J_{FF}$ = 7 Hz, $CF_3{}^iPr^F$), -177.79 (m, $^3J_{FF}$ = 7 Hz, CF^iPr^F). GC-MS: (retention time: 7.11 min): Expected: 364.1 (100%). Found. 364.1 (100%)

***p*-Me-PhC(O)(hfip) (3.4c).** ^{19}F NMR (282 MHz, DMF) δ -74.50 (d, $^3J_{FF}$ = 7 Hz, $CF_3{}^iPr^F$), -179.19 (m, $^3J_{FF}$ = 7 Hz, CF^iPr^F). GC-MS: (retention time: 4.63 min): Expected: 288.1. Found: 288.1

***o*-Me-PhC(O)(hfip) (3.4d).** ^{19}F NMR (282 MHz, DMF) δ -74.19 (d, $^3J_{FF}$ = 7 Hz, $CF_3{}^iPr^F$), -177.46 (m, $^3J_{FF}$ = 7 Hz, CF^iPr^F). GC-MS: (rentention time: 4.34 min): Expected: 288.1. Found: 288.1

***m*-Br-Ph(CO)(hfip) (3.4e).** ^{19}F NMR (282 MHz, DMF) δ -74.50 (d, $^{3}J_{FF}$ = 7 Hz, $CF_3{}^{i}Pr^{F}$), -179.85 (m, $^{3}J_{FF}$ = 7 Hz, $CF^{i}Pr^{F}$). GC-MS: (retention time: 5.16 min): Expected: 351.9(100%), 353.9 (97.3%). Found: 351.9 (100%), 353.9 (93%)

***p*-F-PhC(O)(hfip) (3.4f).** ^{19}F NMR (282 MHz, DMF) δ -73.99 (d, $^{3}J_{FF}$ = 7 Hz, $CF_3{}^{i}Pr^{F}$), -101.26 (m, F-Ar), -178.43 (m, $^{3}J_{FF}$ = 7 Hz, $CF^{i}Pr^{F}$). GC-MS: (retention time: 3.75 min): Expected: 292.0 (100%). Found: 291.9 (100%).

***p*-Br-Ph(CO)(hfip) (3.4g).** ^{19}F NMR (282 MHz, DMF) δ -73.97 (d, $^{3}J_{FF}$ = 8 Hz, $CF_3{}^{i}Pr^{F}$), -178.90 (d'multiplet', $^{3}J_{FF}$ = 8Hz, $CF^{i}Pr^{F}$). GC-MS: (retention time: 5.22 min): Expected: 351.9 (100%), 353.9 (97.3%). Found: 352.1 (100%), 354.0 (90%).

***p*-CN-PhC(O)(hfip) (3.4i).** ^{19}F NMR (282 MHz, DMF) δ -73.9 (d, $^{3}J_{FF}$ = 7 Hz, $CF_3{}^{i}Pr$), -179.45 (d'multiplet', $^{3}J_{FF}$ = 7Hz, $CF^{i}Pr^{F}$). GC-MS: (retention time: 5.30 min). Expected: 299.0 (100%). Found. 299.1 (100%).

***p*-NO_2-PhC(O)(hfip) (3.4j).** ^{19}F NMR (282 MHz, DMF) δ -73.87 (d, $^{3}J_{FF}$ = 7 Hz, $CF_3{}^{i}Pr^{F}$), -179.30 (m, $^{3}J_{FF}$ = 7 Hz, $CF^{i}Pr^{F}$). GC-MS: N/A.

***o*-NO_2-PhC(O)(hfip) (3.4k).** ^{19}F NMR (282 MHz, DMF) δ -73.90 (d, $^{3}J_{FF}$ = 7 Hz, CF_3iPrF), -179.45 (m, $^{3}J_{FF}$ = 7 Hz, $CF^{i}Pr^{F}$). GC-MS: N/A.

2-Naph(CO)iPrF (3.4l). ^{19}F NMR (282 MHz, DMF) δ -74.21 (d, $^{3}J_{FF}$ = 7 Hz, $CF_3{}^{i}Pr^{F}$), -176.83 (m, $^{3}J_{FF}$ = 7 Hz, $CF^{i}Pr^{F}$). GC-MS: (retention time: 6.70 min): Expected: 324.0 (100%). Found: 324.1 (100%).

2-Tp(CO)iPrF (3.4n). ^{19}F NMR (282 MHz, DMF) δ -74.32 (d, $^{3}J_{FF}$ = 7 Hz, $CF_3{}^{i}Pr^{F}$), -179.83 (m, $^{3}J_{FF}$ = 7 Hz, $CF^{i}Pr^{F}$). GC-MS: (retention time: 4.20 min): Expected: 280.1 (100%). Found: 280.0 (100%).

Synthesis of *p*-F-PhCH$_2$(hfip) (3.5a). ^{19}F NMR (282 MHz, DMF) δ -75.86 (d, $^{3}J_{FF}$ = 7 Hz, $CF_3{}^{i}Pr^{F}$), -115.91 (m, F-Ar), -182.76 (t sept, $^{3}J_{FH}$ = 24 Hz, $^{3}J_{FF}$ = 7 Hz, $CF^{i}Pr^{F}$). GC-MS: (retention time: 3.82 min) Expected: 278.0 (100%). Found: 278.1 (100%)[405,406]. See figures S36 for ^{19}F NMR spectra.

Synthesis of *p*-F-PhCH(OH)(hfip) (3.5b). ^{19}F NMR (376.5 MHz, C_6D_6): -70.40 ('quint.', $^{3}J_{FF}$ = $^{4}J_{FF}$ = 9 Hz, $CF_3{}^{i}Pr^{F}$), -73.23 ('quint.', $^{3}J_{FF}$ = $^{4}J_{FF}$ = 9 Hz, $CF_3{}^{i}Pr^{F}$), -111.51 (m, F-Ar), -179.55 (d sept, $^{3}J_{FH}$ = 12 Hz, $^{3}J_{FF}$ = 9 Hz, $CF^{i}Pr^{F}$). GC-MS: (retention time: 5.01 min) Expected: 294.0 (100%). Found: 294.0 (100%)[407-409]. See figures S37-38 for ^{19}F NMR spectra.

3.5.2. Computational Methods

The geometries were optimized at the density functional theory (DFT)[410] level with the hybrid B3LYP[411,412]with the DFT-optimized DZVP2 basis set[413] for H, N, C, F and P atoms and aug-cc-pVDZ-PP[414,415] basis sets for M = Ag, Ni and Cu using Gaussian09 program system.[416] Vibrational frequencies were calculated to show that the structures were minima. The B3LYP/DZVP2/aug-cc-pVDZ-PP(M) geometries were used to predict the NMR chemical shifts for F (^{19}F-NMR) and P (^{31}P-NMR) in C_6H_6 using the ADF program system[417,418] with the BLYP[419] functional and the TZ2P basis set in ADF[420]. Scalar relativistic effects were included at the two-component zero-order regular approximation (ZORA) level for the NMR calculations.[421-423]The ^{19}F-NMR and ^{31}P-NMR chemical shifts are reported relative to their specific standard $CFCl_3$ and H_3PO_4 calculated at the same level.

Using the gas phase geometries, the solvation free energies in DMF at 298 K were calculated using the self-consistent reaction field (SCRF) approach[424] with the COSMO parameters[425,426]as implemented in Gaussian 09[416] at the same B3LYP/DZVP2 level of theory using the COSMO radii. The Gibbs free energy in DMF solution, ΔG_{DMF}, was calculated from Eq. 1.

$$\Delta G_{DMF} = \Delta G_{gas} + \Delta G_{solv} \quad (1)$$

where ΔG_{gas} is the gas phase free energy and ΔG_{solv} is the solvation free energy in DMF. A dielectric constant of 37.22 corresponding to that of bulk DMF was used in the COSMO calculations.

The Natural Population Analysis based on the Natural Bond Orbitals (NBOs)[427,428]using NBO6[429,430]with wavefunctions are calculated at the B3LYP/DZVP2/aug-cc-pVDZ-PP(M) density functional theory level using Gaussian09.

The calculations were performed on a Xeon-based Dell Linux cluster at the University of Alabama, and a local AMD Opteron-based and Intel Xeon-based Linux cluster from Penguin Computing.

Chapter 4

4. Published Contribution

Baker, R. T., Andrella, N. O. Process for Preparation of Hydrofluoroalkenes by Selective Catalytic Consecutive Hydrodefluorination. WO2018039794, March 8, 2018

Selective Copper Complex-Catalyzed Hydrodefluorination of Fluoroalkenes and Ally Fluorides. A Tale of Two Mechanisms.

N. O. Andrella, N. Xu, B. M. Gabidullin, C. Ehm and R. T. Baker *J. Am. Chem. Soc.* **2019**, *141*, 11506 - 11521.

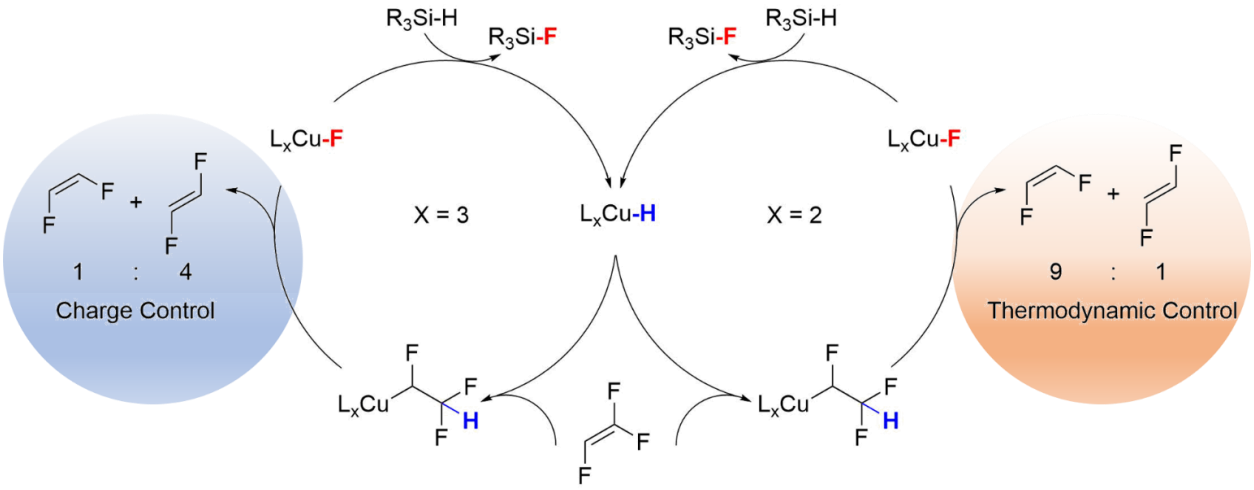

Andrella, Ehm, and Baker wrote the manuscript. Andrella performed most of the experiments, Xu was responsible for some of the reaction optimization.

Ehm was responsible for Computational Studies

Gabidullin was responsible for X-ray diffraction resolution.

4.1. Abstract

The transition to more economically friendly small-chain fluorinated groups is leading to a resurgence in the synthesis and reactivity of fluoroalkenes. One versatile method to obtain a variety of commercially relevant hydrofluoroalkenes involves the catalytic hydrodefluorination (HDF) of fluoroalkenes using silanes. In this work, it is shown that copper hydride complexes of tertiary phosphorus ligands (L) can be tuned to achieve selective multiple HDF of fluoroalkenes. In one example, HDF of hexafluoropropene dimer affords a single isomer of heptafluoro-2-methylpentene in which five fluorines have been selectively replaced with hydrogens. DFT computational studies suggest distinct HDF mechanisms for L_2CuH (bidentate or bulky monodentate phosphines) and L_3CuH (small cone angle monodentate phosphines) catalysts, allowing for stereocontrol of the HDF of trifluoroethylene

4.2. Introduction

The synthesis and chemistry of fluorinated alkenes [FAs] are currently experiencing a renaissance[309, 432-440] due to the need for smaller fluorinated chains[441-444] in materials applications (cf. environmental persistence of long-chain fluorocarbons)[443,444] and the development of economical late-stage fluoroalkylation processes,[395,438-440]including cross-metathesis.[445] Moreover, selected unsaturated hydrofluoroalkenes have been identified as low global warming potential refrigerants [e.g. $H_2C{=}CFCF_3$, R-1234yf] and blowing agents [e.g. (Z)-$CF_3HC{=}CHCF_3$, R-1336mzz(Z)] when compared to their saturated counterparts [i.e. hydrofluorocarbon refrigerants and blowing agents, such as R-134a, R-401a, R-245fa, etc.].[446] Most currently used synthetic routes to the latter employ well-established technologies (i.e. halogen exchange, dehydro-halogenation) that require harsh/caustic conditions, HF and expensive reactors.[446] Catalytic hydrodefluorination [HDF] represents a potential

alternative.[353,354] Selective and potentially consecutive C-F bond activation and substitution by C-H bonds could provide new routes to these valuable compounds and additional previously unavailable FAs.

Detailed studies of metal-catalyzed HDF have been focused largely on fluoroarenes but these reaction conditions are not easily transposed to FAs, as their mechanisms can be quite different. For example, fluoroarene HDFs generally proceed by attack of the hydride at the C_{α}-F carbon (Scheme 4.1a,b) [400,447-451] while FAs typically undergo hydride attack at the C_{β}-F carbon (Scheme 4.1c,d). To further complicate matters, the addition of M-H to the FA can proceed either via the more traditional insertion mechanism (Scheme 4.1c) or, as is shown herein, by nucleophilic addition of the hydride, generating an intimate ion pair (Scheme 4.1d). It can be expected that the disparity between the activation energies of these processes could lead to significantly different outcomes, especially when considering product distribution in a multi-HDF reaction

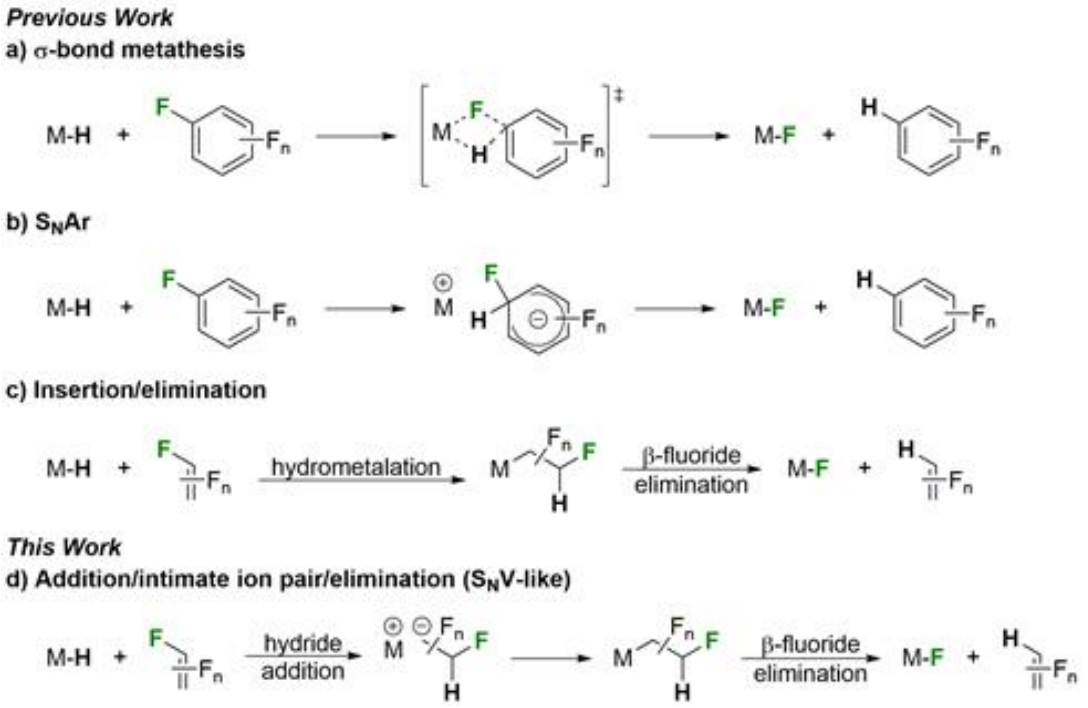

Scheme 4.1. HDF of fluoroarenes *vs* fluoroalkenes.

Furthermore, selectivity issues with HDF of fluoroarenes are less problematic because, as fluorine is removed, HDF becomes more difficult. On top of this, the use of directing groups can increase selectivity. However, such strategies are not necessarily available when using FAs as substrates.[452,453] Product selectivity must arise from the inherent reactivity of the catalyst or rely on thermodynamic distribution of isomers with the former often leading to uncontrolled multi-HDF and the latter leaving little control for obtaining the desired product.

In studies of HDF of hexafluoropropene (HFP, **4.1a;** Scheme 4.2), Jones *et al.* reported the use of stoichiometric zirconocene dihydride for consecutive substitution but selectivity could only be achieved with careful control of the Zr/FA stoichiometry.[454456] Similarly, using a stoichiometric ruthenium hydride complex, Whittlesey and co-workers converted **4.1a** to a 5:3 mixture of mono- and dihydrodefluorinated products.[455] Holland *et al.* demonstrated the iron complex-catalyzed HDF of FAs although turnover numbers (ToNs) were limited and high

temperature was required (100 °C).[456] In contrast, Lentz and co-workers showed that Ti-based catalysts are active under ambient conditions, ToNs up to 125.[457] However, dihydrodefluorination was only observed in trace amounts. Another contribution from the Lentz group showed that HDF of FAs using Al or Ga hydrides can be catalyzed by N- and O-donors with ToNs up to 87.[458-460]

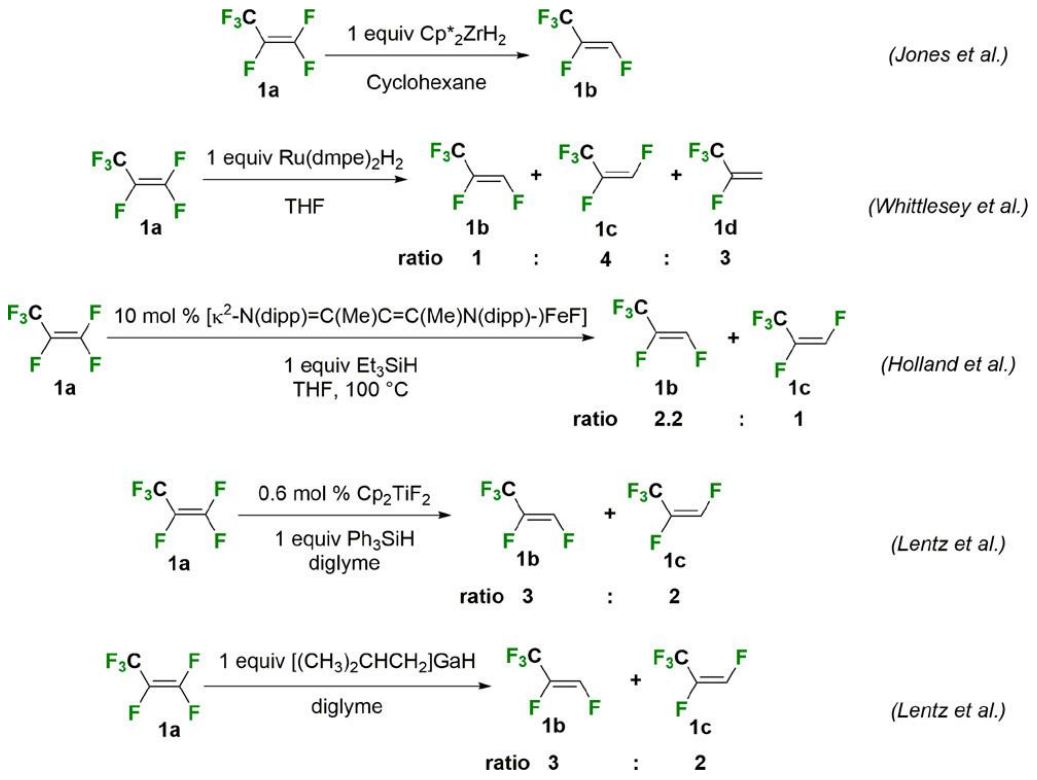

Scheme 4.2. Some examples of the HDF of HFP

Recent studies have identified the potential of copper complexes for catalyzed HDF of FAs (Scheme 4.3).[461-464] For example, the groups of Shi and of Ito have reported the HDF of *gem*-difluoroalkenes to *E*- and *Z*-terminal monofluoroalkenes with high stereoselectivity using copper(I) catalysts and base. Building on this body of knowledge, we recently reported that isolated phosphine copper hydride complexes readily insert HFP, followed by rapid β-fluoride elimination to yield Cu-F and 1,2,3,3,3-pentafluoropropene (PFP, **4.1b, 4.1c**). Using similar

methodology employing silanes to regenerate Cu-H from Cu-F, a catalytic HDF could be established (Scheme 4.3).

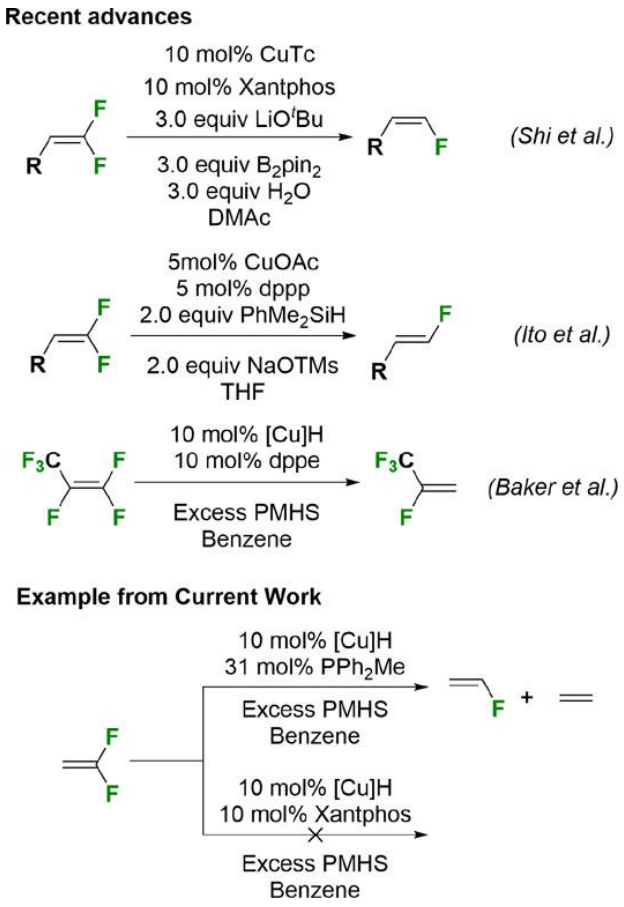

Scheme 4.3. Copper complex-catalyzed HDF of fluoroalkenes. [PMHS = polymethylhydrosiloxane]

As such, described herein is the reactivity of P-ligated [Cu]-H with various FAs, development of tunable selectivity in Cu complex-catalyzed HDF, and discovery of a new catalytic HDF pathway. The latter allows for stereocontrol with some FAs and for the HDF of less electrophilic FAs, like vinylidene difluoride (**4.2e**) (Scheme 4.3, **bottom**).

4.3. Results and Discussion

4.3.1. Catalyzed HDF Reactions.

Ligand Screen.

Extending our previous work to include catalytic HDF, excess dimethylphenyl silane (vs **4.1a**) was added to the reaction of a catalytic amount of $[CuH(PPh_3)]_6$ (10 mol %) with **4.1a** at 45 °C for 8 h. Heating the reaction at 45 °C provided the optimal rate, as higher temperatures were found to decompose the catalyst (reaction turned brown) or lead to HFP oligomerization. As expected, this reaction led readily to a mixture of *E*- and *Z*-1,2,3,3,3-pentafluoropropene isomers (PFP, **4.1b,c**) but, unexpectedly, also 2,3,3,3-tetrafluoropropene (**4.1d**), in a rare double HDF (Table 4.1, entry 1). It is notable that substitution of (*E*)-PFP, **4.1b**, is significantly favored vs the *Z*-isomer, **4.1c**, such that **4.1b** has been entirely consumed while **4.1c** still remains. No additional HDF was observed after another 24 h. No differences in reactivity were observed when employing less expensive tetramethyldisiloxane (TMDS) (Table 4.1, entry 2) or even moisture-tolerant waste product polymethylhydrosiloxane (PMHS) (Table 4.1, entry 3). Similarly, the change in solvent had little impact on the reaction outcome, except for DMF, which gave the same product ratios independent of ligand, followed by rapid catalyst deactivation (see Supporting Information (SI) Table S1). However, while toluene and tetrahydrofuran (THF) both worked well on NMR scale they failed to match benzene for consistent results when scaled to 1 L of HFP. Monitoring the conversion of **4.1a** by ^{19}F NMR spectroscopy showed that addition of 3 equiv or even excess PPh_3 gave no change in the HDF product slate (Table 4.1, entries 4,5)

Table 4.1. Ratios of hexafluoropropene HDF products.

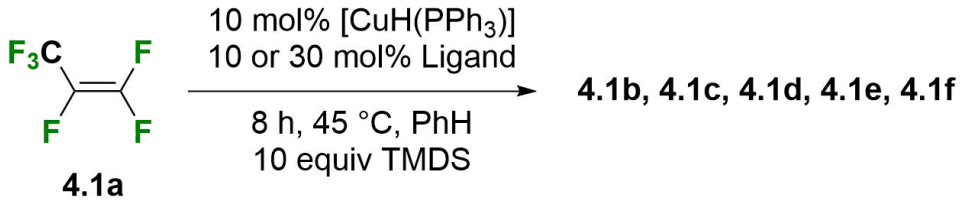

Entry	Ligand	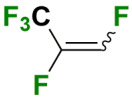		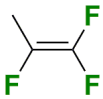	
		4.1b/1c	**4.1d**	**4.1e**	**4.1f**
1	None[a]	1[e]	1.7		
2	None	1[e]	1.7		
3	None[b]	1[e]	1.6		
4	PPh_3	1[e]	1.5		
5	PPh_3[c]	1[e]	1.5		
6	P(*o*-tolyl)$_3$	9.5	1		
7	*t*BuXphos	1[e]	1.2		
8	PCy_3	1[e]	1.3		
9	dppe		11		1
10	dppf		1		3.0
11	Xantphos	1	2.4		

12	$P(OEt)_3$			1	2.4
13	$P(OPh)_3$[a]	1			
14	P(O-*o*-tolyl)$_3$	35	1		

[a]$PhMe_2SiH$ was used in place of TMDS. [b]PMHS was used in place of TMDS; N.B. PMHS forms a biphasic mixture with benzene. [c]60 mol % of PPh_3. [d]Complete conversion of HFP not achieved after 8 h. [e]only Z-isomer **4.1c** was observed. [f]Ratios are based on ^{19}F NMR integration of products vs internal standard. All reactions gave 100% conversion of HFP unless indicated otherwise. Following the reaction, the headspace of the reaction was sampled to confirm solution product distribution.

In contrast, the HDF product distribution showed a pronounced ligand effect (Table 4.1). When employing bulky electron-rich ligands, like tBuXphos or PCy_3 (Table 4.1, entries 7,8), similar ratios to that of no added ligand were observed. Using the bulky aromatic phosphine, P(*o*-tolyl)$_3$, however, the reaction converted HFP to **4.1b/c** isomers and then quickly ceased to be functional. This was based qualitatively on a color change from orange to green and, quantitatively, upon addition of more HFP that failed to react. For **4.1a**, bidentate ligands generated more efficient HDF catalysts. Bis(phosphines) dppe, dppf and Xantphos all readily converted **4.1a** to **4.1d** and even 1,1-difluoropropene, **4.1f**, although the latter likely arises from HDF of 1,1,2-trifluoropropene, **4.1e**. While dppe provided the highest selectivity for **4.1d**, Xantphos produced **4.1f** more slowly than dppf. Interestingly, π-acidic triethylphosphite ($P(OEt)_3$) gave selective tetra-substitution, yielding primarily **4.1f** at the same rate as dppf. This increased efficiency of the $P(OEt)_3$/CuH catalytic mixture is contrary to the expected activity increase with hydricity using the more σ-donating phosphines, dppf and Xantphos. Both $P(OPh)_3$ and P(O-*o*-tolyl)$_3$ provided significantly reduced reactivity, however, suggesting ligand size is also an important factor.

Substrate Scope.

Using these optimized conditions with dppf or Xantphos, the scope was investigated for the HDF reaction of various perfluorinated substrates (Scheme 4.4). Both chlorotrifluoroethylene (**4.3a**) and HFP analogue, trifluoromethyl trifluorovinyl ether (**4.4a**), yielded a 4:1 mixture of *cis*:*trans* 1,2-difluoroethylene (**4.2c,d**), respectively. During the first few hours of the latter reaction trifluoromethyl 1,2-difluorovinyl ether (**4.4b**) was observed as a single isomer but then eventually consumed, presumably via β-OCF_3 elimination (Scheme 4.5). Isomer **4.2c** is presumably formed preferentially due to the *gauche* effect[465] as the *cis* isomer is also the most thermodynamically stable, suggesting a late transition state.

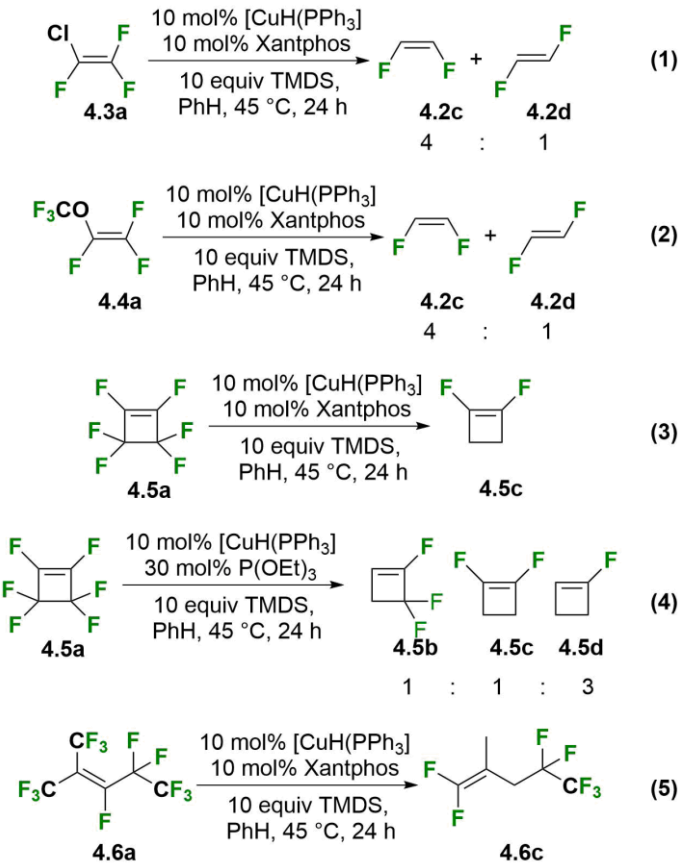

Scheme 4.4. Selective and multiple HDF of various perfluorinated substrates.

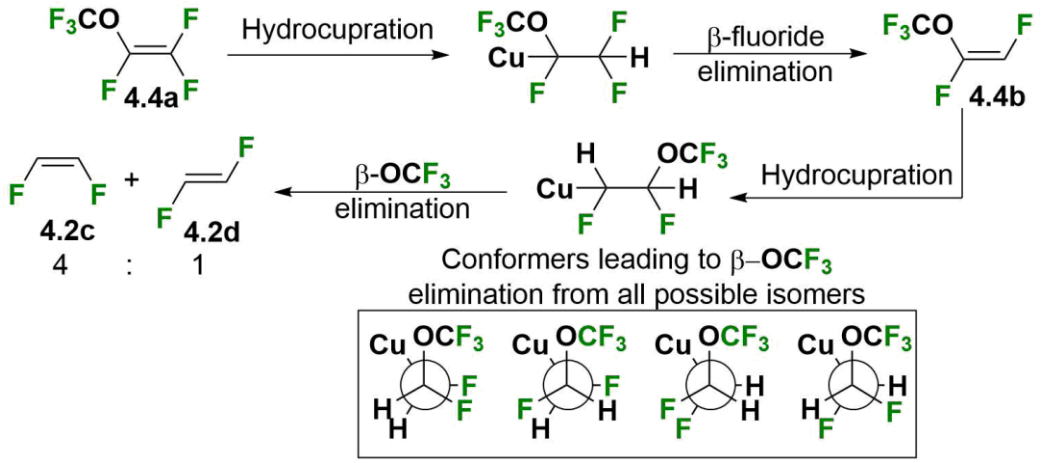

Scheme 4.5 Top: HDF of 4a leading to a 4:1 mixture of **4.2c,d** via β-OCF_3 elimination. **Bottom:** The gauche effect increasing selectivity for **4.2c**.

The HDF of perfluorocyclobutene (**4.5a**) and HFP dimer, perfluoro-2-methylpent-2-ene (**4.6a**) proceeded readily, yielding multi-HDF products. FA **4.5a** was selectively converted to 1,2-dicyclobutene (**4.5c**) via triple HDF whereas **4.6a** underwent quintuple HDF to generate the di-alkyl substituted *gem*-difluoroalkene **4.6c**, exclusively. The isomer of **4.6a**, perfluoro-4-methylpent-2-ene (**4.6b**), also underwent multiple HDF but in an unselective manner, generating multiple products (see the SI for details).

Switching to the use of $P(OEt)_3$, the HDF of **4.5a**, produced a mixture of **4.5b**, 1,2-difluorocyclobutene (**4.5c**) and 1-fluorocyclobutene (**4.5d**) in a 1:1:3 ratio before catalyst deactivation. As with **4.1a**, this ligand produced a significantly more active HDF catalyst than the electron-donating bis(phosphines). FA **4.6a**, as above, yielded only **4.6c**, demonstrating that this product is too electron-rich to undergo further HDF.

The above electrophilic substrates (i.e. **4.1a**, **4.5a**, **4.6a** and **4.6b**) did not provide an avenue to test the impact of stronger σ-donating ligands as they react readily with electron-rich phosphines with cone angles smaller than tricyclohexylphosphine (PCy_3).[437,466,467]

Likewise, the decomposition of CuH complexes containing N-heterocyclic carbenes and nitrogen chelates is well documented, excluding these ligands from consideration.[468-470] With this in mind, the HDF of less electrophilic trifluoroethylene, **4.2b**, was performed. Using the optimized reaction conditions and the Xantphos/CuH catalytic mixture, **4.2b** was readily converted to *cis*:*trans* (**4.2c:4.2d**) in a 7:1 ratio, reflecting the thermodynamic preference, whereas use of $P(OEt)_3$ gave no reaction. Using three equivalents of basic phosphine $PMePh_2$, however, inverted the **4.2c:4.2d** ratio to 1:3.7. As with HFP, hydride addition always occurs regioselectively, suggesting that Cu-H addition to **4.2b** occurs with the FHC= fragment oriented towards the copper.

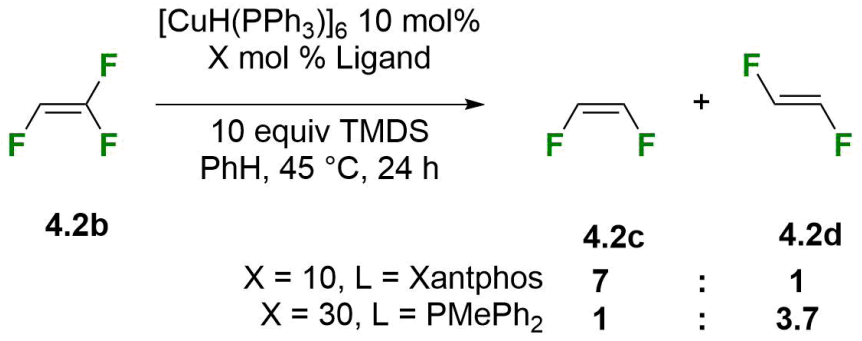

Scheme 4.6. Ligand-induced inversion of stereoselectivity in HDF of trifluoroethylene

In contrast to the above substrates, tetrafluoroethylene (**4.2a**) reacts with the copper hydride complexes to yield thermally stable copper 1,1,2,2-tetrafluoroethyl complexes.[229,230] As previously reported, addition of a Lewis acid (or base) is required to induce β-fluoride elimination,[439] presumably via an outer-sphere fluoride-elimination mechanism (Scheme 4.7).

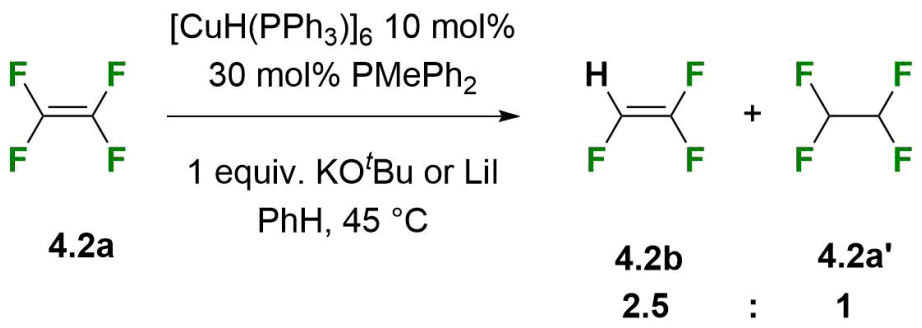

Scheme 4.7. HDF of 2a leading to a mixture of **4.2b**, **4.2a'** and incomplete conversion of **4.2a**.

Cu-tetrafluoroethyl complexes.

Interestingly, the Cu tetrafluoroethyl complex with $PMePh_2$ can be easily and safely prepared using TFE Safe Supply™ (See experimental). Treatment of Stryker's reagent, 3 equiv. $PMePh_2$ and 1.5 equivalents of tetramethyldisiloxane [TMDS] with **4.2a**:CO_2 in benzene at 70 °C afforded the Cu-CF_2CF_2H complex [$(PMePh_2)_3Cu(CF_2CF_2H)$] (**4.7a**) in good yield (70%) and excellent purity [>90%, Scheme 4.8]. The use of this methodology with Xantphos or $P(OEt)_3$ did not yield the desired product. The synthesis of the former complex was instead carried out with limonene-inhibited **4.2a**. In our first attempt, [(Xanpthos)Cu(CF_2CF_3)] (**4.7b'**) was formed concomitantly with [(Xantphos)Cu(CF_2CF_2H)] (**4.7b**). Hence, to avoid this byproduct 10 % TMDS was added to prevent its formation. Using this approach **4.7b** could be successfully prepared.

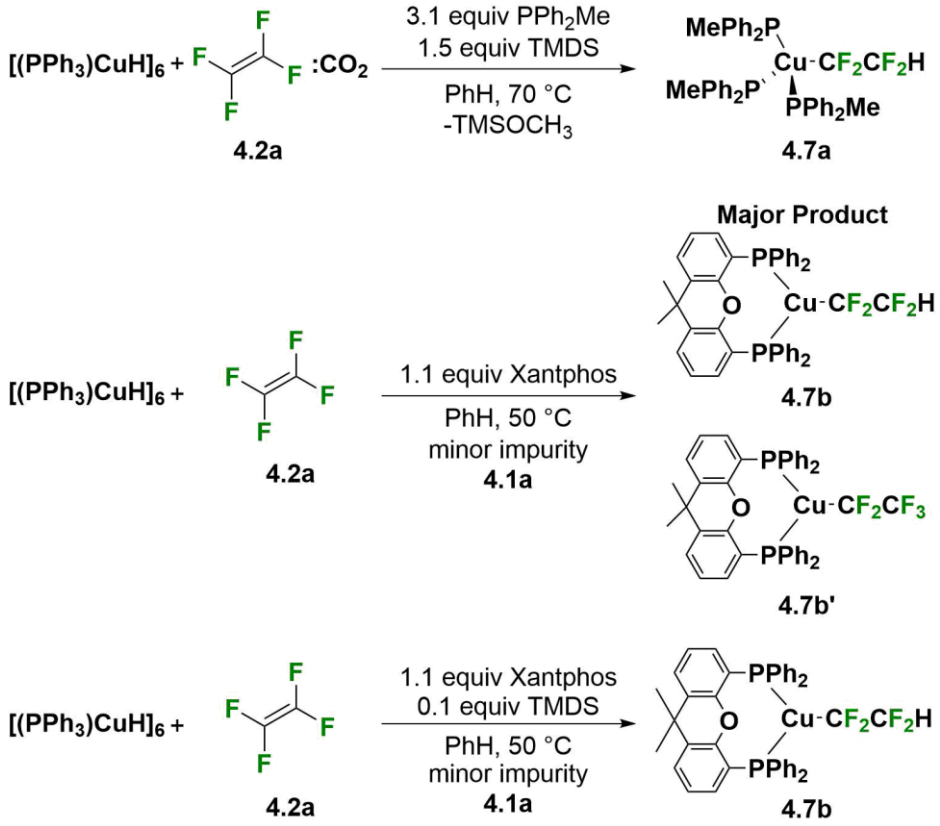

Scheme 4.8. Synthesis of complexes **4.7a** and **4.7b**.

The ^{19}F NMR spectrum of **4.7a** in C_6D_6 displays two resonances which can be easily differentiated based on their J_{FH} coupling constants: CF_2H = 50 Hz and CF_2R < 1 Hz (unresolved). The ^{31}P NMR spectrum contains a broad singlet at -8 ppm and the molecular structure was confirmed by single crystal X-ray diffraction (Figure 4.1). Again, the disparity between the reactivity of the ligands based on cone-angle should be highlighted, although, another layer of complication arises considering only $PMePh_2$ could effectively reduce CO_2, showing that σ-donating phosphines are important in the reduction of less electrophilic substrates.

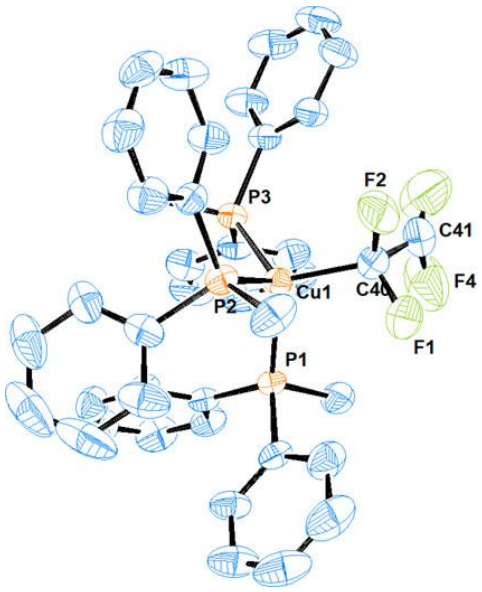

Figure 4.1. ORTEP representation of the molecular structure of **4.7a**. Thermal ellipsoid probabilities are set to 35%, hydrogen atoms omitted for clarity.

With three seemingly unrelated observations in hand - a) Using $P(OEt)_3$ in the HDF of HFP (**1a**) generates an active HDF catalyst on par with dppf, b) Using a small cone-angle, strong σ-donating phosphine ($PMePh_2$ vs $P(OEt)_3$) allows for HDF of **4.2b**; and c) Changing from Xantphos to $PMePh_2$ inverts isomer ratios of **4.2c,d** in the HDF of **4.2b** from 7:1 to 1:3.7 - mechanistic studies and computations were carried out in an attempt to consolidate them.

4.3.2. Mechanistic DFT Studies.

To gain deeper insight into the HDF mechanism(s) in these P-ligated copper-hydride systems, we conducted solvent corrected (PCM: benzene) DFT studies at the TPSSh(PCM)/TZ/TPSSTPSS-(PCM)/DZ level of theory. For details and expected accuracy of the method see computa-tional details and supporting information. A model phos-phine ligand, L = PMe_3, was chosen to fully analyze possi-ble reaction pathways in the LCu-H, L_2Cu-H and L_3Cu-H systems in the HDF of three prototypical FAs of varying fluorine content, i.e. tetrafluoroethylene (2a), trifluoroeth-ylene (2b) and 1,1-difluoroethylene (2e). Relevant transi-

tion states (TS) and resting states (RS) were then analyzed for realistic systems, i.e. L = PPh_3, $PMePh_2$ and PMe_2Ph, dppe and Xantphos, to understand the pronounced influ-ence of the ligands on the selectivity of HDF of **4.2b**.

PMe_3 model system. 4.2a.

We considered HDF in the present systems to take place in an LCu, L_2Cu and/or L_3Cu system (L = PMe_3) via a) insertion-elimination sequence,[471] b) 'S_NV'-like H-addition as for example observed for early transition metal- catalyzed HDF followed by Cu-C bond formation and subsequent F-elimination[452] c) single electron transfer,[472,473] d) σ-bond metathesis [400,445,448,452,474-478] or e) 'S_NV'-like H-addition followed by immediate F-elimination.[452,460,476] The latter two mechanisms could be quickly excluded; a *σ*-bond metathesis TS could not be located and ion pairs are stable, showing no tendency for immediate F-elimination. SET can be excluded based on the known low electron affinity of (per)fluorinated alkenes.[450,452] An oxidative addition – reductive elimination pathway[452] can be excluded based on the experimental observation of **4.7a,b**. Both insertion and H-addition pathways for hydrometallation could be found.

The first two PMe_3 ligands in $(PMe_3)_3Cu$-H (**A**) are relatively weakly bound (ΔG_{323K} = 7.8 + 5.1 kcal/mol). Nonetheless, this penalty raises the barrier for HDF in the LCu-H system significantly over the corresponding barriers in the L_2 and L_3 systems (see supporting information). Therefore, we will focus the discussion on the competition between L_2 and L_3 HDF pathways Figure 4.2 shows important transition states and Figure 4.3 the PES for the two competing mechanisms for the example of **4.2a**.

Hydrometallation in the L_2 system starts with dissociation of one phosphine ligand from L_3Cu-H (**A**, +7.8 kcal/mol) to form L_2Cu-H (**B**). Thereafter, coordination of **4.2a** (alkene coord.

TS(B-C), +12.6 kcal/mol) forming Cu-olefin complex **C** followed by alkene insertion into the Cu-H bond (HM **TS(C-D)**, +9.1 kcal/mol) represents the lowest energy pathway for HDF to form $L_2Cu\text{-}CF_2CF_2H$ (**D**).

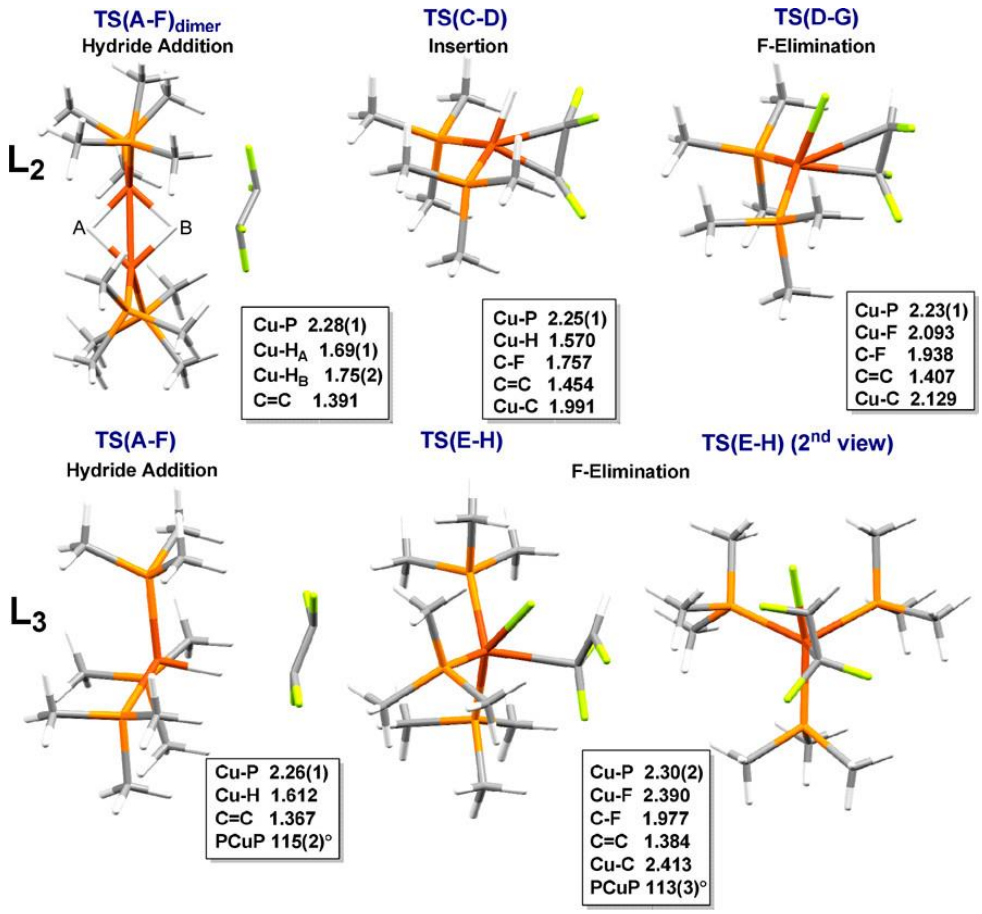

Figure 4.2. Graphical depiction of important transition states in the HDF system of **4.2a** with $L_3/L_2Cu\text{-}H$. L = PMe_3. Bond distances in Å, bond angles in deg. Level of theory TPSSTPSS(PCM)/DZ. Solvent = benzene.

The insertion barrier from the Cu-H(alkene) complex **C** is very small (+3.2 kcal/mol) and overall, the coordination **TS(B-C)** is rate limiting in this process. Nucleophilic H-addition via **TS(B-D)**, although possible in the L_2 system, is associated with a much higher barrier (+17.7 kcal/mol; see discussion of the L_3 system for further details).

Within the L_2 hydrometallation pathway, alkene coordination is endergonic, but irreversible, as insertion from the alkene complex has a much lower barrier than dissociation of the alkene. That insertion of the FA into the Cu-H bond is associated with only a very small barrier is unsurprising; **TS(C-D)** is geometrically very early compared to the Cu-H(alkene) complex **C** (Cu-H bond length + 0.01 Å, see also Figure 4.3), as coordination to the late TM copper has already activated the C=C double bond and Cu-H bonds are rather weak (~ 60 kcal/mol).[478] Hydrometallation leads to **D** (-38.7 kcal/mol), which can be further stabilized by coordination of another phosphine forming $L_3Cu\text{-}CF_2CF_2H$ (-50.4 kcal/mol, **E**).

HDF can also proceed without the release of one phosphine ligand in the L_3 system. Unlike in the L_2 system, where synchronous hydrometallation via insertion is favored, insertion into the Cu-H bond in the L_3 system proceeds via a two-step, asynchronous, mechanism. Nucleophilic H-addition in this system via TS(A-F) has a very low barrier (+7.4 kcal/mol) and proceeds to a contact ion pair (CIP F, -17.7 kcal/mol); the barrier is lower than all barriers in the L_2 system, making this the preferred HDF pathway. The low barrier can be understood as a direct result of the destabilization of a C=C double bond by multiple fluorine substituents and the weak Cu-H bond.[479,480] Coordination of a third phosphine stabilizes the forming cation in the TS with respect to the L_2 system. TS(A-F) is essentially ‘dagger-like’ and requires minimal space around Cu. Forming a solvent-separated ion pair (SIP, +17.5 kcal/mol) from the CIP is associated with a significant increase in energy (see supporting information). However, full separation is not necessary, as slight reorientation of the anion leads to formation of a Cu-C bond, ultimately yielding $L_3Cu\text{-}CF_2CF_2H$ (E).

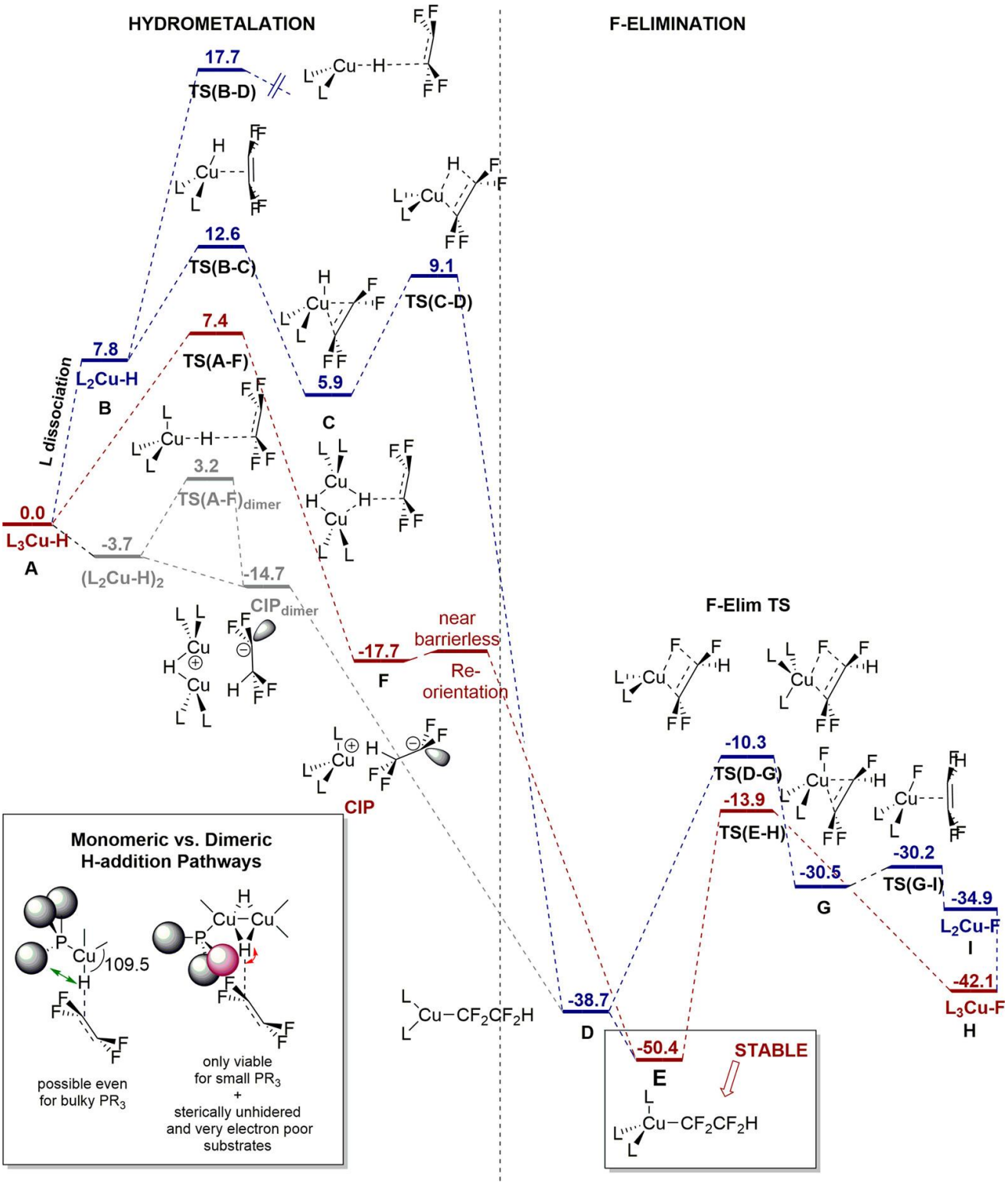

Figure 4.3. PES for HDF of tetrafluoroethylene (**4.2a**) with L_3/L_2Cu-H. L = PMe_3. L_2 pathway in blue, L_3 pathway in maroon. CIP = contact ion pair. Level of theory TPSSh-D0(PCM)/TZ// TPSSTPSS(PCM)/DZ. T = 323 K. p = 0.1 bar. Solvent = benzene. Gibbs free energies in

kcal/mol. PES after the high energy TS12-14 on the H-addition pathway in the L_2 system not shown.

Insertion of **4.2a** into the Cu-H bond is irreversible, as the reverse elimination barriers are > 58 kcal/mol. From the resting state **E** (-50.4 kcal/mol), F-elimination can again proceed, after phosphine decoordination, via L_2 **TS(D-G)** (-10.3 kcal/mol) or, interestingly, also directly from the L_3 species (-13.9 kcal/mol) via **TS(E-H)**. The latter one is preferred for formation of **4.2b**. The lowest F-elimination pathway is still associated with a significant barrier (36.5 kcal/mol); moreover, elimination is endergonic (+8.3 kcal/mol). In line with experiment, where **4.7b** was isolated, **E** is therefore predicted to be stable under experimental conditions with respect to F-elimination and Lewis acids need to be added to shift the equilibrium to the product side by removal of fluoride via salt metathesis, enforcing HDF of **4.2a**. The F-elimination **TS(E-H)** in the L_3Cu system is rather unusual and geometrically not late like the corresponding **TS(D-G)** in the L_2 system but rather central. On the one hand, the Cu-C bond is much more elongated (15 2.016, 14 1.979, **TS(E-H)** 2.413, **TS(D-G)** 2.129 Å) and the forming C=C bond is shorter (**TS(E-H)** 1.384, **TS(D-G)** 1.407 Å). On the other hand, the forming Cu-F bond is much longer in the L_3 system (**TS(E-H)** 2.390, **TS(D-G)** 2.093 Å). Substantial charge separation occurs in both TS, (see Table 4.2**),** with the NPA charge on the eliminating F exceeding 0.6 e^-; charge separation is somewhat more extensive in the L_3 **TS(E-H)** and leads to a slightly higher dipole moment (5.6 D in L_2 vs. 6.1 D in L_3).

The extensive charge delocalization in the TS explains the experimentally observed rate dependence on the solvent. Wiberg bond indices[481,482] support the notion that TS(E-H) is central in the L_3 system and less covalent, as WBIs for the Cu-F, Cu-C and F-C bonds are < 0.24, in all cases lower than in the corresponding L_2 system TS(D-G). In contrast to L_2, where elimination proceeds to RS G with copper-coordinated alkene, elimination in the L_3 system

proceeds directly to L_3Cu-F (H) and the separated olefin **4.2b**. Decoordination of the olefin via TS(G-I) leads to L_2Cu-F I, which can be further stabilized via coordination of a third phosphine to form H. Overall, F-elimination in both the L_2 and L_3 system is reminiscent of the H-addition pathway in the L_3 system, which similarly shows extensive charge separation.

Table 4.2. NPA charges (q) on fragments and Wiberg bond indices (WBI) in L_2 TS(D-G) and L_3 TS(E-H) Elimination TS.

	q (e^-)		WBI		
Fragment	L_2	L_3	Bond	L_2	L_3
Cu	-0.02	-0.24	Cu-F	0.28	0.15
F_2C=CFH	-0.02	-0.05	Cu-C	0.34	0.24
F	-0.62	-0.67	F-C	0.37	0.23
			C=C	1.38	1.5

The first coordination sphere of copper in the F-elimination TS(E-H) can essentially be described as five-coordinate in the L_3 system, consisting of three phosphines, a FA and a fluoride ligand. However, Cu d^{10} does not possess the ability to engage in sp^3d-hybridization required for trigonal-bipyramidal binding of five ligands. The geometry of the P_3Cu fragment barely changes from the resting state E; P-Cu-P angles are 113(3)°for RS and TS, WBIs for the Cu-P bonds in TS(E-H) are with 0.72(1) even higher than in the L_2 system TS(D-G) with 0.64(1). Therefore, it appears that the system is better described as tetrahedral, with one coordination site being simultaneously occupied by both a fluoride and the alkene in the F-elimination TS (Figure 4.4). Both the HOMO and the HOMO-1 are concentrated on the Cu, F and the alkene, which supports

this notion. The H-addition TS in the L_2 system is substantially higher in energy, as it only benefits from stabilization of the partial cationic charge by two phosphines, not three as in the L_3 system.

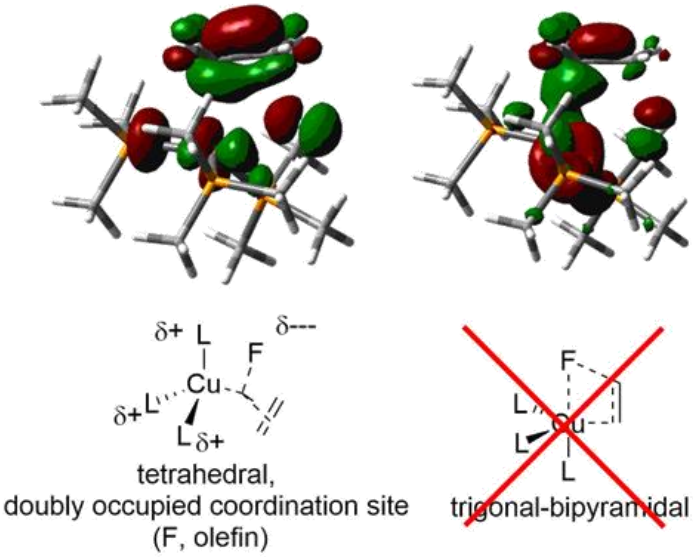

Figure 4.4. HOMO (left) and HOMO-1 (right) of the L_3 F-elimination TS(E-H). Bottom: tetrahedral vs. trigonal-bipyramidal geometry in the L_3Cu(F, alkene) F-elimination TS. L = PMe_3.

In conclusion, in the PMe_3/Cu system, HDF proceeds preferentially via a three-step nucleophilic H-addition/Cu-C bond formation/F-elimination sequence in an L_3 ligand environment along all steps. This pathway offers the possibility for lower barriers compared to the traditional L_2 mechanism. Phosphine ligands that allow for an L_3 environment can subsequently enable HDF in systems where ligands enforcing a traditional L_2 mechanism fail. Interestingly, the mechanism described here for FAs differs distinctively from the concerted SBM described by the group of Zhang for fluorinated arenes using a similar phosphine-stabilized copper hydride system.[400] We could not locate such TS for alkene systems. This presents a distinct difference from early transition metal systems, as in the case of Ti-catalyzed HDF, SBM

TS could be found for both alkene and arene HDF systems,[450,452] although they are only kinetically relevant in the latter case.

PMe_3 model system. 4.2b and 4.2e.

Figure 4.5 shows trends in HM and F-Elimination barriers for all three tested FAs (Table S8-10 shows all relevant RS and TS). Barriers for hydrometallation via H-addition/Cu-C bond formation (L_3 pathway) or insertion (L_2 pathway) increase with decreasing fluorine content of the FA; therefore no 'runaway' defluorination can occur, i.e. that multiple defluorinations are preferred. Due to the stabilization of the corresponding anions, hydrometallation in L_3 environment via H-addition/Cu-C carbon bond formation is the preferred mechanism for the highly fluorinated FAs **4.2a** and **4.2b**, and likely others like **4.1a**; hydrometallation via phosphine decoordination/insertion is preferred for more electron-rich FAs with lower fluorine content like **4.2e**. F-elimination becomes easier the lower the fluorine content of the forming FA is and is exergonic for both, 2b and 2e. The L_3 elimination mechanism is preferred for all three FAs by 4-5 kcal/mol.

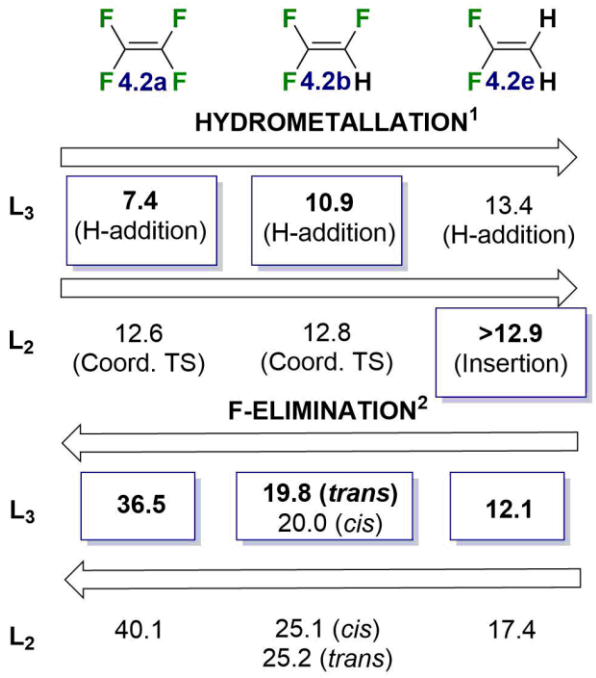

Figure 4.5. Trends in hydrometallation and F-elimination barrier heights for **4.2a**, **4.2b** and **4.2e** in the L_2 and L_3 ligand environment. L = PMe_3. [1] from the isolated reactants L_3CuH and FA. [2] from the L_3CuR resting state. Level of theory TPSSh-D0(PCM)/TZ// TPSSTPSS(PCM)/DZ. T = 323 K. p = 0.1 bar. Solvent = benzene. Gibbs free energies in kcal/mol.

Real systems. 4.2a and $(Ph_3P)_3Cu$-H.

In this system, the H-addition L_3 pathway is favored by 13.4 kcal/mol over the phosphine decoordination/hydrometallation L_2 pathway, indicating that bulkier phosphines and/or less donating phosphines do not change the preferred pathway. This preference stems entirely from the coordination energy of the third phosphine. It has been shown that modern dispersion-corrected functionals allow relatively accurate prediction of transition metal – phosphine bonds;[483] see also the benchmark test for the current method in the supporting information. Even assuming that the error on the Cu-P bond strength of $(PPh_3)_2HCu\text{-}PPh_3$ is on the order of 5-10 kcal/mol does not change the preference.

However, while were able to locate the L_3-F elimination TS for **4.2a** (-1.8 kcal/mol *vs* L_2), all optimization attempts for **4.2b** lead to decoordination of one phosphine (see Supporting

Information for an example structure for one TS with decoordinatied phosphine). It appears that only phosphines with a small cone angle (Tolman cone angles:[484] PMe_3 118°, $PMePh_2$ 122°, PMe_2Ph 136°, PPh_3 145°) can allow for this TS also in cases where the alkyl fragment is less stabilized. Unlike the 'dagger-like' H-addition TS, the F-elimination TS needs significant space around the central metal to accommodate both the FA product and the fluoride ligand.

Real systems. Ligand induced selectivity differences.

One of the striking observations in the present systems is the ability to tune the *cis/trans* product selectivity in the HDF of **4.2b**. We computationally tested the catalyst selectivity for several phosphines, i.e. for the monodentate phosphines PPh_3, $PMePh_2$ and PMe_2Ph, and two bidentate phosphines with varying bite angle, dppe and Xantphos.

The experimentally observed selectivity for Xantphos (2c/2d, *cis/trans* 7:1 = $\Delta\Delta G^{\ddagger}_{50°C}$ = 1.4 kcal/mol) is nicely reproduced by DFT (1.2 kcal/mol), but the error for dppe is somewhat larger (predicted *cis* preference 0.4 kcal/mol, experimentally observed $\Delta\Delta G^{\ddagger}_{50°C}$ =1.4 kcal/mol, see SI). For $PMePh_2$ and PMe_2Ph, both, the L_2 pathway and the L_3 pathway are possible. DFT predicts that the L_3 pathway is preferred by 6-9 kcal/mol. Moreover, while F-elimination in the L_2 system is predicted to yield a 1:1 ratio of *cis* and *trans*, only the L_3 system is in line with the experimentally observed preference for *trans* elimination. The experimental selectivity for $PMePh_2$ and PMe_2Ph (*cis*/*trans* 1:4 = $\Delta\Delta G^{\ddagger}_{50°C}$ = 0.9 kcal/mol) appears to be somewhat overestimated (DFT: 1.5-2.0 kcal/mol). However, repeated product re-insertion into the Cu-F bond could diminish the kinetic *trans* preference of these catalysts somewhat, if regeneration of the catalyst is not fast enough. The possibility for re-insertion of FAs in the Cu-F bond could be successfully demonstrated by the experimental observation of **4.7b'**.

Table 4.3. Barriers for FHC=CFH elimination in various L_xCu-$CFHCF_2H$ systems. Level of theory TPSSh-D0(PCM)/TZ// TPSSTPSS(PCM)/DZ. Solvent = benzene. T = 323K, p = 0.1 bar. Energies in kcal/mol.

	cis $\Delta^{\ddagger}G_{elim}$	*trans* $\Delta^{\ddagger}G_{elim}$	ΔG_{Elim} (cis/trans)
L_2 systems			
dppe*	28.3	28.7	-9.6/-8.9
Xantphos*	25.6	26.8	-9.2/-8.9
PPh_3	23.8	26.1	-14.4/-13.8
$PMePh_2$	26.8	26.8	-8.9/-8.3
PMe_2Ph	28.1	27.9	-3.1/-2.5
L_3 systems			
$PMePh_2$	22.8	20.8	-8.9/-8.3
PMe_2Ph	20.4	19.0	-3.1/-2.5

[a]Level of theory TPSSh-D0(PCM)/TZ//TPSSTPSS(PCM)/DZ. Solvent = benzene. T = 323 K, p = 0.1 bar. Energies are in kilocalories per mole. [b] Resting state is assumed to be $L(PPh_3)Cu$-$CFHCF_2H$, L = dppe or Xantphos.[485]

Experimental trends, i.e. the preference for the *cis* isomer **4.2c** for ligands where F-elimination must proceed in the L_2 environment and for *trans* isomer **4.2d** for systems where it can proceed in the L_3 environment are very well reproduced. The model also correctly predicts that the F-elimination barrier is smaller in bidentate systems with larger bite angle (Xantphos vs. dppe). Product **4.2c** (*cis*) is preferred by 0.9 kcal/mol over **4.2d** (*trans*),[486] but clearly the

ligand environment can modulate the product distribution in the present copper hydride systems, from enhanced *cis* preference all the way to a switch to *trans* preference.

We considered that the pronounced shift in selectivity could stem from short H-F contacts in the TS, as the *trans* TS often has more short contacts of this type. This has been postulated to lead to stabilizing TS interactions in other systems,[487,488] but NBO[482,489] does not locate any significant interactions between H-F in these systems (WBI < 0.002). Steric interactions could conceivably be responsible for the differences in the L_2 systems and, in line with experimental observations, a *cis* preference would be expected in this case. The distribution of steric bulk in L_2 systems as indicated by buried volume maps shown in Figure 4.6 leads to shorter ligand-FA contacts and thus increased steric repulsion in the *trans* TS (Table 4.4).

In the more *trans* selective system L_3, pseudo C_3-symmetric distribution of the phosphines equally distributes the steric bulk, offering no possibility for either of the two FHC=CFH isomers to avoid it (Figure 4.6). Unfavorable dipole-dipole interactions between the FA and L_xCuF can only play a role in the *cis* TSs (Figure 4.7) leading to **4.2c**; this is due to the relative orientation of the two dipoles in the *cis* TSs and the lack of a dipole for **2d**. Interestingly, the *trans* preference in the phosphine systems follows qualitatively Tolman's electronic parameter (Table 4.4), which point to electronic effects being responsible for the switch.

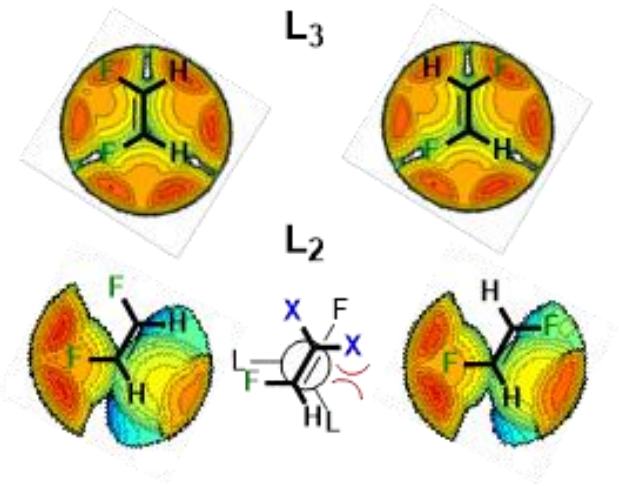

Figure 4.6. Symmetric distribution of steric bulk in L_3 systems and origin of *cis*-preference in L_2 systems (L = PMe_3) and map of steric bulk generated with SambVca 2.0[279] from L_3Cu-H; sphere radius of 3.5 Å.

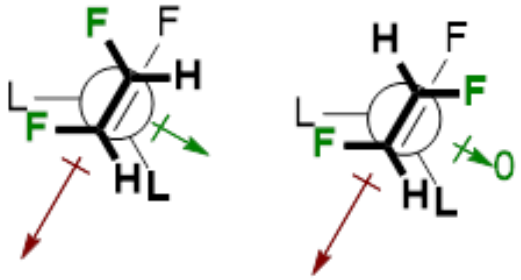

Figure 4.7. Unfavorable dipole-dipole interactions in L_3 TS leading to **4.2c** (left) vs lack of dipole-dipole interactions in L_3 TS leading to **4.2d** (right). L_2Cu-F fragment dipole orientation in maroon, FA dipole orientation in green.

Table 4.4. Ligand dependence of the preference for the *cis* FHC=CFH isomer in different L_2 and L_3 systems, Tolman's electronic parameter ν and differences between the shortest ligand-FA contacts ($l_{cis\text{-}trans}$) in the L_2 ligand environment and deformation energy difference of the FA fragments in the TS ($E_{Def.\ cis\text{-}trans}$).

	ΔΔG‡		**ν**	**$L_{cis\text{-}trans}$**	**$E_{Def.\ cis\text{-}trans}$**
	L_2	**L_3**			
Ph_3P	**-2.5**		**2068.9**	**0.137**	**-2.2**

Xantphos	**-1.2**			**0.066**	**-0.4**
dppe	**-0.8**			**0.015**	**-1.2**
Ph_2MeP	**-0.2**	**2.0**	**2065.1**	**-0.023**	**-0.9/-1.0**
$PhMe_2P$	**0.0**	**1.5**	**2065.3**	**-0.025**	**-0.7/-0.3**
Me_3P	**0.1**	**0.4**	**2064.1**	**-0.048**	**-0.6/-1.9**

Although the unusual *cis* preference for the two isomers of FHC=CFH has been the subject of considerable research efforts in the past, it appears that no definitive conclusion on its origin has been reached, yet.[489-498] Nonetheless, most authors appear to agree that the preference is of electronic origin.[490,497] In the absence of a definitive consensus on the origin of the *cis* preference, we deem a quantitative analysis of the trends here impossible. However, tentatively the preference switch can be explained as follows: The Hammond postulate assumes that electronic and steric changes from the reactants to the TS and further to the products occur gradually.[498,499] While TS of the L_3 type are central with respect to the overall TS geometry, they are later than L_2 type TS with respect to the forming olefin, as the forming C=C bond is much shorter (see also Figure 4.2). A shift from the L_2 to the L_3 environment should therefore increase the preference for the thermodynamic product; this is not observed for **4.2c**/**4.2d**. Table 4.4 shows that the energy difference between the FA fragments in the *cis*/*trans* TS favors the *trans* isomer in all cases, indicating that the electronic stabilization of *cis*-1,2-difluoroethene occurs very late and that initially only the steric repulsion by the F atoms prevails. It appears that within the L_2 pathway, FA deformation and unfavorable dipole-dipole interactions in the *cis* TS favor the *trans* isomer, but this is more than compensated for by unfavorable steric interactions in the *trans* TS. L_2 leads preferentially to formation of the *cis* isomer **4.2c**. An increase in the

FA-Cu distance in the L_3 environment weakens unfavorable dipole-dipole interactions in the *cis* TS and the symmetric distribution of steric bulk lessens steric differences. Subsequently, the FA deformation dominates, which leads to a preference for the *trans* isomer **4.2d**.

To the contrary, increased selectivity for the thermodynamic product upon L_2/L_3 switch is indeed observed experimentally in the HDF of the bulky α-trifluoromethyl styrene (**4.8a**). Use of the small cone angle phosphite $P(OEt)_3$ increases the selectivity for the thermodynamic product *Z*-β-fluoro-α-methyl styrene (**4.8c**) from 2.8:1 (Xantphos/$PMePh_2$) to 7.2:1 [$P(OEt)_3$] (DFT, L = $P(OMe)_3$: $\Delta\Delta G^{\ddagger}$ L_2 1.3 kcal/mol, L_3 2.3 kcal/mol). No HDF is observed for **4.2b** with this ligand class. Phosphites are electron-poor and DFT indicates that F-elimination in such a system could lead to F/OR exchange on the organophosphite ligand during HDF of **4.2a**.[500]

4.3.3. Experimental Mechanistic Studies.

To confirm these DFT revelations, mechanistic studies were carried out. First, the L_2CuH systems like Xantphos follow the previously reported insertion-elimination mechanism, as supported by DFT calculations (*vide supra*) and, therefore, focus was given to mechanistic studies on the HDF mechanism of a phosphine ligand, $PMePh_2$, that can allow for coordination of a third phosphine during catalysis (*vide supra*).

Control experiments for the HDF of **4.2b** demonstrated that all three components of the reaction mixture are required. The product ratio of the HDF of **4.2b** using $PMePh_2$ is altered (**4.2c**:**4.2d**, 1:1) when no silane is present; no such alteration is observed for Xanthphos. This experiment suggests that re-insertion of **4.2c**/**4.2d** into Cu-F occurs if no silane is present. Similarly, TMDS does not achieve HDF at RT without a source of copper. Nor does the mixture of phosphine and TMDS, confirming that the copper plays a crucial role in this HDF reaction. However, when the reaction was attempted with varying concentrations of silane; no rate

dependence was observed. As a significant rate increase with increasing solvent polarity was observed, the silane substituents were varied to elaborate further on its role. Interestingly, the reaction only progresses smoothly at RT when either triphenylsilane (Ph_3SiH) or TMDS are used. When triethoxysilane [$(EtO)_3SiH$] is used, the reaction turns over once at RT and then ceases operation at this temperature. If heated to 45 °C, the reaction progresses with some loss of selectivity. This is reminiscent of Lentz's observations in Ti(III) complex-catalyzed HDF, where $(EtO)_3SiH$ led to fast catalyst deactivation via formation of alkoxytitanium compounds.[477] The alkyl silanes either require heating (i.e. triethylsilane) or are ineffective (i.e. triisopropylsilane). Interestingly, diphenylsilane also does not work at room temperature, and requires heating to 70 °C but the reaction mixture quickly becomes black. The most productive silanes are those with somewhat more electron-withdrawing functional groups.

Based on the stoichiometric reactions of $PMePh_2$/$(PPh_3CuH)_6$/**4.2b**, a fast equilibrium between the resulting products is suspected. In line with observations (see above), this would lead to an increased ratio **4.2c**/**4.2d** ratio tending towards a thermodynamic distribution. On this note, as the rate of Cu-F to Cu-H conversion becomes slow, a secondary reaction becomes competitive (Scheme 4.9) leading eventually to complete catalyst deactivation via formation of a suspected copper(I)-alkenyl complex by formal HF elimination. Additionally, byproduct 1,1,1,2-tetrafluoroethane (**4.2b'**) suggests that the generated Cu-alkyl reacts quickly with HF, explaining why it is not observed over the course of the reaction.

To probe the elementary steps further, the source of the hydride was sought by carrying out the reaction with a deuterated reagent. When the reaction is carried out with stoichiometric amounts of Cu-H and a slight excess of triethylsilyl deuteride, the major product contains mostly

protons, confirming that Cu-H adds to the FA, and that the silane likely does not participate in this event.

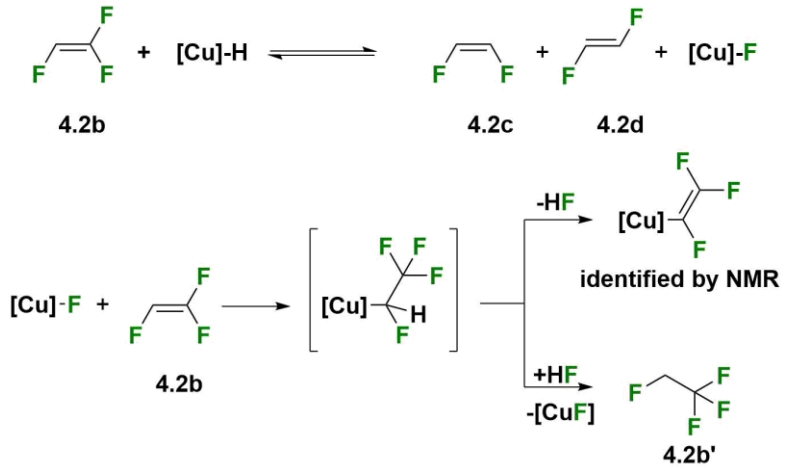

Scheme 4.9. Reaction of copper hydride with **4.2b** leading to the formation of a suspected copper trifluorovinyl complex and R-134a (**4.2b'**).

Effects controlling selectivity for the L_2CuH or L_3CuH mechanism.

With the DFT and experimental support for the L_3CuH mechanism, other FAs were examined to determine the effects of FA substitution on the ability to access the L_3CuH mechanism. For consistency with reactions using the Xantphos catalyst, these reactions were carried out in benzene at 45 °C. First, mono-substituted FAs were explored to determine if β-fluoride elimination is crucial in accessing analogs of **TS(E-H)**. As such, FAs $XFC{=}CF_2$ [X = Cl (**4.3a**), I (**4.3b**) or OCF_3 (**4.4a**)] were used. Unfortunately, when iodotrifluoroethylene, **4.3b**, was treated with stoichiometric copper hydride, the expected $HFC{=}CF_2$, **4.2b**, was observed as the major product, independent of the choice of ligand. It is suspected that this is occurring via *σ*-bond metathesis of the C-I bond. However, with chlorotrifluoroethylene (**4.3a**), when using Xantphos, the observed product was a mixture of *cis/trans*-1,2,-difluoroethylene, **4.2c**/**4.2d**. This result suggests that the first HDF step produces 1-chloro-1,2-difluoroethylene (**4.3a'**) arising

from addition of the hydride at the CF_2 carbon. This new alkene is considerably more reactive than **4.3a**, such that addition of Cu-H to **4.3a'** dominates. Consistent, with this result, $PMePh_2$ yields the same product distribution as that observed with Xantphos. This indicates that β-fluoride elimination is necessary to access analogues of **TS(E-H)**. To confirm this, the HDF of **4.4a** was attempted with $PMePh_2$ and $P(OEt)_3$ and **4.2c,d** were produced in the same ratio as the Xantphos reaction (*vide supra*). β-X elimination (X = Cl or OCF_3), excluding fluoride, generally proceeds through the known analogous transition states of **TS(D-G)**.

On another note, as the activation energies for the L_3CuH hydride addition mechanism are considerably lower, this could explain why $P(OEt)_3$ is competitive in efficiency in the HDF of **4.1a** with the dppf or Xantphos ligands. Although, it would be expected that accessing analogues of TS(A-F), depends on a delicate balance of the stabilization of Cu^+ and the carbanion (Alk). To explore this idea, 1,1-difluoroethylene (**4.2e**) was used as the Xantphos catalyts could not hydrodefluorinate this substrate (Scheme 4.10, bottom). Interestingly, use of $P(OEt_3)$ also afforded no HDF product from 2e. However, the use of $PMePh_2$ led to the efficient HDF of 2e to a 3:1 mixture of vinyl fluoride (2f) and ethylene (Scheme 4.10, Top) although calculations show that this substrate could be hydrometallated via both mechanisms (Figure 4.5). As such, a larger cone-angle, stronger σ-donating phosphine ligand, PCp_3, was also tested with no HDF product detected. Again, because ligand size is so important, $PMePh_2$ likely leads to greater Cu^+ stabilization, thus balancing the more destabilized carbanion, H_2CR^-, in the L_3CuH mechanism.

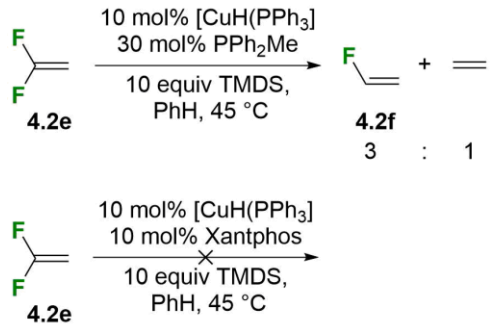

Scheme 4.10. Hydrodefluorination of 1,1-difluoroethylene (**4.2f**)

These results indicate that an electronic limit to the HDF of FAs via the L_3CuH mechanism exists. (i.e. in cases where the stabilization of the Cu^+ is simply not great enough to offset destabilization of the Alk^-). Therefore, alkyl substituted FAs were tested (Scheme 4.11).

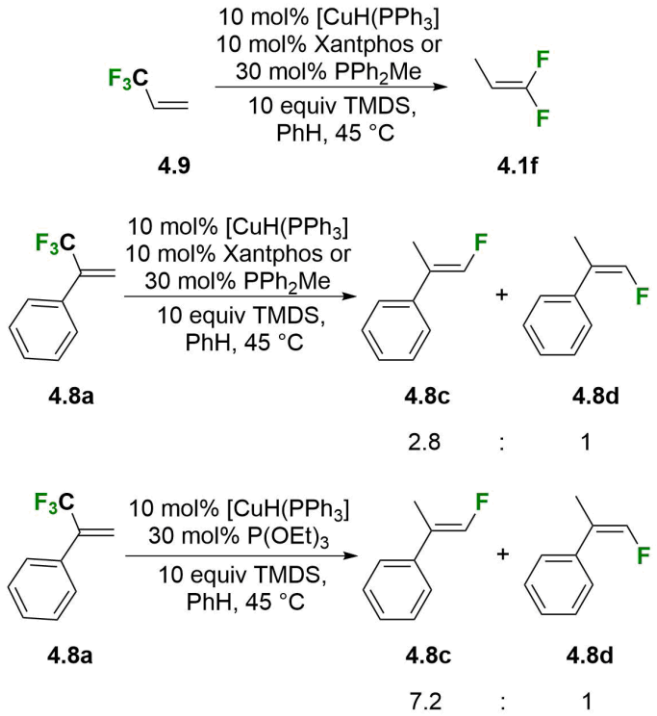

Scheme 4.11. Hydrodefluorination of allyl trifluoropropene and α-trifluoromethyl styrene (bottom)

In this case, 1,1,1-trifluoropropene (**4.9**) was subjected to HDF to generate **4.1f** in situ. Naturally, 1f is not hydrodefluorinated by the Xantphos system, like that observed in the HDF of

4.1a. Nor is **4.1f** hydrodefluorinated by the $PMePh_2$ system, as suspected. Still, if a stabilizing element is introduced onto the Alk^-, HDF through the L_3CuH mechanism should proceed. Hence, α-trifluoromethyl styrene (**4.8a**) could be used to generate β-difluoro-α-methyl styrene (**4.8b**) in situ. In this case, Xantphos or $PMePh_2$ both yielded the same product distribution of *E*/*Z*- β-fluoro-α-methyl styrene (**4.8c,d**) in a ratio of 2.8:1 respectively. As expected, the steric congestion near Cu, from addition with the =CPhMe carbon oriented towards the copper, proves too much to accommodate a third $PMePh_2$ necessary for the L_3 mechanism. As such, the L_2 mechanism dominates for control of the product ratio in both cases. Nevertheless, if our hypothesis is correct even the weaker σ-donating but smaller ligand should function, because significant Alk^- stabilization should come from the benzylic functionality, $PhCHR^-$. Indeed when $P(OEt)_3$ was used, the HDF of **4.8a** to **4.8b** and on to **4.8c,d** proceeded smoothly to provide an increased ratio of 7.2:1 respectively. Apparently, the L_3 mechanism provides an increased *E*/*Z* ratio from 2.8:1 to 7.2:1. The E/Z ratio is reinforced because **4.8c** is both the least polar and most thermodynamically stable, as confirmed by DFT (*vide supra*).

4.4. Conclusion

In summary, new P-ligated copper hydride complex-catalyzed routes for the HDF of fluoroalkenes using silanes have been developed. With our technology, hexafluoro-propene (**4.1a**) can be selectively converted to fourth-generation refrigerant CH2=CF(CF_3) (**4.1d**) or to 1,1-difluoropropene (**4.1f**). While the (dppe)Cu-H system stops at the double HDF, giving the highest yield of **4.1d**, small cone-angle, less electron-rich $P(OEt)_3$ allows for the quad-ruple HDF of **4.1a** to **4.1f**. Furthermore, the use of PMHS provides a simplified separation procedure because it forms a biphasic mixture with benzene. On evaluating the HDF substrate scope we found that use of a smaller cone-angle, electron-rich ligand such as $PMePh_2$ leads to L_3Cu-H

reactivity with electron-poor or bulky fluoroalkenes not observed with the L_2CuH systems. DFT studies identified both inser-tion/elimination and hydride transfer mechanisms. In the latter, F-elimination involves a doubly-occupied coordina-tion site at copper. Both hydrometallation and F-elimination in the L_2 as well as the L_3 system proceed via TSs showing significant charge separation, explaining the experimentally observed rate dependence on the solvent. DFT results are nicely in line with experimental observations. We propose that the phosphine choice can modulate the position of the F-elimination TS with respect to the product and thereby modulate product selectivity, as ex-perimentally observed for **4.2b** and **4.8a**. It appears that in the case of **4.8a**, tuning the position of the F-elimination TS rein-forces the preference for the thermodynamic product. In the case of **4.2b**, the switch from L_2 to L_3 environment leads to a switch from thermodynamic to kinetic product. We believe that this effect can be traced to a breakdown of the assumption that steric and electronic changes occur gradually from RS to TS to product in this specific case.

The work presented herein demonstrates a new variant of copper-catalyzed hydrodefluorination which requires no additive and allows for some control of new FA synthesis, making a host of new variants accessible for further studies. For example, with the renewed interest in FAs as amide bioisosteres this approach may provide an expedient route to their synthesis.

With tetrafluoroethylene both (P-P)CuH and P3Cu-H complexes (**4.7a**,**4.7b**) could be successfully synthesized. In fact, the reactivity of these complexes is currently being assessed as a potential route for the introduction of the 1,1,2,2-tetrafluoroethyl ($-CF_2CF_2H$) moiety to organic electrophiles.[501]

4.5.Experimental Section

4.5.1. General Procedures.

Experiments were conducted under nitrogen, using Schlenk techniques or an MBraun glove box. All solvents were deoxygenated by purging with nitrogen. Tetrahydrofuran (THF) and toluene were dried on columns of activated alumina using a J. C. Meyer (formerly Glass Contour®) solvent purification system. Chlorobenzene, *m*dimethoxybenzene, benzene, cyclopentyl methyl ether (CPME) and Benzene-d6 (C_6D_6) were dried by stirring over activated alumina (ca. 10 wt. %) overnight, followed by filtration. All solvents were stored over activated (heated at ca. 250 °C for >10 h under vacuum) 4 Å molecular sieves. Glassware was oven-dried at 120 °C for >2 h. The following chemicals were obtained commercially, as indicated: Dimethylformamide (DMF, Alfa Aesar Anhydrous 99.8%), hexafluoropropene (**4.1a**, Synquest 98.5%), trifluoroethylene (**4.2b**, Synquest 98%), chloro trifluoroethylene (**4.3a**, Synquest, 99%), iodo trifluoroethylene (**4.3b**, Synquest, 97%), trifluoromethyl trifluorovinyl ether (**4.4a**, Synquest, 99%), vinylidene difluoride (**4.2e**, Arkema Inc., 99%), alpha-trifluoromethyl styrene (**4.8a**, Synquest, 97 %), hexafluorocyclobutene (**4.5a**, Synquest 98%), 3,3,3-trifluoropropene (**4.9**, Synquest, 99%), perfluoro(4-methyl-2-pentene) (**4.6b**, Synquest, 95%), perfluoro(2-methyl-2-pentene) (**4.6a**, Synquest, 96%), triethylesilane (Sigma-Aldrich, 99%), triethyl(silane-*d*) (Sigma-Aldrich, 97 atom % D), triisopropylsilane (Oakwood chemicals, 98%), triphenylsilane (Oakwood chemicals, 97%), triethoxysilane (Sigma-Aldrich, 95%), diphenylsilane (Oakwood chemicals, 97%), tetramethyldisiloxane (TMDS, Sigma-Aldrich, 97 %), poly(methylhydrosiloxane) (PMHS, Sigma-Aldrich, average M_n: 1,700-3,200), triphenylphosphine (PPh_3, Oakwood chemicals, 99%), tri(*o*-tolyl)phosphine ($P(o\text{-tolyl})_3$, Alfa Aesar, 98%), 2-di-tert-butylphosphino-2′,4′,6′-triisopropylbiphenyl (tbuXphos, Sigma-Aldrich,

97%), 1,2-bis(diphenylphosphino) ethane (dppe, Strem chemicals, 99%), 1,1'-bis(diphenylphosphino) ferrocene (dppf, Accela ChemBio Inc., 99%), 4,5-bis(diphenylphosphino)-9,9-dimethylxanthene (Xantphos, Accela ChemBio Inc., 99%), triethylphosphite ($P(OEt)_3$, Sigma-Aldrich, 98%), triphenylphosphite ($P(OPh)_3$, Alfa Aesar, 97%), tri-ortho-tolyl phosphite ($P(O\text{-}o\text{-tolyl})_3$, Alfa Aesar), methyldiphenylphosphine ($PMePh_2$, Acros Organics, 99%), dimethylphenylphosphine (PMe_2PhMe, Acros Organics, 97%). The following chemicals were synthesized as previously reported: 1,3-bis(2,6-diisopropylphenyl)imidazolidin-2-ylidene (SIPr)[502] and $[(PPh_3)CuH]_6$.[503] Tetrafluoroethylene (**4.2a**) was prepared by pyrolysis of polytetrafluoroethylene (Scientific Polymer Products, powdered) under vacuum, using a slightly modified literature procedure [10-20 mTorr, 650 °C, 30 g scale, product stabilized with R(+)-limonene (Aldrich, 97%), giving **4.2a** of ca. 97% purity][504] or by pyrolysis of $KO_2CCF_2CF_3$ under vacuum, producing TFE Safe Supply®.[505] ^1H, ^{19}F, $^{31}P\{^1H\}$, and $^{13}C\{^1H\}$ NMR spectra were recorded on a 300 MHz Bruker Avance instrument at room-temperature (21-23 °C) unless stated otherwise. ^1H NMR spectra were referenced to residual proton peaks associated with the deuterated solvents (C_6D_6: 7.16 ppm). ^{19}F NMR spectra were referenced to internal standard α,α,α-trifluorotoluene (CF_3Ph) [unless stated otherwise] (Sigma-Aldrich, 99%, deoxygenated by purging with nitrogen, stored over activated 4 Å molecular sieves), set to – 63.5 ppm. $^{31}P\{^1H\}$ NMR data were referenced to external H_3PO_4 (85 % aqueous solution), set to 0.0 pm. Electrospray ionization mass spectral data were collected using an Applied Biosystem API2000 triple quadrupole mass spectrometer. Elemental analyses were performed by Ján Veizer Stable Isotope Laboratory, University of Ottawa (Ottawa, Ontario, Canada). Note that the NMR spectra (^1H, ^{19}F, $^{19}F\{^1H\}$, and $^{31}P\{^1H\}$ for the title compounds are displayed at the end of the Supporting Information (Annex D).

4.5.2. General Experimental Procedure for Hydrodefluorination of Gaseous Fluoroalkenes, NMR Scale.

$[(PPh_3)CuH]_6$ (5 mg, 0.0153 mmol, 10 mol %) was placed in a 7 ″ nmr tube and mixed with 400 µL of solvent. A ligand (31 mol % or 11 mol %) and silane (10 equiv) were added. The tube was capped with a rubber septum, removed from the glovebox, further sealed by tightly wrapping the cap with a strip of parafilm and shaken to ensure a homogenous solution. 3 mL of gaseous fluoroalkene was then added to the reaction via air-tight syringe. The reaction was monitored by ^{19}F NMR over 8 hours at various temperatures. See Annex D for ^{1}H NMR and ^{19}F NMR spectra. Compounds **4.1b[**506,507], **4.1c[**506,507], **4.1d**[508], **4.1e**[509], **4.1f**[445], **4.2c**[510], **4.2d**[510], **4.2f**[510], **4.4b**[511], **4.5b**[512] and **4.5c**[512], **4.5d**[512] were identified using available literature data.

Z-3,3,3,2,1-pentafluoropropene (4.1b). ^{1}H NMR (300 MHz, C_6D_6): δ 6.13 (ddq, $^{2}J_{HF}$ = 68, $^{3}J_{HF}$ = 15, $^{4}J_{HF}$ = 1 Hz, =CHF). ^{19}F NMR (282 MHz, C_6D_6): -72.59 (ddq, $^{3}J_{FF}$ = 14, $^{4}J_{FF}$ = 6, $^{4}J_{FH}$ = 1 Hz, CF_3), -155.07 (ddq, $^{2}J_{FH}$ = 68, $^{3}J_{FF}$ = 7, $^{4}J_{FF}$ = 6 Hz, =CFH), -158.97 ppm (ddq, $^{3}J_{FH}$ = 15, $^{3}J_{FF}$ = 7, $^{4}J_{FF}$ = 6 Hz, =CF(CF_3)).

E-3,3,3,2,1-pentafluoropropene (4.1c): ^{1}H NMR (300 MHz, C_6D_6): δ 5.93 (dd, $^{2}J_{HF}$ = 68, $^{3}J_{HF}$ = 4 Hz, = CHF). ^{19}F NMR (282 MHz, C_6D_6): -70.09 (dd, $^{3}J_{FF}$ = 19, $^{4}J_{FF}$ = 12 Hz, CF_3), -165.93 (ddq, $^{2}J_{FH}$ = 68, $^{3}J_{FF}$ = 137, $^{4}J_{FF}$ = 19 Hz, =CFH), -180.12 ppm (ddq, $^{2}J_{FH}$ = 4 $^{3}J_{FF}$ = 137, $^{4}J_{FF}$ = 12 Hz, =CF(CF_3)).

3,3,3,2-tetrafluoropropene (4.1d): ^{1}H NMR (300 MHz, C_6D_6): δ 4.36 (ddq, $^{2}J_{HH}$ = 5, $^{3}J_{HF}$ = 13, $^{3}J_{HF}$ = 1 Hz, =CH_{2cis}), 4.49 (br dd, $^{2}J_{HH}$ = 4, $^{3}J_{HF}$ = 52 Hz, =CH_{2trans}). ^{19}F NMR (282 MHz, C_6D_6): -73.28 (d, $^{3}J_{FF}$ = 10 Hz, CF_3), -124.12 ppm (ddq, $^{3}J_{FH}$ = 52, $^{3}J_{FH}$ = 13 Hz, $^{3}J_{FF}$ = 10 Hz. =CF(CF_3)).

1,1,2-trifluoropropene (4.1e): ^{19}F NMR (282 MHz, C_6D_6): -106.32 (ddq, $^2J_{FF}$ = 93, $^3J_{FF}$ = 32, $^4J_{FH}$ = 5 Hz, $=CF_{2cis}$), -126.15 (ddq, $^2J_{FF}$ = 93, $^3J_{FF}$ = 115, $^4J_{FH}$ = 5 Hz, $=CF_{2trans}$), -167.19 ppm (ddq, $^3J_{FF}$ = 115, $^3J_{FF}$ = 32, $^3J_{FH}$ = 17 Hz, $=CF(CH_3)$).

1,1-difluoropropene (4.1f): ^{19}F NMR (282 MHz, C_6D_6): -89.67 (ddq, $^2J_{FF}$ = 50, $^3J_{FH} \approx {}^4J_{FH}$ = 3 Hz, $=CF_{2trans}$), -93.45 ppm (ddq, $^2J_{FF}$ = 50, $^3J_{FH}$ = 25, $^4J_{FH}$ = 2 Hz, $=CF_{2cis}$).

Z-1,2-difluoroethylene (4.2c): ^{1}H NMR (300 MHz, C_6D_6): δ 5.54 (m). ^{19}F NMR (282 MHz, C_6D_6): δ -163.09 ppm (m).

E-1,2-difluoroethylene (4.2d): ^{1}H NMR (300 MHz, C_6D_6): δ 6.68 (m). ^{19}F NMR (282 MHz, C_6D_6): -187.73 ppm (dd, $^2J_{FH}$ = 49, $^3J_{FH}$ = 30 Hz).

Vinyl fluoride (4.2f): ^{1}H NMR (300 MHz, C_6D_6): δ 6.14 (ddd, $^2J_{HF}$ = 85, $^3J_{HH}$ = 13, $^3J_{HH}$ = 5 Hz), 4.54 (ddd, $^3J_{HF}$ = 20, $^2J_{HH}$ = 12, $^3J_{HH}$ = 3 Hz), 4.00 (ddd, $^3J_{HF}$ = 54, $^2J_{HH}$ = 5, $^3J_{HH}$ = 3 Hz). ^{19}F NMR (282 MHz, C_6D_6): -115.97 ppm (ddd, $^2J_{FH}$ = 85, $^3J_{FH}$ = 54, $^3J_{FH}$ = 20 Hz).

Z-Trifluoromethyl-1,2-difluorovinyl ether (4.4b): ^{19}F NMR (282 MHz, C_6D_6): -54.78 (m, OCF_3), -118.28 (m, F), -122.22 ppm (dm, $^2J_{FH}$ = 59 Hz).

1,4,4-trifluorocyclobutene (4.5b): ^{19}F NMR (282 MHz, C_6D_6): δ -106.52 (m, 2F), -113.45 ppm (m, 1F).

1,2-difluorocyclobutene (4.5c): ^{1}H NMR (300 MHz, C_6D_6): δ 1.67 (m, 2H) ppm. ^{19}F NMR: (282 MHz, C_6D_6) -118.57 ppm (m, 4F).

1-fluorocyclobutene (4.5d): ^{19}F NMR (282 MHz, C_6D_6): -84.23 ppm (m, 1F).

4.5.3. General Experimental Procedure for Hydrodefluorination of Non-Gaseous Fluoroalkenes, NMR Scale.

$[(PPh_3)CuH]_6$ (5 mg, 0.015 mmol, 10 mol %) was placed in a 7 ″ nmr tube and mixed with 400 µL of solvent. A ligand (31 mol % or 11 mol %), silane (10 equiv, 1.45 mmol) and fluoroalkene (0.145 mmol) were added. The tube was capped, removed from the glovebox, further sealed by tightly wrapping the cap with a strip of parafilm and shaken to ensure a homogenous solution. The reaction was monitored by ^{19}F NMR over 8 h at various temperatures. See Annex D for ^{19}F NMR spectra. Compounds **4.6c**[513], **4.8b**,[514,515] **4.8c[**514,515] and **4.8d[**514,515] were identified using available literature data.

1,1,4,4,5,5,5-heptafluoro-2-methylpent-1-ene (4.6c). ^1H NMR (300 MHz, C_6D_6): δ 2.13 (t, $^3J_{HF}$ = 19 Hz, CH_2), 1.22 (m, CH_3). ^{19}F NMR (282 MHz, C_6D_6): -86.42 (s, CF_3), -92.00 (d, $^2J_{FF}$ = 44 Hz, 1F), -92.64 (d, $^2J_{FF}$ = 44 Hz, 1F), -117.07 ppm (tm, $^3J_{FH}$ = 19 Hz, CF_2).

1,1-difluoro-2-methyl-2-phenylethyl-1-ene (4.8a): ^1H NMR (300 MHz, C_6D_6): δ 1.59 (dd, $^4J_{HF} \approx {}^4J_{HF}$ = 3 Hz, Me). ^{19}F NMR (282 MHz, C_6D_6): -91.99 (dq, $^2J_{FF}$ = 44, $^4J_{FH}$ = 3 Hz), -92.30 ppm (dq, $^2J_{FF}$ = 44, $^4J_{FH}$ = 2 Hz).

(E)-1-fluoro-2-methyl-2-phenylethyl-1-ene (4.8b): ^1H NMR (300 MHz, C_6D_6): δ 7.4 – 6.9 (Ar), 6.58 (dq, $^2J_{HF}$ = 85, $^4J_{HH}$ = 2 Hz, $1H_{(FHC=)}$), 1.80 (dd, $^4J_{HF}$ = 4, $^4J_{HF}$ = 2 Hz, Me). ^{19}F NMR (282 MHz, C_6D_6): -131.66 ppm (dq, $^2J_{FF}$ = 85, $^4J_{FH}$ = 4 Hz).

(Z)-1-fluoro-2-methyl-2-phenylethyl-1-ene (4.8c): ^1H NMR (300 MHz, C_6D_6): δ 7.4 – 6.9 (Ar), 6.22 (dq, $^2J_{HF}$ = 84, $^4J_{HH}$ = 2 Hz, $1H_{(FHC=)}$), 1.80 (dd, $^4J_{HF}$ = 5, $^4J_{HF}$ = 2 Hz, Me). ^{19}F NMR (282 MHz, C_6D_6): -131.66 ppm (dq, $^2J_{FF}$ = 84, $^4J_{FH}$ = 5 Hz).

Synthesis of [(PMePh$_2$)$_3$Cu(CF$_2$CF$_2$H)] (4.7a). The red complex [(PPh$_3$)CuH]$_6$ (3.16 g, 9.69 mmol based on monomeric unit), PPh$_2$Me (6.01 g, 30 mmol) and TMDS (1.4 mL, 8 mmol or 16 mmol hydride equivalents) were placed in a 350 mL ampule and mixed with 30 mL of benzene. The reaction vessel was attached via a three-way valve to an **4.2a**:CO$_2$ canister with a regulator and a Schlenk line. The solution was degassed using a regular freeze/pump/thaw method. The **4.2a**:CO$_2$ was added to the degassed solution with the regulator set to 5 psi and the reaction mixture stirred at 70 °C. After 10 minutes, the regulator pressure dropped to 0 and more **4.2a**:CO$_2$ was added. After ~2h, the solution became clear with some black precipitate. The solvent was removed in vacuo, leaving a thick liquid. 10 mL of Et$_2$O was added, and the solution was then filtered through a Celite-padded fritted funnel (30 mL medium pore). The ampule was rinsed 2 more time with 10 mL of Et$_2$O. All volatiles were removed in vacuo and 50 mL of methylcyclohexane were added to the solution. Upon standing, the product crystallized from solution. The white microcrystalline powder was collected (30 mL medium-pore fritted funnel), triturated with pentane (2 x 20 mL), and dried in vacuo to yield 5.17 g of **4.7a** (6.8 mmol, 69 % based on [(PPh$_3$)CuH]$_6$). ^{1}H NMR (300 MHz, C$_6$D$_6$): δ 7.23 (m, 16H, PMePh$_2$), 6.89 (m, 25H, PMePh$_2$), 6.75 (tt, 1H, $^2J_{HF}$ = 52, $^3J_{HF}$ = 5 Hz, -CF$_2$H), 1.55 (br, 12H, PMePh$_2$) ppm. ^{19}F NMR (282 MHz, C$_6$D$_6$): −96.68 (dt, $^3J_{FF}$ = $^3J_{FH}$ = 5 Hz, CF$_2$), -124.89 ppm (dt, $^2J_{FH}$ = 52,$^3J_{FF}$ = 5 Hz, -CF$_2$H). ^{31}P{^{1}H} NMR (121 MHz, C$_6$D$_6$): −19.99 ppm (br, PMePh$_2$). Anal. Calcd for C$_{41}$H$_{40}$CuF$_4$P$_3$: C, 64.35, H, 5.27. Found: C, 60.49, H, 5.31. (These values reflect those expected for phosphine oxidation prior to combustion. Anal. Calc. for C$_{41}$H$_{40}$CuF$_4$O$_3$P$_3$: C, 60.56, H, 4.96.) See Annex D for ^{1}H, ^{19}F, and ^{31}P{^{1}H} NMR spectra.

Synthesis of [(Xantphos)Cu(CF$_2$CF$_2$H)] (4.7b). The red complex [(PPh$_3$)CuH]$_6$ (25 mg, 0.077 mmol based on monomeric unit), Xantphos (40 mg, 0.077 mmol) and TMDS (2 μL, 0.008

mmol) were placed in a 7 " NMR tube mixed with 400 μL of C_6D_6. The tube was capped with a rubber septum, removed from the glovebox, further sealed by tightly wrapping the cap with a strip of parafilm and shaken to ensure a homogenous solution. 3 mL of gaseous **4.2a** was added to the reaction via air-tight syringe. The reaction was monitored by ^{19}F NMR over 8 hours at various temperatures. Compound **4.7b** was identified by comparing to **4.7a**. ^{19}F NMR (282 MHz, C_6D_6): −103.9 (br m, CF_2), -125.45 ppm (br dm, $^2J_{FH}$ = 52, -CF_2H). $^{31}P\{^1H\}$ NMR (121 MHz, C_6D_6): −16.74 ppm (br m, Xantphos). See Annex D for ^{19}F and $^{31}P\{^1H\}$ NMR spectra.

4.5.4. Computational Details.

All geometries were fully optimized by using the Gaussian 09 software package[416] in combination with an external optimizer (PQS, OPTIMIZE routine of Baker[516,517]) and the BOpt software package.[518] Following the protocol proposed in ref.[519], all relevant minima and transition states were fully optimized at the TPSSTPSS level[520] of theory employing correlation-consistent polarized valence double-ζ Dunning (DZ) basis sets with cc-pVDZ quality[521,522]from the EMSL basis set exchange library, using a small core pseudo-potential on Cu.[523] The density fitting approximation (Resolution of Identity, RI) [524-527] was used at the optimization stage and for single-point energy corrections. Solvent effects (benzene, ε = 2.2706) were included with the polarizable continuum model approach (PCM) at both stages.[528] All calculations were performed at the standard Gaussian 09 SCF convergence using an ultrafine grid [Scf=Tight and Int(Grid=ultrafine)]. The nature of each stationary point was checked with an analytical second-derivative calculation (no imaginary frequency for minima, exactly one imaginary frequency for transition states, corresponding to the reaction coordinate). The accuracy of the TS was confirmed with an IRC scan on preliminary gas phase calculations. Transition states were located using a suitable guess and the Berny algorithm (Opt=TS)[529] or a

relaxed potential energy scan to arrive at a suitable transition-state guess, followed by a quasi-Newton or eigenvector-following algorithm to complete the optimization.

Final single-point energies were calculated at the TPSSh level of theory[530] employing triple-ζ Dunning (TZ) basis sets (cc-pVTZ quality).[521] Grimme dispersion corrections without damping (keyword -zero) were added at this stage using the standalone dftd3 program.[531,532] Enthalpies and Gibbs free energies were then obtained from TZ single-point energies and thermal corrections from the TPSSTPSS(PCM)/cc-pVDZ-(PP) vibrational analyses; entropy corrections were scaled by a factor of 0.67 to account for decreased entropy in the condensed phase.[533-535] $\Delta\%V_{Bur}$ was calculated using the SambVca 2.0 program.[490] Maps of steric bulk were generated using the same program. NBO 3.1 was used for NBO analysis.[536]

The correct prediction of copper-phosphine bond strengths is crucial for the competition of mechanisms described in this paper. Metal-phosphine bond strengths are known to be challenging to predict and dispersion corrections are critically needed for their accurate description.[483] To our knowledge, no accurate experimental data is available for Cu-P bonds. In the absence of this data, we decided to benchmark the protocol against available gas phase bond dissociation energies of copper complexes with labile binding of ligands,[479] i.e. Cu(0)-NH_3,[537] Cu^+CO[538] and the 1st and 2nd binding energies in $Cu^+(ethene)_2$[539,540] and $Cu^+(acetonitrile)_4$[541]. A labile metal phosphine bond was included in the benchmark via the complex $NiCN_2(PEt_3)_3$, in the solvents dichloroethane and enthanol.[483] For this set of 8 bonds, the protocol including Grimme's dispersion corrections with no damping produces an MAD of 1.8 kcal/mol. Becke-Johnson damping leads to an overestimation of bond dissociation energies and a higher discrepancy (MAD 4.2 kcal/mol). Finally, in a limited test set, we included

dispersion corrections during optimization via the use of the B97D functional,[337] but this did not noticeably change the predictions.

Chapter 5.

5. Unpublished Contributions

Straightforward Tetrafluoroethylation of Aryl-Iodides and Acid Chlorides from a Cu-CF_2CF_2H Complex and Facile C-F Bond Activation: From ArF_6 to ArF with (IPr)Ni(C_6H_6).

N. O. Andrella, N. Xu and R. T. Baker manuscript in preparation and

N. O. Andrella, R. T. Baker and S. Ogoshi, manuscript in preparation

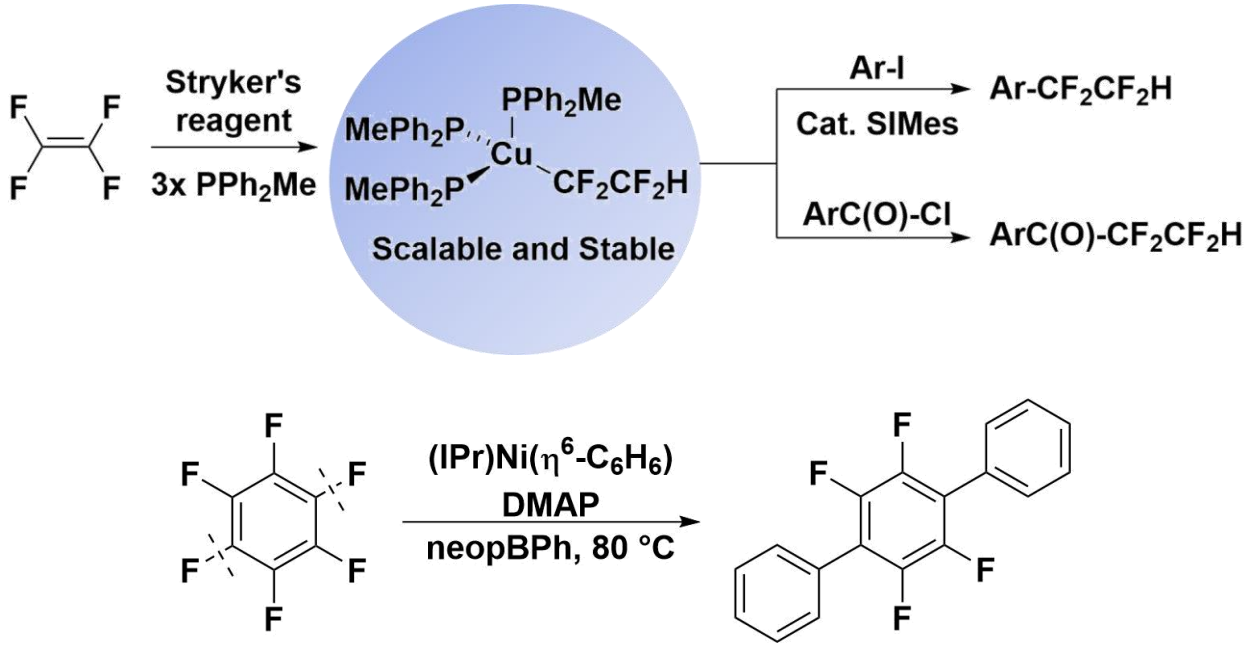

Andrella, Baker and Ogoshi wrote the manuscript. Andrella performed most of the experiments, Xu responsible for the scope of aryl iodides.

5.1. Abstract

The synthesis of C-R^F (Ar^F or fluoroalkyls) compounds remains challenging for synthetic chemists. In particular, the cross-coupling of C-X (X = Boron, Halogen) synthons with fluorinated moieties, using typical reaction conditions (e.g. Suzuki-Miyaura). Therefore, the new synthetic methodologies were envisioned. Using our reported complex, $[(PMePh_2)_3CuCF_2CF_2H]$, a new methodology for tetrafluoroethylation was developed. This complex is sufficiently stable under the reaction conditions to permit the fluoroalkylation of aryl iodides and a broad scope of acid chlorides. This is the first time either Ar-CF_2CF_2H or ArC(O)-CF_2CF_2H have been prepared from Ar-I or ArC(O)Cl. Furthermore, the reaction of (IPr)Ni(η6-C6H6) (**5.4**) with a series of fluoroarenes, C_6F_6-nHn [n = 0, 1, 4 or 5] yielded the C-F bond activated products $[(IPr)NiF(-C_6F_5)]_2$, $[(IPr)NiF(-C_6F_4H)]_2$, $[(IPr)NiF(-m-C_6FH_4)]_2$ and $[(IPr)NiF(-p-C_6FH_4)]_2$. Unexpectedly, the reaction of **5.4** with *o*-$C_6F_2H_4$ afforded a Ni(I) complex $[(IPr)Ni(-o-C_6FH_4)]_2$. With the addition of DMAP, the $[(IPr)NiF(-C_6F_5)]_2$ product was used in a nickel-mediated, base-free Suzuki-type cross-coupling reaction. This observation provides insight for the development of a catalytic reaction and expands the potential of nickel complexes for late-stage fluoroarylation.

5.2. Introduction

The use of fluorine atoms in pharmaceuticals and agrochemicals has for some time now been crucial in the development of new compounds.[15,31,355,550] The discovery of manmade bio-active fluorinated compounds (e.g. fluorouracil and fluorocortisone) spurred a search for new routes for their synthesis.[10,15,25,31,49] Several of these fluorinated compounds contain a C_{Ar}-F bond including one of the more successful drugs, atorvastatin (i.e. Lipitor®,Figure 5.1).[551]

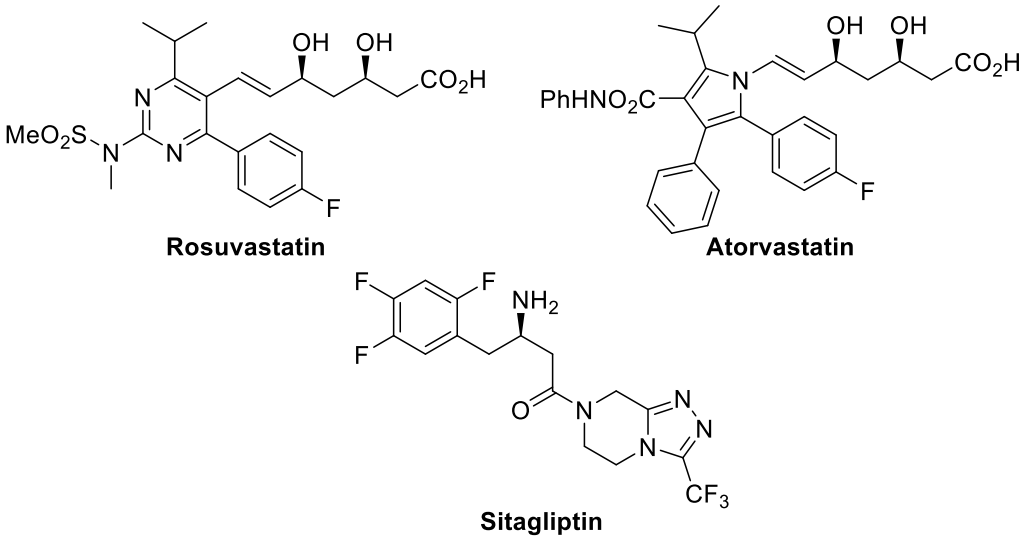

Figure 5.1. Some C_{Ar}-F containing drugs.

As such, more and more fluorinated pharmaceuticals and agro-chemicals have been introduced to the market. Trifluoromethylated compounds have also become increasingly popular and have by and large received the most attention.[92,111,124,128,130,134,140,141,147,148,163,164] Thus, the construction of other C-R^F (R^F = fluoroalkyl) bonds, excluding CF_3, remains underdeveloped.[162,229,230,272,365,399,387,390,391] However, recent advancements have brought other fluoroalkyl fragments to the fore, such as -CF_2H and -CF_2CF_3. In fact, variations on the fluoroethyl fragment have been an area of interest for quite some time.[542-546] For example, Desflurane® is a popular general anesthetic containing a -$CFHCF_3$ group but only a few synthetic methodologies exist for the introduction of such groups.[547]

Although, significant headway has been achieved in late-stage fluorination, the more popular routes generally start with a fluorinated precursor.[552,553,554] One such route that has been explored is the use of fluorinated aromatics as a coupling partner by C-F bond activation.[216,555-567] This route has recently seen some success, several challenges remain:

a) selective C-F vs C-H bond activation, and b) current reaction condition require high-temperature >100 °C and the use of strong Lewis acids. Generally, transition metal-mediated and -catalyzed routes were built on conditions first developed by Mcloughlin and Thrower. [382] In this discovery, it was found that copper metal could couple Ar-I and I-R^F [when used in the appropriate solvent, i.e. DMF] to generate Ar-R^F compounds. It was later introduced, that the use (-mediated or -catalyzed) of Cu^I-CF_3 complexes could achieve this same coupling reaction.[261, 275, 281] Various conditions have now been identified to carry out this reaction. For example, 1,10-phenanthroline (phen), di-tert-butylbipyridine (dtbpy) and 1,3-bis(2,4,6-trimethylphenyl)-4,5-dihydroimidazol-2-ylidene (SIMes) have all been shown to be suitable ligands.[548]

Building on these previous reports, transition metal catalyzed routes, especially with nickel and copper, have thus far proven to be the most useful. In 2006, Radius *et al.* reported the first Suzuki-type cross-coupling reaction using perfluoroarenes.[566] The reaction was enabled by a dimeric Ni^0 complex bearing two N-heterocyclic carbene ligands on each Ni atom, $[(I^iPr_2)_2Ni_2(\mu,\eta^2,\eta^2\text{-COD})]$ with the first step being oxidative addition of a C_{Ar}-F bond. In 2011, Ogoshi *et al.* reported a Hiyama cross-coupling with fluoroarenes using the same catalyst but the reaction still required high-temperatures.[300] Presumably, higher temperatures are required, as compared to perfluoroarenes, because C-F bond activation energy increases with decreasing F-substitution.[568] Recently, Johnson *et al.* found that $Ni(PEt_3)_4$ requires addition of $AlMe_3$ to effect the oxidative addition of C_{Ar}-F bonds.[569] In general, enhanced reactivity is observed with electronically unsaturated Ni complexes (< $16e^-$) that can potentially coordinate fluoro-arenes as π-ligands or through the C_{Ar}-F bond. Recent successes with copper for the introduction of other R^F groups focused on the use of fluoroalkenes [inexpensive and abundant fluorinated precursors]. In 2014, Ogoshi *et al*. synthesized Ar-CF_2CF_2-Ar via a (phen)Cu-CF_2CF_2Ar

complex.[227,228] Ar-CF_2CF_3 and Ar-CF_2CF_2OAr compounds have since been synthesized in a similar fashion.[229,230,272,292] In 2017 Hu *et al.* prepared 1,1,2,2-tetrafluoroethyl, -CF_2CF_2H, containing compounds by addition of E-H nucleophiles to tetrafluoroethylene (TFE).[229] However, this approach was limited to the synthesis of O- and N-CF_2CF_2H compounds. In fact, very few methods exist for the synthesis of C-CF_2CF_2H containing compounds.[546,549]

In a report by Singh and Shreeve, Ar-CF_2CF_2H could be prepared by reacting Ar-C(O)C(O)H compounds with deoxofluor. Very recently, we reported the facile synthesis of a new Cu-CF_2CF_2H complex, which could be successfully coupled with Ph-I, in a preliminary reaction.[see Chapter 4] Advantageously, in our synthetic protocol TFE can be used safely either on industrial or laboratory scale, because it uses a non-explosive 50:50 mixture of TFE:CO_2, so-called TFE Safe Supply®.[505]

Herein we report the synthesis and characterization of new $FNi^{II}Ar^F$ complexes and their reactivity under Suzuki-type cross-coupling reaction conditions and two previously unknown tetrafluoroethylation reactions with our Cu-CF_2CF_2H complex (**4.7a**). We demonstrate the tetrafluoroethylation of a) aryl iodides, effected by a catalytic amount of exogeneous ligand, and b) acid chlorides. The reaction with RC(O)Cl proved to be highly efficient, selective and of broad scope, yielding new tetrafluoroethyl ketones in up to 97% yield.

5.3. Results and Discussion

5.3.1. Copper Mediated and Catalyzed Synthesis of C-CF_2CF_2H Compounds

Based on our results of hydrometallation of TFE, we investigated the stoichiometric reactions between $[CuH(PPh_3)]_6$, TFE, ligand and aryl iodides. Initially, we attempted generating CuH *in situ* but none of the conditions used produced the desired product in appreciable yields

(for details, see the Annex E). Similarly, we could not identify reaction conditions which could couple the *in situ* generated Cu-CF_2CF_2H complexes to iodo benzene. DMF was chosen as a suitable solvent because it was found that polar solvents facilitate the addition of copper hydride to TFE. Additionally, using labile bidentate phosphine ligands such as dppe or DPEphos, yielded $PhCF_2CF_2H$, 20%. Changing the solvent to xylenes did not greatly influence the reaction but showed that aromatic solvents were suitable for such transformations.

As such, continuing with the originally discovered conditions, using isolated complex **4.7a**, we carried out a detailed study on the solvent and ligands (Table 5.1).

Table 5.1. Optimization of reaction conditions using complex **4.7a**.

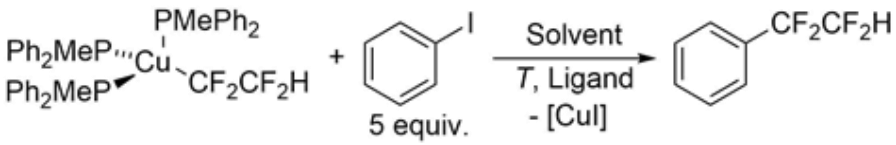

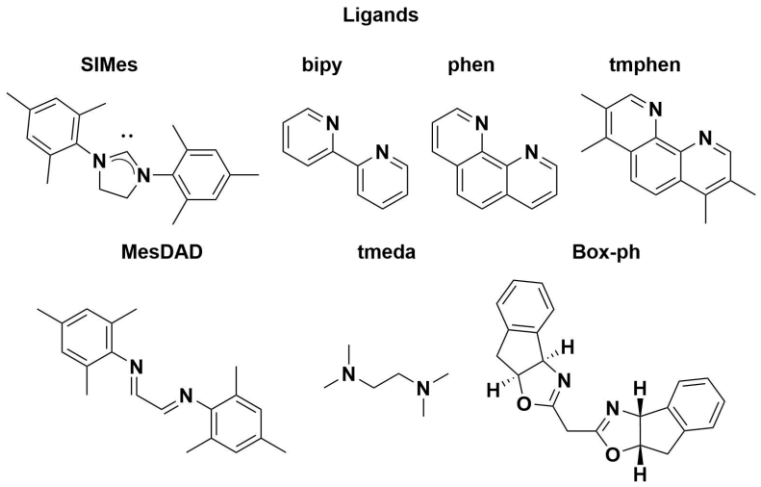

Entry	Solvent	T [°C]	Ligand	Yield[a] [%]
1	C_6D_6	80	SIMes	80

2	DMF	80	SIMes	85
3	THF	80	SIMes	3
4	DMSO	80	SIMes	50
5	DME	80	SIMes	56
6	CPME	60	SIMes	56
7	MeCN	80	SIMes	18
8	Toluene	80	SIMes	83
9	C_6D_6	80	bipy	75
10	C_6D_6	80	phen	68
11	C_6D_6	80	dmphen	58
12	C_5D_6	80	tmeda	32
13	C_6D_6	80	Box-ph	0
14	C_6D_6	80	MesDAD	55
15	C_6D_6	80	SIMes	82
16	C_6D_6	80	phen	42

[a] Yields are based on ^{19}F NMR integration of products vs internal standard. All reactions gave 100% conversion of [Cu]-CF_2CF_2H unless indicated otherwise.

First, the reaction conditions were optimized using complex **4.7a** as the limiting reagent and employing iodobenzene in excess (5 equiv.) for 24 h. Under these conditions, many solvents could be used in combination with SIMes to perform this transformation in good yield. Albeit, when THF is used (entry 3), the reaction does not go to completion and a significant amount of starting material remains. This is likely a consequence of not being able to heat the reaction to 80 °C. If a higher boiling point ether is used instead (e.g. 1,2-dimethoxyethane [DME] or cyclopentyl methyl ether [CPME], entries 5 and 6 respectively) the reaction still proceeds in decent yields, 56%. In DMSO yields are lower (entry 4, 50%) and HCF_2CF_2H is produced as a significant by-product. These results recall the reactivity of $[(PPh_3)_3CuCF_3]$, where HCF_3 was also observed in significant amounts in some solvents. However, when DMF is used (entry 2, 85%) little to no HCF_2CF_2H is formed and yields are on par with reactions in benzene or toluene. As such, we focused first on the use of ligands that are usually employed in trifluoromethylation reactions. Of the nitrogen ligands tested (bipy, phen, mesDAAD and dmphen) all performed well, with bipy giving the highest yields (entry 9, 75%), except for tmeda and Box-ph (entries 12 and 13, 32% and 0% respectively) in which HCF_2CF_2H was the major product.

With the original conditions still providing the best yields, an attempt to switch the limiting reagent of the iodobenzene reaction was made. It was found that an excess of **4.7a,** 1.3 equivalents, could be used to effectively carry out this reaction. Comparatively, use of phen under these conditions (entry 16, 42%), provided lower yields. Increasing the amount of **4.7a** beyond this ratio does not offer any additional benefits. Importantly, under these conditions, the yields depended heavily on the concentrations used, with the highest yields resulting from the most concentrated reactions. Any higher concentrations then those used, were impractical

because of the insolubility of **4.7a**, although ball-milling might prove useful to further optimize these conditions.

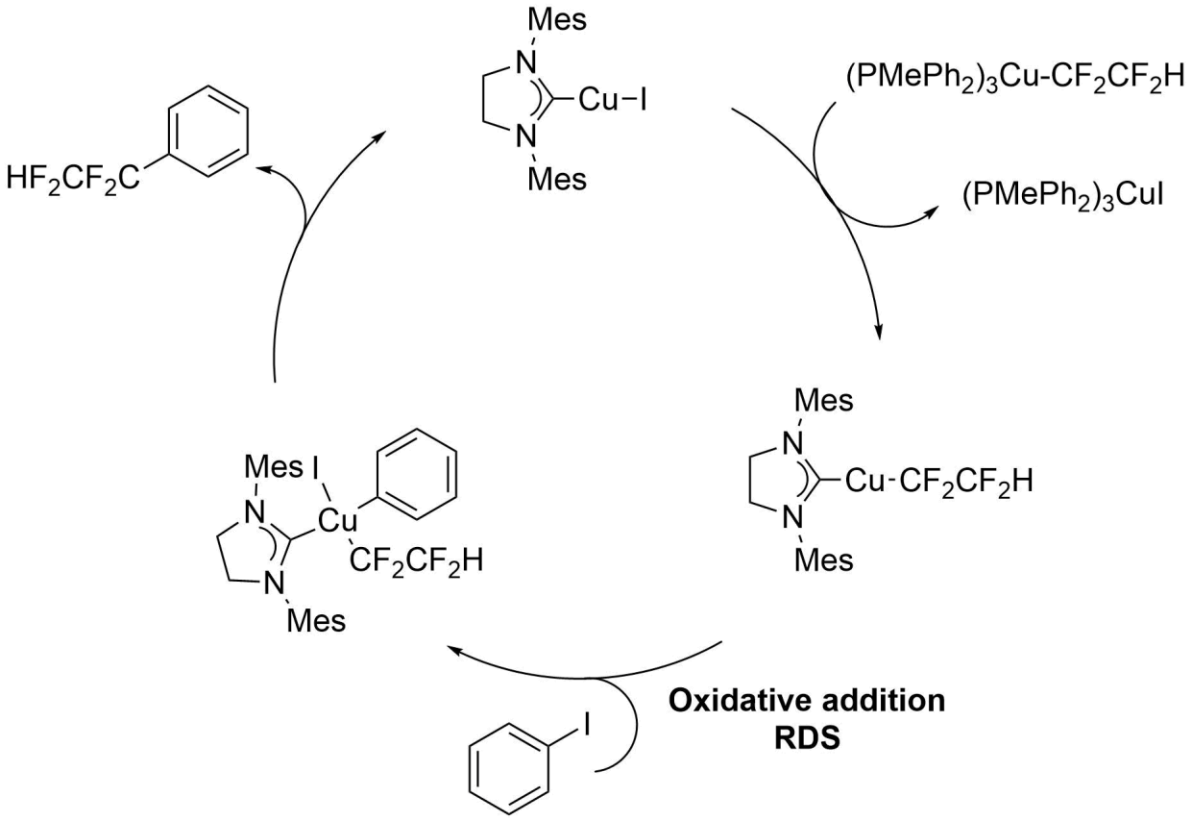

Scheme 5.1. Plausible mechanism for the cross-coupling of aryl iodides and **4.7a**, using a catalytic amount of SIMes.

With the optimized reaction conditions in hand, the scope of substrate reactivity of **4.7a** was explored (Table 5.2) and found to be highly dependent on the electronics and substitution pattern of the aryl iodide. In line with the dependence on the concentration of iodobenzene and results of other fluoro-alkylation reactions with copper, we suspect the limiting step to be the oxidative addition of the Ar-I bond to a copper(I) fluoroalkyl complex.

Table 5.2. Tetrafluoroethylation of aryl iodides with **4.7a** and a catalytic amount of SIMesCuCl.

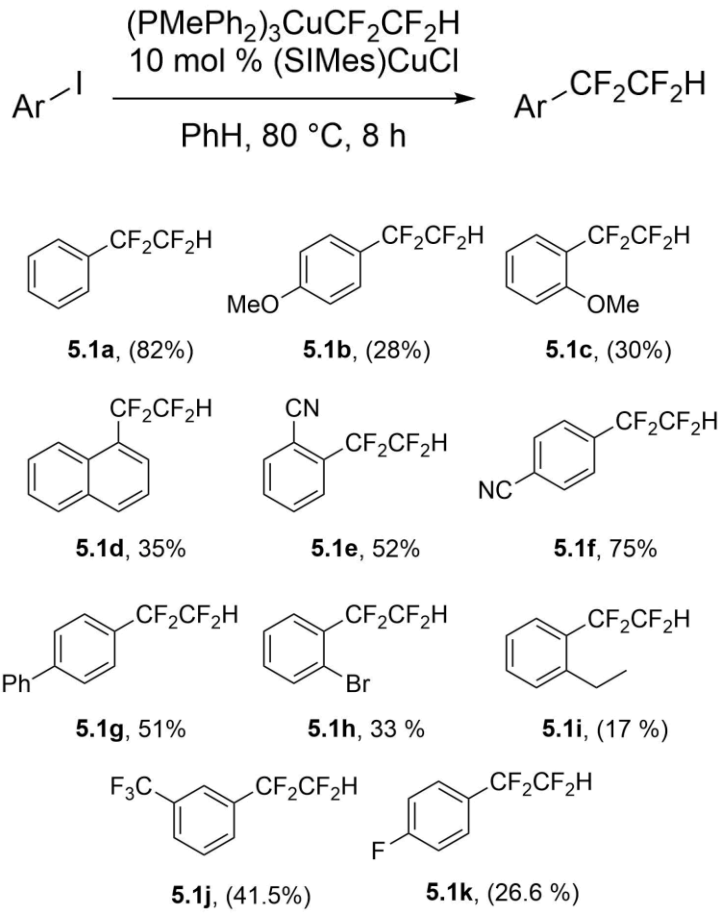

[a] Unless otherwise noted, reactions were performed using **4.7a** (0.07 mmol) and ArI (0.05 mmol). Yields were determined by ^{19}F NMR spectroscopy using $PhCF_3$ as an internal standard. [b] 0.2 mmol of **4.7a** was used. Isolated yields given in parentheses.

Typically, electron-rich arenes (**5.1b**, **5.1c** and **5.1i**) did not efficiently undergo tetrafluoroethylation giving poor yields. Prolonged heating of the reaction mixture did not lead to increased yields because most, if not all, of **4.7a** had decomposed over the course of the reaction. Other electron-poor functional groups such as cyano (**5.1e** and **5.1f**, ortho and para respectively), meta-trifluoromethyl (**5.1j**) and bromo (**5.1h**) were tolerated and moderate yields were obtained. Predictably, substitution in the *ortho* position (**5.1e**, **5.1h**, **5.1i)** leads to lower yields, except for **5.1c** which likely benefits from the *ortho* effect. The substrate bearing the *para*-phenyl (**5.1g**)

showed good yields but *para*-fluoro (**5.1k**) was quite low. However, the naphthyl derivative (**5.1d**) only produced moderate yields, possibly due to the volatility of this product.

To further demonstrate the utility **4.7a**, its reactivity was tested with acid chlorides. As expected, complex **4.7a** reacted smoothly with 2-Me-$C_6H_4C(O)Cl$ (**5.2a**) with gentle heating (50 °C). The choice of solvent was based on the optimization reaction conditions of aryl iodides, see above. Use of DMF, for example, gave multiple products. Interestingly, this reactivity echoes previous reports of fluoroalkylations of acid chlorides using tetrahedral copper complexes. In some of those reports, the $L_2Cu\text{-}R^F$ phosphine complexes were demonstrated to be ineffective in this transformation with yields < 50%. Only by addition of a small bidentate nitrogen ligand, to generate $L_3Cu\text{-}R^F$, did these make useful reagents. As in our case, the use of a smaller phosphine ligand from the onset, provides a much quicker route to the $L_3Cu\text{-}R^F$ complex to achieve similar utility.

Table 5.3. Tetrafluoroethylation of acid chlorides with **4.7a**.

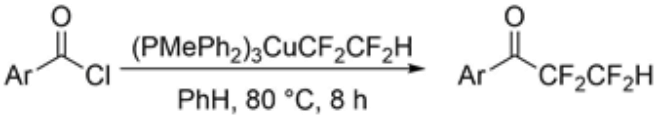

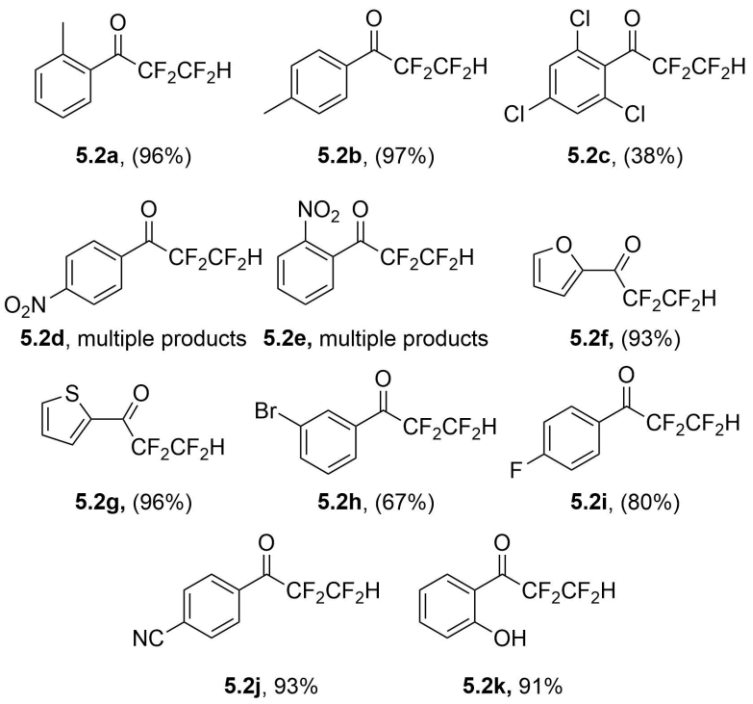

[a] Unless otherwise noted, reactions were performed using **4.7a** (0.07 mmol) and Ar(O)Cl (0.05 mmol). Yields were determined by ^{19}F NMR spectroscopy using $PhCF_3$ as an internal standard. [b] 0.2 mmol of **4.7a** was used. Isolated yields given in parentheses.

Various acid chlorides were reacted with **4.7a** to generate the corresponding ketones **5.8** in great yields (Table 5.3). Unlike the reaction with aryl iodides, even electron-rich substrates reacted smoothly with **4.7a**. In fact, substitution at either the *para* or *ortho* positions were tolerated (**5.8a**, **b** and **k**). Both 2-furanoyl chloride (**5.8f**) and 2-thienoyl chloride (**5.8g**) were tetrafluoroethylated in near quantitative yield. Halogenated aryl rings in either *ortho*, *meta* or *para* are all well tolerated (**5.8c**, **5.8h** and **5.8i**, yields) but the more sterically hindered, **5.8c**, required longer reaction times to go to completion. Like the reactivity of the scope for the aryl iodides, electron-withdrawing functional groups in the *para* position reacted smoothly with *para*-cyano (**5.8j**) giving quantitative yields. However, substitution of the nitro group in the *ortho* or *para* position gave rise to a plethora of side-products, likely due to single-electron transfer chemistry.

5.3.2. Nickel Mediated C_{Ar^F}-C Cross-Coupling Reactions

Building on the success of NHC ligated Ni^0 complexes in C-F bond activation reactions, a recently reported complex by Ogoshi *et al.* (IPr)Ni(η^6-C_6H_6) (**5.3**) was treated with a series of fluoro-arenes. Reaction in neat C_6F_6 at room temperature afforded complex **5.4a** (Scheme 5.2). The collection of single-crystal X-ray diffraction data unambiguously verified the dimeric nature of **5.4a** (Figure 5.2).

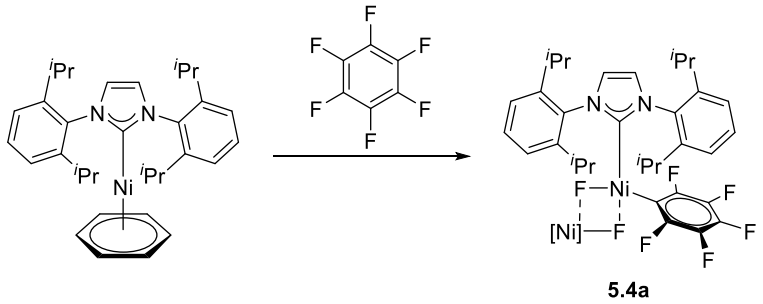

5.4a

Scheme 5.2. Synthesis of complex **5.4a**

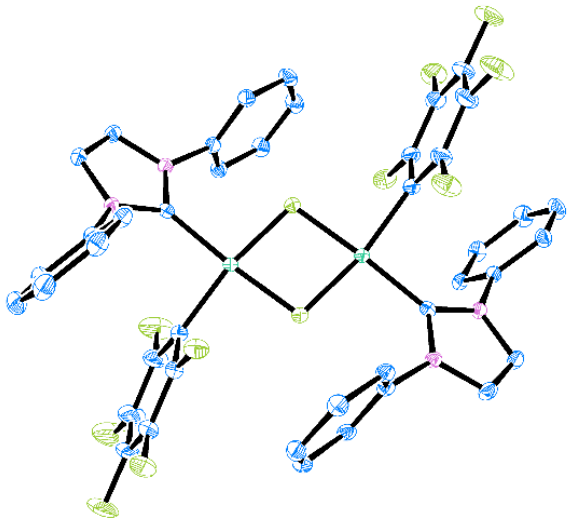

Figure 5.2. ORTEP representation of the molecular structure of **5.4a.** Thermal-ellipsoid probabilities are set to 35% with hydrogen atoms and 2,6-iso-propyl groups omitted for clarity.

The molecular structure of complex **5.4a** exhibits a tetrahedral coordination about the Ni with C_2 symmetry and features a bridging fluoride. There is a slight distortion of the C_6F_5 from

planarity, likely resulting from the steric bulk of the IPr ligand. The ^{19}F NMR spectrum of **5.4a** in C_6D_6 is consistent with the structure determined in the solid state. Interestingly, the Ni-F chemical shift (-470 ppm) is significantly further upfield then previously reported complexes.[564] With these initial reaction conditions in hand, the scope of fluoro-arene C-F bond activation was explored. It was found complex **5.3** undergoes facile oxidative addition, although yields are low (≤ 50 %), with some of the series of ArF compounds tested (Figure 5.3) with increasing temperature as the fluorination level is decreased, with the highest temperature required (60 °C) for fluorobenzene.

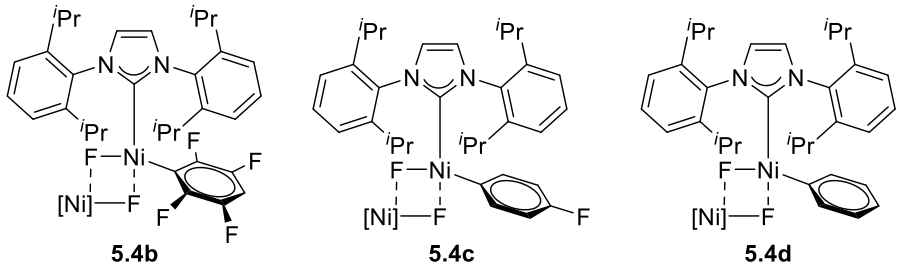

Figure 5.3. Isolated products from the reactions of **5.4** with various fluoroarenes.

All structures were unambiguously confirmed by single-crystal X-ray diffraction data (See SI). The Ni-F bond length is similar for all complexes ~1.89Å. Interestingly, no discernable trend in Ni-C_{Ar} bond length versus the degree of fluorination of the phenyl ring is observed, with only slight variations from 1.879 Å to 1.886 Å. Again, the ^{19}F NMR showed a discernable upfield signal in the range of -400 to -450 ppm, with the chemical shift being dependent on the degree of fluorination.

Unexpectedly, if the same conditions were used with 1,2-difluorobenzene a dimeric $Ni^{I}(C_6H_4F)$ (**5.5**) complex was isolated from the reaction mixture (Scheme 5.3). Although the exact mechanism for the formation of this complex is not known, it is possible that a Ni^{II} complex, analogous to complex **5.4**, is generated *in situ*, followed by a conproportionation with

left-over **5.3** to yield **5.5** and $[IPrNi^{I}F]_n$. This competing reaction may rationalize the low yields observed for complexes **5.4a-d**.

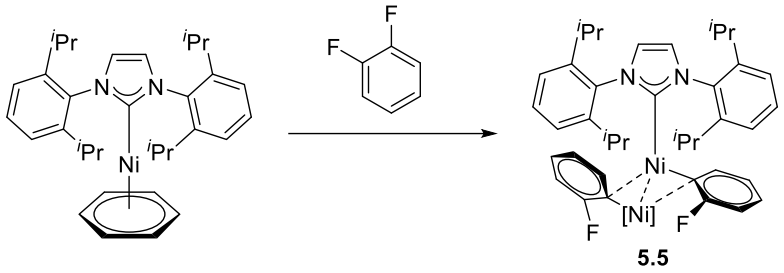

5.5

Scheme 5.3. Synthesis of complex **5.5.**

The molecular structure of complex **5.5** (Figure 5.4) exhibits a trigonal planar coordination about the Ni with C_2 symmetry and features a bridging aryl group that is σ-bonded to one Ni (Ni-C = 1.931 Å and π-bonded to the other (η^1Ni-C_{Ar} = 1.971Å). These bonds are considerably longer then their Ni^{II} counterparts, but in-line with other Ni^{I}-Ar complexes. The dimer exhibits a very close Ni^{I}-Ni^{I} contact of 2.407 Å, suggesting a bonding interaction. Indeed, the ^{19}F NMR spectrum is typical of a diamagnetic complex with a sharp signal for the Ar-F fluorine. This suggests a Ni-Ni single bond or bridging ligand-facilitated, strong anti-ferromagnetic coupling between the paramagnetic Ni^{I} centers.

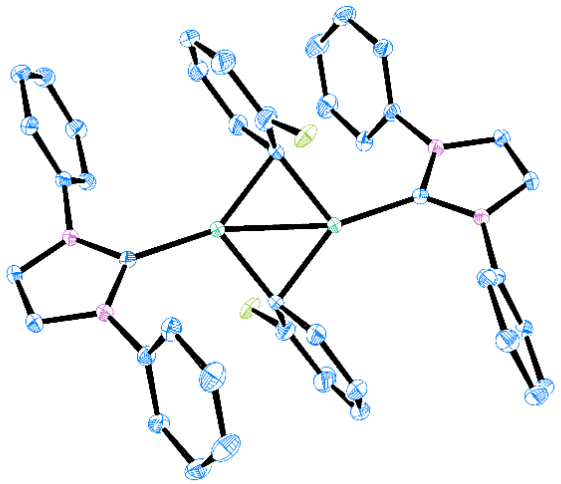

Figure 5.4. ORTEP representation of the molecular structure of **5.5**. Thermal-ellipsoid probabilities are set to 35% with hydrogen atoms and 2,6-iso-propyl groups omitted for clarity.

With initial reactivity with ArF compounds in hand, a stoichiometric study on the reactivity of complex **5.4a** was carried out to achieve a base-free Suzuki-type cross-coupling reaction. Unfortunately, attempted catalytic conditions did not produce the desired product. We therefore focused our attention on stoichiometric reactions of **5.4a** with aryl boronic esters. In a first attempt **5.4a** was mixed with a boronic ester in C_6D_6 but no reaction was observed.

As such, we hypothesized that no transmetallation reaction was occurring because the dimeric nature of **5.4a** was inhibiting the reaction. Thus, the dimer was treated with dimethylaminopyridine (DMAP) to generate **5.6a**. Based on the distinct downfield shift of the Ni-F signal, and color change (orange to yellow) upon addition of DMAP, we suspect that DMAP is coordinated and **5.6a** is monomeric. As expected, addition of aryl boronic acid ester to this complex, leads to a successful cross-coupling reaction (Scheme 5.4). Interestingly, C_6F_5-Ph, the expected product, is not observed. Instead, a mixture of 4-H-C_6F_4-Ph (**5.7**), minor, and 4-Ph-C_6F_4-Ph (**5.8)**, major, are observed. These results suggest that the development of a catalytic reaction is attainable and further elaboration on these results is ongoing. It is suspected that the

initial transmetallation occurs to generate **5.6a'**, which undergoes rapid reductive elimination, to produce C_6F_5-Ph, which then undergoes facile C-F bond oxidative addition at the *para*-position generating **5.6b'**, which likely undergos slow homolysis of Ni-C_{Ar} bond, producing **5.7**, or undergoes transmetallation and reductive elimination to give **5.8**. The role of water in the production of **5.7** has not yet been ruled out.

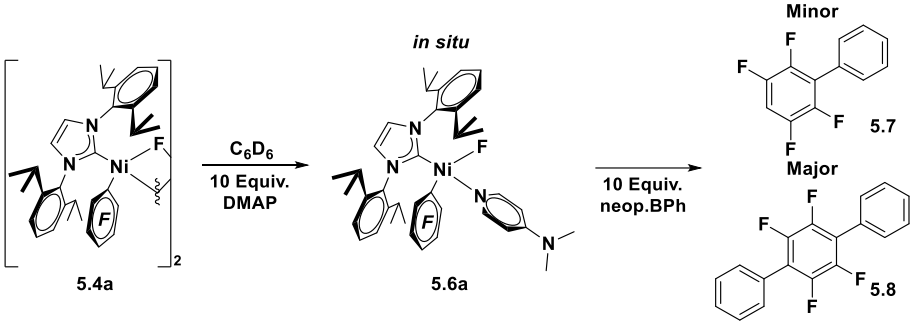

Scheme 5.4. Nickel-mediated base-free Suzuki cross-coupling of **5.4a** and phenylboronic acid neopentylglycol ester.

5.4. Conclusions

In summary, we have outlined the synthesis and characterization of dimeric NHC-NiArF complexes and a rare Ni^I complex and a new synthetic methodology for the introduction of the -CF_2CF_2H group. This reaction uses our previously reported Cu-CF_2CF_2H complex (**4.7a**), which can be easily and safely synthesized from TFE Safe Supply®. We have demonstrated that the nickel complexes, **5.4**, can be easily synthesized under mild conditions by exposure of **5.3** to various Ar-F compounds. Furthermore, we have explored the reactivity of such complexes under various additive-free Suzuki cross-coupling conditions. These results highlight the importance of dimer dissociation to achieve transmetallation of Ar-B with Ni-F complexes. Finally, a mild/base-free nickel complex-mediated cross-coupling of hexafluorobenzene and a boronic acid

ester was demonstrated. Furthermore, the Cu-CF_2CF_2H complex, **4.7a**, can undergo coupling reactions with electron-poor or -neutral aryl iodides in good yields, with addition of either SIMes or bipy in catalytic amounts. This complex, **4.7a**, is an effective reagent for the tetrafluoroethylation of a broad scope of acid chlorides. This protocol represents the first practical synthesis of tetrafluoroethyl ketones from the corresponding acid chlorides. Ongoing studies are focused on the development of a catalytic variant of these reactions and there utility in late-stage introduction of fluoro-alkyls and fluoro-arenes.

5.5. Experimental Section.

5.5.1. General Procedure

Experiments were conducted under nitrogen, using Schlenk techniques or an MBraun glove box. All solvents were deoxygenated by purging with nitrogen. Tetrahydrofuran (THF), acetonitrile (MeCN) and toluene were dried on columns of activated alumina using a J. C. Meyer (formerly Glass Contour®) solvent purification system. 1,2-Dimethoxyethane (DME), cyclopentyl methyl ether (CPME) and benzene-d_6 (C_6D_6) were dried by stirring over activated alumina (ca. 10 wt. %) overnight, followed by filtration. All solvents were stored over activated (heated at ca. 250 °C for >10 h under vacuum) 4 Å molecular sieves. Glassware was oven-dried at 120 °C for >2 h. The following chemicals were obtained commercially, as indicated: dimethylformamide (DMF, Alfa Aesar Anhydrous 99.8%), dimethylsulfoxide (DMSO, Alfa Aesar Anhydrous 99.8%), iodobenzene (Alfa Aesar, 98 %), all other aryl iodides (SiGMA), all acid chlorides (SIGMA), 1,10-phenanthroline (Sigma-Aldrich, phen), 2,2'-bipyridine (SIGMA, bipy), 2,9-dimethy-1,10-phenanthroline (Sigma-Aldrich, dmphen), tetramethylethylenediamine (Sigma-Aldrich, tmeda), [3aR-[2(3′ aR*,8′ aS*),3′ aβ,8′ aβ]]-(+)-2,2′ -Methylenebis

[3a,8a-dihydro-8H-indeno[1,2-d]oxazole] (Box-ph, Sigma), triphenylphosphine (PPh_3, Oakwood chemicals, 99%), tri(*o*-tolyl)phosphine ($P(o\text{-tolyl})_3$, Alfa Aesar, 98%), 2-di-tert-butylphosphino-2′,4′,6′-triisopropylbiphenyl (tbuXphos, Sigma-Aldrich, 97%), 1,2-bis(diphenylphosphino)ethane (dppe, Strem chemicals, 99%), 1,1'-bis(diphenylphosphino)ferrocene (dppf, Accela ChemBio Inc., 99%), 4,5-bis(diphenylphosphino)-9,9-dimethylxanthene (Xantphos, Accela ChemBio Inc., 99%), triethylphosphite ($P(OEt)_3$, Sigma-Aldrich, 98%), triphenylphosphite ($P(OPh)_3$, Alfa Aesar, 97%), tri-ortho-tolyl phosphite ($P(O\text{-}o\text{-tolyl})_3$, Alfa Aesar), methyldiphenylphosphine ($PMePh_2$, Acros Organics, 99%), dimethylphenylphosphine (PMe_2PhMe, Acros Organics, 97%). The following chemicals were synthesized as previously reported: 1,3-bis(2,6-diisopropylphenyl)imidazolidin-2-ylidene (SIPr), 1,3-bis(2,3,6-trimethylphenyl)imidazolidin-2-ylidene (SIMes), $[(PPh_3)CuH]_6$, (SIMes)CuCl and (SIPr)CuCl. Electrospray ionization mass spectral data were collected using an Applied Biosystem API2000 triple quadrupole mass spectrometer and elemental analyses were performed by Ján Veizer Stable Isotope Laboratory, University of Ottawa. NMR spectra (^1H, ^{19}F, $^{31}P\{^1H\}$, and $^{13}C\{^1H\}$) were recorded on a 300 MHz Bruker Avance instrument at room temperature (21-23 °C) unless stated otherwise. ^1H NMR spectra were referenced to residual proton peaks associated with the deuterated solvents (C_6D_6: δ 7.16) and $^{31}P\{^1H\}$ NMR data were referenced to external H_3PO_4 (85 % aqueous solution), set to 0.0 pm. ^{19}F NMR spectra were referenced to internal standard α,α,α-trifluorotoluene (CF_3Ph) [unless stated otherwise] (Sigma-Aldrich, 99%, deoxygenated by purging with nitrogen, stored over activated 4 Å molecular sieves), set to – 63.5 ppm. NMR spectra for the title compounds are displayed at the end of the Supporting Information, Annex D.

General Experimental Procedure for Tetrafluoroethylation of Aryl Iodides, NMR Scale. The copper complex **4.7a** (53 mg, 0.07 mmol) and [(1,3-bis(2,4,6-trimethylphenyl)-4,5-

dihydroimidazol-2-ylidene) copper(I) chloride] (3 mg, 0.007 mmol) were loaded into an NMR tube and mixed with C_6D_6. Aryl iodide (0.054 mmol) and $PhCF_3$ (3 μL, 0.02 mmol) were then added to the solution. The reaction was heated at 80 °C for 8 h. Compounds **5.1a-c**,**h-k** were identified using available literature data. See Annex D.

1,1,2,2-tetrafluoroethylbenzene (5.1a): ^{19}F NMR (282 MHz, C_6D_6): δ −115.98 (dt, $^3J_{FF}$ = $^3J_{FH}$ = 7 Hz, CF_2), −136.54 (dt, $^2J_{FH}$ = 51, $^3J_{FF}$ = 7 Hz, CF_2H). GC-MS (retention time 3.85 min): expected, 178.0; found, 178.0.

(4-methoxy)phenyl-1,1,2,2-tetrafluoroethane (5.1b): ^{19}F NMR (282 MHz, C_6D_6): δ −113.34 (dt, $^3J_{FF}$ = $^3J_{FH}$ = 4 Hz, CF_2), −134.99 (dt, $^2J_{FH}$ = 55, $^3J_{FF}$ = 4 Hz, CF_2H). GC-MS (retention time 4.10 min): expected, 208.0; found, 208.1.

(2-methoxy)phenyl-1,1,2,2-tetrafluoroethane (5.1c): ^{19}F NMR (282 MHz, C_6D_6): δ −117.305 (dt, $^3J_{FF}$ = $^3J_{FH}$ = 9 Hz, CF_2), −137.63 (dt, $^2J_{FH}$ = 54, $^3J_{FF}$ = 9 Hz, CF_2H). GC-MS (retention time 4.08 min): expected, 208.0; found, 208.1.

(2-bromo)phenyl-1,1,2,2-tetrafluoroethane (5.1h)*:* ^{19}F NMR (282 MHz, C_6D_6): δ −115.14 (tt, $^3J_{FF}$ = $^3J_{FH}$ = 7 Hz, CF_2), −136.51 (dt, $^2J_{FH}$ = 51, $^3J_{FF}$ = 7 Hz, CF_2H). GC-MS (retention time 4.54 min): expected, 255.9 (100%), 257.9 (97%); found, 255.9 (100%), 257.9 (94%).

(2-ethyl)phenyl-1,1,2,2-tetrafluoroethane (5.1i): ^{19}F NMR (282 MHz, C_6D_6): δ −110.97 (tt, $^3J_{FF}$ = $^3J_{FH}$ = 7 Hz, CF_2), −134.86 (dt, $^2J_{FH}$ = 51, $^3J_{FF}$ = 7 Hz, CF_2H). GC-MS (retention time 4.32 min): expected, 206.1; found, 206.1.

(3-trifluoromethyl)phenyl-1,1,2,2-tetrafluoroethane (5.1j)*:* ^{19}F NMR (282 MHz, C_6D_6): δ -63.77 (CF_3), −114.88 (m, CF_2), −136.10 (dt, $^2J_{FH}$ = 54, $^3J_{FF}$ = 7 Hz, CF_2H). GC-MS (retention time 3.97 min): expected, 246.0; found, 246.0.

(4-fluoro)phenyl-1,1,2,2-tetrafluoroethane (5.1k)*:* ^{19}F NMR (282 MHz, C_6D_6): δ −115.14 (tt, $^3J_{FF}$ = $^3J_{FH}$ = 7 Hz, CF_2), −136.51 (dt, $^2J_{FH}$ = 51, $^3J_{FF}$ = 7 Hz, CF_2H). GC-MS (retention time 3.65 min): expected, 197.03; found, 197.03.

General Experimental Procedure for Tetrafluoroethylation of Aryl Iodides, Isolation. The copper complex **4.7a** (250 mg, 0.33 mmol) and [(1,3-bis(2,4,6-trimethylphenyl)-4,5-dihydroimidazol-2-ylidene) copper(I) chloride] (17 mg, 0.04 mmol) were loaded into scintillation vial and mixed with toluene. Aryl iodide (0.22 mmol) was then added to the solution and the reaction was heated at 80 °C for 8 h. Compounds **5.1d-g** were identified using available literature data. See Annex D.

2-(1,1,2,2-tetrafluoro)ethylnaphthalene (5.1d): ^{1}H NMR(400 MHz, $CDCl_3$): δ 8.20 (m, Ar, 1H), 8.02 (m, Ar, 1H), 7.93 (m, Ar, 1H), 7.81 (m, Ar, 1H), 7.62 – 7.51 (ov m, Ar, 3H), 6.17 (tt, $^2J_{HF}$ = 54, $^3J_{HF}$ = 4 Hz, 1H, CF_2H). ^{19}F NMR (282 MHz, C_6D_6): δ −113.20 (dt, $^3J_{FF}$ = $^3J_{FH}$ = 5 Hz, CF_2), −137.53 (dt, $^2J_{FH}$ = 54, $^3J_{FF}$ = 6 Hz, CF_2H). GC-MS (retention time 3.85 min): expected, 178.0; found, 178.0. Yield: 33%

(2-cyano)phenyl-1,1,2,2-tetrafluoroethane (5.1e): ^{1}H NMR(400 MHz, $CDCl_3$): δ 7.85 (m, Ar, 1H), 7.79 – 7.64 (ov m, Ar 3H), 6.11 (tt, $^2J_{HF}$ = 54, $^3J_{HF}$ = 3 Hz, 1H, CF_2H). ^{13}C{^{1}H} δ 134.93, 132.77, 132.16, 131.78, 129.12, 128.55 (t, J_{CF} = 8 Hz), 116.29, 114.62 (tt, J_{CF} = 253 Hz, J_{CF} = 30 Hz), 109.76 (tt, J_{CF} = 252, J_{CF} = 41 Hz). ^{19}F NMR (282 MHz, C_6D_6): δ −115.68 (dt, $^3J_{FF}$ = $^3J_{FH}$ =

4 Hz, CF_2), −137.29 (dt, $^2J_{FH}$ = 54, $^3J_{FF}$ = 4 Hz, CF_2H). GC-MS (retention time 3.85 min): expected, 178.0; found, 178.0.

(4-cyano)phenyl-1,1,2,2-tetrafluoroethane (5.1f): ^{1}H NMR(400 MHz, $CDCl_3$) δ 7.80 (dm, $^3J_{HH}$ = 8 Hz, Ar, 2H), 7.69 (dm, $^3J_{HH}$ = 8 Hz, Ar 2H), 5.96 (tt, $^2J_{HF}$ = 54, $^3J_{HF}$ = 2 Hz, 1H, CF_2H). $^{13}C\{^1H\}$ δ 134.03 (t, J_{CF} = 25 Hz), 132.36, 127.51 (t, J_{CF} = 8 Hz), 117.65, 115.62 (m), 114.77 (tt, J_{CF} = 248, J_{CF} = 28 Hz), 109.86 (tt, J_{CF} = 251, J_{CF} = 43 Hz). ^{19}F NMR (282 MHz, C_6D_6): δ −115.302 (dt, $^3J_{FF}$ = $^3J_{FH}$ = 4 Hz, CF_2), −135.11 (dt, $^2J_{FH}$ = 54, $^3J_{FF}$ = 4 Hz, CF_2H). GC-MS (retention time 3.85 min): expected, 178.0; found, 178.0.

4-(1,1,2,2-tetrafluoro)ethylbiphenyl (5.1g): ^{1}H NMR(400 MHz, $CDCl_3$) δ 7.72 – 7.35 (over m, Ar, 9H), 7.69 (dm, $^3J_{HH}$ = 8 Hz, Ar 2H), 5.95 (tt, $^2J_{HF}$ = 54, $^3J_{HF}$ = 3 Hz, 1H, CF_2H). ^{19}F NMR (282 MHz, C_6D_6): δ −114.31(dt, $^3J_{FF}$ = $^3J_{FH}$ = 4 Hz, CF_2), −134.99 (dt, $^2J_{FH}$ = 54, $^3J_{FF}$ = 4 Hz, CF_2H). GC-MS (retention time 3.85 min): expected, 178.0; found, 178.0.

General Experimental Procedure for Tetrafluoroethylation of Acid Chlorides, NMR Scale. The copper complex **4.7a** (53 mg, 0.07 mmol) was loaded into an NMR tube and mixed with C_6D_6. Acid Chloride (0.054 mmol) and $PhCF_3$ (3 μL, 0.02 mmol) were then added to the solution and the reaction was heated at 60 °C for 8 h. Compounds **5.2a-c**, **f-i** were identified using available literature data. See Annex D.

2-Me-PhC(O)CF_2CF_2H (5.2a): ^{19}F NMR (282 MHz, C_6D_6): δ −119.76 (m, CF_2), −140.16 (dm, $^2J_{FH}$ = 53 Hz, CF_2H). GC-MS (retention time 3.85 min): expected, 178.0; found, 178.0.

4-Me-PhC(O)CF_2CF_2H (5.2b): ^{19}F NMR (282 MHz, C_6D_6): δ −119.68 (dd, $^3J_{FF}$ = $^3J_{FH}$ = 7 Hz, CF_2), −136.54 (dm, $^2J_{FH}$ = 54 Hz, CF_2H). GC-MS (retention time 3.85 min): expected, 178.0; found, 178.0.

2,4,6-Cl_3-PhC(O)CF_2CF_2H (5.2c): ^{19}F NMR (282 MHz, C_6D_6): δ −122.87 (m , CF_2), −138.50 (dt, $^2J_{FH}$ = 51, $^3J_{FF}$ = 6 Hz, CF_2H). GC-MS (retention time 3.85 min): expected, 178.0; found, 178.0.

2-(-CHCHCHCHO-)C(O)CF_2CF_2H (5.2f): ^{19}F NMR (282 MHz, C_6D_6): δ −123.10 (m, CF_2), −139.33 (dt, $^2J_{FH}$ = 53, $^3J_{FF}$ = 7 Hz, CF_2H). GC-MS (retention time 3.85 min): expected, 178.0; found, 178.0.

2-TpC(O)CF_2CF_2H (5.2g): ^{19}F NMR (282 MHz, C_6D_6): δ −120.98 (m, CF_2), −139.34 (dt, $^2J_{FH}$ = 52, $^3J_{FF}$ = 7 Hz, CF_2H). GC-MS (retention time 3.85 min): expected, 178.0; found, 178.0.

3-Br-PhC(O)CF_2CF_2H (5.2h): ^{19}F NMR (282 MHz, C_6D_6): δ −119.74 (m, CF_2), −139.61 (dm, $^2J_{FH}$ = 52 Hz, CF_2H). GC-MS (retention time 3.85 min): expected, 178.0; found, 178.0.

4-F-PhC(O)CF_2CF_2H (5.2i): ^{19}F NMR (282 MHz, C_6D_6): δ −101.73 (m, Ar-F), −119.62 (dd, $^3J_{FF}$ = $^3J_{FH}$ = 7 Hz, CF_2), −139.76 (dm, $^2J_{FH}$ = 52 Hz, CF_2H). GC-MS (retention time 3.85 min): expected, 178.0; found, 178.0.

General Experimental Procedure for Tetrafluoroethylation of Acid Chlorides, Isolation. The copper complex **1a** (806 mg, 1.06 mmol) was loaded into an NMR tube and mixed with toluene. Acid Chloride (0.964 mmol) was then added to the solution and the reaction

was heated at 60 °C for 8 h. Compounds **5.2j**,**k** were identified using available literature data. See Annex D

4-CN-PhC(O)CF_2CF_2H (5.2j): Is not yet fully characterized.

2-OH-PhC(O)CF_2CF_2H (5.2k): Is not yet fully characterized.

General Experimental Procedure for the Reaction of Fluoroarenes with Ni^0, NMR Scale. The red complex (IPr)Ni[η^6-(C_6H_6)] (**5.3**) (20 mg, 0.04 mmol) was loaded into an NMR tube and mixed with the respective fluoroarene ($C_6F_nH_{6-n}$). The reaction was left to sit at room temperature for 24 h, unless indicated otherwise.

Synthesis of (IPr)NiF(-C_6F_5) (5.4a). Orange crystals of **5.4a** were collected from the reaction mixture. ^{1}H NMR (400 MHz, C_6D_6): δ 7.31 (Ar, 2), 7.05 (Ar, 4), 6.06 (IPrCH, 2), 2.76 (IPr ^{i}PrCH, quint., 4), 1.46, (IPr ^{i}PrMe, d, 12), 0.82 (IPr ^{i}PrMe, d, 12). ^{19}F NMR (376 MHz, C_6D_6, internal standard: C_6F_6= -164.5): -116.48 (Ar-F, md, $^3J_{FF}$ = 27 Hz, 2F), -164.78 (Ar-F, t, $^3J_{FF}$ = 20 Hz, 1F), -168.10 (Ar-F, dt, $^3J_{FF}$ = 27, $^3J_{FF}$ = 20 Hz, 2F), -470.3 ppm (Ni-F, s).

Synthesis of (IPr)NiF(-*p*-$C_6H_1F_4$) (5.4b). Yellow crystals of **5.4b** were collected from the reaction mixture. This product is not yet fully characterized.

Synthesis of (IPr)NiF(-*p*-C_6H_4F) (5.4c). Yellow crystals of **5.4c** were collected from the reaction mixture. This product is not yet fully characterized.

Synthesis of (IPr)NiF(-C_6H_5) (5.4d). This reaction was heated to 60 °C. Yellow crystals of **5.2d** were collected from the reaction mixture. ^{1}H NMR (400 MHz, C_6D_6): δ 7.46 (Ar, 2), 7.39 (Ar, 4), 6.69 (Ph, 5), 6.29 (IPrCH, 2), 2.81 (IPr ^{i}PrCH, quint., 4), 1.26, (IPr ^{i}PrMe, d, 12), 0.91 (IPr ^{i}PrMe, d, 12). ^{19}F NMR (376 MHz, C_6D_6): -399.7 ppm (Ni-F, s).

Synthesis of (IPr)NiF(-C_6H_5) (5.5). This reaction was heated to 40 °C. Green crystals of **6.3** were collected from the reaction mixture. This product is not yet fully characterized.

Reaction of Phenylboronic Acid Neopentylglycol Ester with 5.4a and Dimethylamino- Pyridine (DMAP), NMR Scale. The orange complex [(IPr)NiF(-C_6F_5)] (**5.4a**) (20 mg, 0.03 mmol) was loaded into an NMR tube and mixed with C_6D_6. DMAP (4 mg, 0.03 mmol), was then added to the solution. After the reaction turned yellow, phenylboronic acid neopentylglycol ester (25 mg, 0.16 mmol) was added. The reaction was heated at 60 °C for 8 h. Compound **5.7** and **5.8** were identified using available literature data. See Annex E for NMR spectra.

Chapter 6.

6. Conclusions

Organofluorine compounds have become ubiquitous in everyday life but their modern-day synthesis still generally relies on archaic synthetic protocols. Albeit, these syntheses have uncompromised advantages when dealing with small-molecules with little to no functional groups. However, as discussed throughout this *Thesis* these protocols generally fail to yield the desired selectivity. Furthermore, their simplicity necessitates the use of the most abundant forms of fluorine such as HF. Although industrially we have developed protocols for the safe handling and storage of these compounds, there remains an inherent danger to their use. To add, many of these protocols generate ozone-depleting chlorofluorocarbons as intermediates.

As the demand for fluorinated chemicals has increased, so too have synthetic methods for introducing fluorine and fluorocarbon groups. The application of green chemistry principles to organofluorine synthesis remains an underused strategy and a source for potential growth in this field. With this in mind, we endeavored to develop new routes to organofluorine compounds using commercially available feedstocks coupled with coinage metal-mediated or -catalyzed reactions.

In Chapter 2 we presented the advantages offered by low-coordination number on perfluoronickelacyclopentanes enabled by a bulky N-heterocyclic carbene ligand. DFT studies reproduced the agostic interaction observed in the solid-state structure and identified a second isomer of similar energy that demonstrates the potential bidentate nature of diaryl NHC ligands. Prior to our discovery, when phosphite or phosphine complexes $L_2Ni(C_4F_8)$ were exposed to a Lewis acid, P migration to the carbenium ion was always observed. This resulted in a

synthetically limited methodology for production of phosphonium fluoroalkyls (Assuming that the Ni-C_{RF} bond could be hydrogenolyzed, although this has never been demonstrated). Additionally, beyond Wittig type chemistry the utility of phosphonium fluoroalkyls are unknown to the author. As such, in terms of reactivity, the pseudo-three coordinate perfluoronickelacyclopentane enabled a rare Cα-F fluoride abstraction, using a Lewis acid, which did not result in ligand migration to the carbon. Instead a rare Ni-C^F bond migration resulting in a ring contraction to a perfluorocyclobutyl complex was observed. Similar reactivity was enabled by exposure of this complex to *Brønsted* acids with pKa < 5. However, when a *Brønsted* acid with a pKa > 5 was used, a novel ring functionalization, Cα-F to Cα-X (X = OAc,) and competing Ni-C^F bond protonolysis was observed; the latter pathway dominates with bulky 2,4,6-trimethylbenzoic acid. Finally, the low-coordinate scaffold has allowed access to low pressure/low temperature hydrogenolysis of both Ni-C^F bonds under much milder conditions than reported previously by Baker et al. using a 4-coordinate bis(phosphite) complex.[185]

In Chapter 3 our approach shifted from oxidative cyclization to M-X insertion reactions. There has been an increase in pesticides containing the hexafluoro-isopropyl (hfip) fragment. To avoid the expense of R^F-I compounds, researchers found previously that insertion of inexpensive hexafluoropropene [HFP] into the Ag-F bond forms stable silver hfip complexes. While these complexes are not efficient hfip transfer agents, they have been employed to prepare analogous copper complexes that are capable of such transfers. Although copper-hfip complexes can be generated from Cu metal or Cu(OAc) and $ICF(CF_3)_2$ they have not been generated directly from inexpensive HFP. As such, we investigated the synthesis of metal-hfip complexes using HFP to expand on their reactivity. A methodology was developed to achieve the successful hfip transmetallation to nickel using an Ag-hfip complex. After treatment of the Ni complex with

$ZnPh_2$ we showed that reductive elimination could be promoted by addition of CO to give benzoyl-hfip. Wanting to eliminate the use of silver, copper hfip complexes were synthesized directly from HFP. These are the first isolated and fully characterized Cu-hfip complexes which allow for a comparison to a series of copper fluoroalkyl complexes. Using these well-defined Cu-hfip complexes the successful transfer of hfip to organic substrates (aroyl and benzyl chlorides) was achieved. We identified competing β-fluoride elimination and Cu-C bond homolysis or protonolysis which was supported by computations that probe thermodynamics for both homolytic and heterolytic cleavage of the M-hfip bond.

Following on this work, and the observation of a rapid β-fluoride elimination reaction when using Cu-H complexes with HFP, in Chapter 4 a facile copper-catalyzed hydrodefluorination of a variety of FAs and vinyl fluorides using inexpensive silane sources such as tetramethyldisiloxane or moisture-tolerant polymethylhydrosiloxane (PMHS) is developed. This is a significant improvement from previous findings on copper-catalyzed HDF reactions which generally relied on the use of an additive that limited selectivity. They also used more privileged silanes which are prohibitively more expensive when considering the scalability of the process. Additionally, no reports exist studying the possibility of switching or enhancing the selectivity of a copper catalyzed HDF as we have demonstrated herein. Variation of the tertiary phosphorus ligand leads to unique ligand control for selective multiple hydrodefluorinations of FAs without the need for Lewis acid additives. In turn we discovered, via a combination of experimental and computational results, a new HDF mechanism in which P_3CuH transfers hydride to the FA or allyl fluoride to generate an initial ionic $[P_3Cu]^+$ $(R^FH)^-$ intermediate. This mechanism gives rise to inverted stereoselectivity in the HDF of trifluoroethylene. This L_3Cu mechanism also provides a more active catalyst, allowing for the reduction of previously unreactive FAs such as

vinylidene difluoride. This HDF proceeds through a three-step nucleophilic H-addition/Cu-C bond formation/F-elimination sequence in an L_3 ligand environment along all steps. F-elimination in the L_3Cu system is possible without ligand decoordination; extensive charge separation allows for the simultaneous occupation of one ligand site in the tetrahedral TS by both a fluorine and the forming fluoroalkene. Lastly, isolation and full characterization of a P_3Cu-CF_2CF_2H complex allows for a comparison with related copper fluoroalkyl complexes.

Chapter 5 expanded on the reactivity of the (SIPr)Ni(η^6-benzene) complex with various fluorinated aromatics. It was found that this complex reacts smoothly with most Ar-F bonds independent of the degree of fluorination, yielding new $Ni^{II}FAr$ complexes. In one exception 1,2-difluorobenzene instead yielded a dimeric Ni^{I} complex; the exact mechanism of this reaction is still unknown. We found that the isolated Ni^{II} complexes could be used in a DMAP-assisted Suzuki type cross-coupling reaction with aryl boronic acid esters but only when DMAP is added to access the monomeric complex (SIPr)(DMAP)NiF(C_6F_6). Interestingly, this complex showed enhanced activity such that 4-Ph-C_6F_4-Ph was observed as the major product. Moreover, with the convenient synthesis of a new P_3Cu-CF_2CF_2H complex in hand, in Chapter 5, I sought to explore the reactivity of this complex with various organic substrates. To date, no pharmaceutical or agrochemicals exist with this functional group (-CF_2CF_2H). I believe that the limited availability for the synthesis of this group is the culprit. Especially in the context of the discovery of pentafluoroethyl-containing bio-active compounds, the advent of this copper complex and this study on its reactivity, the possibility to assay the tetrafluoroethyl group in bio-active compounds could prove fruitful. I found that by addition of ligands employed in similar reactions, i.e. the cross-coupling of aryl iodides with Cu-CF_3, Cu-CF_2CF_2H could be successfully coupled with various aryl iodides, using 10 mol % of SIMesCuCl. This is a rare example of the synthesis of

Ar-CF_2CF_2H. To expand the scope of coupling partners, and in line with the reactivity of our Cu-hfip complex, acid chlorides were also explored. We found that the stochiometric reaction works well, without the use of additives, to synthesize new $ArC(O)CF_2CF_2H$ compounds.

6.1. Outlook

As mentioned, the synthesis and chemistry of organofluorine compounds is currently experiencing a renaissance due to the need for smaller fluorinated chains in materials applications (cf. environmental persistence of long chain fluorocarbons). The contributions in this *Thesis* open the door for the eventual development of coinage metal-catalyzed reactions.

Future studies on fluoronickelacycle chemistry would benefit from the development of Ni^0 complexes from which the NHC is not in equilibrium with the dissociated form. As such, an improvement to retain the reactivity enabled by the pseudo-three coordinate complex would be the incorporation of a hemi-labile functionality on the ligand. This would provide an avenue for a bidentate mode of coordination to the Ni^0 and, kinetically speaking, disfavor ligand decoordination and prevent side reactions.

Expanding and improving the scope of reactivity of both the Cu-hfip and Cu-CF_2CF_2H complexes (presented in Chapters 4 and 5) in cross-coupling reactions could hold the greatest value. The synthesis of these complexes can be easily scaled up and used in the development of new biologically active compounds. However, to date the optimal cross-coupling conditions, especially with Ar-I, remain elusive or are dependent on the electronic nature of the substitution of the aromatic ring. For the Cu-hfip system preliminary reactions suggest that use of the better oxidant, Ph_2I^+, could produce Ar-hfip compounds. As for Cu-CF_2CF_2H, no bio-active compounds currently exist with this functionality, and the synthesis of such compounds could be

useful in the development of pharmaceuticals and agrochemicals. Lastly, there has been renewed interest in fluorovinyl groups as bioisosteres of amides and our new copper hydride-catalyzed route, Chapter 4, offers a greener, more cost-effective method for their incorporation.

Fluoro-organometallic chemistry of the coinage metals has been experiencing a resurgence. Our works builds on this body of knowledge by focusing on the boundaries of the reactivity of these M-R^F complexes (i.e. Ni, Cu and Ag). In so doing, we have contributed significantly to the field, from preparing: the first pseudo-three coordinate perfluoro-nickelacyclopentane, the first direct route to a copper-hfip complex and the unknown copper-CF_2CF_2H complex, the first facile synthesis of organo-CF_2CF_2H compounds, and lowest reported reaction temperature for C-F bond activation using nickel complexes. In collaborating with computational experts: fundamental insights into the thermodynamic stability of the M-hfip complexes were established, and mechanistic probing of copper hydride complex-catalyzed HDF aided in identifying an unprecedented pathway. With these additions, we are on the cusp of developing more efficient coinage metal-catalyzed processes which could rival those of precious metal-catalyzed variants.

Appendix A

X-ray Crystallography.

Table A.1. Crystal data and structure refinement

Complex	**2.2**	**2.3**	**2.4a**	**2.5c**
ID code	tb060	tb065	tb070	tb132_5
Formula	$C_{24}H_{41}F_8N_2NiO_3P$	$C_{31}H_{38}F_8N_2Ni$	$C_{35}H_{45}F_{10}N_2NiO_3S$	$C_{33}H_{41}F_7N_2NiO_2$
Mw	647.27	649.34	822.50	689.39
Color	yellow	Light red	pink	yellow
Temp (K)	200(2)	200(2)	200(2)	200(2)
Crystal system	Monoclinic	Orthorhombic	Monoclinic	Monoclinic
Space group	P2(1)/c	P2(1)2(1)2(1)	P2(1)/c	P2(1)/c
a/Å	15.5474(12)	10.8851(4)	10.2361(5)	9.7181(4)
b/ Å	9.9548(8)	15.5440(6)	16.5042(8)	18.2160(7)
c/ Å	19.6379(15)	18.9208(7)	22.6115(11)	19.2228(7)
α/°	90.00	90	90	90
β/°	92.862(4)	90	90.960(2)	92.180(2)
γ/°	90.00	90	90	90
V/Å^3	3035.6(4)	3201.4(2)	3819.4(3)	3400.5(2)
Z	4	4	4	4
Dc/g cm^{-1}	1.416	1.347	1.430	1.347
μ/mm^{-1}	0.768	0.675	0.648	0.640
F(000)	1352	1352	1708	1440
Crystal size/mm	0.17x0.12x0.10	0.21x0.11x0.07	0.19x0.11x0.07	0.14x0.11x0.09
2θ range/°	2.08-28.47	2.15-28.32	1.53-28.36	1.54-23.43
Index range	-20<h<20 -13<k<13 -25<l<26	-14<h<14 -20<k<20 -25<l<25	-13<h<13 -21<k<21 -30<l<28	-10<h<10 0<k<20 0<l<21
Indep. reflns collected/unique	29150/7565	45918/7927	65889/9440	11781/6216
Max. and min. transmission	0.9271 and 0.8805	0.9543 and 0.8713	0.9561 and 0.8868	0.7449 and 0.5352
(Rint)	0.0226	0.0281	0.0396	?
R1, wR2 (I>2θ(I))	0.0326, 0.0838	0.0266, 0.0643	0.0580, 0.1410	0.0687, 0.1292
R1, wR2(all data)	0.0399, 0.0880	0.0318, 0.0663	0.0727, 0.1513	0.1053, 0.1475
Goodness of fit, F^2	1.011	1.035	1.046	1.062

Data/restraints/para	7565/0/352	7927/0/380	9440/0/469	9216/0/407
Largest diff. peak,	0.944, -0.261	0.327, -0.224	0.944, -0.717	0.871, -0.423

Table A.1. …Continued

Complex	**2.7**	**3.1a**	**3.2a**	**3.3a**
ID code	tb187_a	tb197	tb198	tb226
Formula	$C_{33}H_{41}F_8N_2NiO_2$	$C_{12}H_{19}AgF_7N$	$C_{17}H_{18}BrF_7N_2Ni$	$C_{39}H_{30}CuF_7P_2$
Mw	708.39	418.15	521.95	757.11
Color	yellow	colorless	light pink	colorless
Temp (K)	200(2)	200(2)	200(2)	200(2)
Crystal system	Orthorombic	Monoclinic	Orthorhombic	Monoclinic
Space group	P 21 21 21	P21/c	Cmca	P21/c
a/Å	10.994(2)	8.1927(5)	28.5021(8)	10.6766(4)
b/ Å	16.858(3)	14.9823(10)	23.4222(7)	20.3224(8)
c/ Å	18.465(4)	12.9081(8)	12.1675(3)	32.5627(13)
α/°	90	90	90	90
β/°	90	90.271(3)	90	95.297(2)
γ/°	90	90	90	90
V/Å^3	3422.3(12)	1584.39(17)	8122.8(4)	7035.1(5)
Z	4	4	16	8
Dc/g cm^{-1}	1.375	1.753	1.707	1.430
μ/mm^{-1}	0.642	1.336	2.989	0.776
F(000)	1476	832	4160	3088
Crystal size/mm	0.321x0.229x0.17	0.91x0.16x0.16	0.45x0.43x0.33	0.81x0.240x0.07
2θ range/°	1.636-27.949	2.08-27.99	1.43-27.90	1.61-28.36
Index range	-14<h<7 -15<k<21 -24<l<21	-10<h<10 -19<k<19 -17<l<16	-36<h<36 -30<k<30 -16<l<14	-14<h<14 -27<k<26 -43<l<43
Indep. reflns collected/unique	15281/7779	20731/3799	28965/4919	67390/17397
Max. and min. transmission	0.838 and 0.896	0.746 and 0.562	0.746 and 0.538	0.746 and 0.573
(Rint)	0.0874	0.0245	0.0482	0.0766
R1, wR2	0.0837, 0.1040			
R1, wR2(all data)	0.1750, 0.1307	0.0228, 0.0570	0.0532, 0.1177	0.0466, 0.0975
(I>2θ(I))		0.0279, 0.0600	0.0903, 0.1420	0.1085, 0.1294
Goodness of fit,	1.111	1.056	1.032	1.032
Data/restraints/pa^2	7779/0/424	3799/0/201	4919/144/344	17397/63/911
Largest diff.	1.196, -0.570	1.053, -0.311	2.204, -1.449	0.637, -0.904

Table A.1. …Continued

Complex	**3.3b**	**3.2c**	**4.7a**	**6.2a**
ID code	tb232	tb256re_new	tb270_0m_a	
Formula	$C_{3}H_{23}CuF_{7}N_{2}P$	$C_{35}H_{49}F_{7}NiP_{2}$	$C_{86}H_{90}Cu_{2}F_{8}OP_{6}$	$C_{66}H_{72}F_{12}N_{4}Ni_{2}$
Mw	675.04	723.39	1604.47	3039.38
Color	orange	light yellow	colorless	orange/yellow
Temp	200(2)	200(2)	200(2)	123
Crystal	Monoclinic	Monoclinic	Monoclinic	Triclinic
Space	P21/n	P21/n	P21/n	P -1
a/Å	9.7205(1)	16.6206(4)	10.0120(18)	11.06173(7)
b/ Å	30.924(3	18.9727(4)	18.468(3)	13.08380(9)
c/ Å	10.9867(7)	22.3699(5)	21.823(4)	21.79463
α/°	90	90	90	91.7863(5)
β/°	116.2310(10)	98.822(2)	92.408(4)	90.6884(5)
γ/°	90	90	90	105.3684(6)
V/Å^3	2962.5(6)	6970.6(3)	4031.6(13)	
Z	4	8	2	2
Dc/g cm$^-$	1.513	1.379	1.322	1.384
μ/mm^{-1}	0.862	0.710	0.710	1.469
F(000)	1368	3040	1668	1320.0
Crystal	0.92x0.77x0.22	0.36x0.24x0.05	0.700x0.660x0.42	
2θ	2.17-28.32	1.414-25.250	1.445-30.103	
Index	-12<h<12 -40<k<40 -14<l<14	-19<h<19 -22<k<22 -26<l<26	-14<h<14 -26<k<25 -30<l<30	-13<h<13 -16<k<16 -27<l<27
Indep. reflns collected /unique	35681/7252	47813/12603	11763/108288	73893/12297
Max. and min. transmission	0.746and 0.597	0.745 and 0.624		1.000 and 0.915
(Rint)	0.0442	0.0899	0.0412	0.0376
R1, wR2	0.0363, 0.0799	0.0743, 0.01680	0.0389, 0.0974	0.0376,
R1,	1.020	0.1639, 0.2278	0.0638, 0.0.1141	0.0401, 0.1281
Goodnes	0.343, -0.419	1.053	1.060	0.633
Data/rest		12603/0/811	11763/102/505	
Largest		2.590, -0.552	0.607, -0.498	0.79, -0.55

Table A.1. …Continued

Complex	**6.2b**	**6.2d**	**6.3**
ID code			
Formula	$C_{66}H_{70}F_{10}N_4Ni_2$	$C_{66}H_{82}F_2N_4Ni_2$	$C_{66}H_{78}F_2N_4Ni_2$
Mw	2985.73	1086.80	1082.77
Color	light yellow	light yellow	light yellow
Temp	123	123	123
Crystal	Monoclinic	Triclinic	Triclinic
Space	P21/n	P -1	P -1
a/Å	14.4093(5)	11.0865(2)	10.4758(3)
b/ Å	12.1008(4)	12.4575(3)	12.3309(3)
c/ Å	17.5861(5)	12.71041(17)	13.4635(3)
α/°	90	100.4839(14)	64.401(3))
β/°	103.170(3)	105.9107(14)	81.066(2)
γ/°	90	115.3244(19)	66.104(3)
V/Å^3			
Z	2	1	2
Dc/g cm$^-$	1.364	1.260	1.254
μ/mm^{-1}	0.706	1.200	1.199
F(000)	1281.97	580.0	576.0
Crystal	0.200x0.100x0.10		
2θ			
Index	-20<h<20 -16<k<16 -22<l<22	-13<h<13 -15<k<15 -15<l<15	-13<h<13 -15<k<15 -16<l<16
Indep. reflns collected /unique	34095/7675	22176/5789	27233/5803
Max. and min. transmis sion			
(Rint)	0.0523	0.0376	0.0419
R1, wR2			
R1,	0.0712, 0.1583	0.0399, 0.1031	0.0419, 0.1238
Goodnes	1.044	1.068	1.043
Data/rest			
Largest			

Appendix B

Appendix for Chapter 2

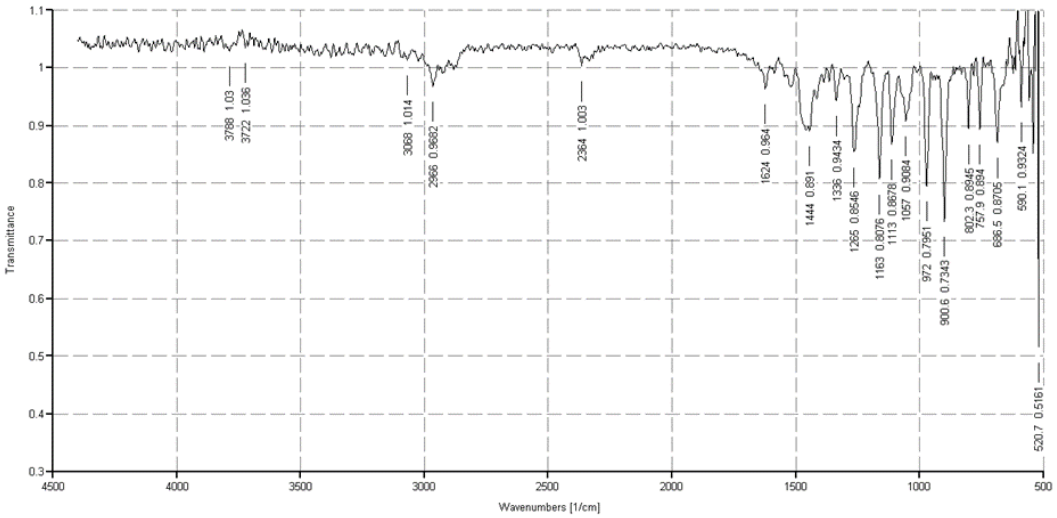

Figure B.1: ATR-IR Spectrum of a powdered sample of **2.7**, collected at room temperature in air.

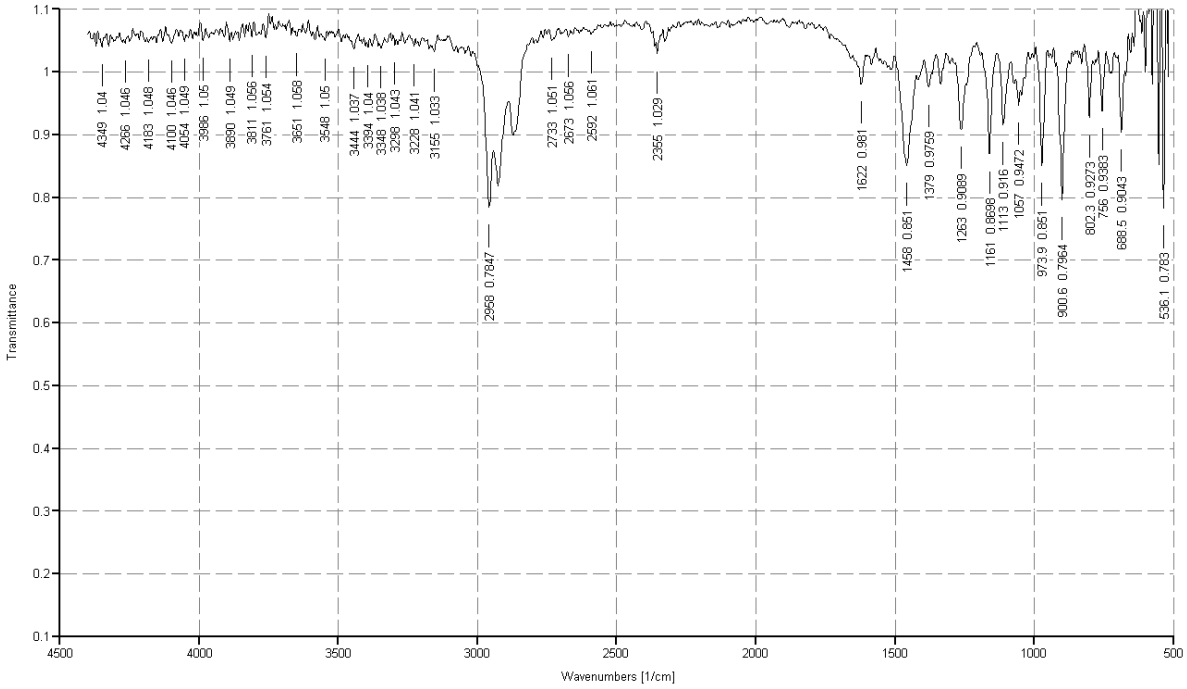

Figure B.2. ATR-IR spectrum of a slurry of **2.7** in hexanes, collected at room temperature in air.

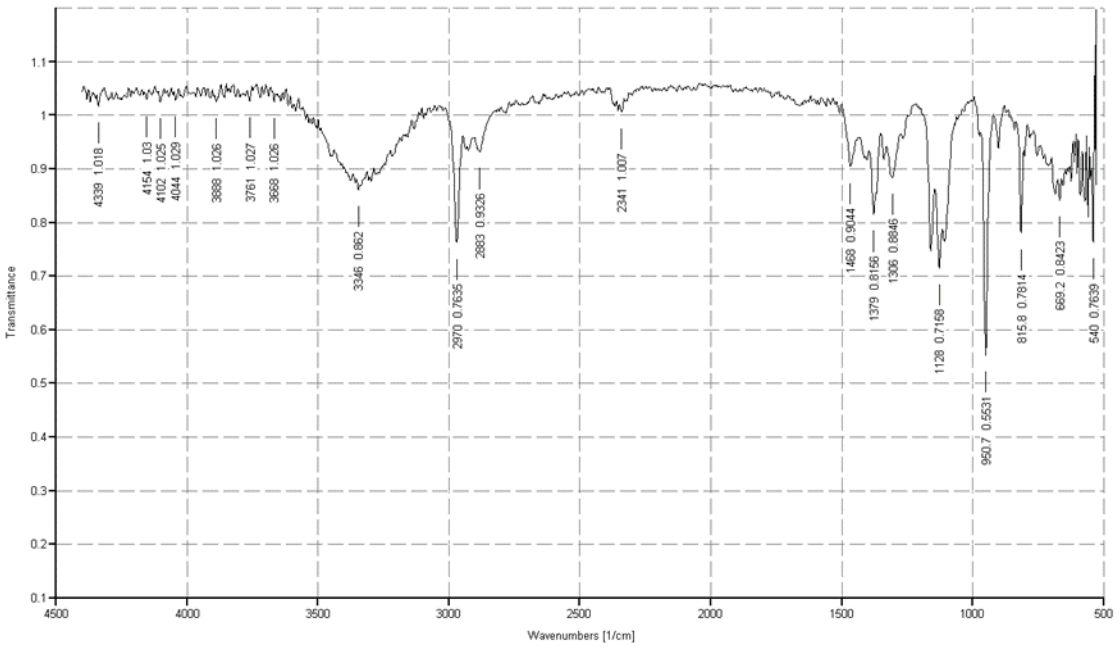

Figure B.3. ATR-IR spectrum of a slurry of **2.**7 in isopropanol, collected at room temperature in air.

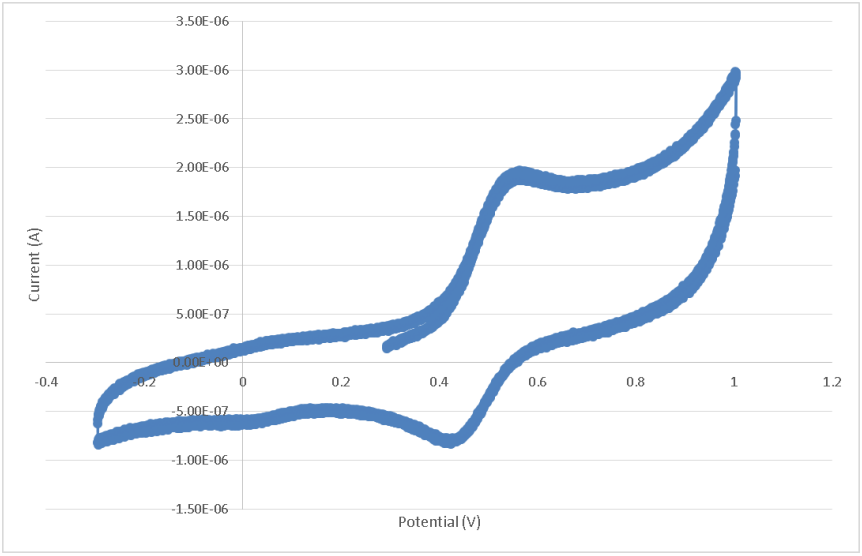

Figure B.4. Cyclic Voltammogram of **2.7** (1 mg/mL in DCM, 10 mM of supporting electrolyte [NBu_4PF_6]), referenced to Cp_2Fe/Cp_2Fe^+. Inset arrow indicates direction of scan at a rate of 200 $mV•s^{-1}$.

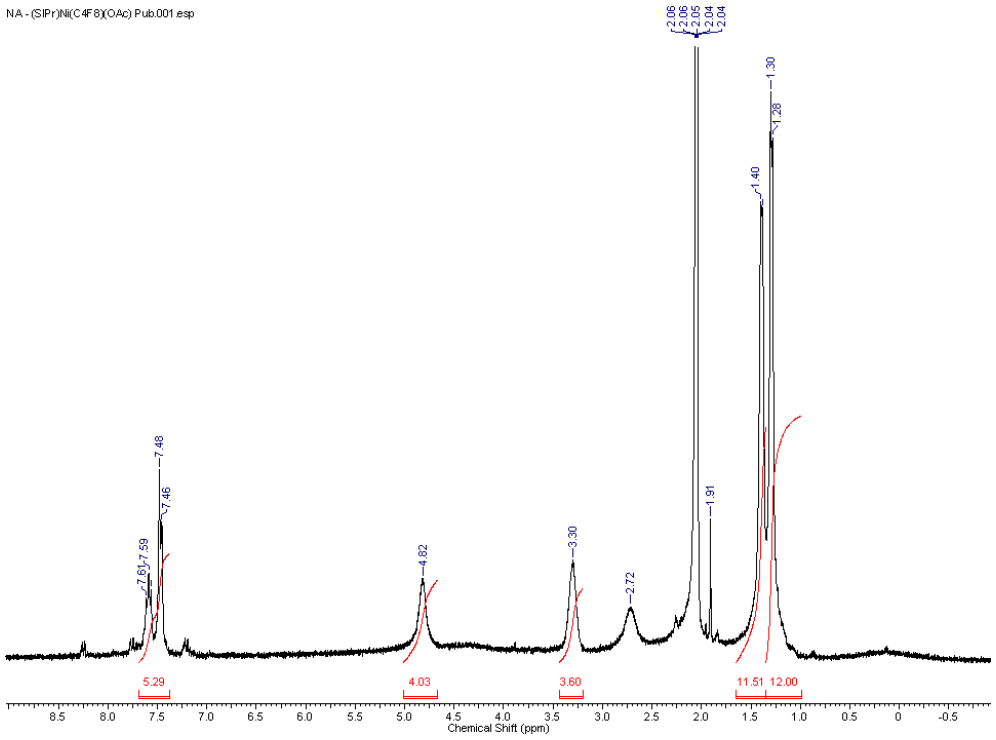

Figure B.5. ^{1}H NMR spectrum (300 MHz, $(CD_3)_2CO$) of **2.7**.

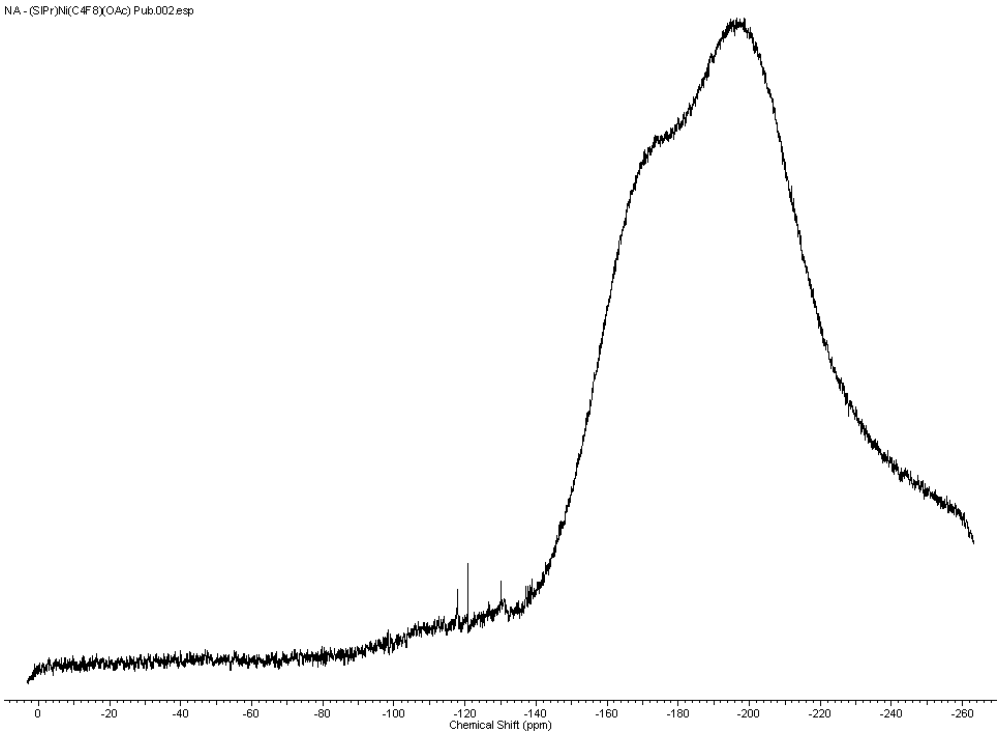

Figure B.6. ^{19}F NMR spectrum (282 MHz, $(CD_3)_2CO$) of **2.7**. Externally referenced to $CFCl_3$.

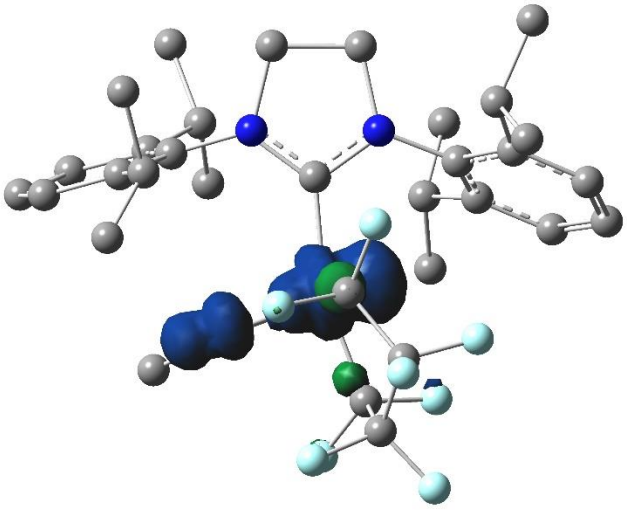

Figure B.7. SOMO of **2.7**, isosurface values of 0.04 au are used. Atomic spin densities: Ni(0.86), acetate(0.16) and carbon (-0.02).

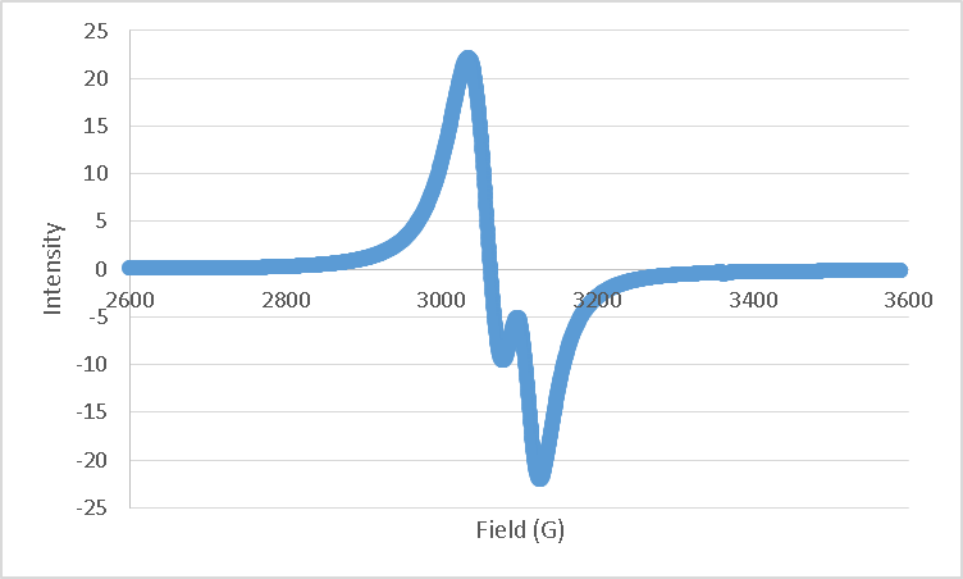

Figure B.8. EPR spectrum (9600 MHz) of **2.7** (26 mg in 0.4 mL dichloromethane).

Appendix C

Appendix for Chapter 4.

Table C.1. Conversion of HFP**(4.1a)** and Product Ratios of the Solvent and mol % of Catalyst Optimization Screen for HDF of HFP **(4.1a**), using dppe.[a]

mol % [$CuH(PPh_3)$] and dppe	Solvent	Conversion of HFP	Products
10	Benzene	> 99 %	11(**1d**) : 1(**1f**)
10	THF	> 99 %	11(**1d**) : 1(**1f**)
10	Toluene	> 99%	11(**1d**) : 1(**1f**)
10	DMF[b]	> 99 %	2**(1d)** : 1**(1f**
1	Benzene	30 %	2(**1b/c**) : 1(**1d**)

[a]Conversion and ratios are based on ^{19}F NMR integration vs internal standard. All reactions were carried out in a sealed NMR tube with a septum cap at 45 °C with 10 equivalents of TMDS after 8 hours. Gas phase sampling confirmed similar ratios in gas phase. [b]The conversion of **4.1a** and product ratios were ligand independent.

Table C.2. Relative Rates for HDF of TrFE (**4.2b**) ($PMePh_2$ 30 mol % / $[CuH(PPh_3)]$ 10 mol %) at 45 °C with 10 equivalents of TMDS.

m-Dimethoxybenzene	3
Chlorobenzene	1
Benzene	1
THF	0.8
CPME	0.8

[a]Reactions were carried out in a sealed NMR tube with a septum cap, monitored until complete conversion of TrFE. Gas phase sampling confirmed similar ratios in gas phase.

Examples of Kinetic Experiments:

HDF of 4.1a with dppe/$[(PPh_3)CuH]]_6$/TMDS

$[(PPh_3)CuH]_6$ (5 mg, 0.015 mmol, 10 mol % Cu) was placed in a 7 ″ nmr tube and mixed with 400 μL of benzene-d_6 (C_6D_6). 1,2-bis(diphenylphosphino)ethane (dppe, 7 mg, 0.017 11 mol %) and 1,1,3,3-tetramethyldisiloxane (TMDS, 161 mg , 1.21 mmol, 10 equiv) were added. The tube was capped with a rubber septum, removed from the glovebox, further sealed by tightly wrapping the cap with a strip of parafilm and shaken to ensure a homogenous solution. Hexafluoropropene (**4.1a**; 3 mL) was then added to the reaction via air-tight syringe and the tube was placed in the NMR probe at ambient temperature. ^{19}F NMR spectra were obtained every 10 minutes for 60 minutes. At this temperature the conversion of **4.1a** to a mixture of **4.1b**/**4.1c** was slow. Even after 60 minutes, a significant amount of **4.1a** still remained and an intermediate was observed, proposed to be $CuCF(CF_3)(CF_2H)$. The sample was then warmed to 45 °C and the ^{19}F NMR spectrum was acquired after 10 minutes (70 minutes total reaction time) to allow for temperature equilibration. After warming, the intermediate was no longer present, and **4.1a**, **4.1b** and **4.1c** had been entirely consumed, yielding mostly **4.1d**. After continued heating at 45 °C for 60 minutes (130 minutes total reaction time, not shown) no further hydrodefluorination (HDF) was observed.

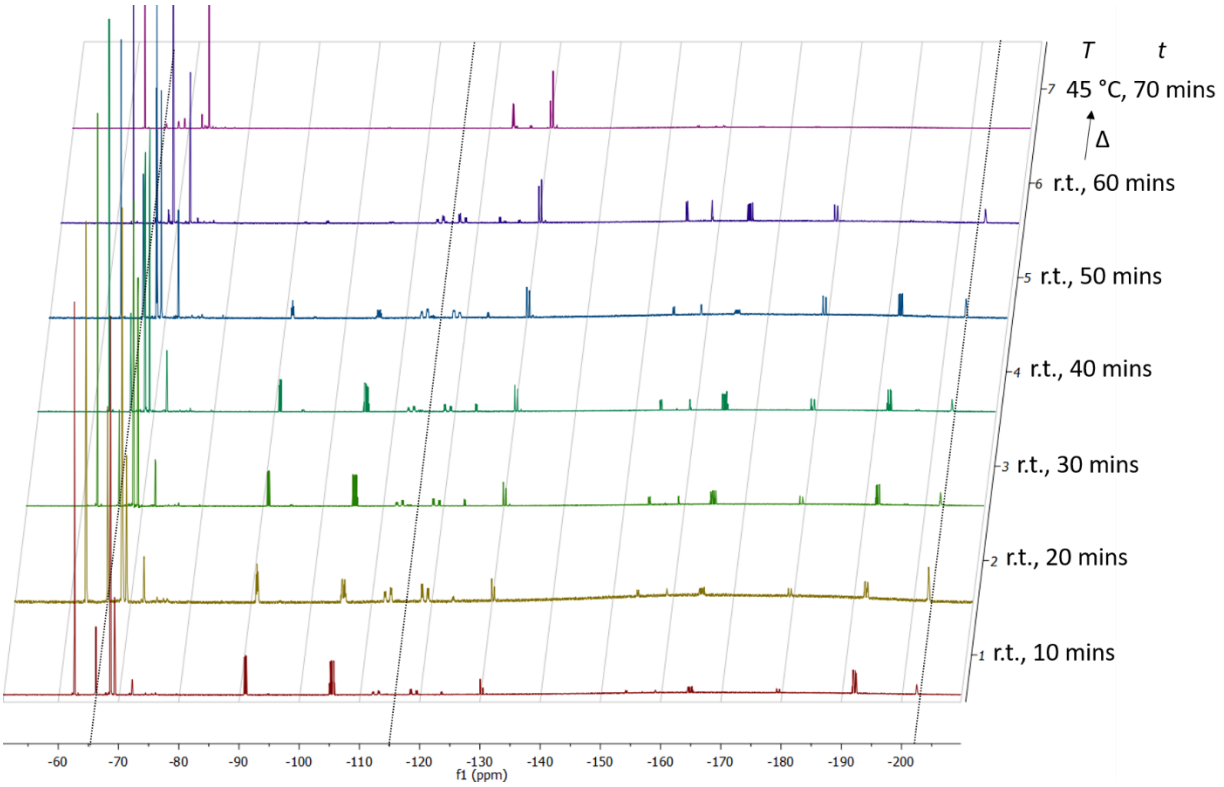

Figure C.1. ^{19}F NMR spectra (282 MHz, C_6D_6) of the conversion of **4.1a** to **4.1d**. The dashed line represents the trace of Cu-$CF(CF_3)(CF_2H)$ across all reactions.(See Table S2 for ^{19}F NMR chemical shift data of products

HDF of 4.2b with $PMePh_2$/$[(PPh_3)CuH]_6$/Ph_3SiH

$[(PPh_3)CuH]_6$ (5 mg, 0.015 mmol, 10 mol %) was placed in a 7 ″ nmr tube and mixed with 400 µL of benzene-d_6 (C_6D_6). Methyldiphenylphosphine ($PMePh_2$, 9 mg, 0.046 mmol, 30 mol %) and triphenylsilane (Ph_3SiH, 78 mg , 0.30 mmol, 2.5 equiv) were added. The tube was capped with a rubber septum, removed from the glovebox, further sealed by tightly wrapping the cap with a strip of parafilm and shaken to ensure a homogenous solution. Trifluoroethylene (**4.2b**, 3 mL) was added to the reaction via air-tight syringe and the tube was placed in the NMR probe at ambient temperature. ^{19}F NMR spectra were obtained every 7 minutes for 90 minutes (14-

minute intervals are shown) At this temperature the conversion of **4.2b** to a mixture of **4.2c**/**4.2d** proceeded smoothly. After ~2 hours, **4.2b** was completely converted.

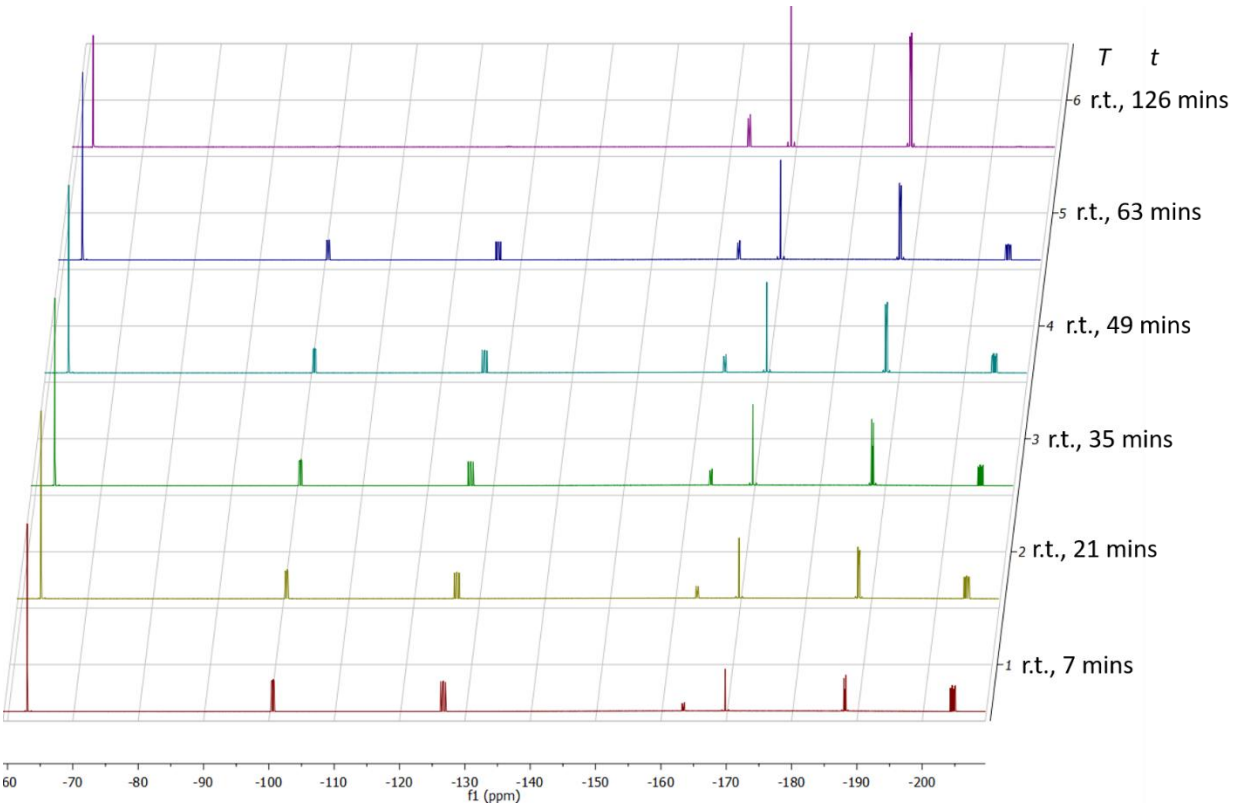

Figure C.2. ^{19}F NMR spectra (282 MHz, C_6D_6) of the conversion of **4.2b** to **4.2c/4.2d**.

HDF of 4.2b with Xantphos/[(PPh$_3$)CuH]]$_6$/Ph$_3$SiH

[(PPh$_3$)CuH]$_6$ (5 mg, 0.015 mmol, 10 mol %) was placed in a 7 ″ nmr tube and mixed with 400 µL of benzene-d$_6$ (C_6D_6). 4,4-bis(diphenylphosphino)-9,9-dimethylxanthene (Xantphos, 10 mg, 0.017 mmol, 11 mol %) and triphenylsilane (Ph_3SiH, 78 mg , 0.30 mmol, 2.5 equiv) were added. The tube was capped with a rubber septum, removed from the glovebox, further sealed by tightly wrapping the cap with a strip of parafilm and shaken to ensure a homogenous solution. Trifluoroethylene (**4.2b**, 3 mL) was added to the reaction via air-tight syringe and the

tube was placed in the NMR probe at ambient temperature. ^{19}F NMR spectra were obtained every 7 minutes for 90 minutes (14-minute intervals are shown), At this temperature the conversion of **4.2b** to a mixture of **4.2c**/**4.2d** proceeded slowly. After ~2 days, **4.2b** still remained.

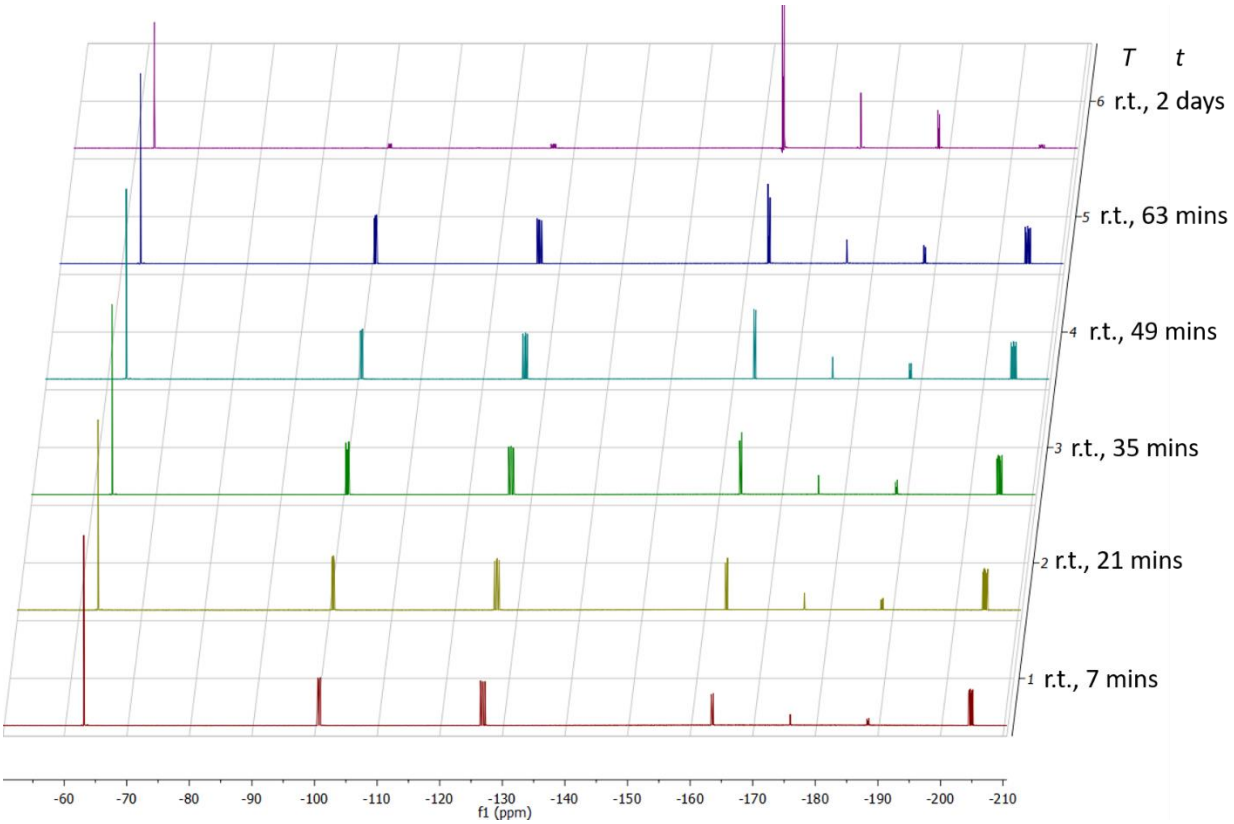

Figure C.3. ^{19}F NMR spectra (282 MHz, C_6D_6) of the conversion of **4.2b** to **4.2c/4.2d**.

NMR Spectra for Title Compounds.

Table C.3. ^{19}F NMR Chemical Shifts of the series **4.1.**

Compound	CF_3	Fα	Fβ
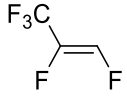 Pentafluoropropene Z	-72.59	-155.07	-158.97

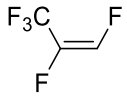 Pentafluoropropene E	-70.09	-180.12	-165.93
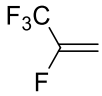 2,3,3,3-Tetrafluoropropene (R-1234yf)	-73.83	-123.99	
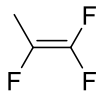 1,1,2-Trifluoropropene		-106.32	-126.15 -167.19
 1,1-Difluoropropene			-89.92 -93.66

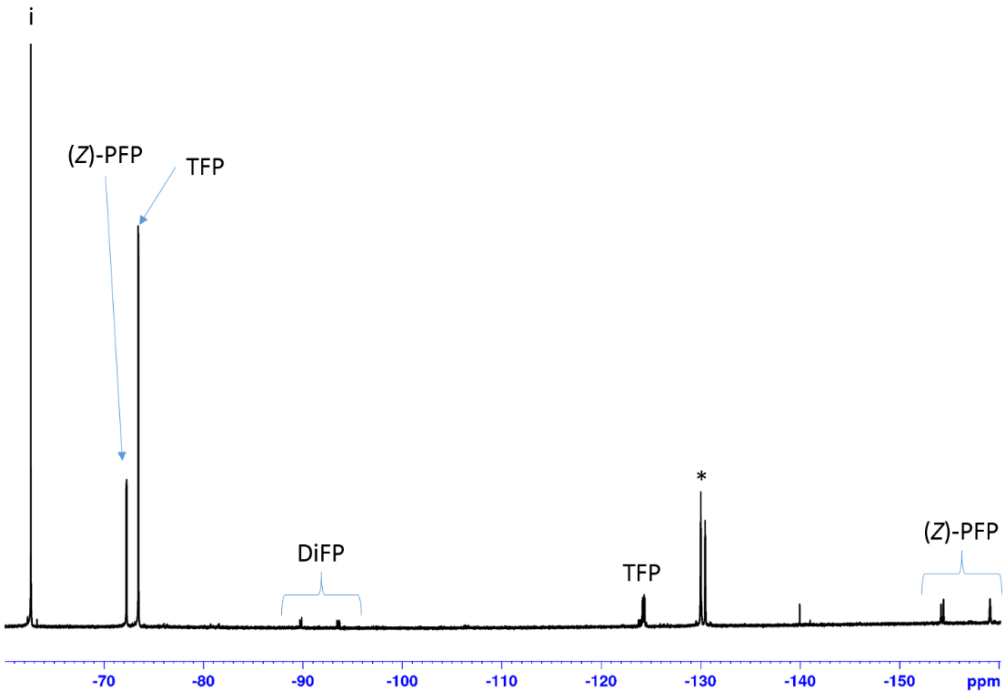

Figure C.4. ^{19}F NMR spectrum (282 MHz, C_6D_6) in situ of the HDF of HFP (**4.1a**) using $[(PPh_3)CuH]_6$ and TMDS after 8 h at 45 °C. The Si-F peak is labeled '*', $PhCF_3$ 'i'.

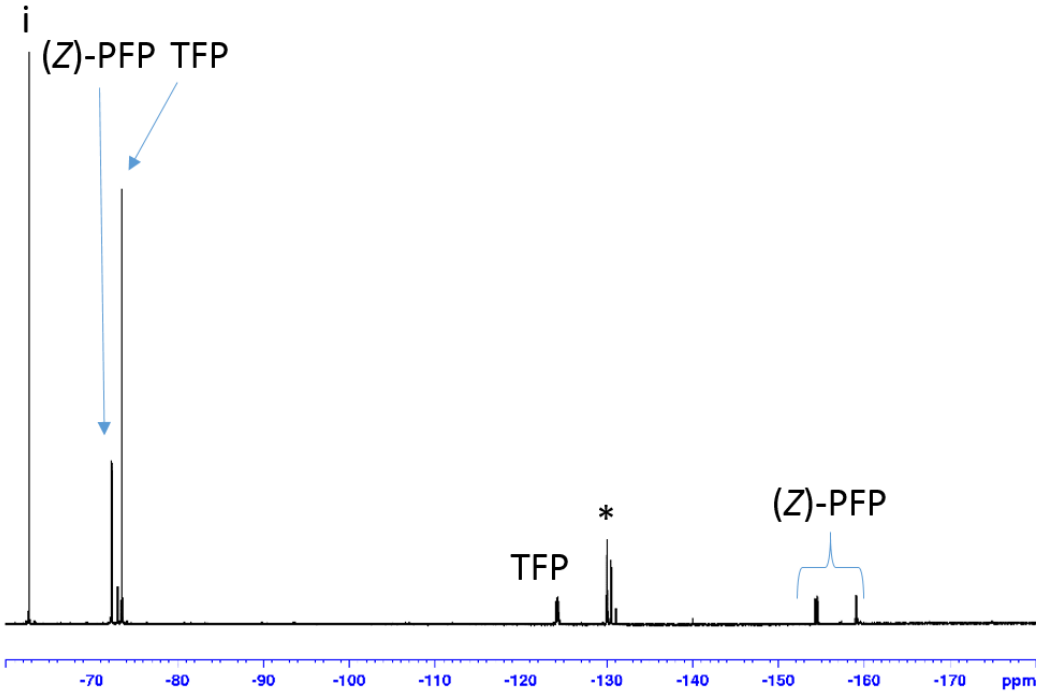

Figure C.5. ^{19}F NMR spectrum (282 MHz, C_6D_6) in situ of the HDF of HFP (**4.1a**) using $[(PPh_3)CuH]_6$, PPh_3 and TMDS after 8 h. The Si-F peak is labeled '*', $PhCF_3$ 'i'.

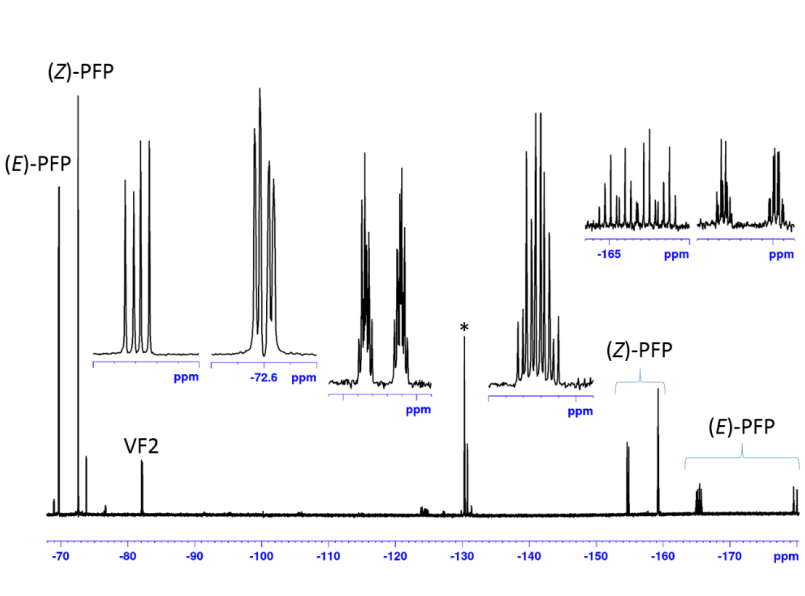

Figure C.6. ^{19}F NMR spectrum (282 MHz, C_6D_6) in situ of the HDF of HFP (**4.1a**) using $[(PPh_3)CuH]_6$, P(o-tolyl)$_3$ and TMDS. The Si-F peak is labeled '*'. The inset shows the expanded (horizontal scale) signal. Vinylidene difluoride (**4.2e**) arises from contamination of the gas stream. $PhCF_3$ was used as an internal NMR standard (not shown).

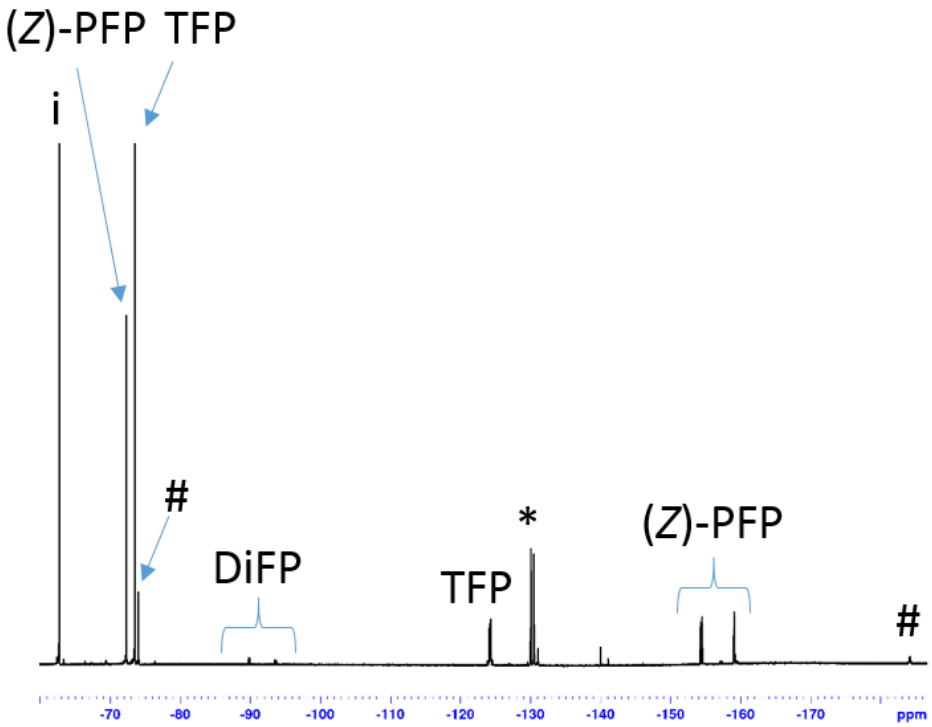

Figure C.7. ^{19}F NMR spectrum (282 MHz, C_6D_6) in situ of the HDF of HFP (**4.1a**) using $[(PPh_3)CuH]_6$, tBuXphos and TMDS. The Si-F peak is labeled '*', $PhCF_3$ 'i' and [Cu]-$CF(CF_3)CH_3$ '#'.

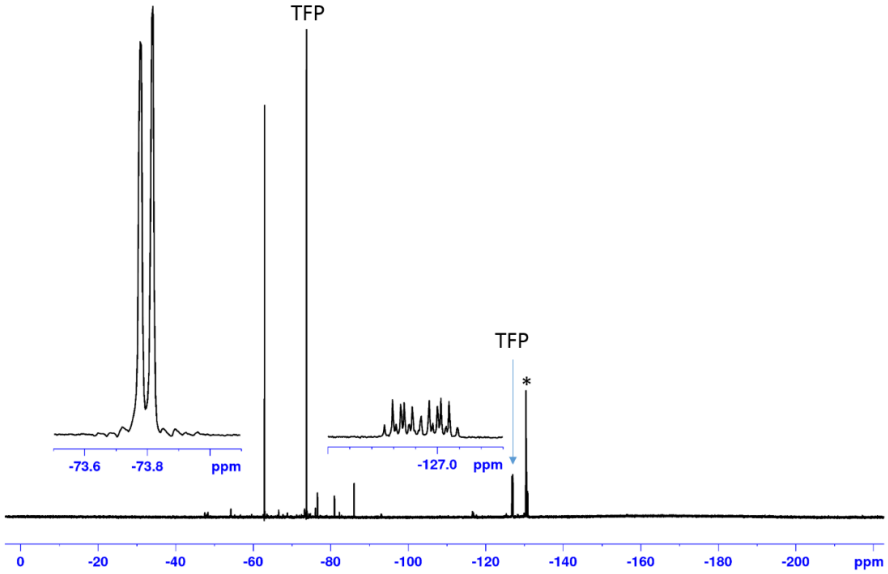

Figure C.8. ^{19}F NMR spectrum (282 MHz, C_6D_6) in situ of the HDF of HFP (**4.1a**) using $[(PPh_3)CuH]_6$, dppe and TMDS. The Si-F peak is labeled '*' and $PhCF_3$ 'i'.

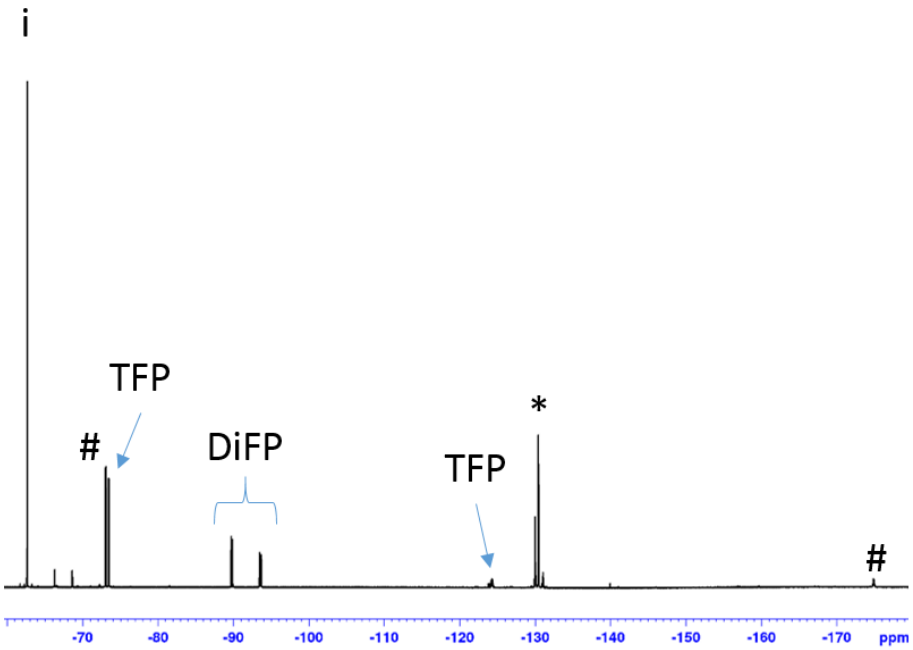

Figure C.9. ^{19}F NMR spectrum (282 MHz, C_6D_6) in situ of the HDF of HFP (**4.1a**) using $[(PPh_3)CuH]_6$, dppf and TMDS. The Si-F peak is labeled '*', $PhCF_3$ 'i' and [Cu]-$CF(CF_3)CH_3$ '#'.

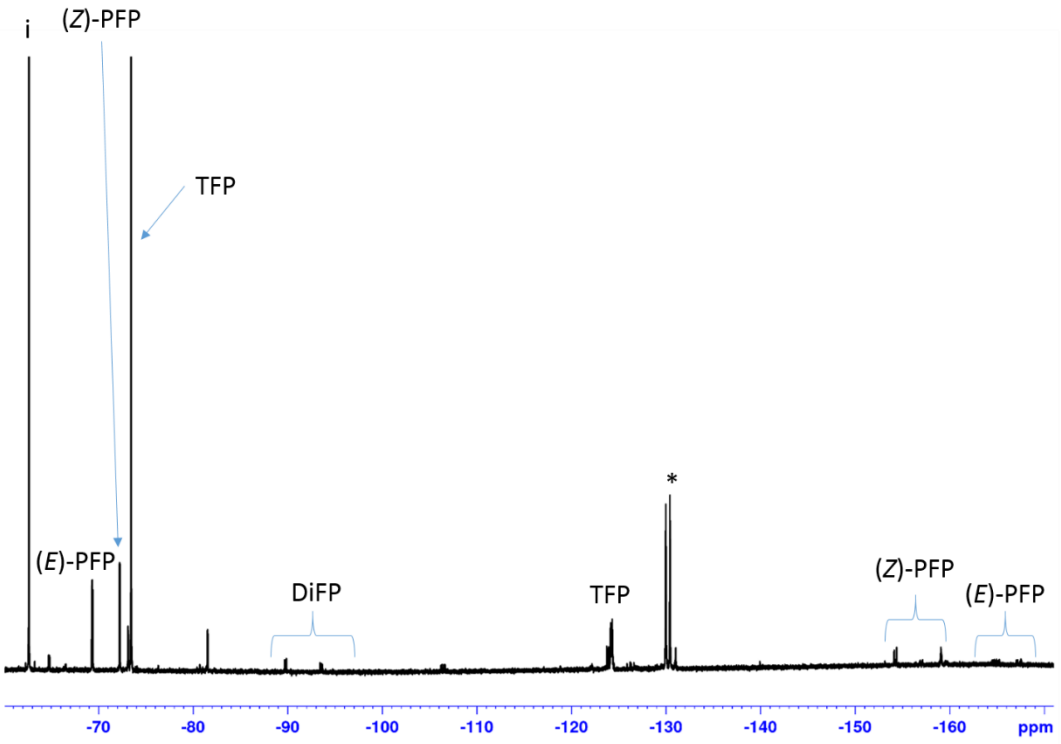

Figure C.10. ^{19}F NMR spectrum (282 MHz, C_6D_6) in situ of the HDF of HFP (**4.1a**) using $[(PPh_3)CuH]_6$, Xantphos and TMDS. The Si-F peak is labeled '*' and $PhCF_3$ 'i'.

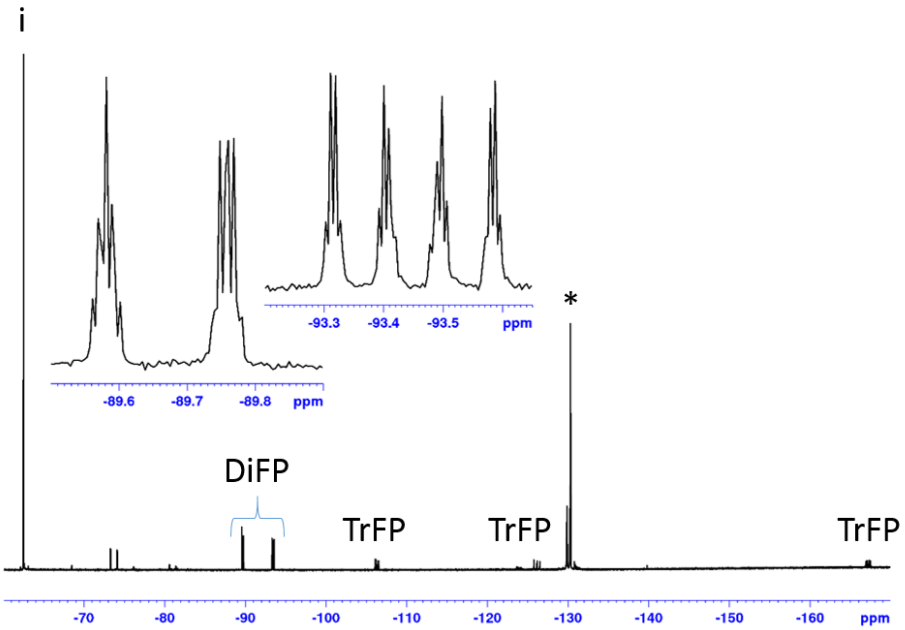

Figure C.11. ^{19}F NMR spectrum (282 MHz, C_6D_6) in situ of the HDF of HFP (**4.1a**) using $[(PPh_3)CuH]$, $P(OEt)_3$ and TMDS. The Si-F peak is labeled '*' and $PhCF_3$ 'i'. The inset shows the expanded (horizontal scale) signal.

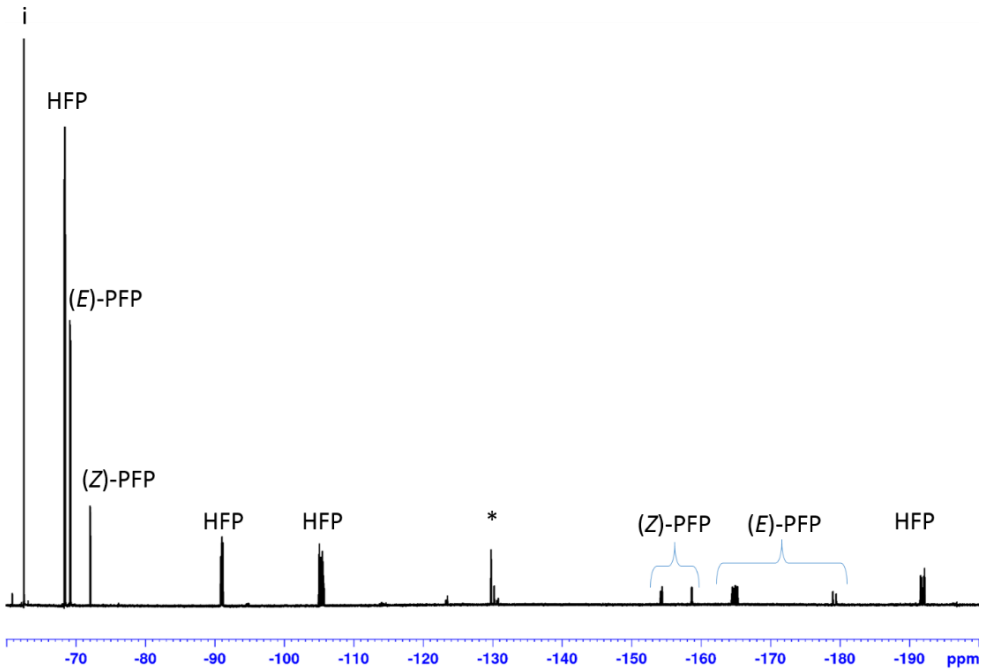

Figure C.12. ^{19}F NMR spectrum (282 MHz, C_6D_6) in situ of the HDF of HFP (**4.1a**) using $[(PPh_3)CuH]_6$, $P(OPh)_3$ and TMDS. The Si-F peak is labeled '*' and $PhCF_3$ 'i'.

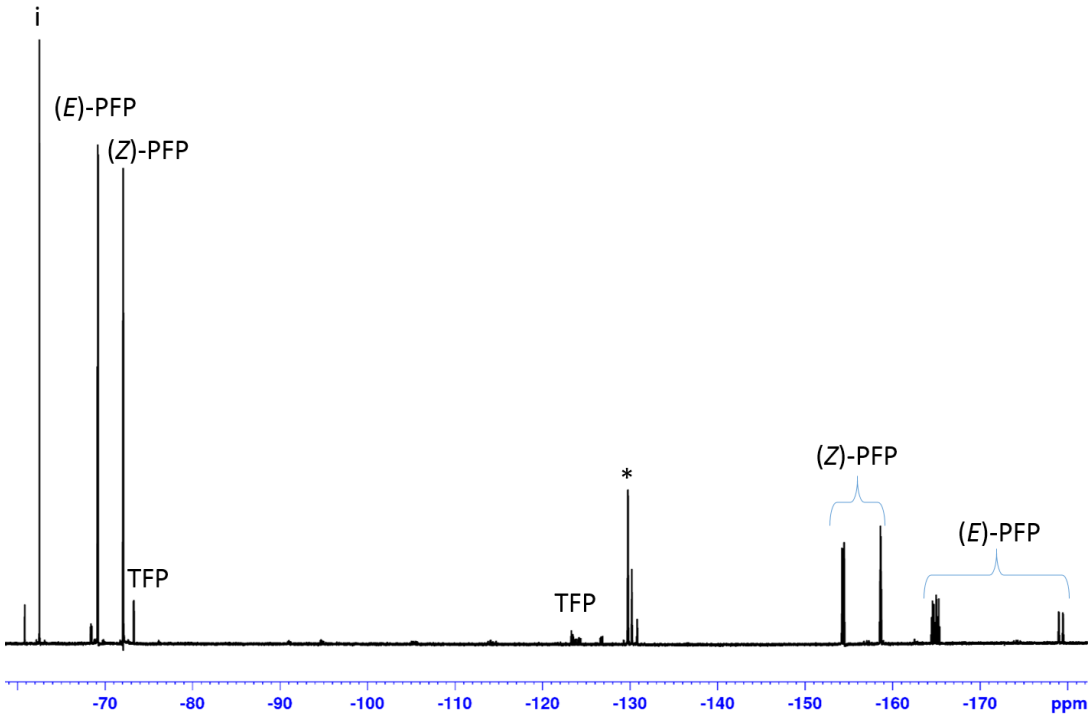

Figure C.13. ^{19}F NMR spectrum (282 MHz, C_6D_6) in situ of the HDF of HFP (**4.1a**) using $[(PPh_3)CuH]_6$, $P(O\text{-}o\text{-}tolyl)_3$ and TMDS. The Si-F peak is labeled '*' and $PhCF_3$ 'i'.

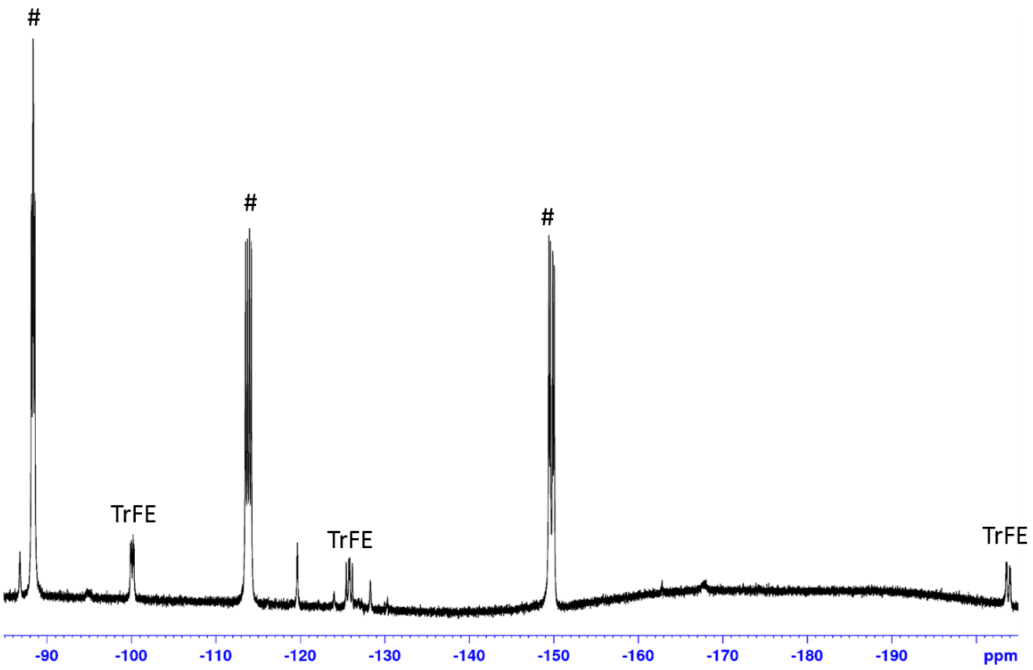

Figure C.14. ^{19}F NMR spectrum (282 MHz, C_6D_6) in situ of the HDF of ITFE (**4.3b**) using $[(PPh_3)CuH]_6$, Xantphos and TMDS. The ITFE peaks are labelled '#'. $CFCl_3$ was used as an external NMR standard.

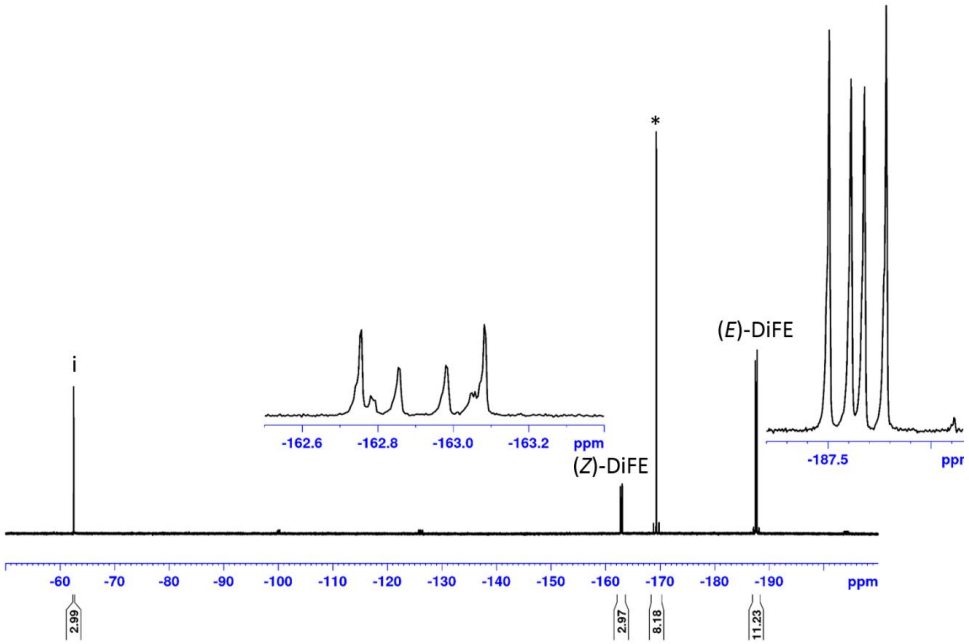

Figure C.15. ^{19}F NMR spectrum (282 MHz, C_6D_6) in situ of the HDF of TrFE (**4.2b**) using $[(PPh_3)CuH]_6$, PPh_2Me and Ph_3SiH. The Si-F peak is labeled '*' and $PhCF_3$ 'i'. The inset shows the expanded (horizontal scale) signal.

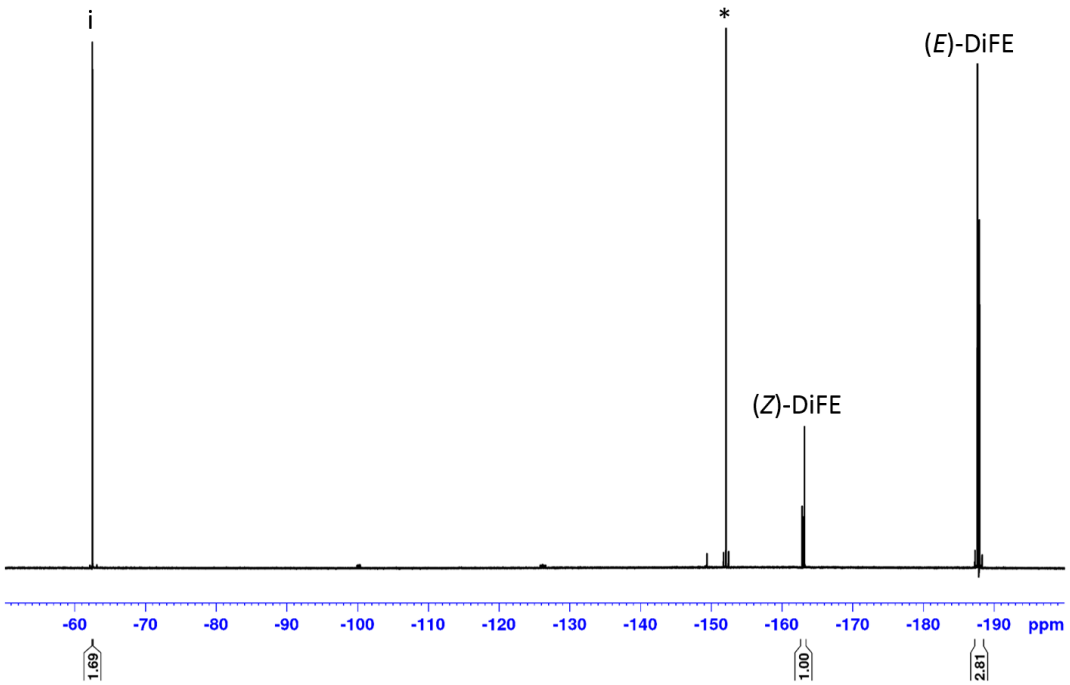

Figure C.16. ^{19}F NMR spectrum (282 MHz, C_6D_6) in situ of the HDF of TrFE (**4.2b**) using $[(PPh_3)CuH]_6$, PPh_2Me and EtO_3SiH. The Si-F peak is labeled '*' and $PhCF_3$ 'i'.

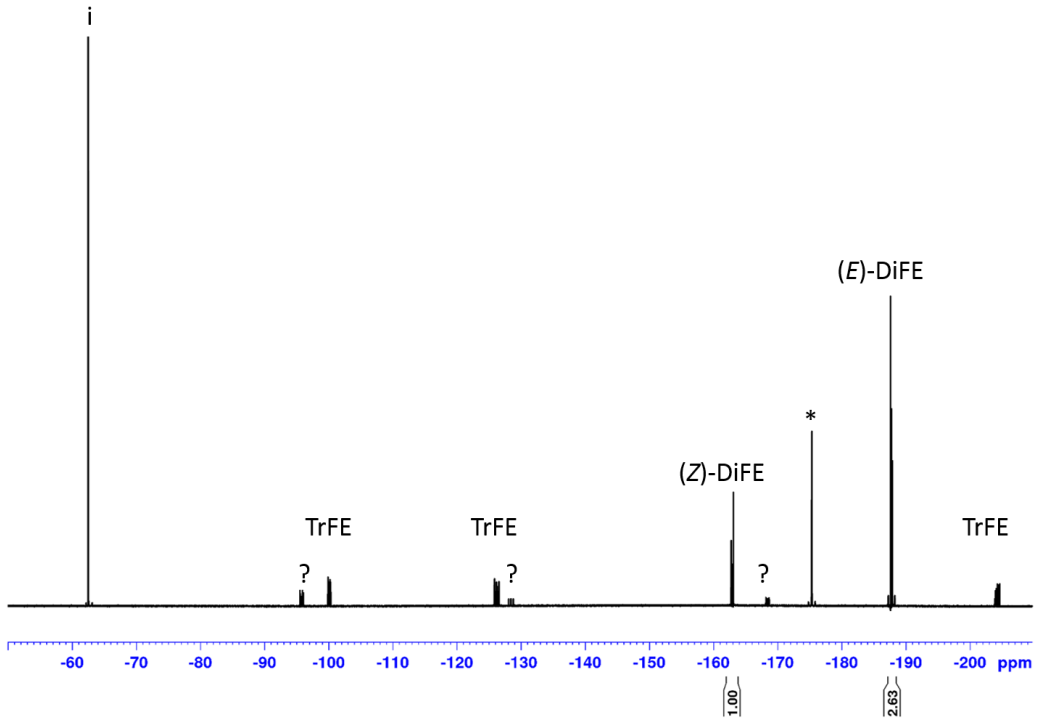

Figure C.17. ^{19}F NMR spectrum (282 MHz, C_6D_6) in situ of the HDF of TrFE (**4.2b**) using $[(PPh_3)CuH]_6$, PPh_2Me and Et_3SiH. The Si-F peak is labeled '*', $PhCF_3$ 'i' and Cu-$CF=CF_2$ '?'.

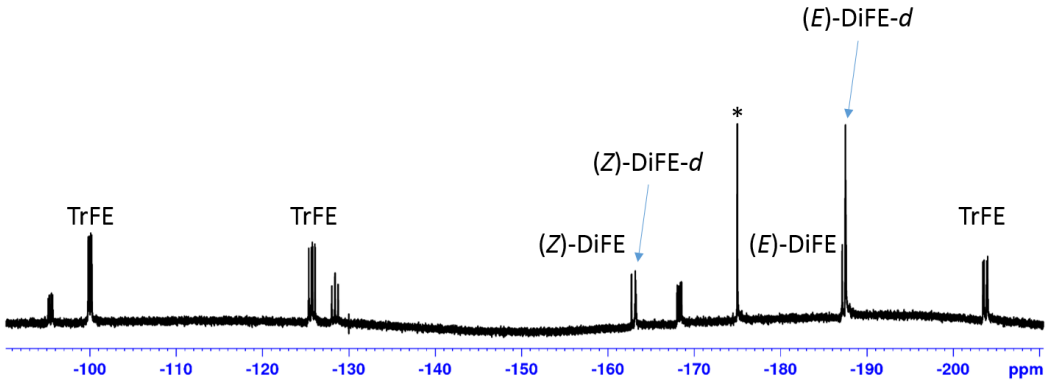

Figure C.18. ^{19}F NMR spectrum (282 MHz, C_6D_6) of the HDF of TrFE (**4.2b**) using $[(PPh_3)CuH]_6$, PPh_2Me and Et_3SiD after 16 h. The Si-F peak is labeled '*'. $CFCl_3$ was used as an external NMR standard.

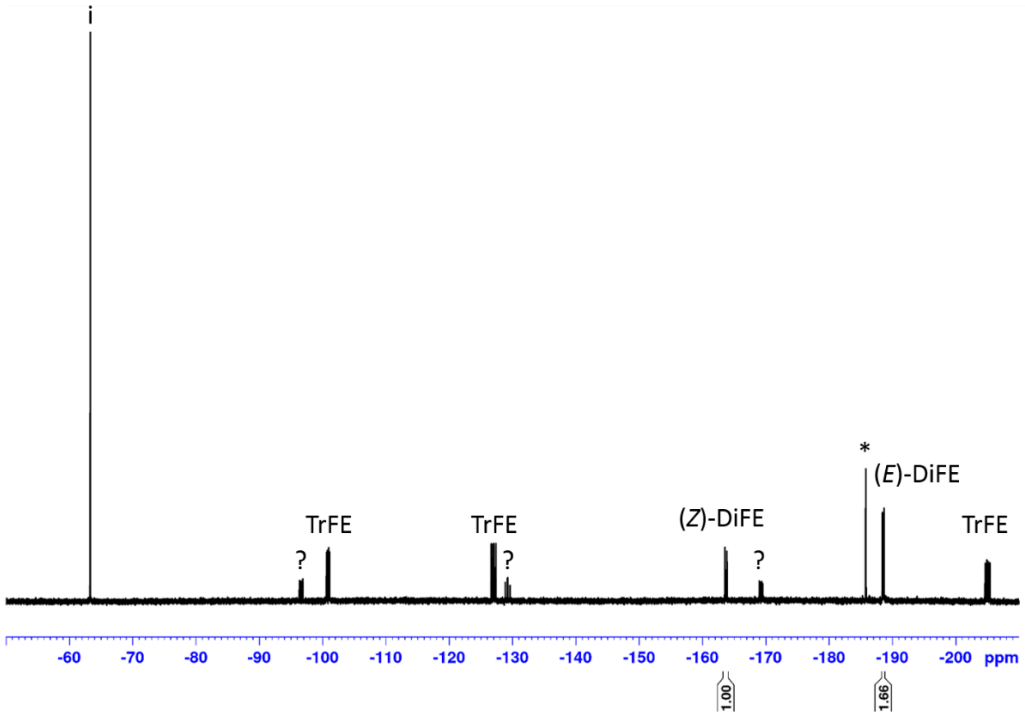

Figure C.19. ^{19}F NMR spectrum (282 MHz, C_6D_6) in situ of the HDF of TrFE (**4.2b**) using $[(PPh_3)CuH]_6$, PPh_2Me and $^{i}Pr_3SiH$. The Si-F peak is labeled '*', $PhCF_3$ 'i' and Cu-$CF{=}CF_2$ '?'.

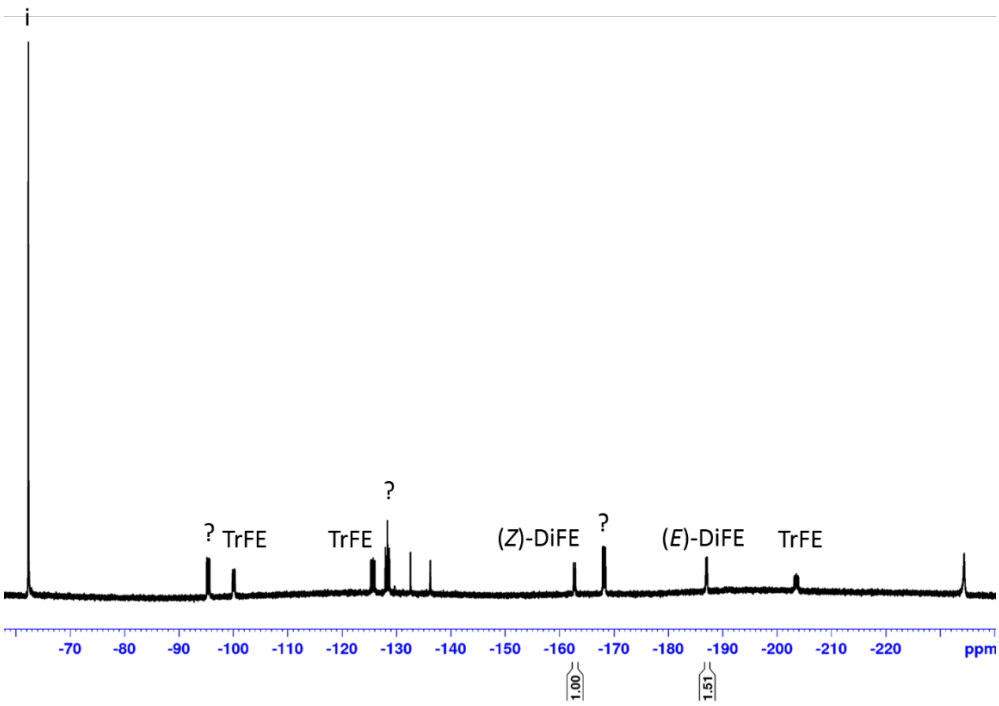

Figure C.20. ^{19}F NMR spectrum (282 MHz, C_6D_6) in situ of the HDF of TrFE (**4.2b**) using $[(PPh_3)CuH]_6$ and PPh_2Me. The $PhCF_3$ peak is labelled 'i' and Cu-$CF{=}CF_2$ '?'.

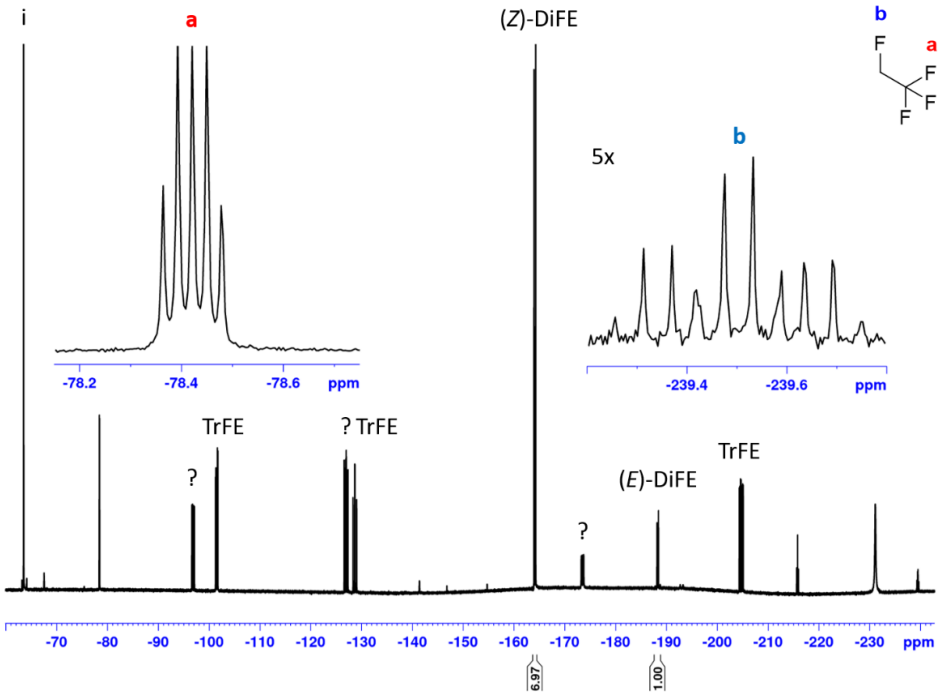

Figure C.21. ^{19}F NMR spectrum (282 MHz, C_6D_6) in situ of the HDF of TrFE (**2b**) using $[(PPh_3)CuH]_6$ and Xantphos. The $PhCF_3$ is labelled 'i' and Cu-$CF{=}CF_2$ '?'.

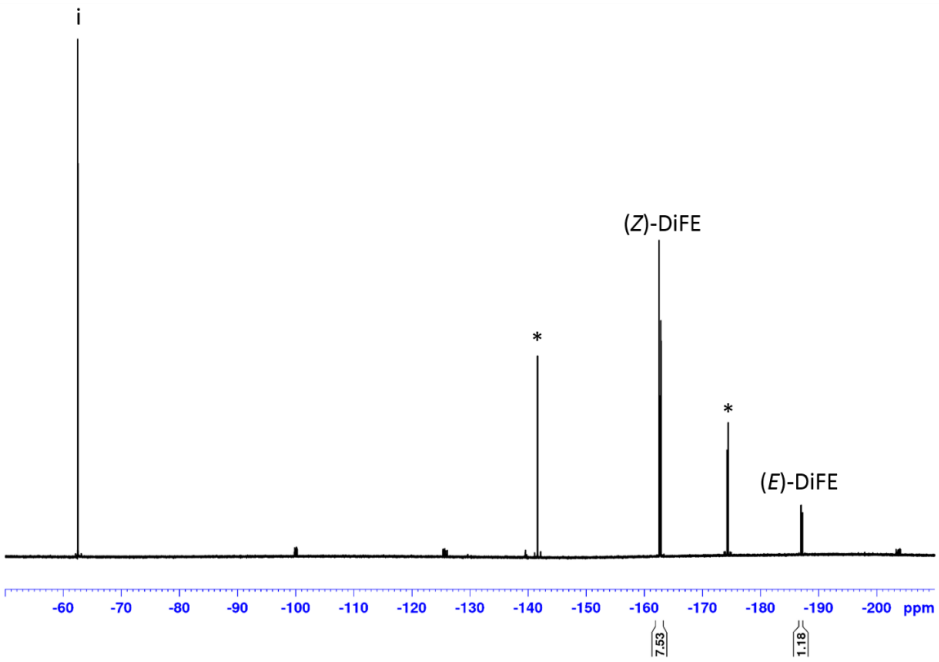

Figure C.22. ^{19}F NMR spectrum (282 MHz, C_6D_6) in situ of the HDF of TrFE (**4.2b**) using $[(PPh_3)CuH]_6$, Xantphos and Ph_2SiH_2. The Si-F peak is labeled '*' and $PhCF_3$ 'i'.

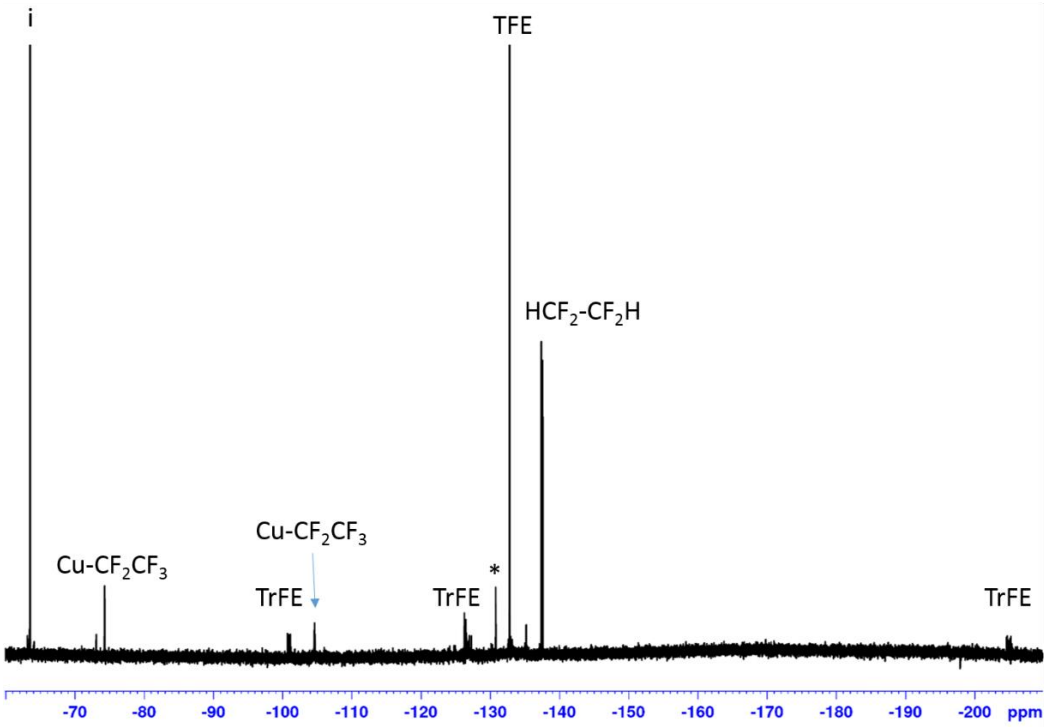

Figure C.23. ^{19}F NMR spectrum (282 MHz, C_6D_6) of the HDF of TFE (**4.2b**) using $[(PPh_3)CuH]_6$, Xantphos and TMDS. The Si-F peak is labeled '*'and $PhCF_3$ 'i'.

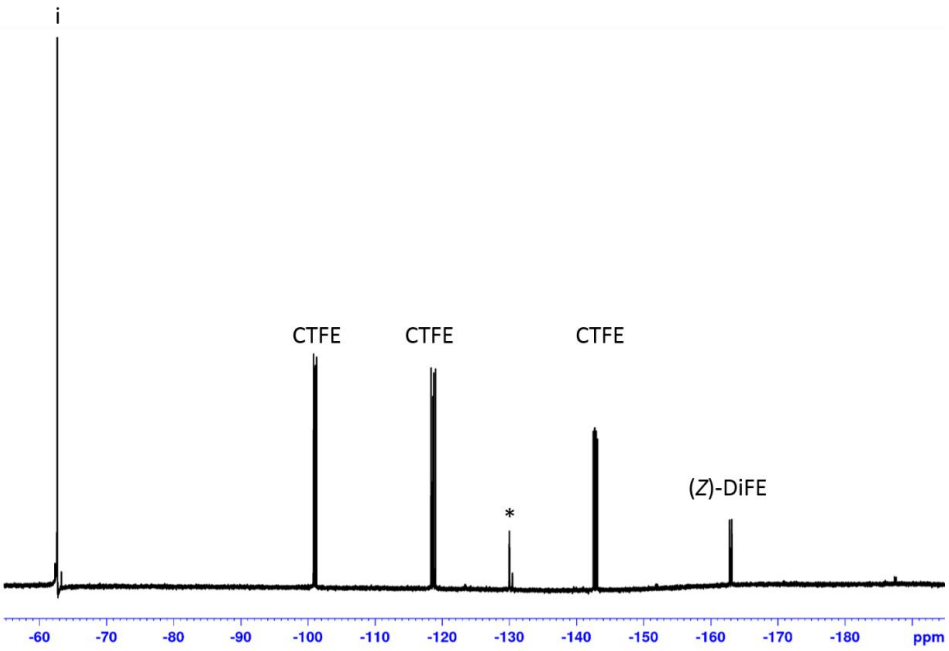

Figure C.24. ^{19}F NMR spectrum (282 MHz, C_6D_6) of the HDF of CTFE (**4.3a**) using $[(PPh_3)CuH]_6$, Xantphos and TMDS. The Si-F peak is labeled '*'and $PhCF_3$ 'i'.

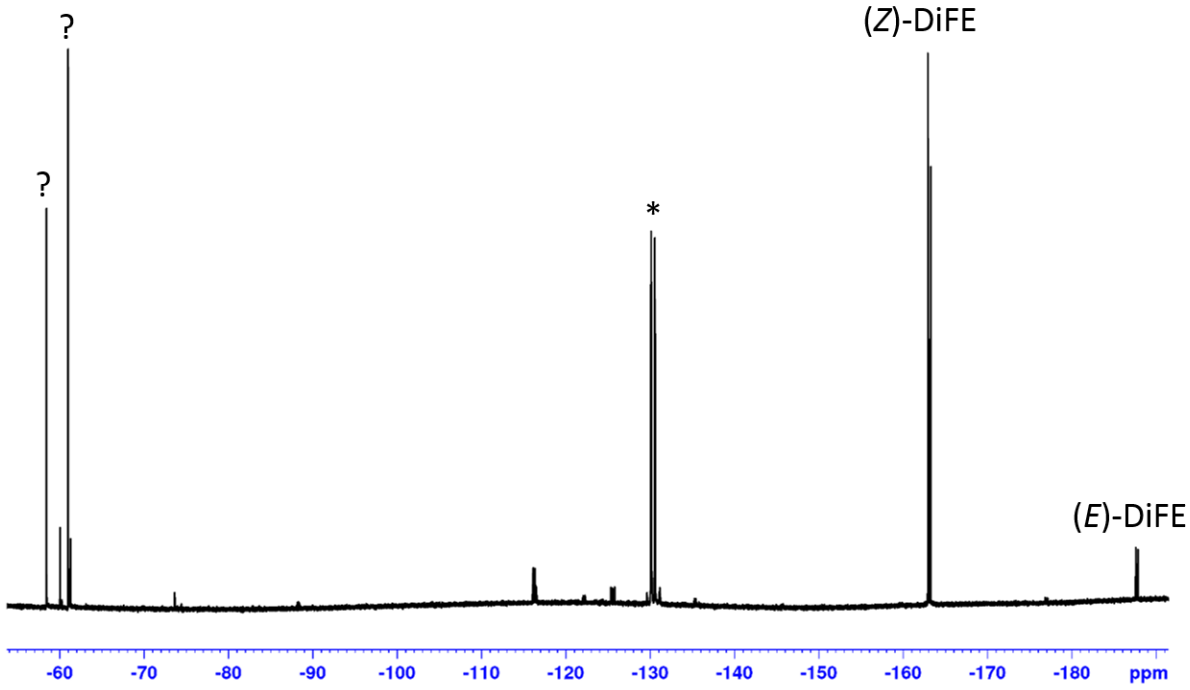

Figure C.25. ^{19}F NMR spectrum (282 MHz, C_6D_6) of the HDF of CF_3OVF_3 (**4.4a**) using $[(PPh_3)CuH]_6$, $P(OEt)_3$ and TMDS. The Si-F peak is labeled '*' and unknown OCF_3 species '?'. $CFCl_3$ was used as an external NMR standard.

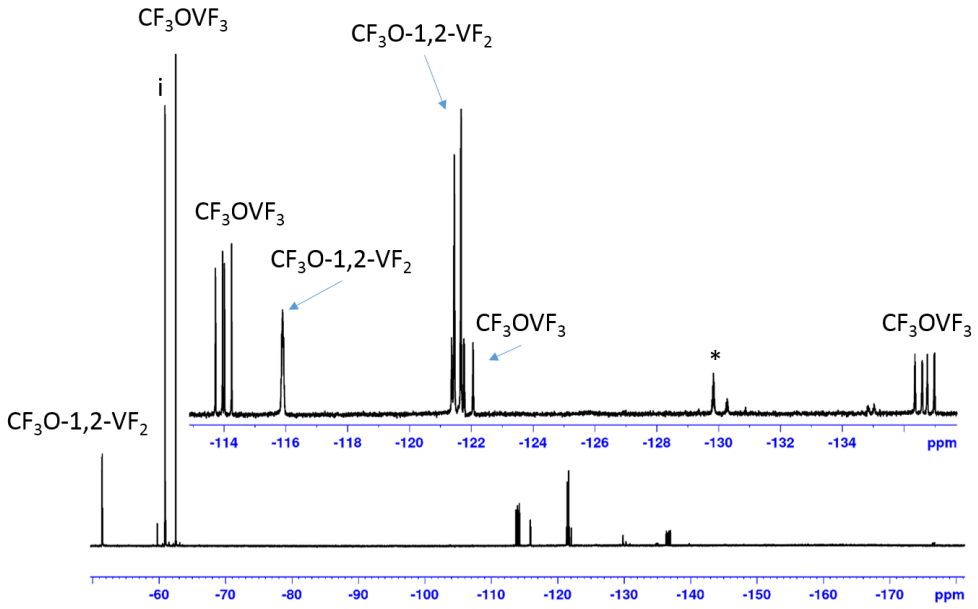

Figure C.26. ^{19}F NMR spectrum (282 MHz, C_6D_6) of the HDF of CF_3OVF_3 (**4.4a**) using $[(PPh_3)CuH]_6$, Xantphos and TMDS after 8 h. The Si-F peak is labeled '*' and $PhCF_3$ 'i'. The inset shows the expanded (horizontal scale) signal.

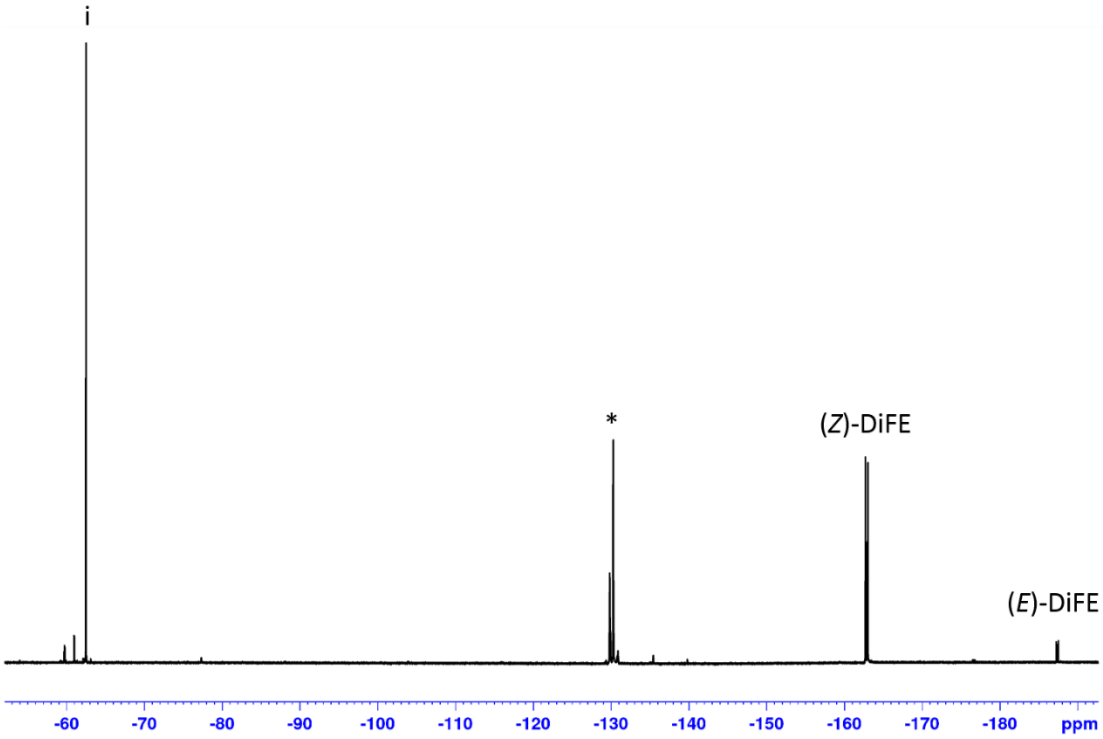

Figure C.27. ^{19}F NMR spectrum (282 MHz, C_6D_6) of the HDF of CF_3OVF_3 (**4.4a**) using $[(PPh_3)CuH]_6$, Xantphos and TMDS after 16 h. The Si-F peak is labeled '*' and $PhCF_3$ 'i'.

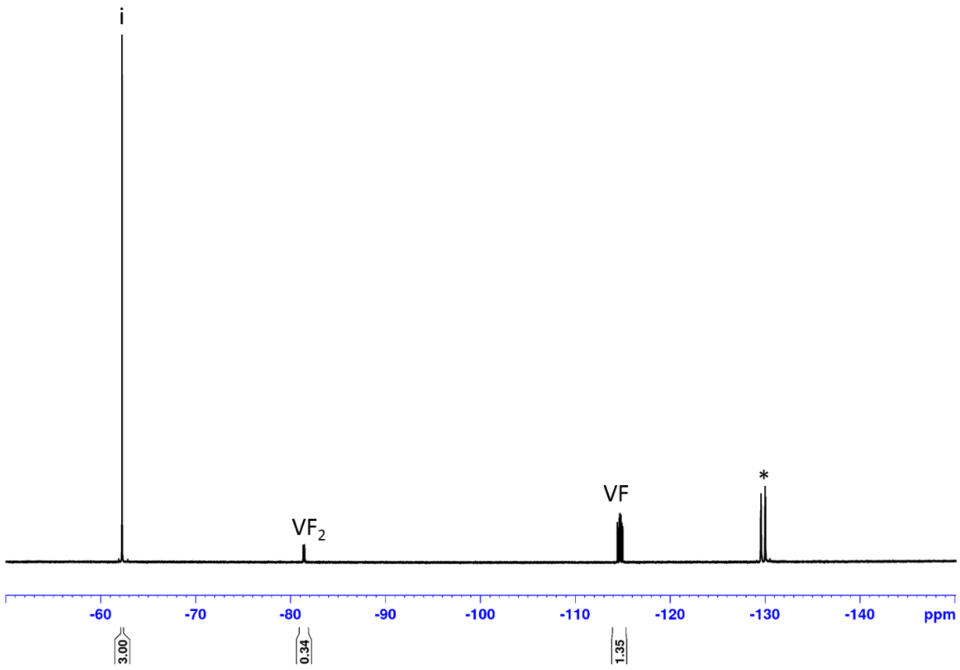

Figure C.28. ^{19}F NMR spectrum (282 MHz, C_6D_6) in situ of the HDF of VdF (**4.2e**) using $[(PPh_3)CuH]_6$, PPh_2Me and TMDS. The Si-F peak is labeled '*' and $PhCF_3$ 'i'.

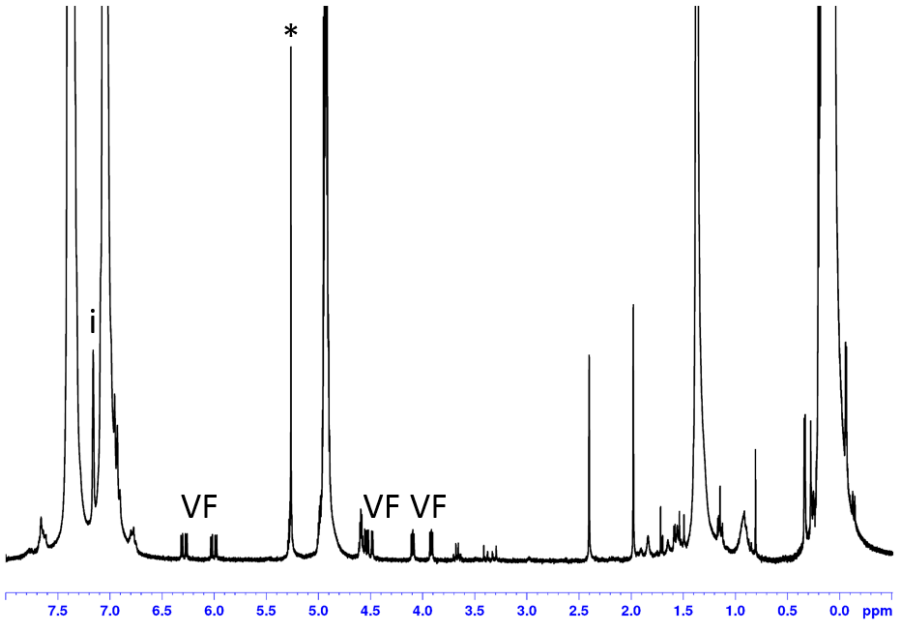

Figure C.29. ^{1}H NMR spectrum (300 MHz, C_6D_6) in situ of the HDF of VdF (**4.2e**) using $[(PPh_3)CuH]_6$, PPh_2Me and TMDS. The residual solvent peak is labeled 'i' and $H_2C{=}CH_2$ '*'

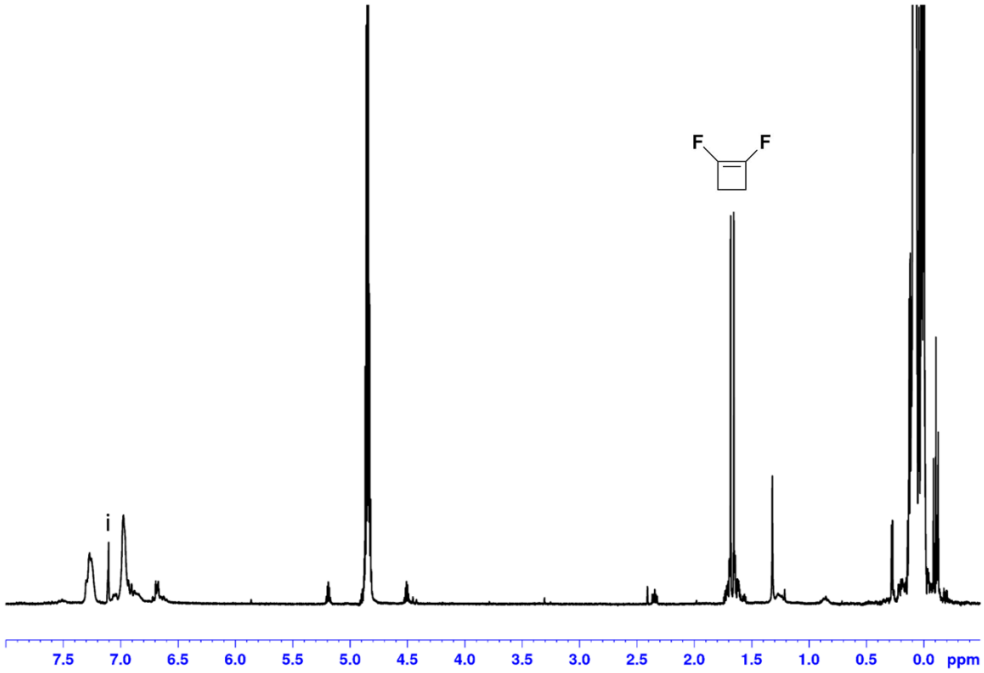

Figure C.30. ^{1}H NMR spectrum (300 MHz, C_6D_6) in situ of the HDF of hexafluorocyclobut-1-ene (**4.5a**) using $[(PPh_3)CuH]_6$, Xantphos and TMDS. The residual solvent peak is labeled 'i'.

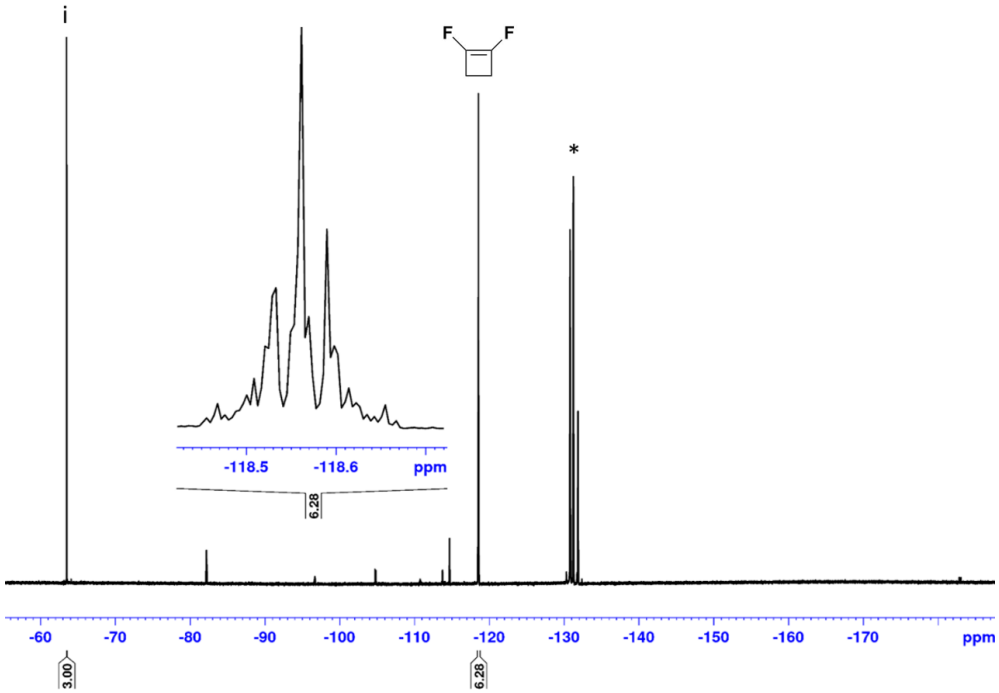

Figure C.31. ^{19}F NMR spectrum (282 MHz, C_6D_6) in situ of the HDF of hexafluorocyclobut-1-ene (**4.5a**) using $[(PPh_3)CuH]_6$, Xantphos and TMDS. The Si-F peak is labeled '*' and $PhCF_3$ 'i'. The inset shows the expanded (horizontal scale) signal.

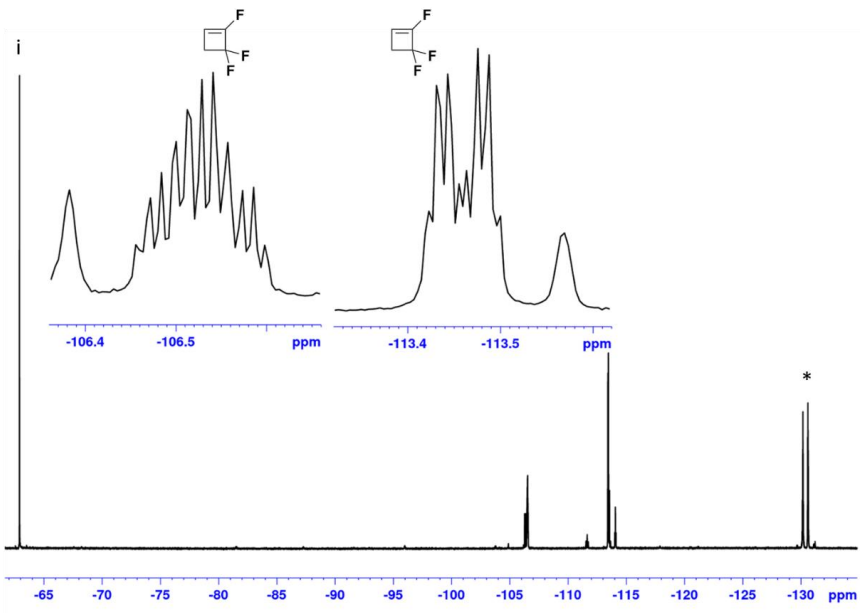

Figure C.32. ^{19}F NMR spectrum (282 MHz, C_6D_6) in situ of the HDF of hexafluorocyclobut-1-ene (**4.5a**) using $[(PPh_3)CuH]_6$, $P(OEt)_3$ and TMDS after 10 min. The Si-F peak is labeled '*' and $PhCF_3$ 'i'. The inset shows the expanded (horizontal scale) signal.

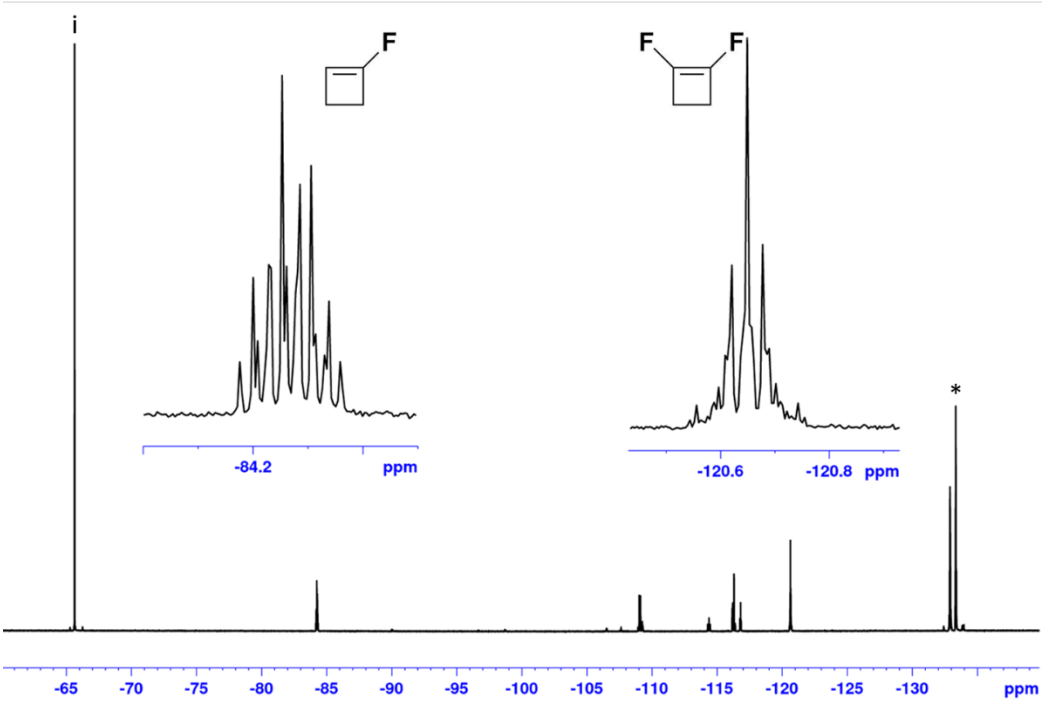

Figure C.33. ^{19}F NMR spectrum (282 MHz, C_6D_6) in situ of the HDF of hexafluorocyclobut-1-ene (**4.5a**) using $[(PPh_3)CuH]_6$, $P(OEt)_3$ and TMDS after 10 h. The Si-F peak is labeled '*' and $PhCF_3$ 'i'. The inset shows the expanded (horizontal scale) signal.

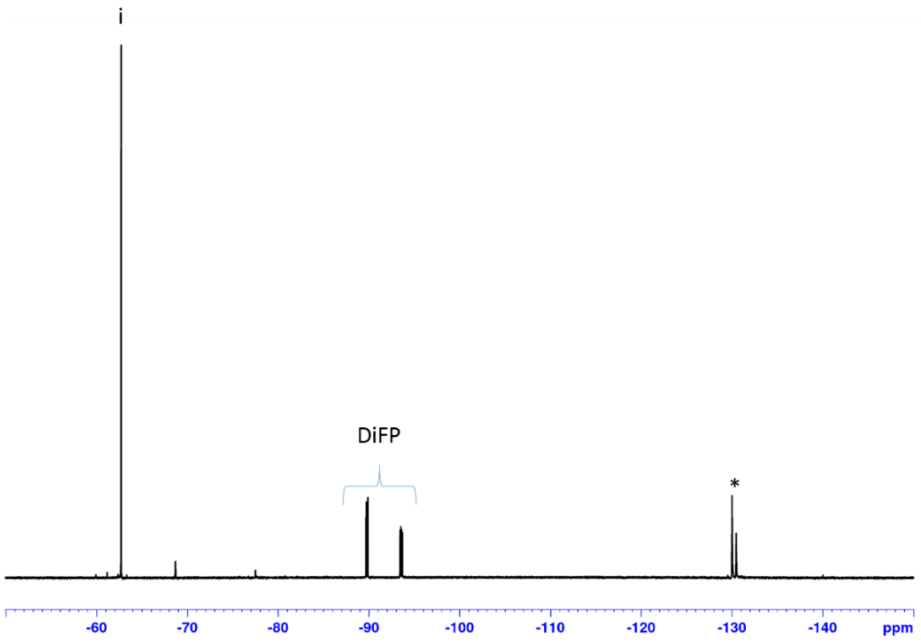

Figure C.34. ^{19}F NMR spectrum (282 MHz, C_6D_6) in situ of the HDF of CF_3V (**4.9**) using $[(PPh_3)CuH]_6$, PPh_2Me and TMDS. The Si-F peak is labeled '*' and $PhCF_3$ 'i'.

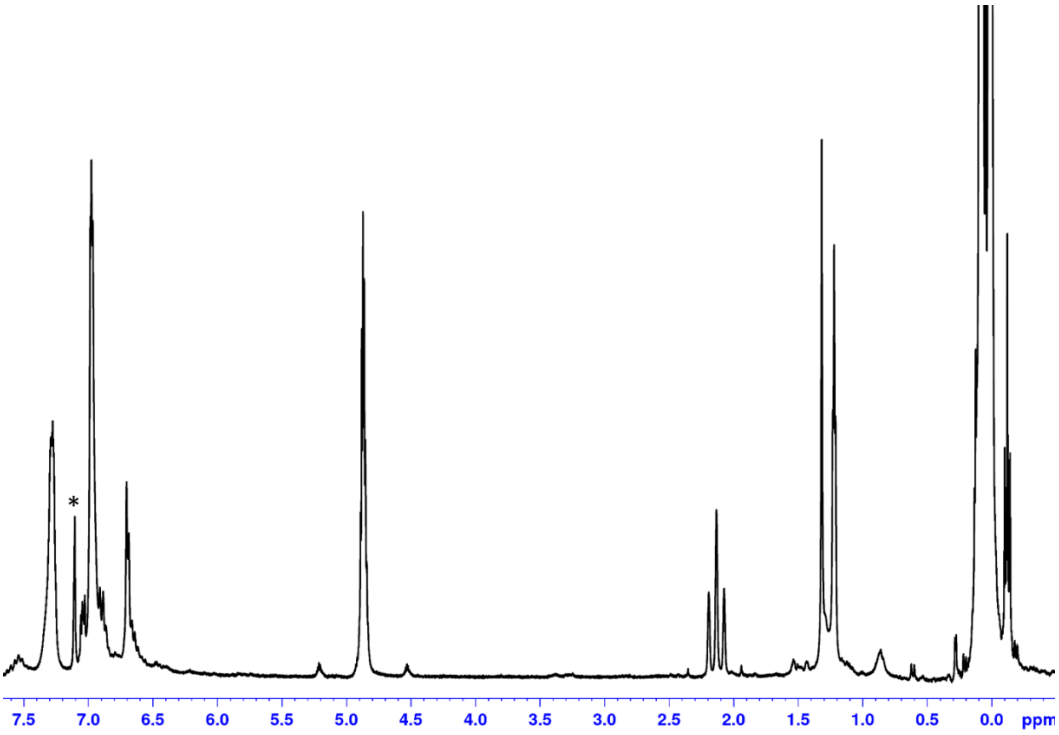

Figure C.35. ^{1}H NMR spectrum (300 MHz, C_6D_6) in situ of the HDF of $CF_3CF_2CF=(CF_3)_2$ (**4.6a**) using $[(PPh_3)CuH]_6$, Xantphos and TMDS. The residual solvent peak is labeled '*'.

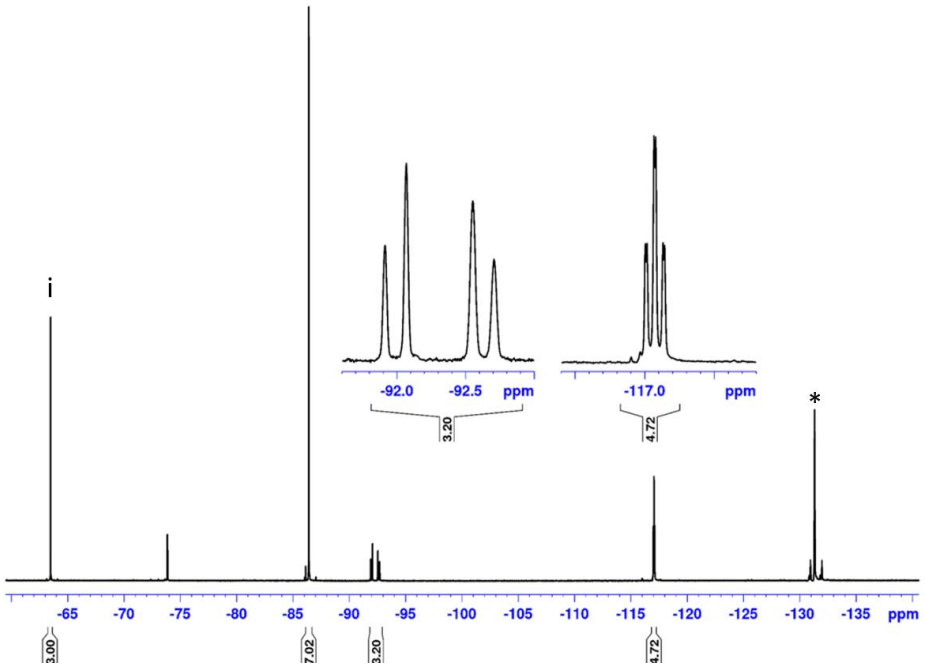

Figure C.36. ^{19}F NMR spectrum (282 MHz, C_6D_6) in situ of the HDF of $CF_3CF_2CF=(CF_3)_2$ (**4.6a**) using $[(PPh_3)CuH]_6$, Xantphos and TMDS. The Si-F peak is labeled '*' and $PhCF_3$ 'i'. The inset shows the expanded (horizontal scale) signal.

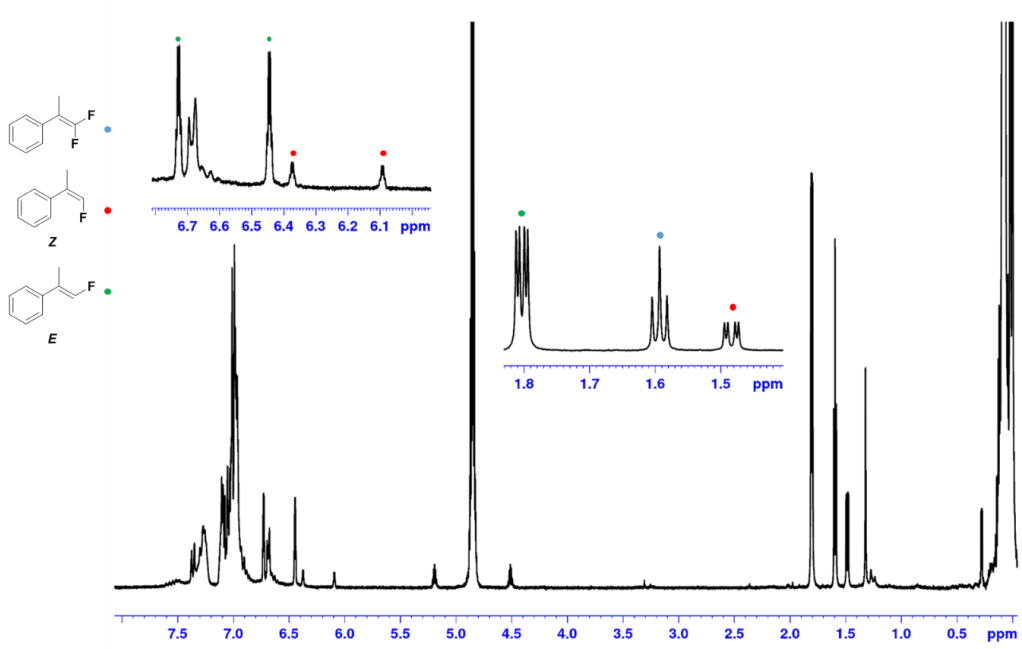

Figure C.37. ^1H NMR spectrum (300 MHz, C_6D_6) in situ of the HDF of α-trifluoromethylstyrene (**4.8a**) using $[(PPh_3)CuH]_6$, Xantphos and TMDS. The inset shows the expanded (horizontal scale) signal.

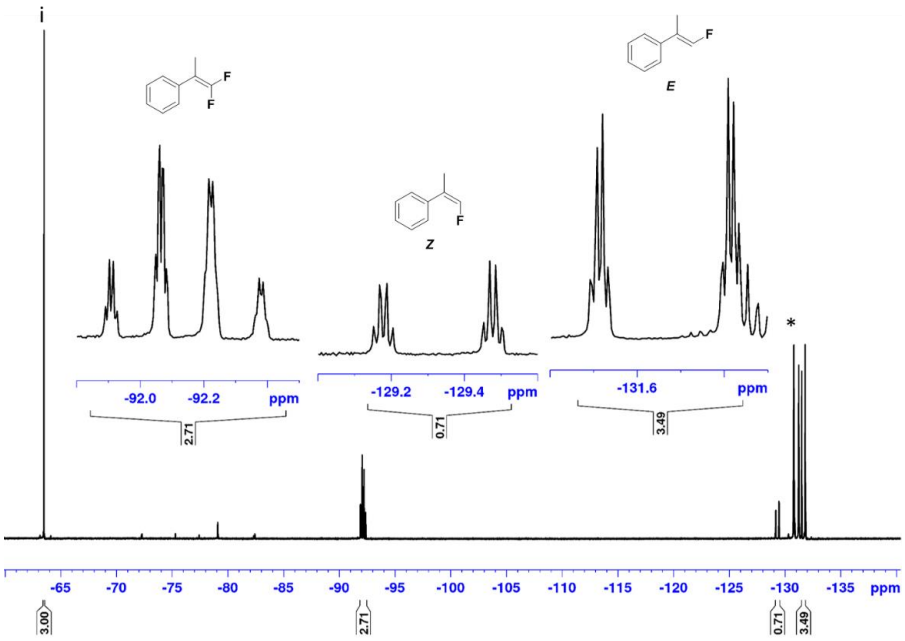

Figure C.38. ^{19}F NMR spectrum (282 MHz, C_6D_6) in situ of the HDF of α-trifluoromethylstyrene (**4.8a**) using $[(PPh_3)CuH]_6$, Xantphos and TMDS. The Si-F peak is labeled '*' and $PhCF_3$ 'i'. The inset shows the expanded (horizontal scale) signal.

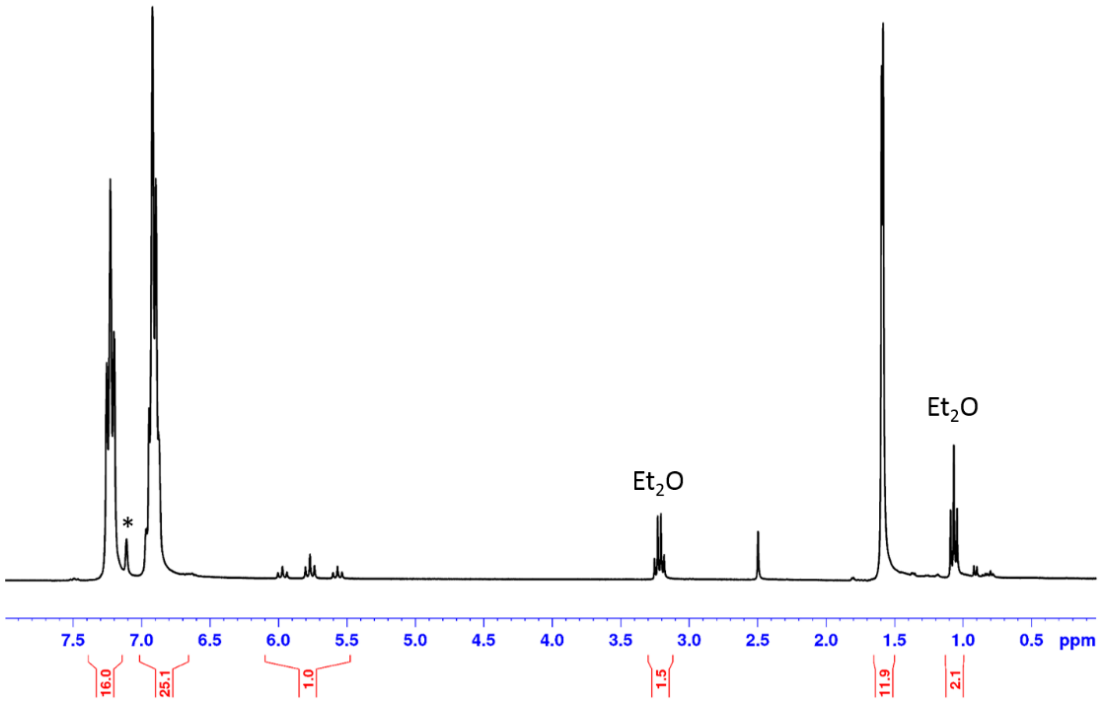

Figure C.39. ^1H NMR spectrum (300 MHz, C_6D_6) of **4.7a**. The residual solvent peak is labeled 'i'.

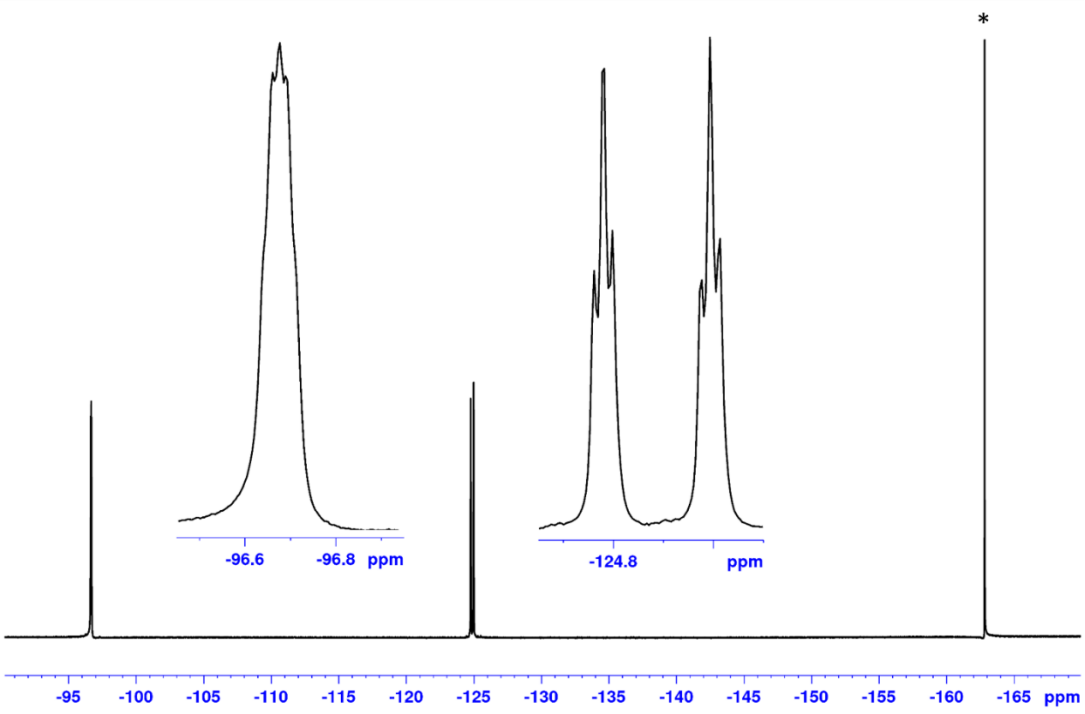

Figure C.40. ^{19}F NMR spectrum (282 MHz, C_6D_6) of **7a.** The C_6F_6 peak is labeled '*'.

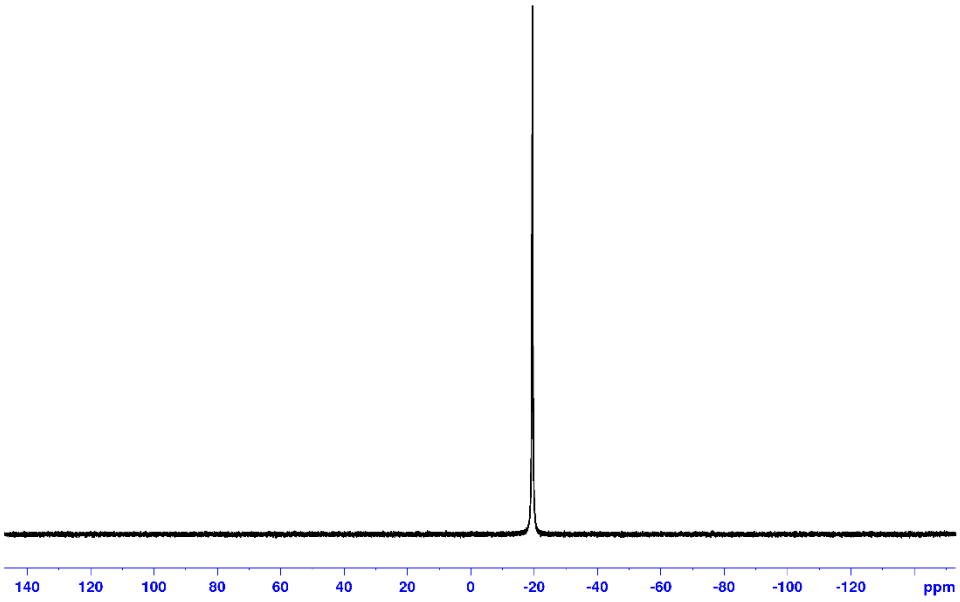

Figure C.41. $^{31}P\{^{1}H\}$ NMR spectrum (181 MHz, C_6D_6) of **4.7a.** H_3PO_4 used as external reference.

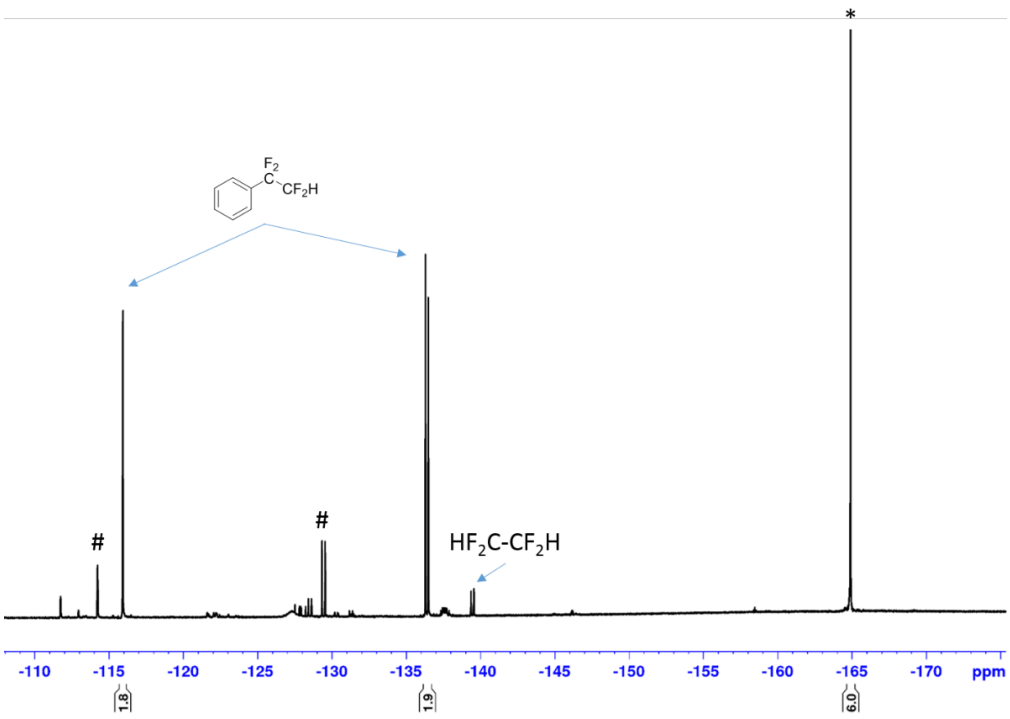

Figure C.42. ^{19}F NMR spectrum (282 MHz, C_6D_6) in situ of the reaction of Ph-I with $(PPh_2Me)_3Cu\text{-}CF_2CF_2H$ and SIMesCuCl (10 mol %). The SIMesCu-CF_2CF_2H peak is labeled '#' and C_6F_6 'i'.

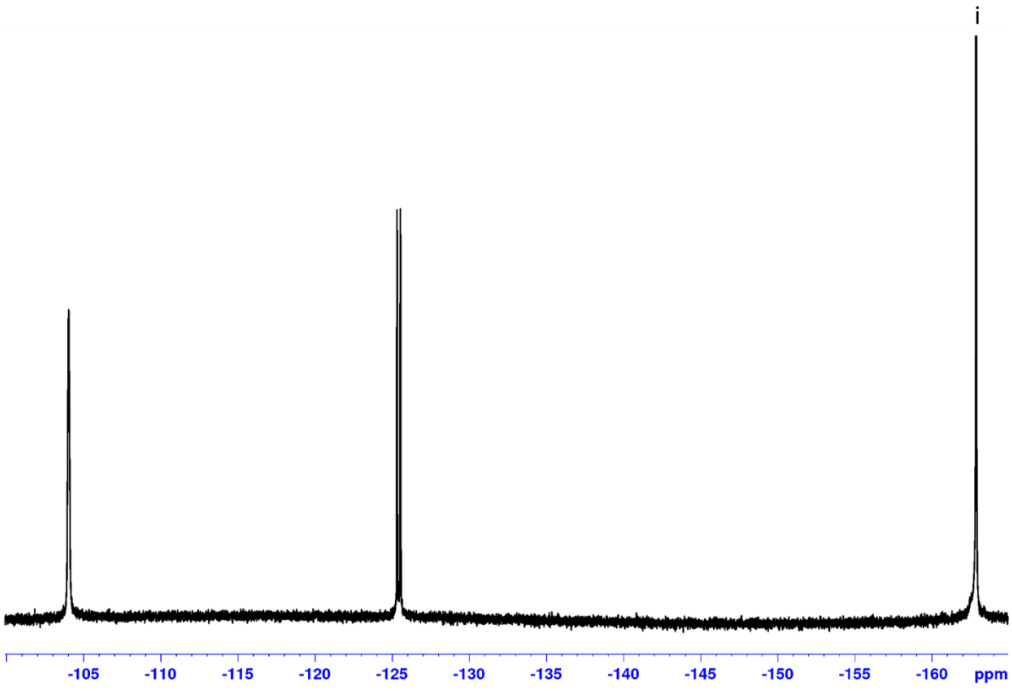

Figure C.43. ^{19}F NMR spectrum (282 MHz, C_6D_6) of **4.7b.** The C_6F_6 peak is labeled '*'.

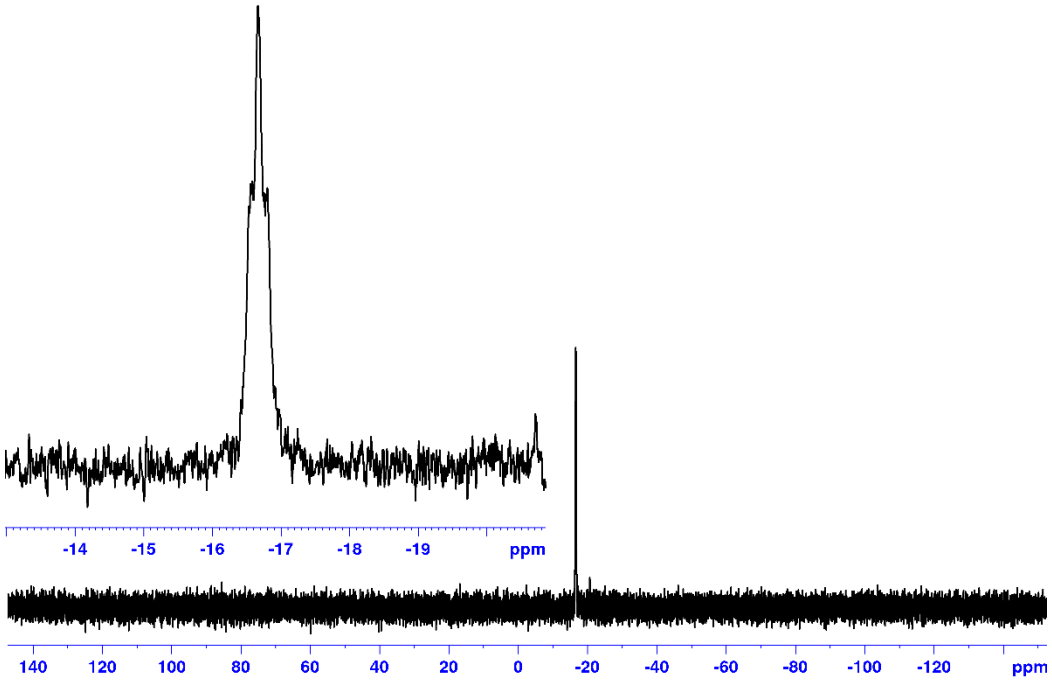

Figure C.44. $^{31}P\{^{1}H\}$ NMR spectrum (181 MHz, C_6D_6) of **4.7b.** H_3PO_4 used as external reference.

Appendix D

Appendix for Chapter 5.3.1

NMR Spectra

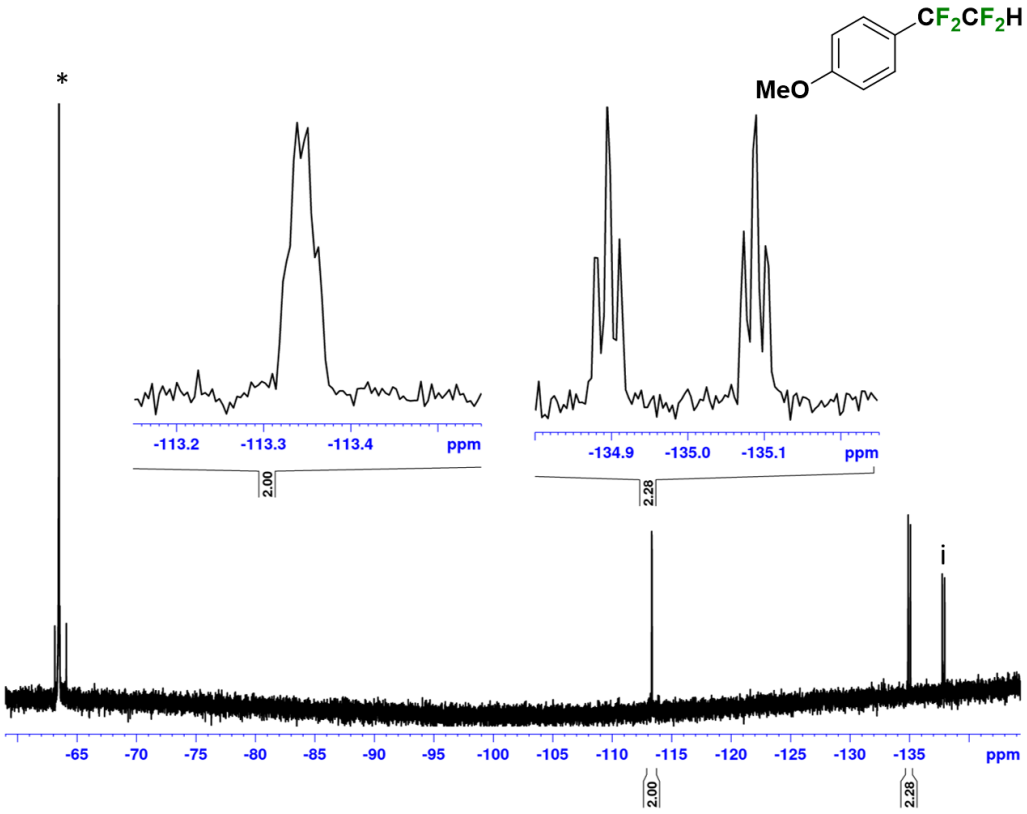

Figure D.1. ^{19}F NMR spectrum (386 MHz, $CDCl_3$) of **5.1b**. $PhCF_3$ (*) and HCF_2CF_2H (i).

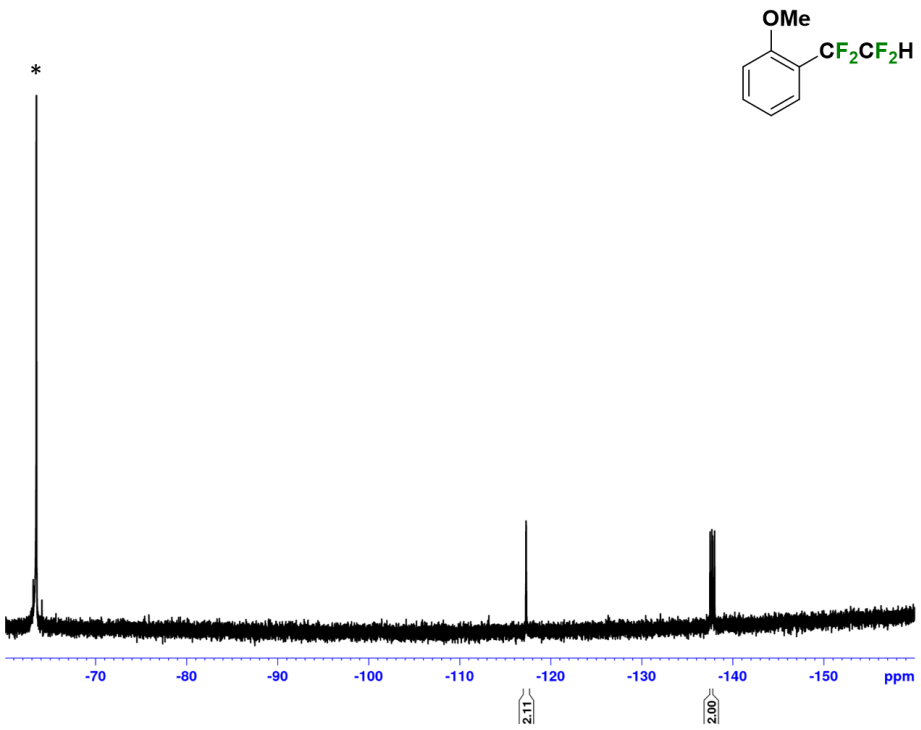

Figure D.2. ^{19}F NMR spectrum (386 MHz, $CDCl_3$) of **5.1c**. $PhCF_3$ (*).

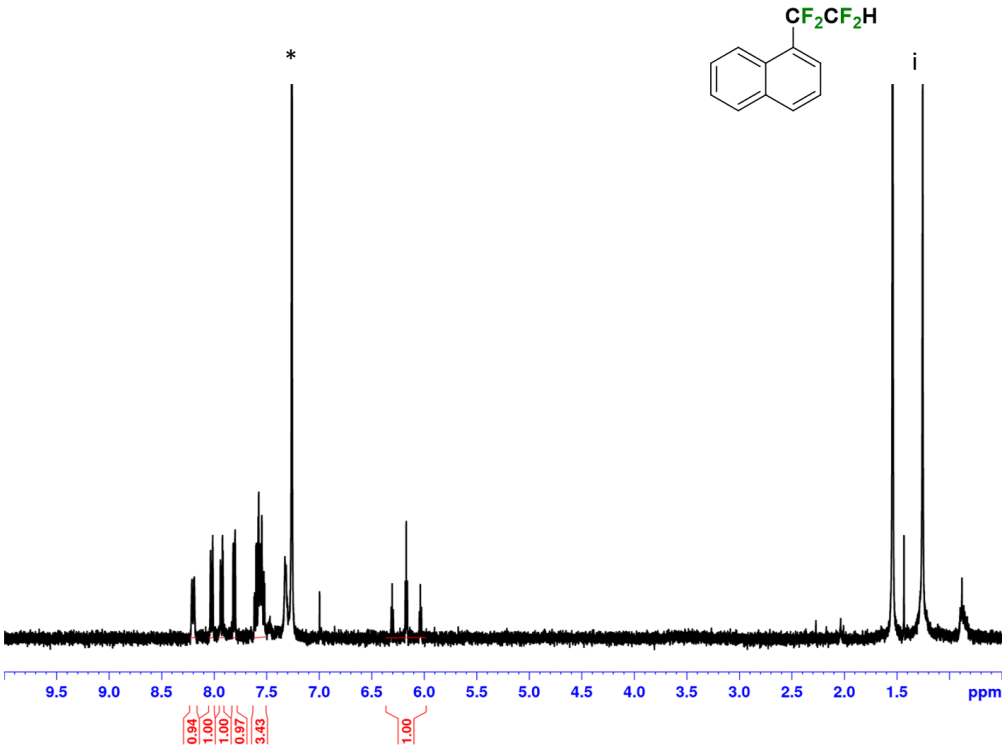

Figure D.3. ^{1}H NMR spectrum (400 MHz, $CDCl_3$) of **5.1d**. $CHCl_3$ (*) and impurity in solvent (i)

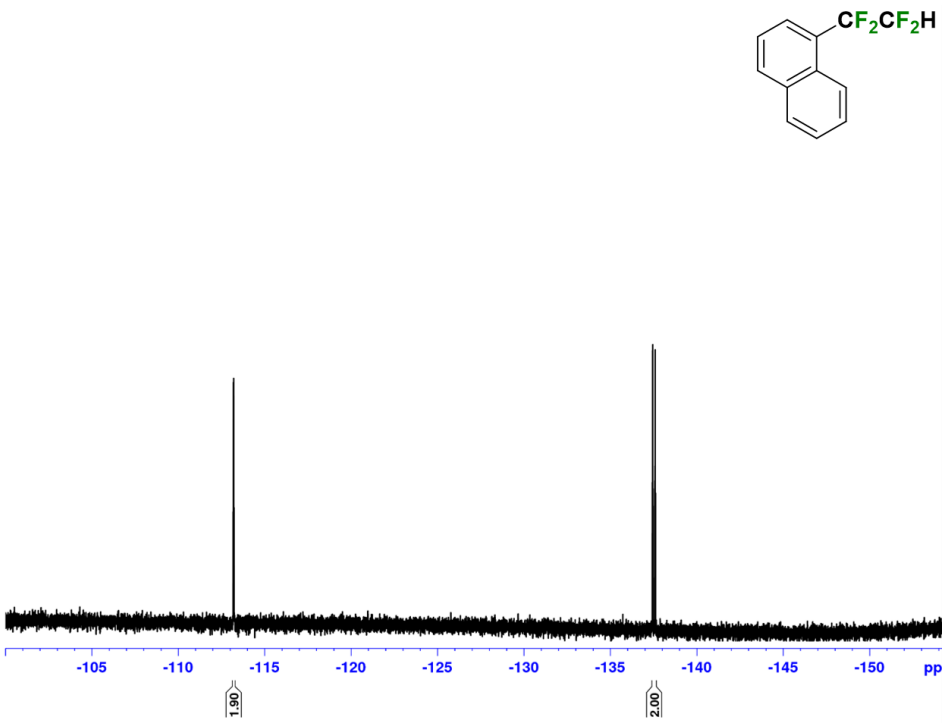

Figure D.4. ^{19}F NMR spectrum (386 MHz, $CDCl_3$) of **5.1d**.

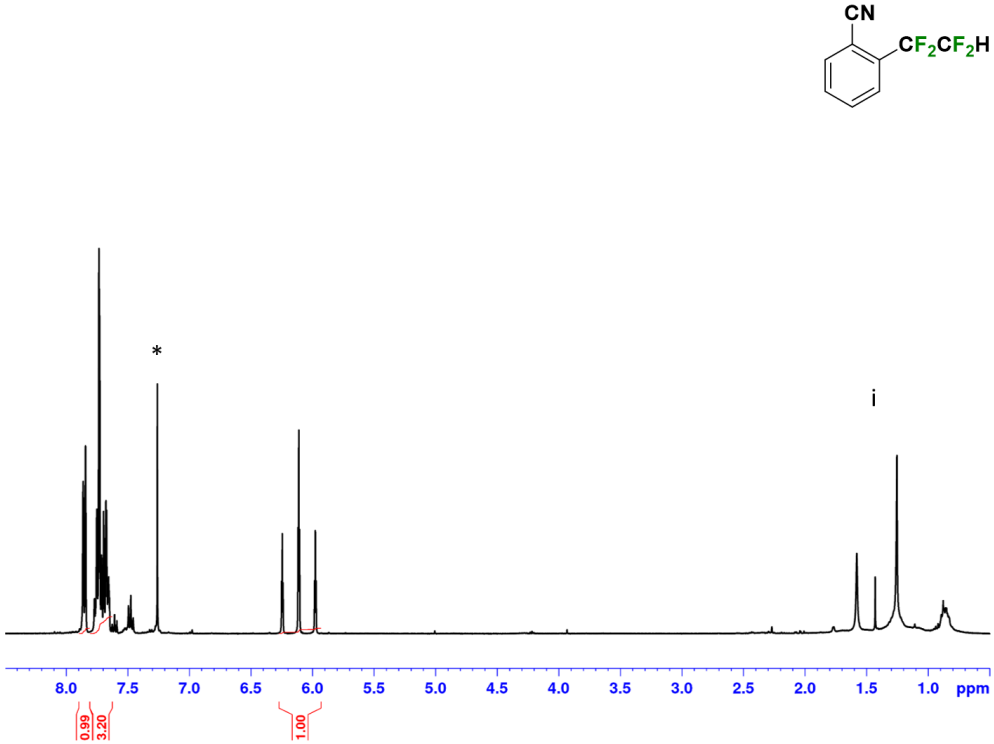

Figure D.5. ^{1}H NMR spectrum (400 MHz, $CDCl_3$) of **5.1e**. $CHCl_3$ (*) and impurity in solvent (i)

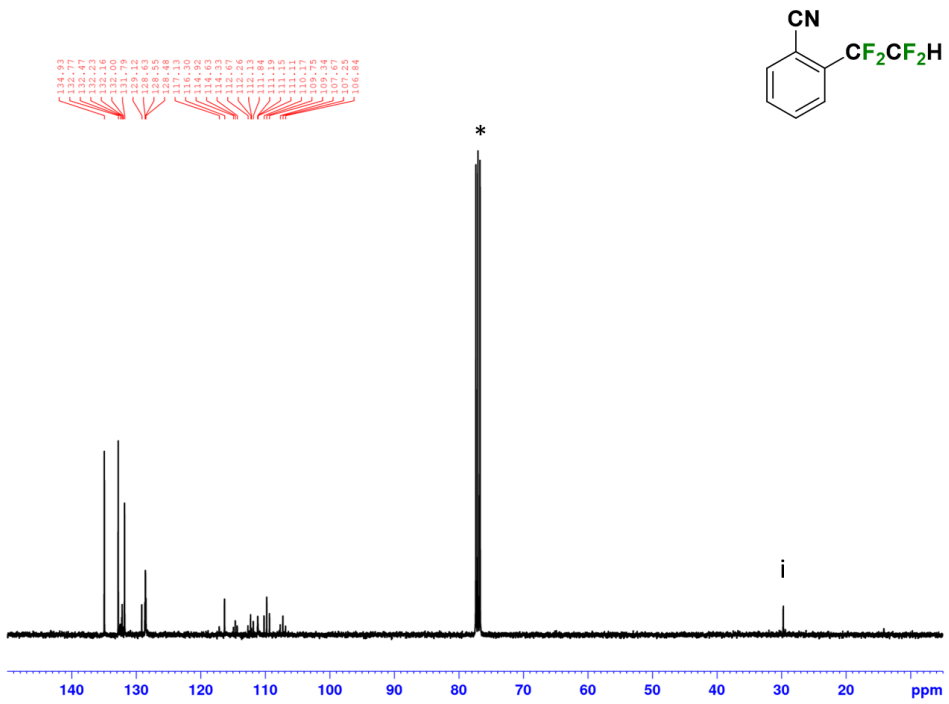

Figure D.6. $^{13}C\{^{1}H\}$ NMR spectrum (100 MHz, $CDCl_3$) of **5.1e**. $CDCl_3$ (*) and and impurity in solvent (i).

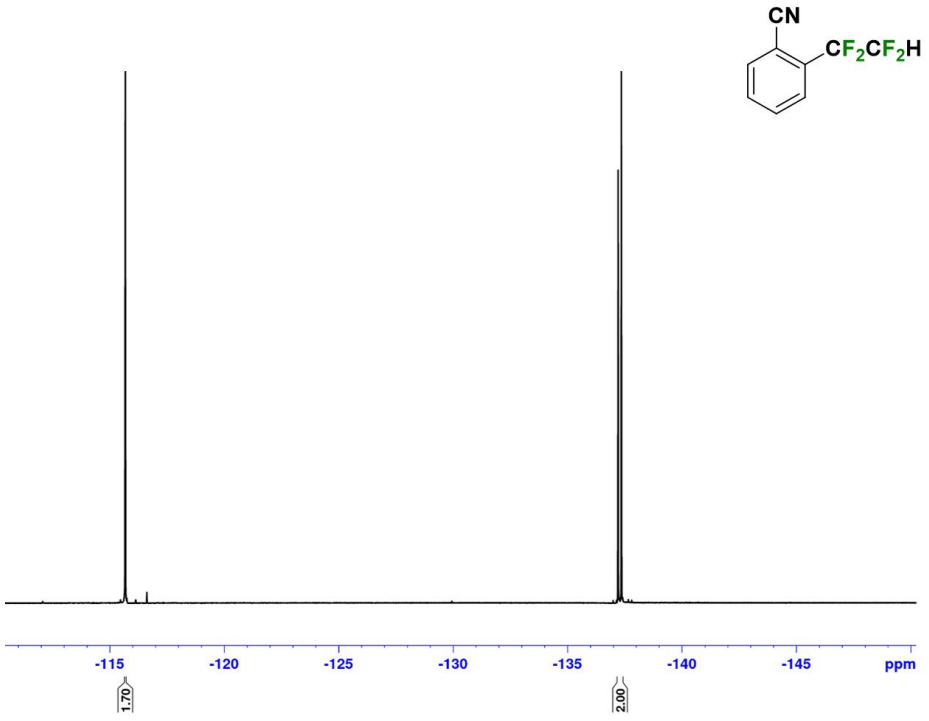

Figure D.7. ^{19}F NMR spectrum (386 MHz, $CDCl_3$) of **5.1e**.

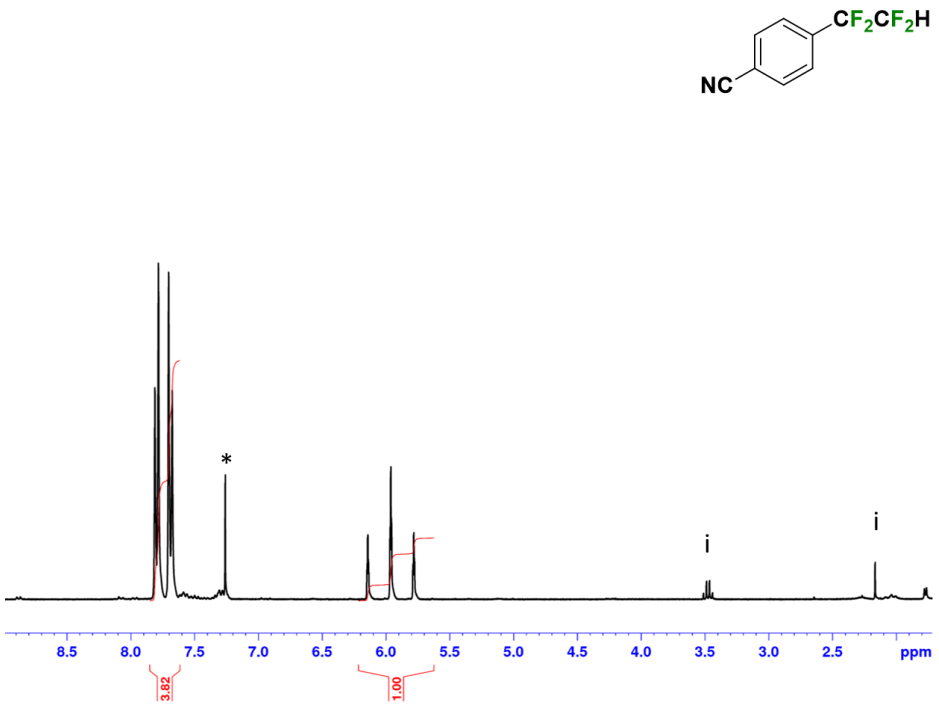

Figure D.8. ^{1}H NMR spectrum (400 MHz, $CDCl_3$) of **5.1f**. $CHCl_3$ (*) and impurity in solvent (i)

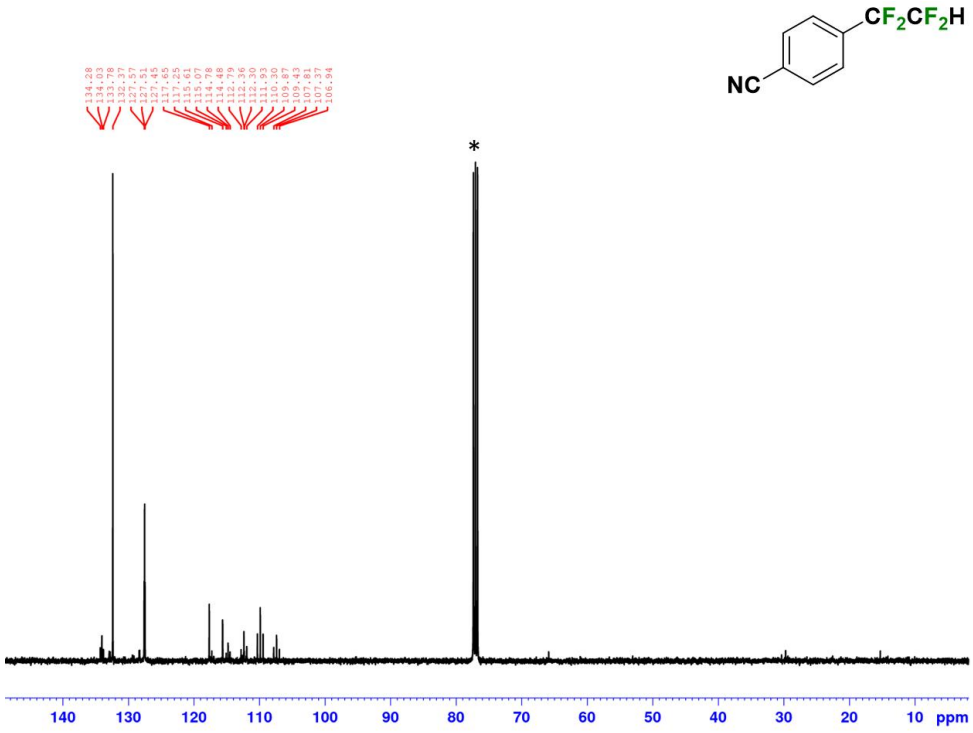

Figure D.9. $^{13}C\{^{1}H\}$ NMR spectrum (100 MHz, $CDCl_3$) of **5.1f**. $CDCl_3$ (*) and and impurity in solvent (i).

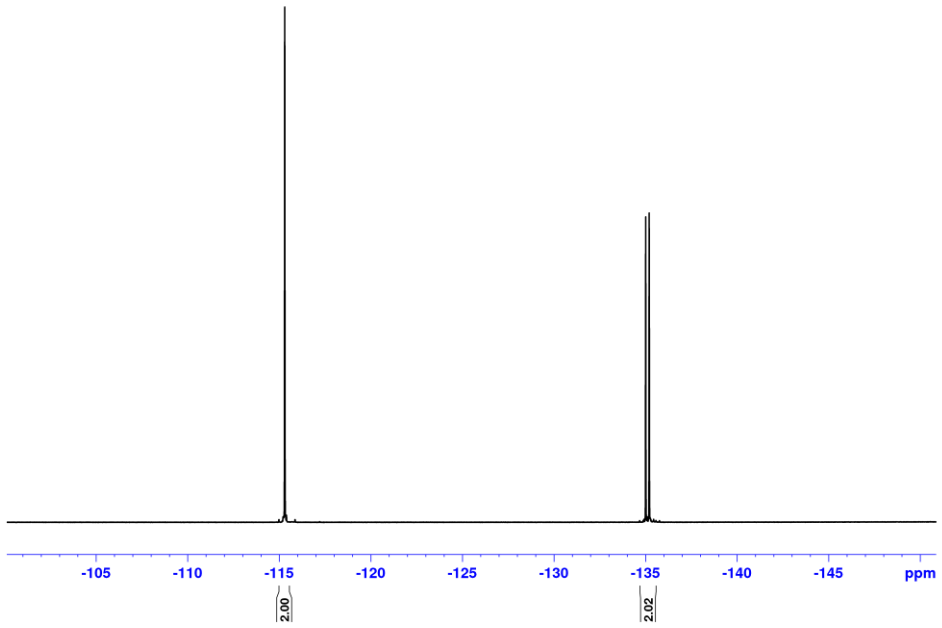

Figure D.10. ^{19}F NMR spectrum (386 MHz, $CDCl_3$) of **5.1f**.

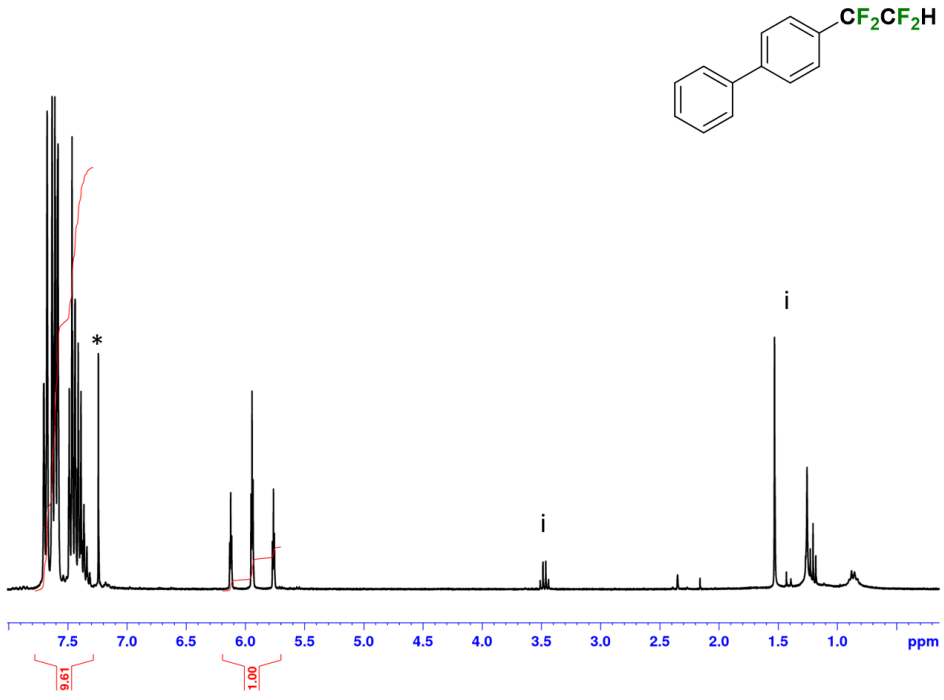

Figure D.11. ^{1}H NMR spectrum (400 MHz, $CDCl_3$) of **5.1g**. $CHCl_3$ (*) and impurity in solvent (i)

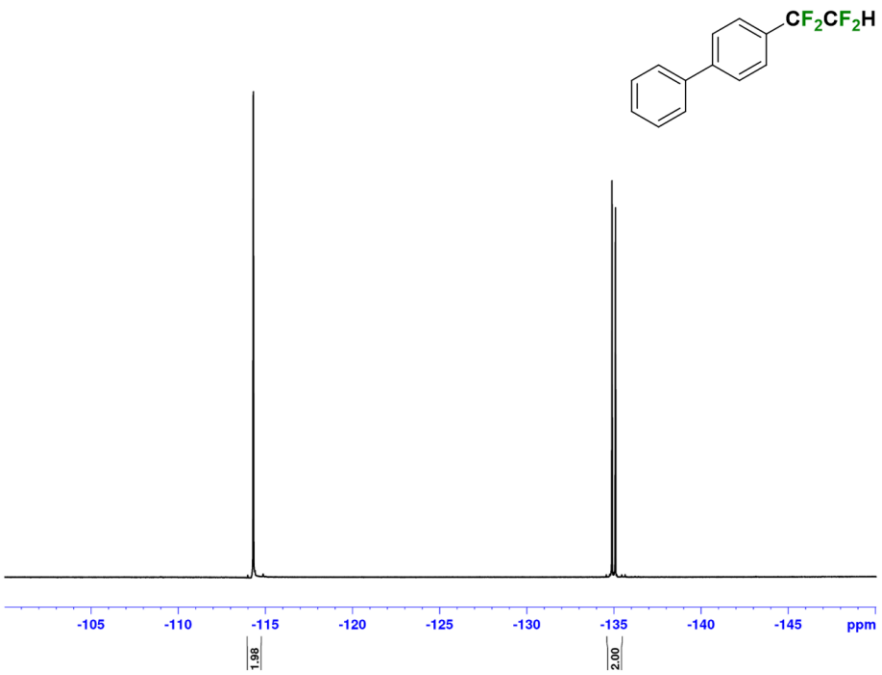

Figure D.12. ^{19}F NMR spectrum (386 MHz, $CDCl_3$) of **5.1g**.

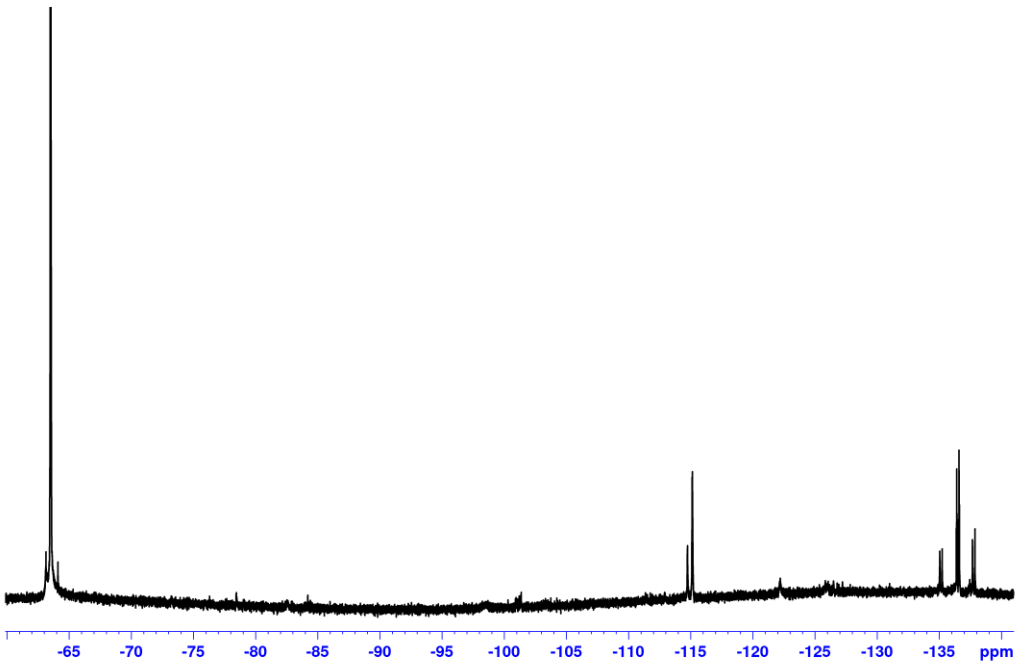

Figure D.13. ^{19}F NMR spectrum (386 MHz, C_6D_6) *in situ* of **5.1h**. $PhCF_3$ (*).

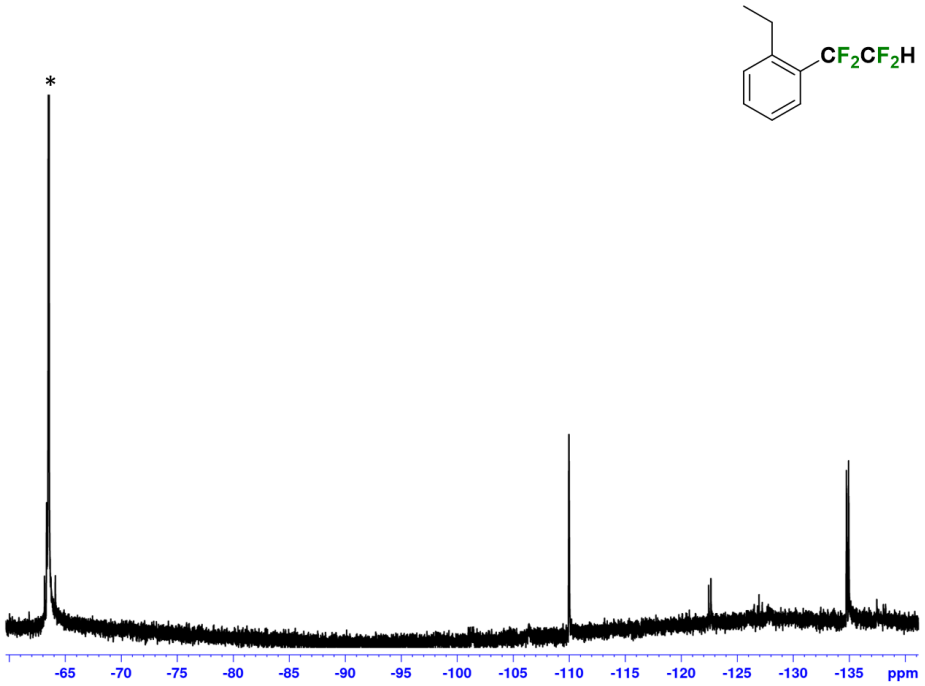

Figure D.14. ^{19}F NMR spectrum (386 MHz, C_6D_6) *in situ* of **5.1i**. $PhCF_3$ (*).

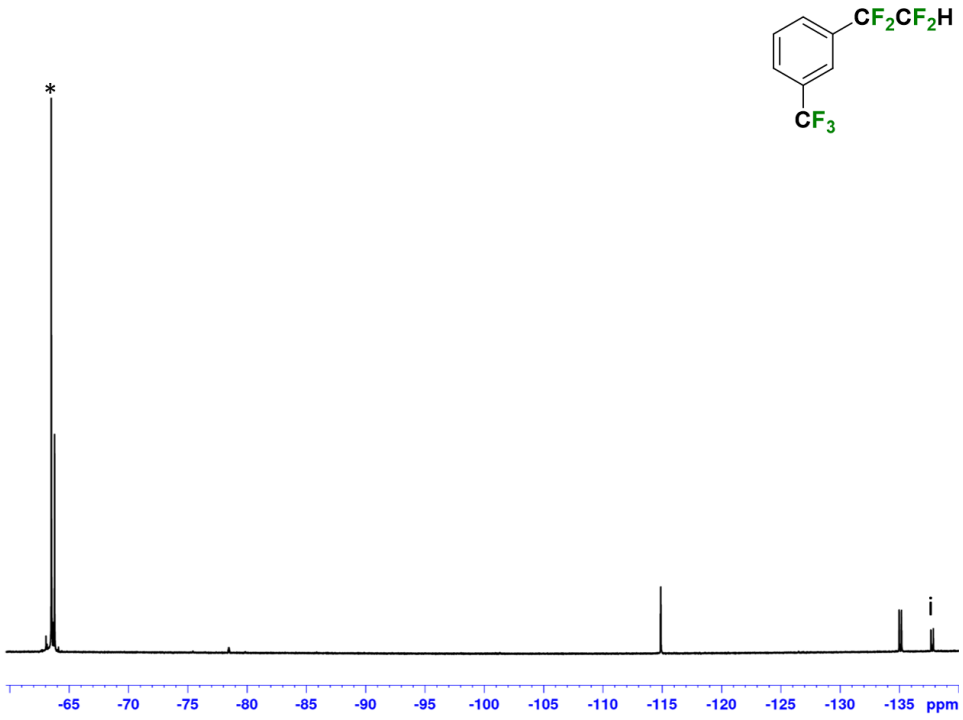

Figure D.15. ^{19}F NMR spectrum (386 MHz, C_6D_6) *in situ* of **5.1j**. $PhCF_3$ (*) and HCF_2CF_2H (i).

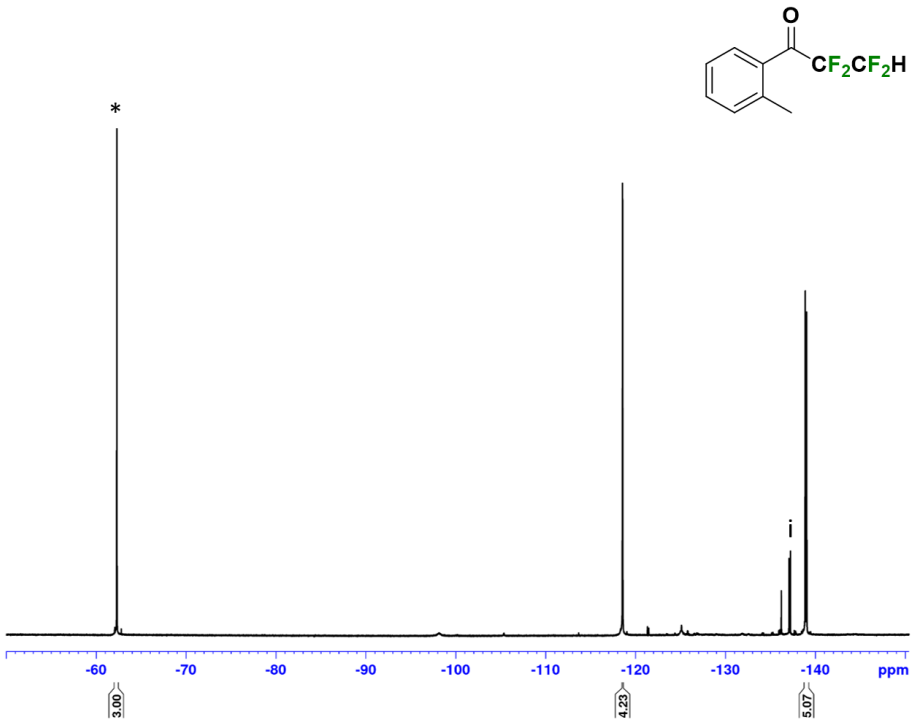

Figure D.16. ^{19}F NMR spectrum (386 MHz, C_6D_6) *in situ* of **5.2a**. $PhCF_3$ (*) and HCF_2CF_2H (i).

Figure D.17. ^{19}F NMR spectrum (386 MHz, C_6D_6) *in situ* of **5.2b**. $PhCF_3$ (*).

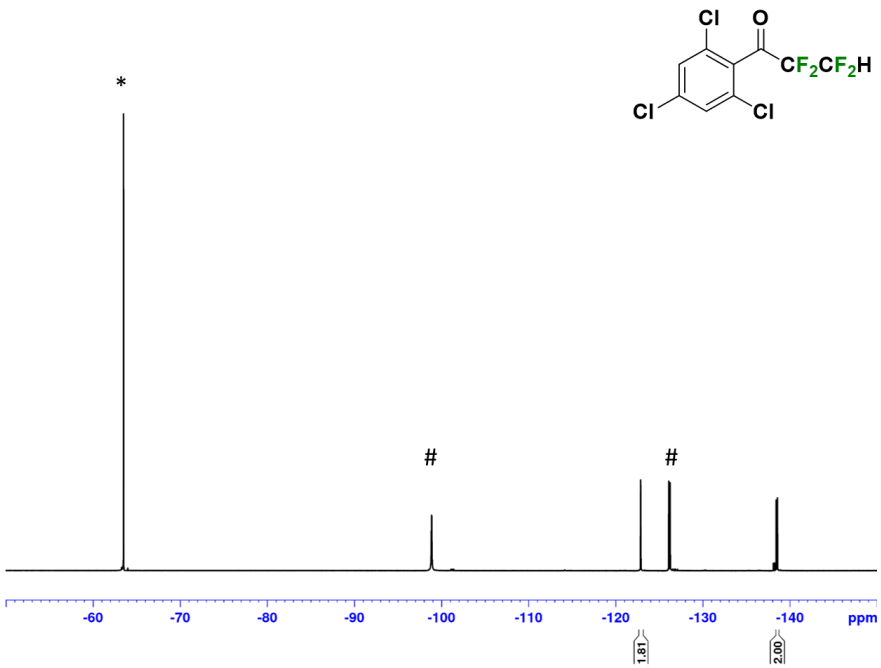

Figure D.18. ^{19}F NMR spectrum (386 MHz, C_6D_6) *in situ* of **5.2c**. $PhCF_3$ (*) and $[Cu]CF_2CF_2H$ (#).

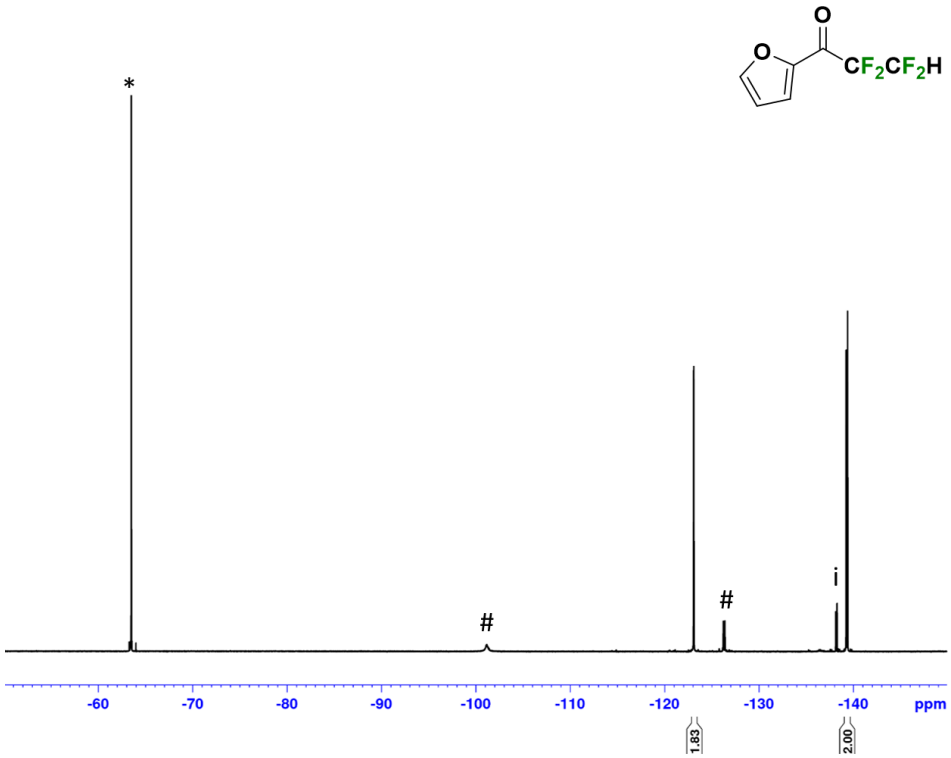

Figure D.19. ^{19}F NMR spectrum (386 MHz, C_6D_6) *in situ* of **5.2f**. $PhCF_3$ (*), HCF_2CF_2H (i) and $[Cu]CF_2CF_2H$ (#).

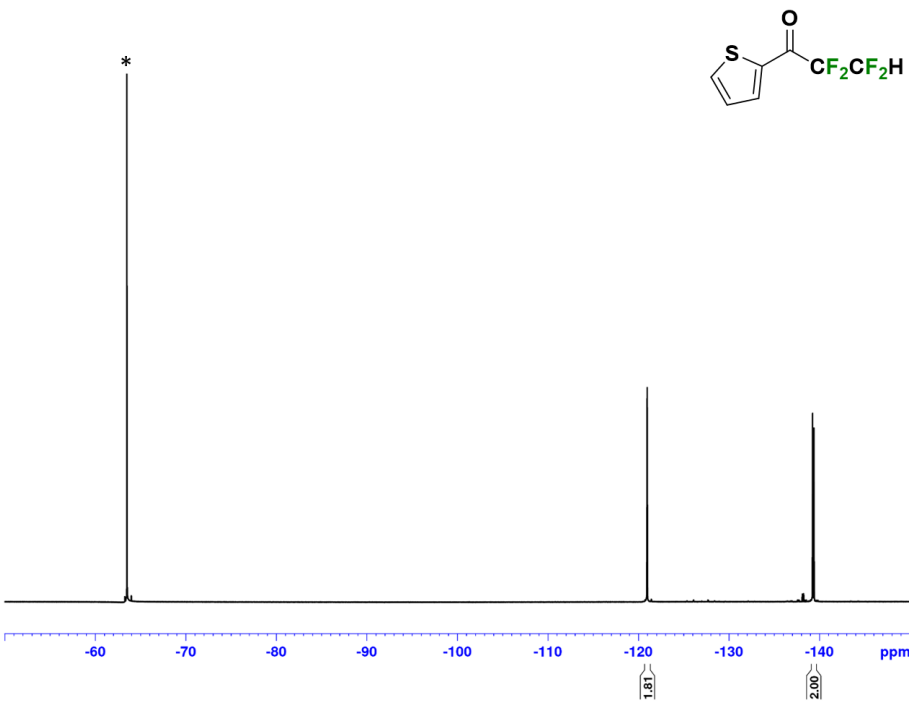

Figure D.20. ^{19}F NMR spectrum (386 MHz, C_6D_6) *in situ* of **5.1g**. $PhCF_3$ (*) and HCF_2CF_2H (i).

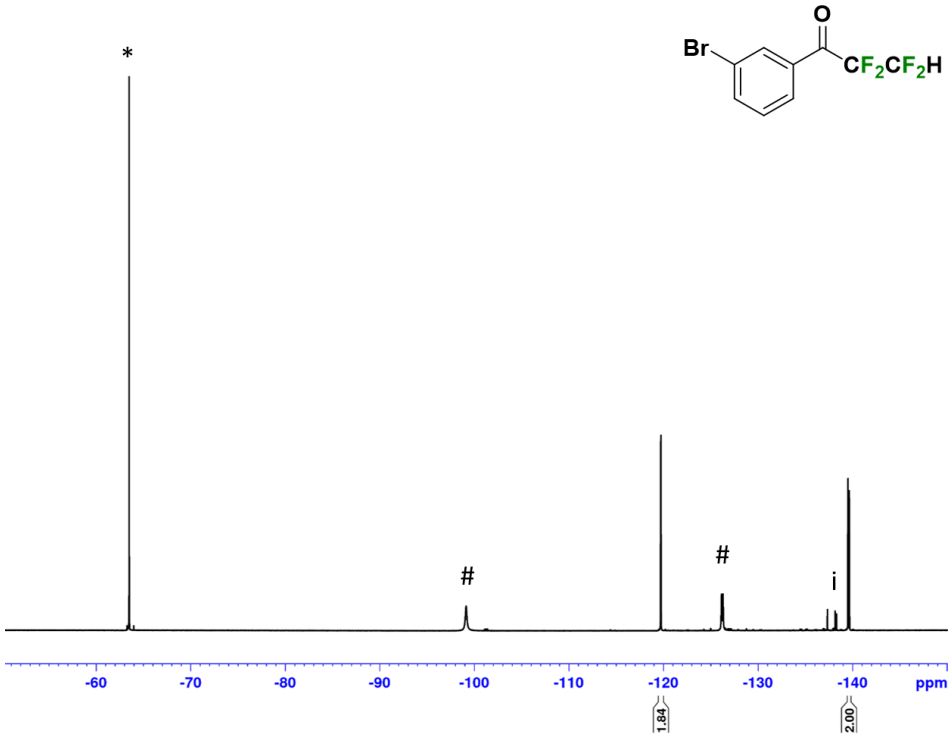

Figure D.21. ^{19}F NMR spectrum (386 MHz, C_6D_6) *in situ* of **5.2h**. $PhCF_3$ (*), HCF_2CF_2H (i) and $[Cu]CF_2CF_2H$ (#).

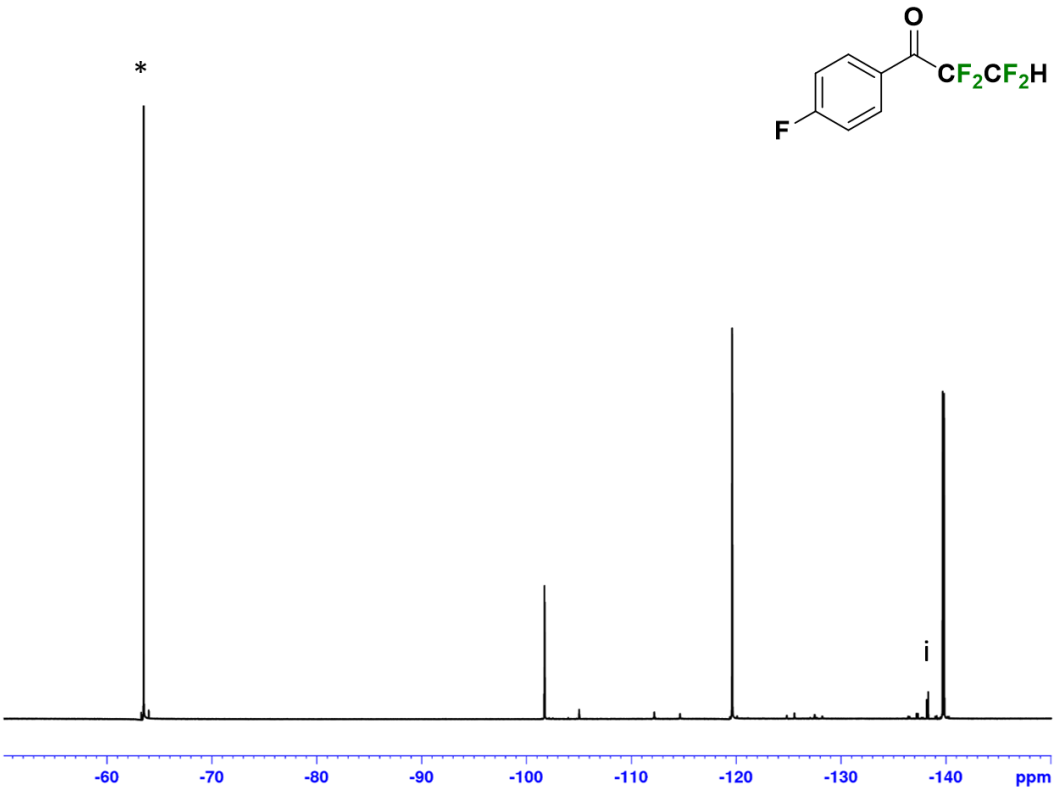

Figure D.22. ^{19}F NMR spectrum (386 MHz, C_6D_6) *in situ* of **5.2i**. $PhCF_3$ (*) and HCF_2CF_2H (i).

Appendix E

Appendix for Chapter 5.3.2

X-ray Structures

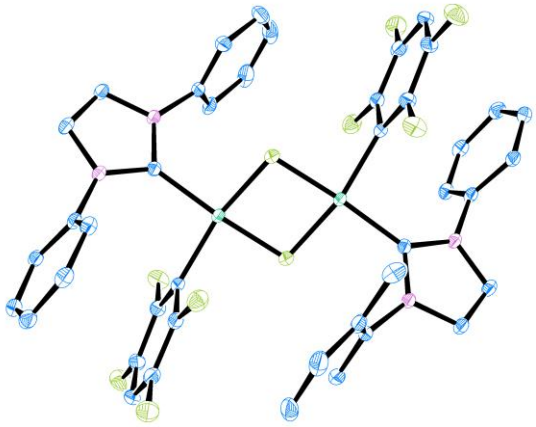

Figure E.1. ORTEP representation of the molecular structure of **5.4b**. Thermal-ellipsoid probabilities are set to 35% with hydrogen atoms and 2,6-iso-propyl groups omitted for clarity.

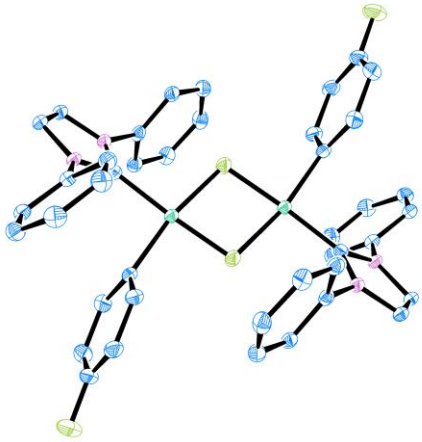

Figure E.2. Preliminary ORTEP representation of the molecular structure of **5.4c**. Thermal-ellipsoid probabilities are set to 35% with hydrogen atoms and 2,6-iso-propyl groups omitted for clarity.

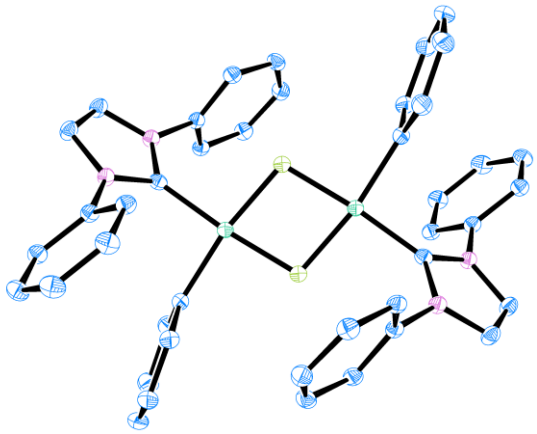

Figure E.3. ORTEP representation of the molecular structure of **5.4d**. Thermal-ellipsoid probabilities are set to 35% with hydrogen atoms and 2,6-iso-propyl groups omitted for clarity.

NMR Spectra

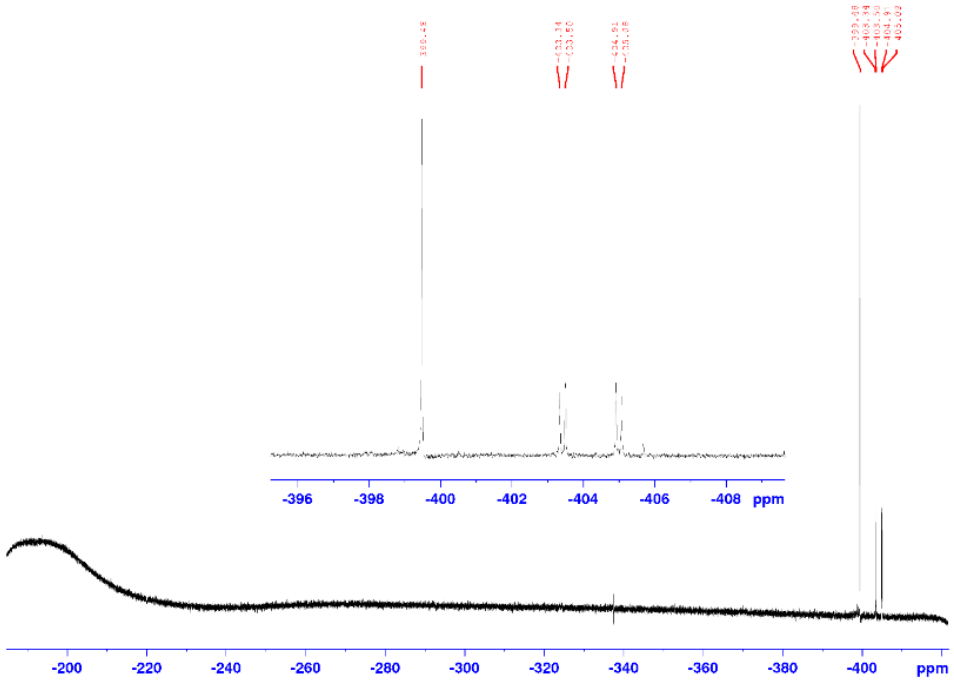

Figure E.4. ^{19}F NMR (386 MHz, C_6H_5F) *in situ* **5.3**

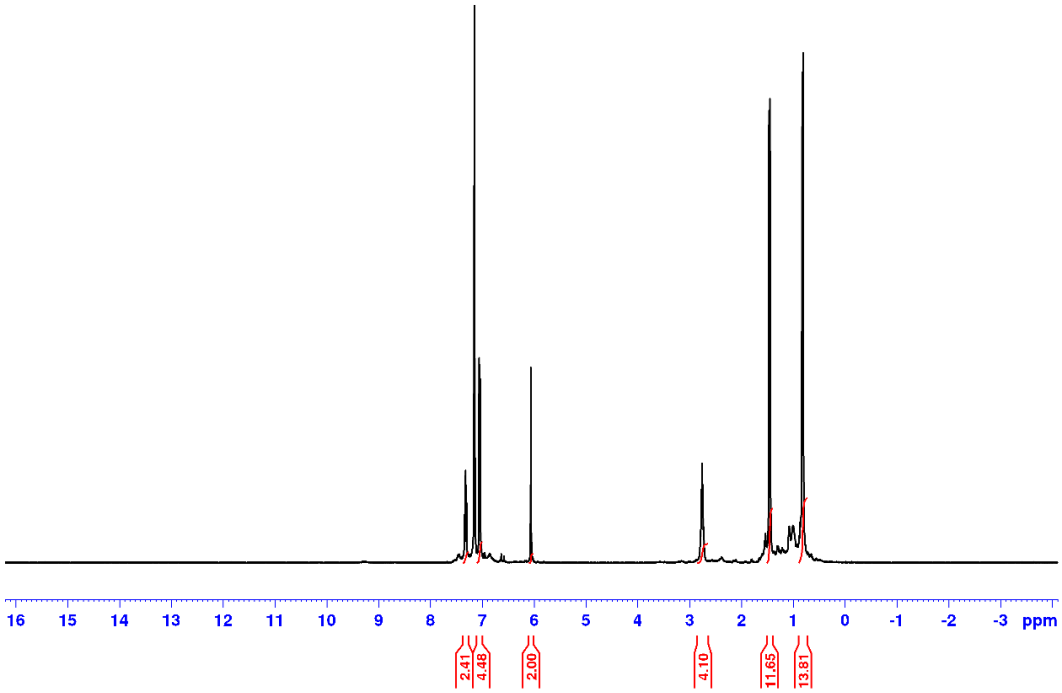

Figure E.5. ^{1}H NMR (400 MHz, C_6D_6) of (IPr)NiF(C_6F_5) **5.4a.**

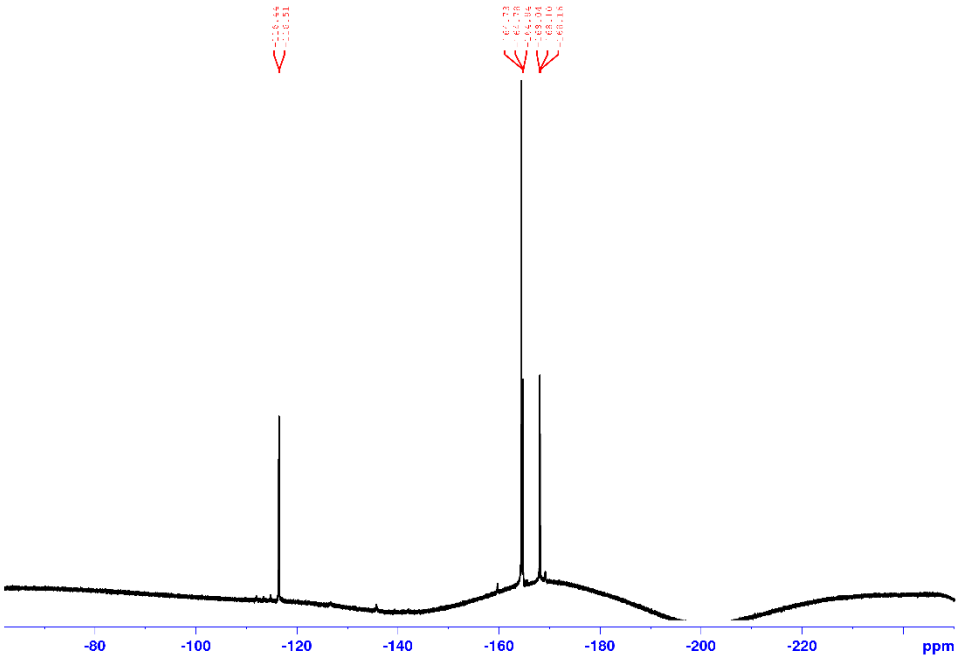

Figure E.6. ^{19}F NMR (386 MHz, C_6D_6) of (IPr)NiF(C_6F_5) **6.2a**. C_6F_6 external reference.

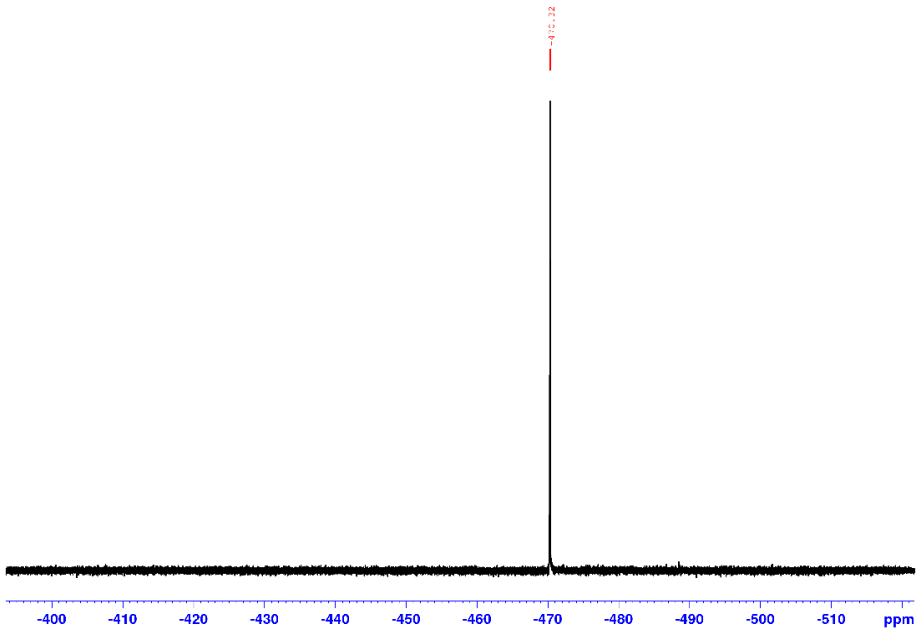

Figure E.7. ^{19}F NMR (386 MHz, C_6D_6) of (IPr)NiF(C_6F_5) **6.2a**. C_6F_6 external reference.

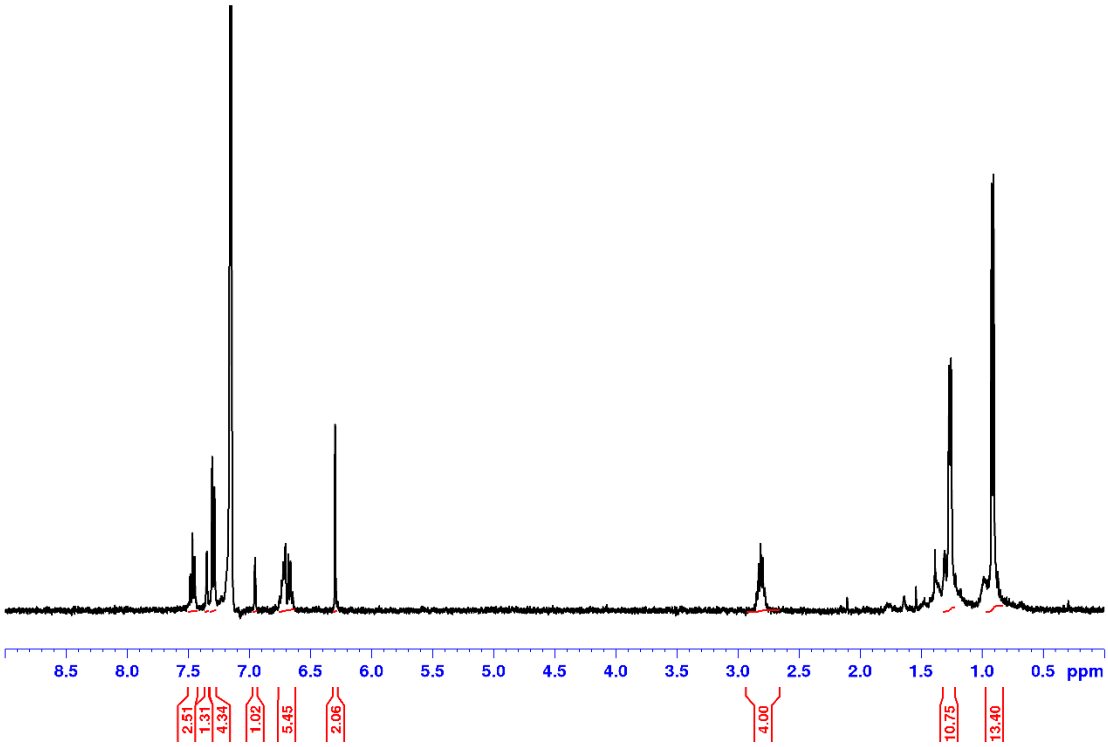

Figure E.8. ^{1}H NMR (400 MHz, C_6D_6) of (IPr)NiF(C_6H_5) **6.2d**.

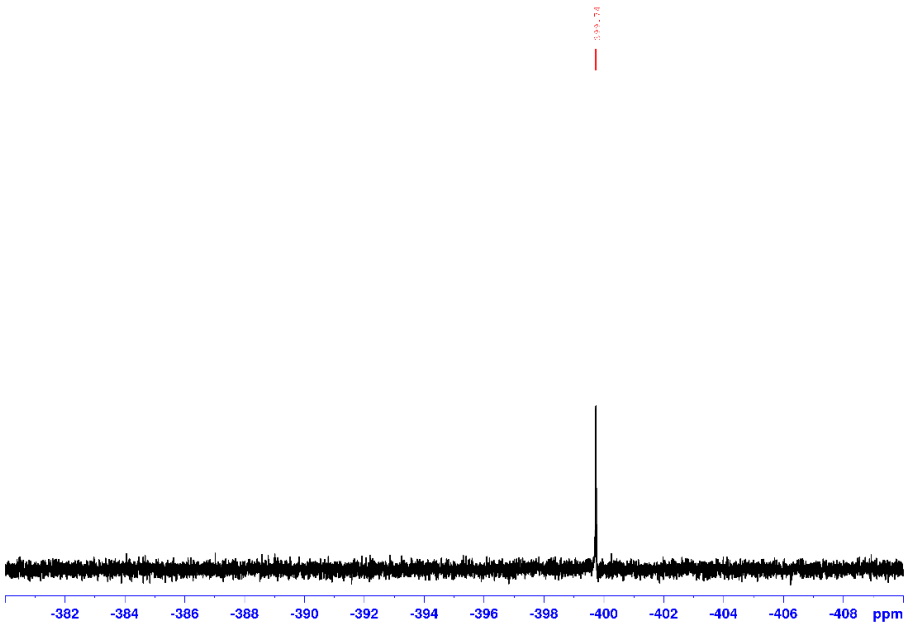

Figure E.9. ^{19}F NMR (386 MHz, C_6D_6) of (IPr)NiF(C_6H_5) **6.2d.** C_6F_6 external reference.

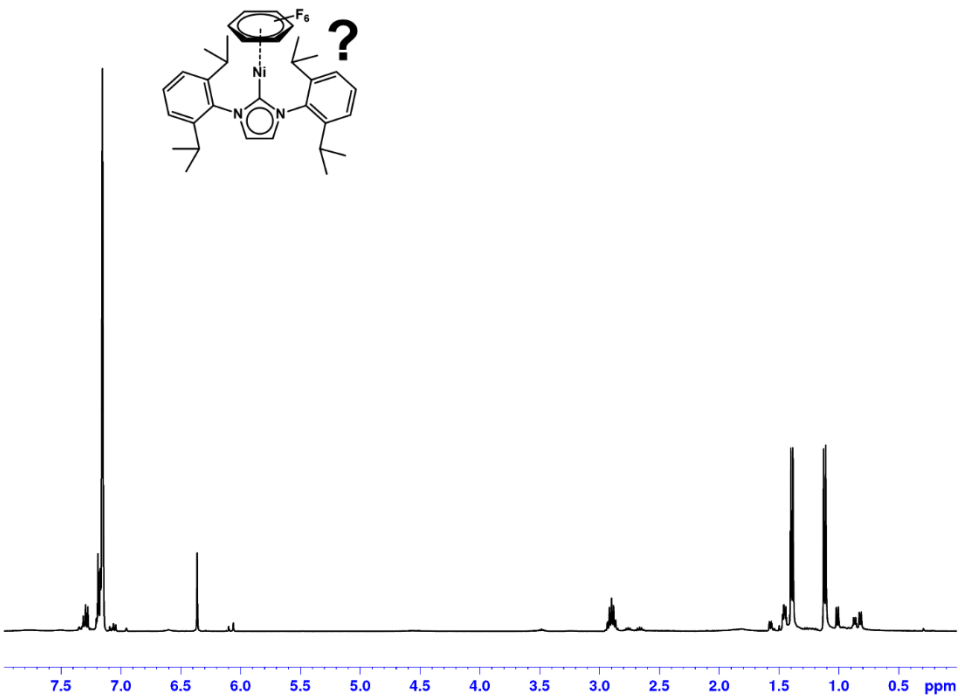

Figure E.10. ^{1}H NMR (400 MHz, C_6D_6) of (IPr)Ni(η^6-C_6F_6) **6.1'**.

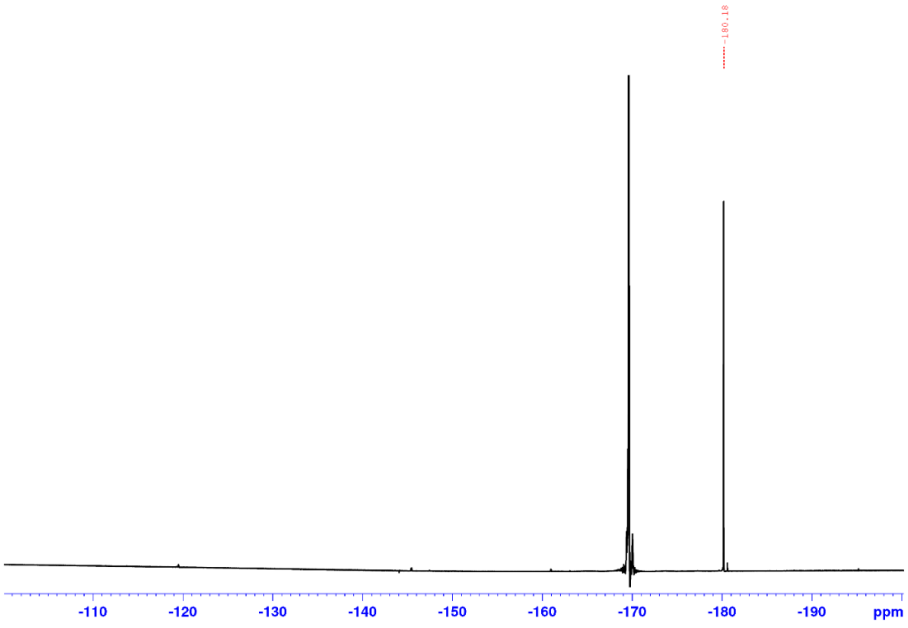

Figure E.11. ^{19}F NMR (386 MHz, C_6D_6) of (IPr)Ni(η^6-C_6F_6) **6.1'**. C_6F_6 external reference

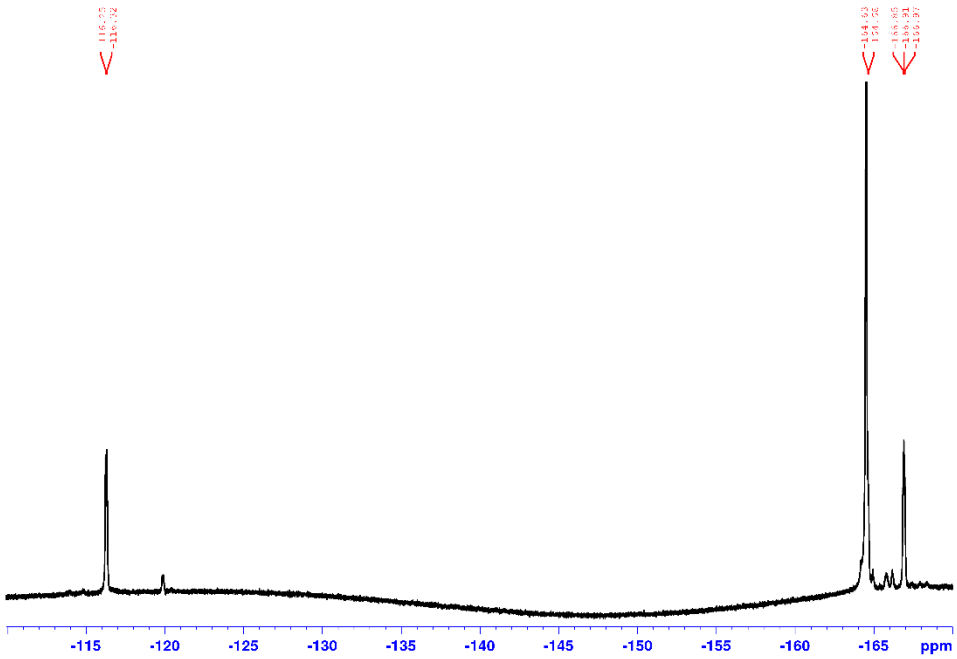

Figure E.12. ^{19}F NMR (386 MHz, C_6D_6) *in situ* of **6.2a** with DMAP. C_6F_6 external reference

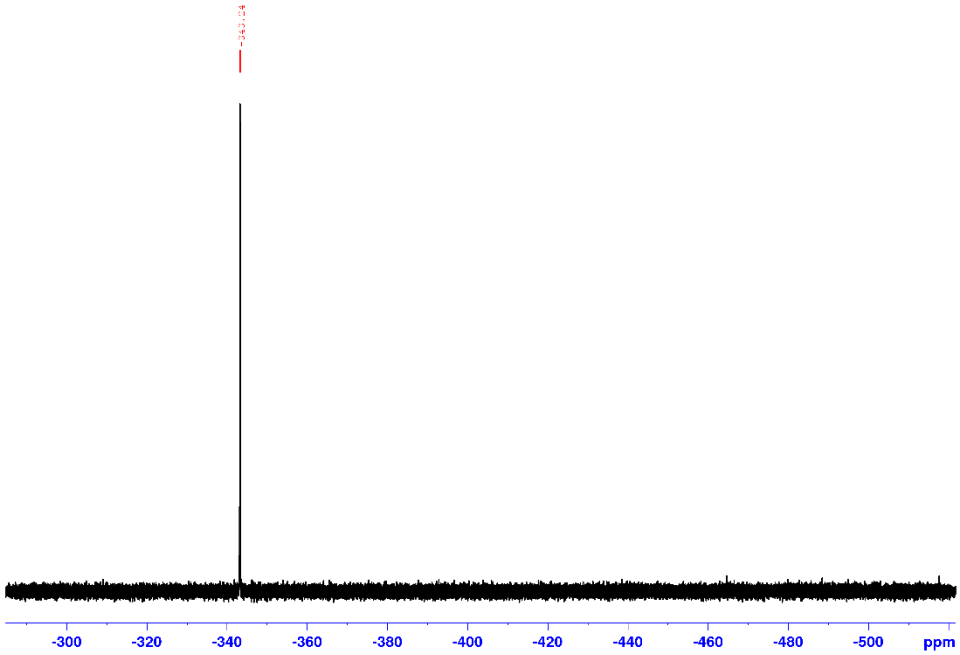

Figure E.13. ^{19}F NMR (386 MHz, C_6D_6) *in situ* of **6.2a** with DMAP. C_6F_6 external reference

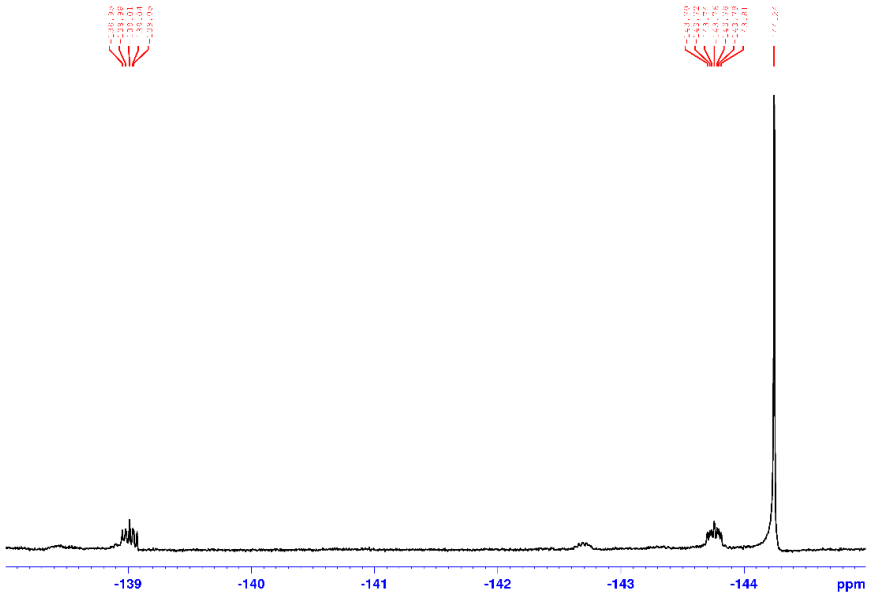

Figure E.14. ^{19}F NMR (386 MHz, C_6D_6) *in situ* of **6.2a** with DMAP and neopBPh after heating at 80 °C overnight. C_6F_6 external reference

References.

1. Chambers, R. D. *Fluorine in Organic Chemistry, 2nd Ed.,* Blackwell: Oxford, **2004**.
2. Kirsch, P. *Modern Fluoroorganic Chemistry: Synthesis, Reactivity, Applications,* Wiley-VCH: Weinheim, Germany, **2013**.
3. Midgley, T.; Henne, A. L. Organic Fluorides as Refrigerants. *Ind. Eng. Chem.*, **1930**, *22*, 542
4. Einecke, E. Fünfzig Jahre Chemie des Fluors. *Angew. Chem.*, **1937**, *50*, 859.
5. Renfre, M. M.; Lewis, E. E. Polytetrafluoroethylene. Heat Resistant, Chemically Inert Plastic. *Ind. Eng. Chem.*, **1946**, *38*, 870.
6. Banks, R. E.; Tatlow, J. C. Synthesis of C-F bonds: The Pioneering Years, 1835–1940. *J. Fluorine Chem.*, **1986**, *33*, 71.
7. Chambers, R. D. *Organofluorine Chemistry: Techniques and Synthons,* Springer-Verlag: Berlin Heidelberg, Germany, **1997**.
8. Hiyama, T. *Organofluorine Compounds: Chemistry and Applications*. H. Yamamoto (Ed.), Springer-Verlag: Berlin Heidelberg, Germany, **2000**
9. Okazoe, T. Overview on the History of Organofluorine Chemistry from the Viewpoint of Material Industry. *Proc. Jpn. Acad. Ser. B. Phys. Biol. Sci.*, **2009**, *85*, 276.
10. Fujiwara, T.; O'Hagan, D. Successful Fluorine-containing Herbicide Agrochemicals. *J. Fluorine Chem.*, **2014**, *167*, 16.
11. Ameduri, B.; Sawada, H. *Fluorinated Polymers: Volume 2: Applications*. Royal Society of Chemistry: Cambridge, UK, **2016**

12. Ameduri, B.; Sawada, H.; Masuda, T. *Fluorinated Polymers: Volume 1: Synthesis Properties Processing and Simulation*. Royal Society of Chemistry: Cambridge, UK, **2016**.
13. Gardiner, J. Fluoropolymers: Origin, Production, and Industrial and Commercial Applications. *Aust. J. Chem.*, **2015**, *68*, 13.
14. Surya Prakash, G. K.; Wang, F. Fluorine: The New Kingpin of Drug Discovery. *Chim. Oggi-Chem. Today*, **2012**, *30*, 30
15. Wang, J.; Sánchez-Roselló, M.; Aceña, J. L.; del Pozo, C.; Sorochinsky, A. E.; Fustero, S.; Soloshonok, V. A.; Liu, H. Fluorine in Pharmaceutical Industry: Fluorine-Containing Drugs Introduced to the Market in the Last Decade (2001-2011). *Chem. Rev.*, **2014**, *114*, 2432.
16. Gillis, E. P.; Eastman, K. J.; Hill, D. M.; Donelly, D. J.; Meanwell, N. A. Applications of Fluorine in Medicinal Chemistry. *J. Med. Chem.*, **2015**, *58*, 8315.
17. Reddy, V. P. *Organofluorine Compounds in Biology and Medicine*. Elsevier B.V.: Amsterdam: Netherlands, **2015.**
18. Böhm, H.-J.; Banner, D.; Bendels, S.; Kansy, M.; Kuhn, B.; Müller, K.; Obst-Sander, U.; Stahl, M. Fluorine in Medicinal Chemistry. *ChemBioChem*, **2004**, *5*, *637*.
19. Percy, J. M. Geminally-difluorinated Pharmaceutical Agents: Synthesis and Applications. *Chim. Oggi-Chem. Today*, **2004**, *22*, 18.
20. Bégué, J. P.; Bonnet-Delpon, D. Why Fluorine is an Invaluable Tool in Medicinal Chemistry. *Chim. Oggi-Chem. Today*, **2005**, *23*, III.
21. Banks, R. E. *Fluorine Chemistry at the Millenium: Fascinated by Fluorine*; Elsevier: Oxford, **2000**.

22. Dolbier Jr., W. R. Fluorine Chemistry at the Millennium. *J. Fluorine Chem.*, **2005**, *126*, 157.

23. Jäckel, C.; Koksch, B. Fluorine in Peptide Design and Protein Engineering. *Eur. J. Org. Chem.*, **2005**, 4483.

24. Pagliaro, M.; Ciriminna, R. New Fluorinated Functional Materials. *J. Mater. Chem.*, **2005**, *15*, 4981.

25. Isanbor, C.; O'hagan, D. Fluorine in Medicinal Chemistry: A Review of Anti-Cancer Agents. *J. Fluorine Chem.*, **2006**, *127*, 303.

26. Kirk, K. L. Selective Fluorination in Drug Design and Development: An Overview of Biochemical Rationales. *Curr. Top. Med. Chem.*, **2006**, *6*, 1447.

27. Thomas, C. J. Fluorinated Natural Products with Clinical Significance. *Curr. Top. Med. Chem.*, **2006**, *6*, 1529.

28. Dinoiu, V. Fluorine Chemistry: Past, Present and Future. *Rev. Roum. Chim.*, **2006**, *51*, 1141.

29. Tressaud, A. *Fluorine and the Environment: Agrochemicals, Archaeology, Green Chemistry & Water*. Elsevier B.V.: Amsterdam, Netherlands, **2006**.

30. Shah, P.; Westwell, A. D. The Role of Fluorine in Medicinal Chemistry. *J. Enzyme Inhib. Med. Chem.*, **2007**, *22*, 527.

31. Müller, K.; Faeh, C.; Diederich, F. Fluorine in Pharmaceuticals: Looking Beyond Intuition. *Science, 317*, 1881.

32. Jeschke, P. *The Unique Role of Halogen Substituents. In the Design of Modern Crop Protection Compounds*. W. Krämer, U. Schirmer (Eds.). Wiley-VCH: Weinheim, Germany, **2008.**

33. Hagmann, W. K. The Many Roles of Fluorine in Medicinal Chemistry. *J. Med. Chem.*, **2008**, *51*, 4359.
34. Ojima, I. *Fluorine in Medicinal Chemistry and Chemical Biology*. Wiley-VCH: Weinheim, Germany, **2009**.
35. Jeschke, P. The Unique Role of Halogen Substituents in the Design of Modern Agrochemicals. *Pest Manag. Sci.*, **2010**, *66*, 10.
36. L. Hunter, The C-F Bond as a Conformational Tool in Organic and Biological Chemistry. *Beilstein J. Org. Chem.*, **2010**, *6*, 38.
37. Vulpetti, A.; Dalvit, C. Fluorine Local Environment: From Screening to Drug Design. *Drug Discov. Today*, **2012**, *17*, 890.
38. Roesky, H. W. *Efficient Preparations of Fluorine Compounds*. Wiley-VCH: Weinheim, Germany, **2012**.
39. Prchalová, E.; Štěpánek, O.; Smrček, S.; Kotora, M. Medicinal Applications of Perfluoroalkylated Chain-containing Compounds. *Future Med. Chem.*, **2014**, *6*, 1201.
40. Champagne, P. A.; Desroches, J.; Hamel, J.-D.; Vandamme, M.; Paquin, J.-F. Monofluorination of Organic Compounds: 10 Years of Innovation. *Chem. Rev.*, **2015**, *115*, 9073.
41. Uneyama, K. *Organofluorine Chemistry*; Blackwell: Oxford, **2006**.
42. Horváth, I. T. *Fluorous Chemistry*; Springer: New York, **2011**.
43. Abraham, R. J.; Jones, A. D.; Warne, M. A.; Rittner, R.; Tormena, C. F. Conformational Analysis. Part 27. NMR, Solvation and Theoretical Investigation of Conformation Isomerism in Fluoro- and 1,1,-Difluoro-Acetone. *J. Chem. Soc., Perkin Trans.*, **1996**, 533.

44. Biffinger, J. C.; Kim, H. W.; DiMagno, S. G. The Polar Hydrophobicity of Fluorinated Compounds. *ChemBioChem*., **2004**, *5*, 622.
45. Carroll, T. X.; Thomas, T. D.; Bergersen H.; Børve, K. J.; Sæthre, L. J. Fluorine as a π Donor. Carbon 1s Photoelectron Spectroscopy and Proton Affinities of Fluorobenzenes. *J. Org. Chem.*, **2006**, *71*, 1961.
46. Goodman, L; Gu, H. B.; Pophristic, V. Gauche Effect in 1,2-Difluoroethane. Hyperconjugation, Bent Bonds, Steric Repulsion. *J. Phys. Chem. A*, **2015**, *109*, 1223.
47. Howard, J. A. K.; Hoy, V. J.; O'Hagan, D.; Smith, G. T. How Good is Fluorine as a Hydrogen Bond Acceptor? *Tetrahedron*, **1996**, *52*, 12613.
48. Wieberg, K. B.; Rablen, P. R. Origin of the Stability of Carbon Tetrafluoride: Negative Hyperconjugation Reexamined. *J. Am. Chem. Soc.*, **1993**, *115*, 614.
49. O'Hagan, D. Understanding Organofluorine Chemistry. An Introduction to the C-F Bond. *Chem. Soc. Rev.*, **2008**, *37*, 308.
50. F. Swarts, *Bulletins de l'Académie royale des sciences, des lettres et des beauxarts de Belgique*, **1892**, *24*, 456.

Fluorination Strategies

51. Booth, H. S.; Mong, W. L.; Burchfield, P. E. Fluorination of Hexachloroethane under Pressure. *Ind. Eng. Chem.*, **1932**, *24*, 328.
52. Rây, P. C. A New Method of Fluorination of Organic Compounds. *Nature*, **1933**, *132*, 173.
53. Bigelow, L. A.; Pearson, J. H. The Action of Elementary Fluorine Upon Aromatic Organic Compounds. II. The Fluorination of Hexachlorobenzene. *J. Am. Chem. Soc.*, **1934**, *56*, 2773.

54. Henne, A. L.; Hubbard, D. M. Fluorochloroethanes and Fluorochloroethylenes. III. *J. Am. Chem. Soc.*, **1936**, *58*, 404.

55. Henne, A. L.; Renoll, M. W. The Fluorination of Aliphatic Substances with Mercurous Fluoride. *J. Am. Chem. Soc.*, **1938**, *60*, 1060.

56. Henne, A. L.; Ladd, E. C. Fluorinated Derivatives of Propane. II. *J. Am. Chem. Soc.*, **1938**, *60*, 2491.

57. Simons, J. H.; Francis, H. T.; Hogg, J. A. The Electrolysis of Solutions of Organic Substances in Liquid Hydrogen Fluoride. *J. Electrochem. Soc.*, **1949**, *95*, 53.

58. Tewksbury, C. I.; Haendler, H. M. Metal Fluorides as Fluorinating Agents. *J. Am. Chem. Soc.*, **1949**, *71*, 2336.

59. Musgrave, W. K. R.; Smith, F. Organic Fluorides. Part I. Fluorination of Hydrocarbons. *J. Chem. Soc.*, **1949**, 3021.

60. Musgrave, W. K. R.; Smith, F. Organic Fluorides. Part II. The Effect of Metals on the Fluorination of Hydrocarbons. *J. Chem. Soc.*, **1949**, 3026.

61. Haszeldine, R. N.; Smith, F. Organic Fluoride. Part V. Fluorination of Hydrocarbons with Cobalt Trifluoride. *J. Chem. Soc.*, **1950**, 3617.

62. Miller, W. T.; Koch, S. D. The Mechanism of Fluorination. III. Fluorine Atom Reactions. The Olefin Dimerization Reaction. *J. Am. Chem. Soc.*, **1957**, *79*, 3084.

63. Fuller, G.; Stacey, M.; Tatlow, J. C.; Thomas, C. R. The Vapour Phase Fluorination of Trichloroethylene with Cobalt Trifluoride and with Manganese Trifluoride. *Tetrahedron*, **1962**, *18*, 123.

64. Stephens, R.; Tatlow, J. C. Fluorocarbon Chemistry. Part I. The Fluorination of Organic Compounds. *Q. Rev. Chem. Soc.*, **1962**, *16*, 44.

65. Maynard, J. T. The Synthesis of Highly Fluorinated Compounds by Use of Potassium Fluoride in Polar Solvents. *J. Org. Chem.*, **1963**, *28*, 112.

66. Nakagawa, S. Process for Manufacturing Trifluoroethylene, US3564064A, **1971**, Daikin Industries Ltd.

67. Sievert, A. C.; Process for the Manufacture of Hydrofluorocarbons, US5406008A, **1989**, E. I. du Pont de Nemours and Co.

68. Jackson, S. C.; Resnick, P. R.; Swearingen, S. H. Producing $CF_3CH_2CF_3$ and/or $CF_3CH{=}CF_2$ by the Conversion of Fluorinated Ethers. US5516946A.

69. Noelke, C. J.; Rao, V. N. M. Pyrolysis Process. US6958422B2, **2005**, Chemours Co FC LLC.

70. Mukhopadhyay, S.; Hsuehsung, T. Novel Catalytic Method for the Production of Fluoroalkylenes from Chlorofluorohydrocarbons. US20060217577A1, **2006**, Honeywell International Inc.

71. Van Der Puy, M.; Cook, G.; Scheidle, P.; Uhrich, K.; Wang, H.; Tung, H. S. Process for Manufacture of Fluorinated Olefins. US20070179324A1, **2009**, Honeywell International Inc.

72. Mukhopadhyay, S.; Tung, H.; Light, B.; Phillips, S.; Ma, J.; Bortz, C.; Van Der Puy, M.; Merkel D.; Bubey, R. Method for Producing Fluorinated Organic Compounds. US20070197842A1, **2011**, Honeywell International Inc.

73. Tirtowidjojo, M. M.; Au-Yeung, H.-S.; Chakraborty, D.; Eiffler, J.; Groenewald, H.; Hirsekorn, K. F.; Kokott, M.; Kruper, W. J. Jr.; Luebbe, T. U.; Meeman, H.; Sexton, S. S.; Wenzel, P.; Wobser, M. Processes for the Production of Hydrofluoroolefins. US8933280B2, **2015**, Blue Cube IP LLC.

74. Wedlinger, L. Method for Preparing Fluoroorganic Compounds. WO 2018/215418 A1, **2018**, Arkema France. PCT.
75. Okamoto, S.; Ueda, K., Kitamoto, T. Method for Producing Trans-1-Chloro-3,3,3-trifluoropropene. EP3404006 (A1), .**2018**, Central Glass Company, Limited.
76. Sharratt, A. Catalyst and Process Using the Catalyst. US20180318797, **2018**, Mexichem Amanco Holding S.A. de C.V.

Synthesis of Tetrafluoroethylene and Hexafluoropropylene

77. Ruff, O.; Die, O. Bildung von Hexafluoräthan und Tetrafluoräthylen aus Tetrafluorkohlenstoff *Bretschneider Zeitschrift fur anorganische und allgemeine Chemie*, **1933**, *21*, 173.
78. Downing, F. B.; Benning, A. F.; and McHarness, R. C. Octafluorocyclobutane and Pyrolytic Process for its Preparation, US2384821A, **1944**, Kinetic Chemicals Inc.
79. Park, J.; Benning, A. F.; Downing, F. B.; Laucius, J.; McHarness, R. C. Synthesis of Tetrafluoroethylene – Pyrolisis of Monochlorodifluoromethane. *Ind. Eng. Chem.*, **1947**, *39*, 354.
80. Forshey, W. O. Jr. Preparation of Tetrafluoroethylene, US2941012, **1960**, E. I. du Pont de Nemours and Co.
81. Barnes, J. J.; Kelch, K. P.; Sandbrook, T. D.; Van Bramer, D. J. Synthesis of Hexafluoropropene, US6924403B2, **2005**, E. I. du Pont de Nemours and Co.

Synthesis of Tetrafluoropropene

82. Mukhopadhyay, S.; Nair, H. K.; Tung, H.; Van Der Puy, M. Processes for Synthesis of Tetrafluoropropene. US7189884B2, **2004**, Honeywell International Inc.

83. Tung, H.; Johnson, R.; Merkel, D. Process for the Manufacture of 1,3,3,3-Tetrafluoropropene. US20050020862A1, **2009**, Honeywell International Inc.
84. Pigamo, A.; Deur-Bert, D.; Wendlinger, L. Catalytic Gas Phase Fluorination of 1230xa to 1234yf. US20110155942A1, **2012**, Arkema France.
85. Nappa, M. J.; Lousenberg, R. D., Jackson, A. Synthesis of 1234yf by Selective Dehydrochlorination of 244BB. US8263817B2, **2012**, E. I. du Pont de Nemours and Co.
86. Smith, J. W.; McGuiness, C. E.; Sharratt, A. P. Process for Preparing 2,3,3,3-Tetrafluoropropene (1234yf). US8536388B2, **2013**, Mexichem Amanco Holding SA de CV.
87. Deur-Bert, D.; Collier, B.; Wendlinger, L. Process for the Preparation of 2,3,3,3-Tetrafluoropropene. US20180327341, **2018**, Arkema France.

Organometallic Catalysis

88. Ertl, G.; Knozinger, H.; Schüth, F.; Weitkamp, J. *Handbook of Heterogeneous Catalysis, 2nd edition;* Wiley-VCH: Weinheim, Germany, **2008**.
89. Beller, M.; Renken, A.; van Santen, R. A., *Catalysis: From Principles to Applications*. Wiley-VCH: Weinheim, Germany, **2012**.
90. Ross, J. R. H. *Heterogeneous Catalysis*; Elsevier: Amsterdam, Netherlands, **2012**.
91. Hagen, J. *Industrial Catalysis: A Practical Approach, 2nd Ed.*; Wiley-VCH: Weinheim, Germany, **2005**.

M-F bond strength

92. Furuya, T.; Kamlet, A. S.; Ritter, T. Catalysis for Fluorination and Trifluoromethylation. *Nature*, **2011**, *473*, 470.

93. Murphy, E. F.; Murugavel, R.; Roesky, H. W. Organometallic Fluorides: Compounds Containing Carbon-Metal-Fluorine Fragments of d-Block Metals. *Chem. Rev.*, **1997**, *97*, 3425

Synthesis using I-R^F

94. Morrison, J. A. *Advances in Organometallic Chemistry: Trifluoromethyl-Containing Transition Metal Complexes, Volume 35*; Academic Press: Oxford, UK, **1993**.
95. Emeléus, H. J.; Haszeldine, R. N. Organometallic Fluorine Compounds. Part I. The Synthesis of Trifluoromethyl and Pentafluoroethyl Mercurials. *J. Chem. Soc.*, **1949**, 2948.
96. Emeléus, H. J.; Haszeldine, R. N. Organometallic Fluorine Compounds. Part II. The Synthesis of Bistrifluoromethylmercury. *J. Chem. Soc.*, **1949**, 2953.
97. King, R. B.; Stafford, S. L.; Treichel, P. M.; Stone, F. G. A. Chemistry of the Metal Carbonyls. XV. Fluorocarbon Derivatives of Iron Carbonyl. *J. Am. Chem. Soc.*, **1961**, *83*, 3604.
98. Mukhedkar, A. J.; Mukhedkar, V. A.; Green, M.; Stone, F. G. A. Reactions of Low-valent Metal Complexes with Fluorocarbons. Part XIII. (π-Cyclopentadienyl)bis(π-ethylene)rhodium. *J. Chem. Soc.*, **1970**, 3158.
99. McBride, D. W.; Dudek, E.; Stone, F. G. A. Chemistry of the Metal Carbonyls. Part XXV. Fluorocarbon Derivatives of Nickel. *J. Chem. Soc.*, **1964**, 1752.
100. Hughes, R. P.; Smith, J. M.; Liable-Sands, L. M.; Concolino, T. E.; Lam, K.-C.; Incarvito, C.; Rheingold, A. L. Syntheses and Crystallographic Studies of [Ir(η^5-C_5Me_5)(L)(R_F)I] (L = CO, PMe_3; R_F = CF_2CF_3, $CF_2CF_2CF_3$, $CF_2C_6F_5$, $CF(CF_3)_2$) Complexes. Cone and Solid Angle Steric Parameters for Perfluoroalkyl Ligands. *J. Chem. Soc., Dalton Trans.*, **2000**, 873.

101. Hughes, R. P.; Maddock, S. M.; Guzei, I. A.; Liable-Sands, L. M.; Rheingold, A. L. Reactions of Halofluorocarbons with Group 6 Complexes $M(C_5H_5)_2L$ (M = Mo, W; L = C_2H_4, CO). Fluoroalkylation at Molybdenum and Tungsten, and at Cyclopentadienyl or Ethylene Ligands. *J. Am. Chem. Soc.*, **2001**, *123*, 3279.

102. Bourgeois, C. J.; Hughes, R. P.; Husebo, T. L.; Smith, J. M.; Guzei, I. M.; Liable-Sands, L. M.; Zakharov, L. N.; Rheingold, A. L. Reaction of Perfluoroalkyl Iodides with $M(C_5H_5)(CO)(PMe_3)$ [M = Rh, Ir]; Evidence for Direct Fluoroalkylation at a CO Ligand. *Organometallics*, **2005**, *24*, 6431.

103. Yuan, J.; Hughes, R. P.; Rheingold, A. Synthesis and Crystallographic Characterization of Dimeric Perfluoroalkyl Iridium Complexes: $[Cp^*Ir(X)(R_F)]_2$ (X = I, R_F = CF_3, CF_2CF_3, $CF_2CF_2CF_3$, $CF(CF_3)_2$, $CF(CF_3)(CF_2CF_3)$; X = Cl and Br, R_F = CF_2CF_3), and a new Perfluoroethylidene complex $Cp^*Ir(PPh_3)(CFCF_3)$. *Inorg. Chim. Acta*, **2010**, *364*, 96.

104. Gil-Rubio, J.; Guerrero-Leal, J.; Blaya, M.; Vicente, J. Reactions of Half-Sandwich Ethene Complexes of Rhodium(I) toward Iodoperfluorocarbons: Perfluoro-alkylation or -arylation of Coordinated Ethene versus Oxidative Addition. *Organometallics*, **2012**, *31*, 1287.

Fluoroalkyl Radicals in Organic Synthesis

105. Dolbier, W. R. Structure, Reactivity, and Chemistry of Fluoroalkyl Radicals. *Chem. Rev.*, **1996**, *96*, 1557.

106. Brace, N. Syntheses with Perfluoroalkyl Radicals from Perfluoroalkyl Iodides. A Rapid Survey of Synthetic Possibilities with Emphasis on Practical Applications. Part One: Alkene, Alkynes and Allylic Compounds. *J. Fluorine Chem.*, **1999**, *93*, 1.

107. Furin, G. G. Some New Aspects in the Application of Perfluoroalkyl Halides in the Synthesis of Fluorine-Containing Organic Compounds. *Russ. Chem. Rev.*, **2000**, *69*, 491.

108. Brace, N. Syntheses with Perfluoroalkyl iodides. A Review. *J. Fluorine Chem.*, **2001**, *108*, 147.

109. Kino, T.; Nagase, Y.; Ohtsuka, Y.; Yamamoto, K.; Uraguchi, D.; Tokuhisa, K.; Yamakawa, T. Trifluoromethlation of Various Aromatic Compounds by CF_3I in the Presence of Fe(II) Compound, H_2O_2 and Dimethylsulfoxide. *J. Fluorine Chem.*, **2010**, *131*, 98.

110. Takagi, T.; Kanamori, T. Iridium-mediated Radical Addition of Perfluoroalkyl Iodide in Water. *J. Fluorine Chem.*, **2011**, *132*, 427.

111. Studer, A. A "Renaissance" in Radical Trifluoromethylation. *Angew. Chem. Int. Ed.*, **2012**, *51*, 8950.

112. Filippini, G.; Nappi, M.; Melchiorre, P. Photochemical Direct Perfluoroalkylation of Phenols. *Tetrahedron*, **2015**, *71*, 4535.

113. Lange, H.; Naumann, D. Perfluoroorganozink-verbindungen: Darstellung und Eigenschaften von $(R_F)_2Zn$-komplexen (R_F = CF_3, C_2F_5, C_3F_7, C_6F_5). *J. Fluorine Chem.*, **1984**, *26*, 435.

114. Kaplan, P. T.; Chen, B.; Vicic, D. A. Synthetic Utility of Dizinc Reagents Derived from 1,4-Diido- and 1,4-Dibromooctafluorobutane. *J. Fluorine Chem.*, **2014**, *168*, 158.

115. Aikawa, K.; Nakamura, Y.; Yokota, Y.; Toya, W.; Mikami, K. Stable but Reactive Perfluoroalkylzinc Reagents: Application in Ligand-Free Copper-Catalyzed Perfluoroalkylation of Aryl Iodides. *Chem. Eur. J.*, **2015**, *21*, 96.

116. Fujiu, M.; Hashimoto, R.; Nakamura, Y.; Aikawa, K.; Ito, S.; Mikami, K. Paradigm Shift from Alkaline (Earth) Metals to Early Transition Metals in Fluoroorganometal Chemistry: Perfluoroalkyl Titanocene(III) Reagents Prepared via Not Titanocene(II) but Titanocene(III) Species. *Chem. Eur. J.*, **2014**, *20*, 2382.

Decarbonylation Reactions

117. McClellan, W. R. Perfluoroalkyl and Perfluoroacyl Metal Carbonyls. *J. Am. Chem. Soc.*, **1961**, *83*, 1598.

118. King, R. B. Applications of Metal Carbonyl Anions in the Synthesis of Unusual Organometallic Compounds. *Acc. Chem. Res.*, **1970**, *3*, 417.

119. Brothers, P. J.; Roper, W. R. Transition-Metal Dihalocarbene Complexes. *Chem. Rev.*, **1998**, *88*, 1293.

120. Panthi, B. D.; Gipson, S. L.; Franken, A. Comparison of the Thermal and Reductive Decarbonylation of a Trifluoroacetyl Diphosphine Complex. *Organometallics*, **2010**, *29*, 5890.

121. Brothers, P. J.; Burrell, A. K.; Clark, G. R.; Rickard, C. E. F.; Roper, W. R. Trifluoromethyl, Difluorocarbene and Tetrafluoroethylene Complexes of Iridium and the Crystal Structures of $IrI(CH_3)(CF_3)(CO)(PPh_3)_2$, $Ir(CF_3)(C_2F_4)(CO)(PPh_3)_2$ and $Ir(CF_3)(=CF_2)(CO)(PPh_3)_2$. *J. Organomet. Chem.*, **1990**, *394*, 615.

122. Kubota, M.; Blake, D. M. Acyl, Alkyl, and Aryl Complexes of Iridium from Acid Chlorides. *J. Am. Chem. Soc.*, **1971**, *93*, 1368.

123. Deacon, G. B.; Faulks, S. J. Decarboxylation Synthesis of Transition Metal Organometallics. VI. Preparations of Polyfluorophenyliridium(I) compounds. *J. Organomet. Chem.*, **1992**, *437*, 239.

124. Maleckis, A.; Sanford, M. S. Catalytic Cycle for Palladium-Catalyzed Decarbonylative Trifluoromethylation using Trifluoroacetic Esters as the CF_3 Source. *Organometallics*, **2014**, *33*, 2653.

125. Hieber, V. W.; Beck, W.; Lindner, E. Trifluoracetyl- und Trifluormethyl-Metallcarbonyle. *Z. Naturforsch., B: Chem. Sci.*, **1961**, *16b*, 229.

126. Maleckis, A.; Sanford, M. S. Synthesis of Fluoroalkyl Palladium and Nickel Complexes via Decarbonylation of Acylmetal Species. *Organometallics*, **2014**, *33*, 3831.

127. Harrison, D. J,; Daniels, A. L.; Korobkov, I.; Baker, R. T. Tetracarbonyl(trifluoromethyl)cobalt(I) $[Co(CO)_4(CF_3)]$ as a Precursor to New Cobalt Trifluoromethyl and Difluorocarbene Complexes. *Organometallics*, **2015**, *34*, 4598.

Trifluoroacetate routes

128. Kiyohide, M.; Etsuko, T.; Midori, A.; Kiyosi, K. A Convenient Trifluoromethylation of Aromatic Halides with Sodium Trifluoroacetate. *Chem. Lett.*, **1981**, *10*, 1719.

129. Carrm G. E.; Chambers, R. D.; Holmes, T. F.; Parker, D. G. Sodium Perfluoroalkane Carboxylates as Sources of Perfluoroalkyl Groups. *J. Chem. Soc. Perkin Trans. I*, **1988**, 921.

130. Lin, X.; Hou, C.; Li, H.; Weng, Z. Decarboxylative Trifluoromethylating Reagent $[Cu(O_2CCF_3)(phen)]$ and Difluorocarbene Precursor $[Cu(phen)_2][O_2CCF_2Cl]$. *Chem. Eur. J.*, **2016**, *22*, 2075.

131. McReynolds, K. A.; Lewis, R. S.; Ackerman, L. K. G.; Dubinina, G. G.; Brennessel, W. W.; Vicic, D. A. Decarboxylative Trifluoromethlation of Aryl Halides using Well-defined Copper-trifluoroacetate and -chlorodifluoroacetate Precursors. *J. Fluorine Chem.*, **2010**, *131*, 1108.

Reactions with $TMSCF_3$

132. Ruppert, I.; Schlich, K.; Volbach, W. Fluorinated Organometallic Compounds. XVIII. First Trifluoromethyl-substituted Organyl(chloro)silanes. *Tetrahedron Lett.*, **1984**, *25*, 2195.

133. Prakash, G. K. S.; Yudin, A. K. Perfluoroalkylation with Organosilicon Reagents. *Chem. Rev.*, **1997**, *97*, 757

134. Liu, X.; Xu, C.; Wang, M.; Liu, Q. Trifluoromethyltrimethylsilane: Nucleophilic Trifluoromethylation and Beyond. *Chem. Rev.*, **2015**, *115*, 683.

135. Barrata-Vallejo, S.; Bonesi, S. M.; Postigo, A. Perfluoroalkylation Reactions of (Hetero)arenes. *RSC Advances*, **2015**, *5*, 62498.

136. Beier, P.; Zibinsky, M.; Prakash, G. K. S. Nucleophilic Additions of Perfluoroalkyl Groups. In Organic Reactions. Wiley-VCH: Weinheim, Germany, **2009**.

137. Prakash, G. K. S.; Zhang, Z. New Nucleophilic Fluoroalkylations. In Modern Synthesis Processes and Reactivity of Fluorinated Compounds: Progress in Fluorine Science. Elsevier B.V.: Amsterdam: Netherlands, **2017**.

138. Ono, T. Synthesis of Highly Branched Perfluoroolefins that are Super-Congested via Multi-Substitution of Trifluoromethyl Groups: Trifluoromethylation of Hexafluoropropene Trimers with Ruppert-Prakash Reagent. *J. Fluorine Chem.*, **2017**, *196*, 128.

139. Krishnamoorthy, S.; Kar, S.; Korthandaraman, J.; Prakash, G. K. S. Nucleophilic Difluoromethylation of Aromatic Aldehydes using Trimethyl(trifluoromethyl)silane ($TMSCF_3$). *J. Fluorine Chem.*, **2018**, *208*, 10.

140. Zhang, C. Advances in Trifluoromethylation or Trifluoromethylthiolation with Copper CF_3 or SCF_3 Complexes. *J. Chem. Sci.*, **2017**, *129*, 1795.

141. Li, M.; Zheng, H.; Xue, X.-S.; Cheng, J.-P. Ordering the Relative Power of Electrophilic Fluorinating, Trifluoromethylating, and Trifluoromethylthiolating Reagents: A Summary of Recent Efforts. *Tetrahedron Lett.*, **2018**, *59*, 1278.

142. Lishchynskyi, A.; Miloserdov, F. M.; Martin, E.; Benet-Buchholz, J.; Escudero-Adán, E. C.; Konovalov, A. I.; Grushin, V. V. The Trifluoromethyl Anion. *Angew. Chem. Int. Ed.*, **2015**, *54*, 15289.

143. Miloserdov, F.; Konovalov, A. I.; Martin, E.; Benet-Buchholz, J.; Escudero-Adán, E. C.; Lishchynskyi, A.; Grushin, V. V. The Trifluoromethyl Anion: Evidence for $[K(crypt\text{-}222)]^+ CF_3^-$. *Helv. Chim. Acta*, **2017**, *100*, e1700032.

144. Tyra, W. E. Oxidative Perfluoroorganylation Methods in Group 12-13 Chemistry: The Reactions of Haloperfluoroorganics and In and InBr, A Convenient New Route to AgR_f (R_f = CF_3, C_6F_5) and Reactions of AgR_f With Group 12-16 Elements. *J. Fluorine Chem.*, **2001**, *112*, 149.

145. Tyrra, W. E. Silver(I) Fluoride and Related Compounds in Chemical Synthesis. *Heteroat. Chem.*, **2002**, *13*, 561.

146. Kremlev, M. M.; Mushta, A. I.; Tyrra, W. E.; Naumann, D.; Fischer, H. T. M.; Yagupolskii, Y. L. Silver Compounds in Synthetic Chemistry Part 5: Selective Syntheses

of Trifluoromethylketones, $RCOCF_3$, from Fluoromethylsilver, $AgCF_3$, and Corresponding Acyl Chlorides, RCOCl. *J. Fluorine Chem.*, **2007**, *128*, 1385.

147. Dubinina, G. G.; Furutachi, H.; Vicic, D. A. Active Trifluoromethylating Agents from Well-Defined Copper(I)-CF_3 Complexes. *J. Am. Chem. Soc.*, **2008**, *130*, 8600.

148. Tomashenko, O. A.; Escudero-Adán, E. C.; Belmonte, M. M.; Grushin, V. V. Simple, Stable, and Easily Accesible Well-Defined $CuCF_3$ Aromatic Trifluoromethylating Agent. *Angew. Chem. Int. Ed.*, **2011**, *50*, 7655.

149. Lee, G.; Korobkov, I.; Baker, R. T. d^8 Nickel and Palladium Difluorocarbenes Derived from Trifluoromethyl POCOP-type Pincer Complexes. *J. Organomet. Chem.*, **2017**, *847*, 270.

150. Taw, F. L.; Clark, A. E.; Mueller, A. H.; Janicke, M. T.; Cantat, T.; Scott, B. L., Hay, P. J.; Hughes, R. P.; Kiplinger, J. L. Titanium(IV) Trifluoromethyl Complexes: New Perspectives on Bonding from Organometallic Fluorocarbon Chemistry. *Organometallics*, **2012**, *31*, 1484.

151. Huang, D.; Caulton, K. G. New Entries to and New Reactions of Fluorocarbon Ligands. *J. Am. Chem. Soc.*, **1997**, *119*, 3185.

152. Huang, D.; Koren, P. R.; Folting, K.; Davidson, E. R.; Caulton, K. G. Facile and Reversible Cleavage of C-F Bonds. Contrasting Thermodynamic Selectivity for Ru-CF_2H vs F-Os=CFH. *J. Am. Chem. Soc.*, **2000**, *122*, 8916.

153. Vicente, J.; Gil-Rubio, J.; Bautista, D. Synthesis and Reactivity of Fluoro Complexes. Part 1. Cyclooctadiene Rhodium(I) Complexes. *Inorg. Chem.*, **2001**, *40*, 2636.

154. Vicente, J.; Gil-Rubio, J.; Guerrero-Leal, J.; Bautista, D. Synthesis of the First Family of Rhodium(I) Perfluoroalkyl Complexes from Rhodium(I) Fluoro Complexes. *Organometallics*, **2004**, *23*, 4871.

155. Grushin, V. V.; Marshall, W. J. Facile Ar-CF_3 Bond Formation at Pd. Strikingly Different Outcomes of Reductive Elimination from $[(Ph_3P)_2Pd(CF_3)Ph]$ and [(Xanthphos)Pd(CF_3)Ph]. *J. Am. Chem. Soc.*, **2006**, *128*, 12644.

156. Naumann, D.; Kirij, N. V.; Maggiarosa, N.; Tyrra, W.; Yagupolskii, Y. L.; Wickleder, M. S. Synthesen und Charakterisierungen der ersten Tris- und Tetrakis(trifluormethyl)palladate(II) und -platinate(II), $[M(CF_3)_3(PPh_3)]^-$ und $[M(CF_3)_4]^{2-}$ (M = Pd, Pt). *Z. Anorg. Allg. Chem.*, **2004**, *630*, 746.

157. Menjón, B.; Martínez-Salvador, S.; Gómez-Saso, M. A.; Forniés, J.; Falvello, L. R.; Martín, A.; Tsipis, A. Oxidative Addition of Halogens to Homoleptic Perfluoromethyl or Perfluorophenyl Derivatives of Platinum(II): A Comparative Study. *Chem. Eur. J.*, **2009**, *15*, 6371.

158. Zopes, D.; Kremer, S.; Scherer, H.; Belkoura, L.; Pantenburg, I.; Tyrra, W.; Mathur, S. Hydrolytic Decomposition of Tetramethylammonium Bis(trifluoromethyl)aurate(I), $[NMe_4][Au(CF_3)_2]$: A Route for the Synthesis of Gold Nanoparticles in Aqueous Medium. *Eur. J. Inorg. Chem.*, **2011**, 273.

159. Leclerc, M. C.; Bayne, J. C.; Lee, G. M.; Gorelsky, S. I.; Vasiliu, M.; Korobkov, I.; Harrison, D. J.; Dixon, D. A.; Baker, R. T. Perfluoroalkyl Cobalt(III) Fluoride and Bis(perfluoroalkyl) Complexes: Catalytic Fluorination and Selective Difluorocarbene Formation. *J. Am. Chem. Soc.*, **2015**, *137*, 16064.

160. Popov, I.; Lindeman, S.; Daugulis, O. Copper-Catalyzed Arylation of 1*H*-Perfluoroalkanes. *J. Am. Chem. Soc.*, **2011**, *133*, 9286.

161. Zanardi, A.; Novikov, M. A.; Martin, E.; Benet-Buchholz, J.; Grushin, V. V. Direct Cupration of Fluoroform, *J. Am. Chem. Soc.*, **2011**, *133*, 20901.

162. Lishchynskyi, A.; Grushin, V. V. Cupration of C_2F_2H: Isolation, Structure, and Synthetic Applications of $[K(DMF)_2][(t\text{-BuO})Cu(C_2F_5)]$. Highly Efficient Pentafluoroethylation of Unactivated Aryl Bromides. *J. Am. Chem. Soc.*, **2013**, *135*, 12584.

163. Novák, P.; Lishchynskyi, A.; Grushin, V. V. Fluoroform-Derived $CuCF_3$ for Low-Cost, Simple, Efficient, and Sage Trifluoromethylation of Aryl Boronic Acids in Air. *Angew. Chem. Int. Ed.*, **2012**, *51*, 7767.

164. Luo, G.; Qu, J. Direct Nucleophilic Trifluoromethylation using Fluoroform: A Theoretical Mechanistic Investigation and Insight into the Effect of Alkali Metal Cations. *New. J. Chem.*, **2013**, *37*, 3274.

165. Konovalov, A. I.; Benet-Buchholz, J.; Martin, E., Grushin, V. V. The Critical Effect of the Countercation in the Direct Cupration of Fluoroform with $[Cu(OR)_2]^-$. *Angew. Chem. Int. Ed.*, **2013**, *52*, 11628.

166. Miloserdov, F. M.; Grushin, V. V. Alcoholysis of Fluoroform. *J. Fluorine Chem.*, **2014**, *167*, 105.

Using M-CF3

167. Treichel, P. M.; Stone, F. G. A. Fluorocarbon Derivatives of Metals. *Adv. Organomet. Chem.*, **1964**, *1*, 143.

168. Morrison, J. A.; Gerchman, L. L.; Eujen, R.; Lagow, R. J. Ligand Exchange Reactions of Bis(trifluoromethyl)mercury; The Preparation of $(CF_3)_4Ge$ and $(CF_3)_2SnBr_2$ from $(CF_3)_2Hg$. *J. Fluorine Chem.*, **1977**, *10*, 333.

169. Lagow, R. J.; Morrison, J. A. New Methods for the Synthesis of Trifluoromethyl Organometallic Compounds. *Adv. Inorg. Chem. Radiochem.*, **1983**, *27*, 293.

170. Krause, L. J.; Morrison, J. A. Formation and Reactions of the (Trifluoromethyl)tin Bromides CF_3SnBr_3 and $(CF_3)_2SnBr_2$. *Inorg. Chem.*, **1980**, *19*, 604.

171. Krause, L. J.; Morrison, J. A. Trifluoromethyl Group 2B Compounds: Bis(trifluoromethyl)cadmium*Base. New, More Powerful Ligand-Exchange Reagents and Low-Temperature Difluorocarbene Sources. *J. Am. Chem. Soc.*, **1981**, *103*, 2995.

172. Zissis, J.-P.; Moreau, P.; Commeyras, A. Synthese et Reactivite d'Organomagnesiens Perfluoroes. V. Synthese et Identification de Nouveaux Composes Perfluoroalkyles du Mercure a Chaine Longue. *J. Fluorine Chem.*, **1981**, *19*, 71.

173. Nair, H. K.; Morrison, J. A. Formation of Group 11 Trifluoromethyl Derivatives by Reaction of $Cd(CF_3)_2$·glyme with Representative Au, Ag, and Cu Complexes: Isolation of $Au(CF_3)_3(PMe_3)$. $Au(CF_3)_3(PEt_3)$, $AuI(CF_3)_2(PMe_3)$, $AuCF_3(PMe_3)$, $AuCF_3(PEt_3)$ and $AgCF_3(PMe_3)$; Observation of $CuCF_3(PMe_3)$. *J. Organomet. Chem.*, **1989**, *376*, 149.

174. Ontiveros, C. D.; Morrison, J. A.; Hani, R.; Geanangel, R. A. *Bis(trifluoromethyl)cadmium·1,2-dimethoxyethane. In Inorganic Syntheses, Volume 24*. J. M. Shreeve (Ed.). Wiley-VCH: Weinheim, Germany, **1986**.

175. Tyrra, W. E.; Naumann, D. Perfluoroorganosilver(I) Compounds. *J. Fluorine. Chem.*, **2004**, *125*, 823.

176. Naumann, D.; Roy, T.; Caeners, B.; Hütten, D.; Tebbe, K.-F.; Gilles, T. Synthesen und Eigenschaften von Pentafluoroethylkupfer(I)- und –(III)-Verbindungen: $Cu(C_2F_5)\cdot D$, $[Cu(C_2F_5)_2]^-$ und $(C_2F_5)_2CuSC(S)N(C_2H_5)_2$. *Z. Anorg. Allg. Chem*., **2000**, *626*, 999.

177. Naumann, D.; Wessel, W.; Hahn, J.; Tyrra, W. Darstellung, NMR-spektroskopische Charakterisierung und Reaktionen von Perfluoralkylsilber(I)-verbindungen. *J. Organomet. Chem.*, **1997**, *547*, 79.

178. Loizou, D. C.; Castillo, J.; Oki, A. R.; Hosmane, N. S.; Morrison, J. A. Synthesis of Cyclopentadienyldinitrosyl(trifluoromethyl)chromium(0), $CpCr(NO)_2CF_3$, and cyclopentadienyldinitrosyl(trifluoromethyl)molybdenum(0), $CpMo(NO)_2CF_3$. Crystal structure of $CpCr(NO)_2CF_3$. *Organometallics*, **1992**, *11*, 4189.

Transmetallation

179. Aikawa, K.; Nakamura, Y.; Yokota, Y.; Toya, W. Mikami, K. Stable but Reactive Perfluoroalkylzinc Reagents: Application in Ligand-Free Copper Catalyzed Perfluoroalkylation of Aryl Iodides. *Chem. Eur. J.*, **2015**, *21*, 96.

180. Serizawa, H.; Ishii, K.; Aikawa, K.; Mikami, K. Copper-Catalyzed Difluoromethylation of Aryl Iodides with (Difluoromethyl)zinc Reagent. *Org. Lett.*, **2016**, *18*, 3686.

181. Xu, L.; Vicic, D. Direct Difluoromethylation of Aryl Halides via Base Metal Catalysis at Room Temperature. *J. Am. Chem. Soc.*, **2016**, *138*, 2536.

182. Gu, Y.; Chang, D.; Leng, X.; Gu, Y.; Shen, Q. Well-Defined, Shelf-Stable (NHC)Ag(CF_2H) Complexes for Difluoromethylation. *Organometallics*, **2015**, *34*, 3065.

183. Liu, S.; Kang, K.; Liu, S.; Wang, D.; Wei, P.; Lan. Y.; Shen, Q. The Difluoromethylated Organogold(III) Complex *cis*-[Au(PCy_3)(4-F-C_6H_4)(CF_2H)(Cl)]: Preparation, Characterization, and Its C(sp^2)-CF_2H Reductive Elimination. *Organometallics*, **2018**, *37*, 3901.

184. Lu, C.; Lu, H.; Wu, J.; Shen, H. C.; Hu, T.; Gu, Y.; Shen, Q. Palladium-Catalyzed Difluoromethylation of Aryl Chlorides and Triflates and Its Applications in the Preparation of Difluoromethylated Derivatives of Drug/Agrochemical Molecules. *J. Org. Chem.*, **2018**, *83*, 1077.

Metallacycle

185. Baker, R. T.; Beatty, R. P.; Farnham, W. B.; Wallace, R. L. Jr. EP 0783472A1, **1997**, E. I. du Pont de Nemours & Co., USA.

186. Browning, J.; Cundy, C. S.; Green, M.; Stone, F. G. A. Hexafluoroacetone and Hexafluorothioacetone Nickel Complexes. *J. Chem. Soc. (A)*, **1969**, 20.

187. Manuel, T. A.; Stafford, S. L.; Stone, F. G. A. Chemistry of the Metal Carbonyls. VII. Perfluoroalkyl Iron Compounds. *J. Am. Chem. Soc.*, **1961**, *83*, 249.

188. Coyle, T. D.; King, R. B.; Pitcher, E.; Stafford, S. L.; Treichel, P. M.; Stone, F. G. A. A Novel Heterocyclic Cobalt compound. *J. Inorg. Nucl. Chem.*, **1961**, *20*, 172.

189. Green, M.; Osborn, R. B. L.; Rest, A. J.; Stone, F. G. A. Perfluoro-allenyl and Butadienyl Transition Metal Complexes. *Chem. Commun. (London)*, **1966**, 755.

190. Green, M.; Osborn, R. B. L.; Rest, A. J.; Stone, F. G. A. Fluorocarbon Platinum Complexes. *Chem. Commun. (London)*, **1966**, 502.

191. Green, M.; Osborn, R. B. L.; Rest, A. J.; Stone, F. G. A. Fluorocarbon Platinum Complexes. *J. Chem. Soc. A*, **1968**, 2525.

192. Cundy, C. S.; Green, M.; Stone, F. G. A. Reaction of Low-valent Metal Complexes with Fluorocarbons. Part XII. Fluoro-olefin Reactions of Zerovalent Nickel Complexes. *J. Chem. Soc. (A)*, **1970**, 1647.

193. Mukhedar, A. J.; Mukhedar, V. A.; Green, M.; Stone, F. G. A. Reactions of Low-valent Metal Complexes with Fluorocarbons. Part XV. Acetylacetonatobis(Methyldiphenyl- or triphenylphosphine) Rhodium. *J. Chem. Soc. (A)*, **1970**, *3166.*

194. Green, M.; Shakshooki, S. K.; Stone, F. G. A. Reactions of Low-valent Metals with Fluorocarbons. Part XVIII. t-Butyl Isocyanide-nickel Complexes. *J. Chem. Soc. (A)*, **1971**, 2828.

195. Browning, J.; Green, M.; Stone, F. G. A Reactions of Low-valent Metal Complexes with Fluorocarbons. Part XVII. Tertiary Arsine-nickel Complexes. *J. Chem Soc. (A)*, **1971**, 453.

196. Stone, F. G. A The role of Fluorocarbons in Oxidative-addition and -elimination Reactions. *Pure Appl. Chem.*, **1972**, *30*, 551.

197. Browning, J.; Empsall, H. D.; Green, M.; Stone, F. G. A. Reactions of Low-valent Metal Complexes with Fluorocarbons. Part XXV. Phosphine, phosphite and cyclo-octa-1,5-diene Platinum Complexes. *J. Chem. Soc., Dalton Trans.*, **1973**, 381.

198. Stone, F. G. A. Synthetic Applications of d^{10} Metal Complexes. *J. Organomet. Chem.*, **1975**, *100*, 257.

199. Xu, W.; Sun, H.; Xiong, Z.; Li, X. Acid Promoted Selective Carbon-Fluorine Bond Activation and Functionalization of Hexafluoropropene by Nickel Complexes Supported with Phosphine Ligands. *Organometallics*, **2013**, *32*, 7122.

200. Ohashi, M.; Shibata, M.; Ogoshi, S. Regioselective C-F Bond Activation of Hexafluoropropylene on Palladium(0): Formation of a Cationic η^2-Perfluoroallylpalladium Complex. *Angew. Chem. Int. Ed.*, **2014**, *53*, 13578.

201. Green, M.; Laguna, A.; Spencer, J. L.; Stone, F. G. A. Reactions of Low-valent Metal Complexes with Fluorocarbons. Part 31. Bis(η-cyclo-octa-1,5-diene)-platinum and -palladium, with Fluoroolefins. *J. Chem. Soc., Dalton Trans.* **1977**, 1010.

202. Stone, F. G. A. Fluorocarbon Metal Compounds – Role Models in Organotransition Metal Chemistry. *J. Fluorine Chem.*, **1999**, *100*, 227.

203. Giffin, K. A.; Harrison, D. J.; Korobkov, I.; Baker, R. T. Activation of C-F and Ni-C Bonds of [P,S]-ligated Nickel Perfluorometallacycles. *Organometallics*, **2013**, *32*, 7424.

204. Giffin, K. A.; Korobkov, I.; Baker, R. T. Brønsted Acid-promoted C-F Bond Activation in [P,S]-ligated Neutral and Anionic Perfluoronickelacyclopentanes. *Dalton Trans.*, **2015**, *44*, 19587.

205. Ohashi, M.; Shibata, M.; Saijo, H.; Kambara, T.; Ogoshi, S. Carbon-Fluorine Bond Activation of Tetrafluoroethylene on Palladium(0) and Nickel(0): Heat or Lewis Acidic Additive Promoted Oxidative Addition. *Organometallics*, **2013**, *32*, 3631.

206. Sicard, A. J. Organometallic Manipulations of Fluoroolefins Mediated or Catalyzed by Low-Coordinate Nickel. MSc Thesis, University of Ottawa, **2016**.

207. Giffin, K. A.; Pua, L. A.; Piotrkowski, S.; Gabidullin, B. M.; Korobkov, I.; Hughes, R. P.; Baker, R. T. Generation of Hydrofluoronickelacycles from Trifluoroethylene and Ni(0): Ligand Effects on Regio-/Stereoselectivity and Reactivity. *J. Am. Chem. Soc.*, **2017**, *139*, 4075.

208. Kaschube, W.; Schröder, W.; Pörschke, K. R.; Angermund, K.; Krüger, C. Amin-Nickel Komplexe VI. Syntheses, Struktur und Reaktivität von (tmeda)Ni(C_2F_4). *J. Organomet. Chem.*, **1990**, *389*, 399.

209. Schröder, W.; Bonrath, W.; Pörschke, K. R. Synthese und Reactivität von (2,6-$^{i}Pr_2$Ph-dad)Ni(C_2F_4). *J. Organomet. Chem.*, **1991**, *408*, C25

210. Ohashi, M.; Kawashima, T.; Taniguchi, T.; Kikushima, K.; Ogoshi, S. 2,2,3,3-Tetrafluoronickelacyclopentanes Generated via the Oxidative Cyclization of Tetrafluoroethylene and Simple Alkenes: A Key Intermediate in Nickel-Catalyzed C-C Bond Forming Reactions. *Organometallics*, **2015**, *34*, 1604.

211. Hacker, M. J.; Littlecot, G. W.; Kemmitt, R. D. W. Reactions of Fluoro-olefins, Chloro-olefins and Related Molecules with Carbonatobis(triphenylarsine)platinum(II) in Ethanol. *J. Organomet. Chem.*, **1973**, 189.

212. Booth, B. L.; Casey, G.; Haszeldine, R. N. Reactions Involving Transition Metals: XII. Some Attempts to Prepare Alkylidynetrirhodium Cluster Compounds. *J. Organomet. Chem.*, **1981**, *219*, 401.

213. Barnes, N. A.; Brisdon, A. K.; Ellis, M. J.; Pritchard, R. G. Recent Advances in Fluorovinyl-containing Compounds. *J. Fluorine Chem.* **2001**, *112*, 35.

214. Anderson, D. J.; Mcdonald, R.; Cowie, M. Carbon-Fluorine Bond Activation in Fluoroolefins: Clear Documentation of Cooperative C-F Bond Activation by Adjacent Metal Centers. *Angew. Chem. Int. Ed.*, **2007**, *46*, 3741.

215. Ohashi, M.; Ogoshi. S. Catalytic Transformations of Fluorinated Olefins. *Topics in Organomet. Chem.*, **2015**, *52*, 197.

216. Ohashi, M.; Kambara, T.; Hatanaka, T.; Saijo, H.; Doi, R.; Ogoshi, S. Palladium-Catalyzed Coupling Reactions of Tetrafluoroethylene with Arylzinc Compounds, *J. Am. Chem. Soc.*, **2011**, *133*, 3256.

217. Jolly, P.; Stone, F. G. A. Reactions of Fluorinated Olefins with Metal Carbonyl Anions. *Chem. Commun. (London)*, **1965**, 85.

218. Jolly, P.; Bruce, M. I.; Stone, F. G. A. Chemistry of Metal Carbonyls. XXXI. Reactions Between some Fluoro Olefins and Carbonyl Metal Anions. *J. Chem. Soc.*, **1965**, 5830.

219. Banger, K. K.; Brisdon, A. K.; Gupta, A. Perfluorovinyl-metal Derivatives: A New One-pot Synthesis. *Chem. Commun.*, **1997**, 139.

220. Banger, K. K.; Brisdon, A. K.; Brain, P. T.; Parsons, S.; Rankin, D. W. H.; Robertson, H. E.; Smart, B. A.; Bühl, M. Experimental and Theoretical Studies of Bis(perfluorovinyl)mercury, $Hg(CF=CF_2)_2$: Synthesis, Characterization, and Structure in the Gaseous and Crystalline Phases. *Inorg. Chem*., **1999**, *38*, 5894.

221. Clark, H. C.; Tsang, W. S. Chemistry of Metal Hydrides. I. Reactions of some Platinum(II) Hydrides. *J. Am. Chem. Soc.*, **1967**, *89*, 529.

222. Clark, H. C.; Tsang, W. S. Chemistry of Metal Hydrides. II. Spectroscopic Studies of Fluorovinylplatinum(II) Derivatives. *J. Am Chem. Soc.*, **1967**, *89*, 533.

223. Green, M. L. H.; Stear, A. N. Fluorocarbon Complexes of Iron, *Z. Naturforsch.*, **1965**, *20b*, 812.

224. Wilford, J. B.; Stone, F. G. A. Chemistry of the Metal Carbonyls. XXVIII. Addition of Rhenium Pentacarbonyl Hydride to Fluoroolefins, *Inorg. Chem.*, **1965**, *4*, 93.

225. Wilford, J. B.; Forster, A.; Stone, F. G. A. Chemistry of the Metal Carbonyls. XXXIII. Synthesis of σ-Tetrafluoroethylcobalt Tetracarbonyl, and Related Reactions. *J. Chem. Soc.*, **1965**, 6519.

226. Miller, W. T. Jr.; Burnard, R. J. Perfluoroalkylsilver Compounds. *J. Am. Chem. Soc.*, **1968**, *90*, 7367.

227. Saijo, M.; Ohashi, M.; Ogoshi, S. Fluoroalkylcopper(I) Complexes Generated by the Carbocupration of Tetrafluoroethylene: Construction of a Tetrafluoroethylene-Bridging Structure. *J. Am. Chem. Soc.*, **2014**, *136*, 15158.

228. Kikushima, K.; Sakaguchi, H.; Saijo, M.; Ohashi, M.; Ogoshi, S. Copper-Mediatd One-Pot Synthesis of Trifluorostyrene Derivatives from Tetrafluoroethylene and Arylboronate. *Chem. Lett.*, **2015**, *44*, 1019.

229. Li, L.; Ni, C.; Xie, Q.; Hu, M.; Wang, F.; Hu, J. $TMSCF_3$ as a Convenient Source of CF_2=CF_2 for Pentafluoroethylation, (Aryloxy)tetrafluoroethylation, and Tetrafluoroethylation. *Angew. Chem. Int. Ed.* **2017**, *56*, 9971.

230. Ohashi, M.; Ishida, N.; Ando, K.; Hashimoto, Y.; Shigaki, A.; Kikushima, K.; Ogoshi, S. CuI-Catalyzed Pentafluoroethylation of Aryl Iodides in the Presence of Tetrafluoroethylene and Cesium Fluoride: Determining the Route to the Key Pentafluoroethyl CuI Intermediate. *Chem. Eur. J.*, **2018**, *24*, 9794.

231. Kelter, P. B.; Mosher, M. D.; Scott, A.; *Chemistry: The Practical Science*, Volume 10; Cengage Learning: New York, 2008.

232. Calderazzo, F. Synthetische und Mechanistische Aspekte Anorganischer Insertionsreaktionen. Insertion von Kohlenmonoxid. *Angew. Chem.*, **1977**, *89*, 305.

233. Hughes, R. P. Organo-Transition Metal Compounds Containing Perfluorinated Ligands. *Adv. Organomet. Chem.*, **1990**, *31*, 183.

234. Grubbs, R. H.; Miyashita, A.; Liu, M.; Burk, P. Preparation and Reactions of Phosphine Nickelacyclopentanes. *J. Am. Chem. Soc.*, **1978**, *100*, 2418.

235. Bennett, M. A.; Glewis, M.; Hockless, D. C.; Wenger, E. Successive Insertion of Tetrafluoroethylene and CO and of Tetrafluoroethylene and Acetylenes into Aryne-nickel(0)bonds. *J. Chem. Soc., Dalton Trans.*, **1997**, 3105.

236. King, R. B.; Bisnette, M. B. Organometallic Chemistry of the Transition Metals XXI. Some π-Pentamethylcyclopentadienyl Derivatives of Various Transition Metals. *J. Organomet. Chem.*, **1967**, *8*, 287.

237. Cotton, F. A.; Wing, R. M. Vibrational Spectra and Bonding in Metal Carbonyls VI. Evidence for a π-Interaction Between Manganese Pentacarbonyl and the Perfluoromethyl group. *J. Organomet. Chem.*, **1967**, *9*, 511.

238. Graham, W. A. G. Approach to the Separation of Inductive and Mesomeric Effects in Complexes of the Types $LMn(CO)_5$ and $LMo(CO)_5$. *Inorg. Chem.*, **1968**, *7*, 315.

239. Hall, M. B.; Fenske, R. F. Electronic Structure and Bonding in Methyl- and Perfluoromethyl(pentacarbonyl)manganese. *Inorg. Chem*, **1972**, *11*, 768.

240. Algarra, A. G.; Grushin, V. V.; Macgregor, S. A. Natural Bond orbital Analysis of the Electronic Structure of $[LnM(CH_3)]$ and $[Ln(M(CF_3)]$ Complexes. *Organometallics*, **2012**, *31*, 1467.

Metal Trifluoromethyl Complexes

241. King, R. B., Bisnette, M. B. Preparation and Decarboxylation of Acyl Derivatives of Cyclopentadienyl Metal Carbonyls. *J. Organomet. Chem.*, **1964**, *2*, 15.

242. Reger, D. L.; Dukes, M. D. Molybdenum Perfluorocarbene Complexes. *J. Organomet. Chem.*, **1978**, *153*, 67.

243. Richmond, T. G.; Crespi, A. M.; Shriver, D. F. Nucleophilic, Electrophilic and Homolytic Reaction Chemistry of Transition-Metal Carbonyl Trihalomethyl Complexes. *Organometallics*, **1984**, *3*, 314.

244. Richmond, T. G.; Shriver, D. F. Electrophilic Halogen Exchange Between Lewis Acids and Transition-Metal Perfluoroalkyl Complexes. Synthesis and Characterization of Transition-Metal α-Haloalkyl Complexes. *Organometallics*, **1984**, *3*, 305.

245. Pitcher, E.; Stone, F. G. A. Spectroscopic Studies on Organometallic Compounds. VII. Infrared Spectra of some Perfluoroalkyl and Perfluoroacyl Metal Carbonyl Compounds. *Spectrochim. Acta*, **1962**, *18*, 585.

246. Gerus, I. I.; Yagupolskii, Y.; Volkov, N. D. Compounds of Transition Metals With σ-Bound Fluorine-containing Groups. II. Reactions of Polyfluoroalyklirontetracarbonyl Iodides and Pentacarbonyl Bromides of Manganese and Rhenium. *Russ. J. Org. Chem.*, **1982**, *18*, 1186.

247. Anderson, S.; Hill, A. F.; Clark, G. R. Reaction of $[Fe[C(O)N^iPr_2](CO)_4]^-$ with Trifluoroacetic Anhydride: Molecular Structure of $[Fe(CF_3)[\eta^2\text{-}C(O)N^iPr_2](CO)_2(PPh_3)$. *Organometallics*, **1992**, *11*, 1988.

248. Beveridge, A. D.; Clark, H. C. Reactivity of Metal-Metal Bonds. *J. Organomet. Chem.*, **1968**, *11*, 601.

249. Deng, J.; Li, Q.; Xie, Y.; King, R. B. Effects of the Strongly Electron-withdrawing Trifluoromethyl Group in Cobalt Carbonyl Chemistry. *J. Fluorine Chem.*, **2013**, *146*, 37.

250. Toscano, P. J.; Lettko, L.; Schermerhorn, E. J.; Waechter, J.; Shufon, K.; Liu, S.; Dikarev, E. V.; Zubieta, J. Synthesis and Characterization of Diphenylglyoximato cobalt(III) Complexes. The Molecular Structures of *trans*-Bis(diphenylglyoximato)(alkyl)(pyridine)cobalt(III), with alkyl=CH_2SiMe_3, CH_2CMe_3 and CF_3. *Polyhedron*, **2003**, *22*, 2809.

251. Liebing, P.; Oehler, F.; Wagner, M.; Tripet, P. F.; Togni, A. Perfluoroalkyl Cobaloximes: Preparation Using Hypervalent Iodine Reagents, Molecular Structures, Thermal and Photochemical Reactivity. *Organometallics*, **2018**, *37*, 570.

252. Zhang, C.-P.; Wang, H.; Klein, A.; Biewer, C.; Stirnat, K.; Yamaguchi, Y.; Xu, L.; Gomez-Benitez, V.; Vicic, D. A Five-Coordinate Nickel(II) Fluoroalkyl Complex as a Precursor to a Spectroscopically Detectable Ni(III) Species. *J. Am. Chem. Soc*, **2013**, *135*, 8141.

253. Tang, F.; Rath, N. P.; Mirica, L. M. Stable Bis(trifluoromethyl)nickel(III) Complexes. *Chem. Commun.*, **2015**, *51*, 3113.

254. Bour, J. R.; Camasso, N. M.; Sanford, M. S. Oxidation of Ni(II) to Ni(IV) with Aryl Electrophiles Enables Ni-Mediated Aryl-CF_3 Coupling. *J. Am. Chem. Soc.*, **2015**, *137*, 8034.

255. Bour, J. R.; Camasso, N. M.; Meucci, E. A.; Kampf, J. W.; Canty, A. J.; Sanford, M. S. Carbon-Carbon Bond-Forming Reductive Elimination from Isolated Nickel(III) Complexes. *J. Am. Chem. Soc.*, **2016**, *138*, 16105.

256. Chong, E.; Kampf, J. W.; Ariafard, A.; Canty, A. J.; Sanford, M. S. Oxidatively Induced C-H Activation at High Valent Nickel. *J. Am. Chem. Soc.*, **2017**, *139*, 6058.

257. D'Accriscio, F.; Borja, P.; Saffon-Merceron, N.; Fustier-Boutignon, M.; Mezailles, N.; Nebra, N. C-H Bond Trifluoromethylation of Arenes Enabled by a Robust, High-Valent Nickel(IV) Complex. *Angew. Chem. Int. Ed.*, **2017**, *56*, 12898.

258. Kieltsch, I.; Dubinina, G. G.; Hamacher, C.; Kaiser, A.; Torres-Nieto, J.; Hutchison, J. M.; Klein, A.; Budnikova, Y.; Vicic, D. A. Magnitudes of Electron-Withdrawing Effects of the Trifluoromethyl Ligand in Organometallic Complexes of Copper and Nickel. *Organometallics*, **2010**, *29*, 1451.

259. Dubinina, G. G.; Brennessel, W. W.; Miller, J. L.; Vicic, D. A. Exploring Trifluoromethylation Reactions at Nickel: A Structural and Reactivity Study. *Organometallics*, **2008**, *27*, 3933.

260. Klein, A.; Vicic, D. A.; Biewer, C.; Kieltsch, I.; Stirnat, K, Hamacher, C. Oxidative Cleavage of CH_3 and CF_3 Radicals from BOXAM Nickel Complexes. *Organometallics*, **2012**, *31*, 5334.

261. Wiemers, D. M.; Burton, D. J. Pregeneration, Spectroscopic Detection and Chemical Reaction of (Trifluoromethyl)copper, an Elusive and Complex Species. *J. Am. Chem. Soc.*, **1986**, *108*, 832.

262. Naumann, D.; Roy, T.; Tebbe, K. F.; Crump, W. Synthesis and Structure of a Surprisingly Stable Tetrakis(trifluoromethyl)cuprate (III) Salt. *Angew. Chem. Int. Ed.*, **1993**, *32*, 1482.

263. Romine, A. M.; Nebra, N.; Konovalov, A. I.; Martin, E.; Bennet-Buchholz, J.; Grushin, V. V. Easy Access to the Copper(III) Anion $[Cu(CF_3)_4]^-$. *Angew. Chem. Int. Ed.*, **2015**, *54*, 2745.

264. Zhang, S.-L.; Bie, W.-F. Isolation and Characterization of Copper(III) Trifluoromethyl Complexes and Reactivity Studies of Aerobic Trifluoromethylation of Arylboronic Acids. *RSC Adv.*, **2016**, *6*, 70902.

265. Zhang, S.-L.; Xiao, C.; Wan, H.-X. Diverse Copper(III) Trifluoromethyl Complexes with Mono-, Bi- and Tridentate Ligands and their Versatile Reactivity. *Dalton Trans.*, **2018**, *47*, 4779.

266. Huang, H.; Rheingold, A.; Hughes, R. P. Synthesis and X-ray Structure of a Diamagnetic Oxo-Bridged Trifluoromethyl-Chromium(V) Complex: Structural and Computational Comparisons between CF_3 and CH_3 Ligands in Two Different Oxidation States of Chromium. *Organometallics*, **2010**, *29*, 3672.

267. Johnson, A.; Puddephatt, R. J. Reactions of Trifluoromethyl Iodide with Methylgold(I) Complexes. Preparation of Trifluoromethyl-gold(I) and -gold(III) Complexes. *J. Chem. Soc., Dalton Trans.*, **1976**, 1360.

268. Sanner, R. D.; Satcher, J. H. Jr.; Droege, M. W. Synthesis and Characterization of (Trifluoromethyl) Gold Complexes. *Organometallics*, **1989**, *8*, 1498.

269. Florke, U.; Haupt, H.-J.; Jones, P. G. Trifluoromethyl(triphenylphosphine)gold(I). *Acta. Crystallogr. C.*, **1996**, *C52*, 609.

270. Winston, M. S.; Wolf, W. J.; Toste, F. D. Photoinitiated Oxidative Addition of CF_3I to Gold(I) and Facile Aryl-CF_3 Reductive Elimination. *J. Am. Chem. Soc.*, **2014**, *136*, 7777.

271. Blaya, M.; Bautista, D.; Gil-Rubio, J.; Vincente, J. Synthesis of Au(I) Trifluoromethyl Complexes. Oxidation to Au(III) and Reductive Elimination of Halotrifluoromethanes. *Organometallics*, **2014**, *33*, 6358.

272. Xie, Q.; Li, L.; Zhu, Z.; Zhang, R.; Ni, C.; Hu, J. From C_1 to C_2: $TMSCF_3$ as a Precursor for Pentafluoroethylation. *Angew. Chem. Int. Ed.*, **2018**, *57*, 13211.

273. Richard, M V C; John, T Manufacture of Organic Compounds Containing Fluorine. US patent 3,408,411, **1968**.

274. Urata, H.; Fuchikami, T. A Novel and Convenient Method for Trifluoromethylation of Organic Halides using $CF_3SiR'_3$/KF/Cu(I) System. *Tetrahedron*, **1991**, *32*, 91.

275. Oishi, M.; Kondo, H.; Amii, H. Aromatic Trifluoromethylation Catalytic in Copper. *Chem. Commun.*, **2009**, 1909.

276. Liu, T.; Shen, Q. Progress in Copper-Mediated Formation of Trifluoromethylated Arenes. *Eur. J. Org. Chem*, **2012**, 6679.

277. Alonso, C.; Marigorta, E. M. de; Rubiales, G.; Palacios, F. Carbony Trifluoromethylation Reactions of Hydrocarbons Derivatives and Heteroarenes. *Chem. Rev.*, **2015**, *115*, 1847.

278. Roy, S.; Gregg, B. T.; Gribble, G. W.; Le, V.-D.; Roy, S. Trifluoromethylation of Aryl and Heteroaryl Halides. *Tetrahedron*, **2011**, *67*, 2161.

279. Senecal, T. D.; Parsons, A. T.; Buchwald, S. L. Room Temperature Aryl Trifluoromethylation via Copper-Mediated Oxidative Cross-Coupling. *J. Org. Chem.*, **2010**, *76*, 1174.

280. Knauber, T.; Arikan, F.; Röschenthaler, G.-V.; Gooßen, L. J. Copper-Catalyzed Trifluoromethylation of Aryl Iodides with Potassium (Trifluoromethyl)trimethoxyborate. *Chem. Eur. J.*, **2011**, *17*, 2689.

281. Morimoto, H.; Tsubogo, T.; Litvinas, N. D.; Hartwig, J. F. A Broadly Applicable Copper Reagent for Trifluoromethylations and Perfluoroalkylations of Aryl Iodides and Bromides. *Angew. Chem. Int. Ed.*, **2011**, *50*, 3793.

282. Weng, Z.; Lee, R.; Jia, W.; Yuan, Y.; Wang, W.; Feng, X.; Huang, K.-W. Cooperative Effects of Silver in Copper-Catalyzed Trifluoromethylation of Aryl Iodides Using M_3SiCF_3. *Organometallics*, **2011**, *30*, 3229.

283. Amii, H. Recent Progress in Catalytic Aromatic Trifluoromethylation. *J. Syn. Org. Chem. Jpn.*, **2011**, *69*, 752.

284. Xu, J.; Luo, D.-F.; Xiao, B.; Liu, Z.-J.; Gong, T.-J.; Fu, Y.; Liu, L. Copper-catalyzed Trifluoromethylation of Aryl Boronic Acids using a CF_3^+ Reagent. *Chem. Commun.*, **2011**, *47*, 4300.

285. Cho, E. J.; Senecal, T. D.; Kinzel, T.; Zhang, Y.; Watson, D. A.; Buchwald, S. L. The Palladium-Catalyzed Trifluoromethylation of Aryl Chlorides. *Science*, **2010**, *328*, 1679.

286. Lundgren, R. J.; Stradiotto, M. Transition-metal-catalyzed Trifluoromethylation of Aryl Halides, *Angew. Chem. Int. Ed.*, **2010**, *49*, 9322.

287. Gladysz, J. A. The Future of Organometallic Chemistry. *Organometallics*, **2011**, *30*, 1.

288. Furuya., T.; Kamlet, A. S.; Ritter, T. Catalysis for Fluorination and Trifluoromethylation. **2011**, *Nature*, *473*, 470.

289. Salinas, S. M. de; Mudarra, A. L.; Benet-Buccholz, J.; Parella, T.; Maseras, F.; Pérez-Temprano, M. H. New Vistas in Transmetalation with Discrete "Ag-CF_3" Species: Implications in Pd-Mediated Trifluoromethylation Reactions. *Chem. Eur. J.*, **2018**, *24*, 11895.

290. Konovalov, A. I.; Lyshchynskyi, A.; Grushin, V. V. Mechanism of Trifluoromethylation of Aryl Halides with $CuCF_3$ and the Ortho Effect. *J. Am. Chem. Soc.*, **2014**, *136*, 13410.

291. Yu, D.-H.; Shao, J.-N.; He, R.-X.; Li, M. Mechanism of Trifluoromethylation Reactions with Well-Defined NHC Copper Trifluoromethyl Complexes and Iodobenzene: A Computational Exploration. *Chin. Chem. Lett.*, **2015**, *26*, 564.

292. Ohashi, M.; Adachi, T.; Ishida, N.; Kikushima, K.; Ogoshi, S. Synthesis and Reactivity of Fluoroalkyl Copper Complexes by the Oxycupration of Tetrafluoroethylene. *Angew. Chem. Int. Ed.*, **2017**, *56*, 11911.

293. Braun, T.; Parsons, S.; Perutz, R. N.; Voith, M. Reactivity of a Nickel Fluoride Complex: Preparation of New Tetrafluoropyridyl Derivatives. *Organometallics*, **1999**, *18*, 1710.

294. Zhu, F.; Yang, G.; Zhou, Z.; Wu, X.-F. Palladium-Catalyzed Carbonylative Coupling of Aryl Iodides with an Organocopper Reagent: A Straightforward Procedure for the Synthesis of Aryl Trifluoromethyl Ketones. *RSC Adv.*, **2016**, *6*, 57070.

295. Kawashima, T.; Ohashi, M.; Ogoshi, S. Selective Catalytic Formation of Cross-Tetramers from Tetrafluoroethylene, Ethylene, Alkynes, and Aldehydes via Nickelacycles as Key Reaction Intermediates. *J. Am. Chem. Soc.*, **2018**, *140*, 17423.

296. Shirataki, H.; Ohashi, M.; Ogoshi, S. Nickel-catalyzed Three-component Coupling Reaction of Tetrafluoroethylene and Aldehydes with Silanes via Oxa-Nickelacycles. *Eur. J. Org. Chem.*, **2019**, 1883.

297. Kawashima, T.; Ohashi, M.; Ogoshi, S. Nickel-Catalyzed Formation of 1,3-Dienes via a Highly Selective Cross-Tetramerization of Tetrafluoroethylene, Styrenes, Alkynes, and Ethylene. *J. Am. Chem. Soc.*, **2017**, *139*, 17795.

298. Ohashi, M.; Ueda, Y.; Ogoshi, S. Nickel(0)-Mediated Transformations of Tetrafluoroethylene and Vinylarenes into Fluorinated Cyclobutyl Compounds. *Angew. Chem. Int. Ed.*, **2017**, *56*, 2435.

299. Fujiwara, M.; Ichikawa, J.; Okauchi, T.; Minami. T. Vinylic C-F Bond Activation with Low-Valent Zirconocene: The Generation and Cross-Coupling of 1-Fluorovinylzirconocene. *Tetrahedron Lett.*, **1999**, *40*, 7261.

300. Saijo, H.; Sakaguchi, H.; Ohashi, M.; Ogoshi, S. Base-Free Hiyama, Coupling Reaction via a Group 10 Metal Fluoride Intermediate Generated by C-F Bond Activation. *Organometallics*, **2014**, *33*, 3669.

301. Fujita, T.; Fuchibe, K.; Ichikawa, J. Transition-Metal-Mediated and -Catalyzed C-F Bond Activation by Fluorine Elimination. *Angew. Chem. Int. Ed.*, **2018**, *58*, 390.

302. Ichitsuka, T.; Fujita, T.; Arita, T.; Ichikawa, J. Double C-F Bond Activation through β-fluorine Elimination: Nickel-Mediated [3+2] Cycloaddition of 2-Trifluoromethyl-1-alkenes with Alkynes. *Angew. Chem. Int. Ed.*, **2014**, *53*, 7564.

303. Ichitsuka, T.; Fujita, T.; Arita, T.; Ichikawa, J. Catalytic Defluorinative [3+2] Cycloaddition of Trifluoromethylalkenes with Alkynes *via* Reduction of Nickel(II) Fluoride Species. *Dalton Trans.*, **2015**, *44*, 19460.

304. Xu, J.; Ahmed, E.-A.; Xiao, B.; Lu, Q.-Q.; Wang, Y.-L.; Yu, C.-G.; Fu, Y. Pd-Catalyzed Regioselective Activation of *gem*-Difluorinated Cyclopropanes: A Highly Efficient Approach to 2-Fluorinated Allylic Scaffolds. *Angew. Chem. Int. Ed.*, **2015**, *54*, 8231.

305. Harrison, D. J.; Lee, G. M.; Leclerc, M. C.; Korobkov, I.; Baker, R. T. Cobalt Fluorocarbenes: Cycloaddition Reactions with Tetrafluoroethylene and Reactivity of the Perfluorometallacyclic Products. *J. Am. Chem. Soc.*, **2013**, *135*, 18296.

306. Heitz, W.; Knebelkamp, A. Synthesis of Fluorostyrenes via Palladium-catalyzed Reactions of Aromatic Halides with Fluoroolefins. *Makromol. Chem., Rapid Commun.*, **1991**, *12*, 69.

307. Miura, T.; Ito, Y.; Murakami, M. Synthesis of *gem*-Difluoroalkenes via β-Fluoride Elimination of Organorhodium(I). *Chem. Lett.*, **2008**, *37*, 1006.

308. Sakaguchi, H.; Ohashi, M.; Ogoshi, S. Fluorinated Vinylsilanes from the Copper-Catalyzed Defluorosilylation of Fluoroalkene Feedstocks. *Angew. Chem Int. Ed.*, **2018**, *57*, 328.

309. Sakaguchi, H.; Uetake, Y.; Ohashi, M.; Niwa, T.; Ogoshi, S.; Hosoya, T. Copper-Catalyzed Regioselective Monodefluoroborylation of Polyfluoroalkenes en Route to Diverse Fluoroalkenes. *J. Am. Chem. Soc.*, **2017**, *139*, 12855.

310. Kojima, R.; Kubota, K.; Ito, H. Stereodivergent Hydrodefluorination of Gem-difluoroalkenes: Selective Synthesis of (Z)- and (E)-Monofluoroalkenes. *Chem. Commun.*, **2017**, *53*, 10688.

311. Purser, S.; Moore, P. R.; Swallow, S.; Gouverneur, V. Fluorine in Medicinal Chemistry. *Chem. Soc. Rev.*, **2008**, *37*, 320.

312. Grushin, V. V. The Organometallic Fluorine Chemistry of Palladium and Rhodium: Studies toward Aromatic Fluorination. *Acc. Chem. Res.*, **2010**, *43*, 160.

313. Brown, J. M.; Gouverneur, V. Transition-Metal-Mediated Reactions for C(sp2)-F Bond Construction: The State of Play. *Angew. Chem. Int. Ed.*, **2009**, *48*, 8610.

314. Hull, K. L.; Anani, W. Q.; Sanford, M. S. Palladium-Catalyzed Fluorination of Carbon-Hydrogen Bonds. *J. Am. Chem. Soc.*, **2006**, *128*, 7134.

315. Wang, F.; Luo, T.; Hu, J.; Wang, Y.; Krishnan, H. S.; Jog, P. V.; Ganesh, S. K.; Prakash, G. K. S.; Olah, G. A. Synthesis of *gem*-Difluorinated Cyclopropanes and Cyclopropenes: Trifluoromethyltrimethylsilane as a Difluorocarbene Source. *Angew. Chem. Int. Ed.*, **2011**, *50*, 7153.

316. Singh, R. P.; Cao, G.; Kirchmeier, R. L.; Shreeve, J. M. Cesium Fluoride Catalyzed Trifluoromethylation of Esters, Aldehydes, and Ketones with (Trifluoromethyl)trimethylsilane. *J. Org. Chem.*, **1999**, *64*, 2873.

317. Arpe, H.-J., *Industrial Organic* Chemistry, Wiley-VCH, Weinheim, 5th edn, 2010

318. *Applied Homogenous Catalysis with Organometallic Compounds*, ed. Cornils, B.; Herrmann, W. A., Wiley-VCH, New York, 1996.

319. Shin, S. K.; Beauchamp, J. L. Identification of Mn(CO)nCF_3- (n = 4, 5) Structural Isomers by IR Multiphoton Dissociation, Collision-Induced Dissociation, and Specific Ligand Displacement Reactions: Studies of the Trifluoromethyl Migratory Decarbonylation Reaction in the Gas Phase. *J. Am. Chem. Soc.*, **1990**, *112*, 2057.

320. Gasafi-Martin, W.; Oberendfellner, G.; von Werner, K. A Facile Synthesis of Metalla-octafluorocyclopentane Complexes of Ruthenium and Nickel. *Can. J. Chem.*, **1996**, *74*, 1922.

321. Burch, R. R.; Calabrese, J. C.; Ittel, S. D. Fluoroorganometallic Chemistry: Carbon-Fluorine Bond Activation in Perfluorometallacyclopentane Complexes. *Organometallics*, **1988**, *7*, 1642.

322. Hughes, R. P. Fluorine as a Ligand Substituent in Organometallic Chemistry: A Second Chance and a Second Research Career. *J. Fluorine Chem.*, **2010**, *131*, 1059

323. Goodman, J.; Grushin, V. V.; Larichev, R. B.; Macgregor, S. A.; Marshall, W. J.; Roe, D. C. Fluxionality of $[(Ph_3P)_3Rh(X)]$: The Extreme Case of X = CF_3. *J. Am. Chem. Soc.*, **2009**, *131*, 4236.

324. Garratt, S. A.; Hughes, R. P.; Kovacik, I.; Ward, A. J.; Willemsen, S.; Zhang, D. Carbon-Fluorine Bond Activation Coupling with Carbon-Hydrogen Bond Formation α to Iridium: Kinetics, Mechanism, and Diastereoselectivity. *J. Am. Chem. Soc.*, **2005**, *127*, 15585.

325. Torrens, H. Carbon-Fluorine Bond Activation by Platinum Group Metal Complexes. *Coord. Chem. Rev.*, **2005**, *249*, 1957.

326. Huang, D.; Koren, P. R.; Folting, K.; Davidson, E. R.; Caulton, K. G. Facile and Reversible Cleavage of C-F Bonds. Contrasting Thermodynamic Selectivity for Ru-CF_2H vs F-Os=CFH. *J. Am. Chem. Soc.*, **2000**, *122*, 8916.

327. Richmond, T. G.; Crespi, A. M.; Shriver, D. F. Nucleophilic, Electrophilic and Homolytic Reaction Chemistry of Transition-Metal Carbonyl Trihalomethyl Complexes. *Organometallics*, **1984**, *3*, 314.

328. Richmond, T. G.; Shriver, D. F. Facile Electrophilic Halogen Exchange Between Boron Trihalides and Transition-Metal Perfluoroalkyl Complexes. A Novel Method for

the Synthesis of Reactive Transition-Metal Haloalkyl Complexes. *Organometallics*, **1983**, *2*, 1061.

329. Crabtree, R. H. NHC Ligans versus Cyclopentadienyls and Phosphines as Spectator Ligands in Organometallic Catalysis. *J. Organomet. Chem.*, **2005**, *690*, 5451.

330. Wilson, D. J. D.; Couchman, S. A.; Dutton, J. L. Are N-Heterocyclic Carbenes "Better" Ligands than Phosphines in Main Group Chemistry? A Theoretical Case Study of Ligand-Stabilized E_2 Molecules, L-E-E-L (L = NHC, phosphine; E = C, Si, Ge, Sn, Pb, N, P, As, Sb, Bi). *Inorg. Chem.*, **2012**, *51*, 7657.

331. Nelson, D. J.; Nolan, S. P. Quantifying and Understanding the Electronic Properties of N-Heterocyclic Carbenes. *Chem. Soc. Rev.*, **2013**, *42*, 6723.

332. Laskowski, C. A.; Miller, A. J.; Hillhouse, G. L.; Cundari, T. R. A Two-Coordinate Nickel Imido Complex that Effects C-H Amination. *J. Am. Chem. Soc.*, **2011**, *133*, 771.

333. Miyazaki, S.; Koga, Y.; Matsumoto, T.; Matsubara, K. A New Aspect of Nickel-Catalyzed Grignard Cross-Coupling Reactions: Selective Synthesis, Structure, and Catalytic Behavior of a T-Shape Three-Coordinate Nickel(I) Chloride Bearing a Bulky NHC Ligand. *Chem. Commun.*, **2010**, *46*, 1932.

334. Hanley, P. S.; Marquard, S. L.; Cundari, T. R.; Hartwig, J. F. Reductive Elimination of Alkylamines from Low-Valent, Alkylpalladium(II) Amido Complexes. *J. Am. Chem. Soc.*, **2012**, *134*, 15281.

335. Ni–C_{RF} bond lengths for structure **2.2** (see ESI†): 1.956(1) Å (trans to P); 1.945(1) Å (trans to C). Ni–C_{NHC} bond length for **2.2**: 1.945(1) Å.

336. See ESI page S14 for low temperature NMR spectra.†

337. Grimme, S. Semiempirical GGA-type Density Functional Constructed with a Long-Range Dispersion Correction. *J. Comput. Chem.*, **2006**, *27*, 1787.

338. See ESI page S29.†

339. Islam, N.; Gosh, D. C., *Theoretical and Computational Research in the 21st Century*, ed. Islam, N., CRC Press, Boca Raton, **2014**, ch. 1, pp. 1-58.

340. Dyatkin, B. L.; Martynov, B. I.; Martynova, L. G.; Kizim, N. G.; Sterlin, S. R.; Stumbrevichute, Z. A.; Federov, L. A. On the Interaction of Perfluoroalkyl Carbanions with Silver Salts. *J. Organomet. Chem.*, ***1973***, *57*, 423.

341. Dyatkin, B. L.; Sterlin, S. R.; Martynov, B. I.; Mysov, E. I.; Knunyants, I. L. Reaction of Perfluoroalkyl Carbanions with Mercury Salts. *Tetrahedron*, **1971**, *27*, 2843.

342. Crossland, R. K.; Wells, W. E.; Shiner Jr., V. J. Sulfonate Leaving Groups, Structure and Reactivity. 2,2,2-Trifluoroethanesulfonate. *J. Am. Chem. Soc.*, **1971**, *93*, 4217.

343. Bourgeois, C. J.; Hughes, R. P.; Yuan, J.; DiPasquale, A. G.; Rheingold, A. L. α- and β-Fluorine Elimination Reactions Induced by Reduction of Iridium-Fluoroalkyl Complexes. Selective Formation of Fluoroalkylidene and Hydrofluoroalkene Ligands. *Organometallics*, **2006**, *25*, 2908.

344. For NMR spectra of compound 4a see pages S21–S22.†

345. Haindl, M. H.; Schmid, M. B.; Zeitler, K.; Gschwind, R. M. What is Your Actual Catalyst? TMS Cleavage Rates of Diarylprolinol Silyl Ethers Studied by *in situ* NMR. *RSC Adv.*, **2012**, *2*, 5941.

346. Cohen, T.; Bennett, D. A.; Mura, A. J. Preparative Methods for .beta.-Acyl Vinyl Anion Equivalents from Enones or Allyl Sulfides. *J. Org. Chem.*, **1976**, *41*, 2506.

347. Jover, J.; Bosque, R.; Sales, J. QSPR Prediction of pK_a for Benzoic Acids in Different Solvents. *QSAR Comb. Sci.*, **2008**, *27*, 563.

348. Riemenschneider, W.; Bolt, H. M., Esters, Organic, in *Ullman's Encyclopedia of Industrial Chemistry*, Wiley-VCH, Weinheim, **2005**.

349. Hughes, R. P.; Zhang, D.; Zakharov, L. N.; Rheingold, A. L. Selective Protonation at a C-F Bond in the Presence of an Iridium-Methyl Bond Gives Diastereoselective Carbon-Fluorine Bond Activation and Carbon-Carbon Bond Formation. A New Path to Carbon Stereocenters Bearing Fluorine Atoms. *Organometallics*, **2002**, *21*, 4902.

350. Kalberer, E. W.; Houlis, J. F.; Roddick, D. M. Protolytic Stability of (dfepe)Pt(Ph)O_2CCF_3: Supporting Evidence for a Concerted S_E2 Protonolysis Mechanism. *Organometallics*, **2004**, *23*, 4112.

351. Unpublished work.

352. Hughes, R. P.; Smith, J. M. Hydrogenolysis of Aliphatic Carbon-Fluorine Bonds in Fluoroalkyl-Iridium Complexes to Give Hydrofluorocarbons. *J. Am. Chem. Soc.*, **1999**, *121*, 6084.

353. Banks, R. E.; Smart, B. E.; Tatlow, J. C. *Organofluorine Chemistry: Principles and Commercial Applications*; Plenum: New York, **1994.**

354. Chambers, R. D. *Fluorine Chemistry at the Millenium;* Elsevier: Amsterdam, **2000**.

355. Gouverneur, V.; Müller, K. *Fluorine in Pharmaceutical and Medicinal Chemistry*; Imperial College Press: London, **2012**.

356. Charpentier, J.; Früh, N.; Togni, A. Electrophilic Trifluoromethylation by use of Hypervalent Iodine Reagents. *Chem. Rev.*, **2015**, *115*, 650.

357. Yang, X.; Wu, T.; Phipps, R. J.; Toste, F. D. Advances in Catalytic Enantioselective Fluorine, Mono-, Di-, and Trifluoromethylation, and Trifluoromethylthiolation Reactions. *Chem. Rev.*, **2015**¸*115*, 826.

358. Gao, P.; Song, X.-R. S.; Liu, X.-Y.; Liang, Y.-M. Recent Developments in the Trifluoromethylation of Alkynes. *Chem. Eur. J.*, **2015**, *21*, 7648.

359. Kyasa, S. K. Fluoroform (CHF_3). *Synlett.*, **2015**, *26*, 1911.

360. Wang, S.-M.; Han, J.-B.; Zhang, C.-P.; Qin, H.-L.; Xiao, J.-C. An Overview of Reductive Trifluoromethylation reactions using electrophilic '+CF_3' Reagents. *Tetrahedron*, **2015**, *71*, 7949.

361. Hu, J.; Zhang, W.; Wang, F. Selective Difluoromethylation and Monofluoromethylation Reactions. *Chem. Commun.*, **2009**, 7465.

362. Lu, Y.; Liu, C.; Chen, Q.-Y. Recent Advances in Difluoromethylation Reaction. *Curr. Org. Chem.*, **2015**, *19*, 1638.

363. Chen, B.; Vicic, D. Transition-Metal-Catalyzed Difluoromethylation, Difluoromethylenation, and Polydifluoromethylenation Reactions. In *Organometall Fluorine Chemistry*; Braun, T.; Hughes, R. P., Eds; Springer US: New York, **2014**; Top. Organomet. Chem. *52*, pp 113-141.

364. Huang, Y.; Ajitha, M. J.; Huang, K.-W.; Zhang, Z.; Weng, Z. A Class of Effective Decarboxylative Perfluoroalkylating Reagents: $[(phen)_2Cu](O_2CR_F$. *Dalton Trans.*, **2016**, *45*, 8468.

365. Sugiishi, T.; Amii, H.; Aikawa, K.; Mikami, K. Carbon-Carbon Bond Cleavage for Cu-Mediated Aromative Trifluoromethylations and Pentafluoroethylations. *Beilstein J. Org. Chem.*, **2015**, *11*, 2661.

366. Landelle, G.; Panossian, A.; Leroux, F. R. Trifluoromethyl Ethers and -Thioethers as Tools for Medicinal Chemistry and Drug Discovery. *Curr. Top. Med. Chem.*, **2014**, *14*, 941.

367. Lee, K. N.; Lee, J. W.; Ngai, M.-Y. Synthesis of Trifluoromethoxylated (Hetero)Arenes *via* OCF_3 Migration. *Synlett.*, **2016**, *27*, 313.

368. Besset, T.; Jubault, P.; Pannecoucke, X.; Poisson, T. New Entries Toward the Synthesis of OCF_3-Containing Molecules. *Org. Chem. Front.*, **2016**, *3*, 1004.

369. Landelle, G.; Panossian, A.; Pazenok, S.; Vors, J.-P.; Leroux, F. R. Recent Advances in Transition Metal-Catalyzed Csp^2-Monofluoro-, Difluoro-, Perfluoromethylation and Trifluoromethylthiolation. *Beilstein J. Org. Chem.*, **2013**, *9*, 2476.

370. Tohnishi, M.; Nakao, H.; Kohno, E.; Nishida, T.; Furuya, T.; Shimizu, T.; Seo, A.; Sakata, K.; Fujioka, S.; Kanno, H. Process for the Production of Perfluoroalkylated Aniline Derivatives. EP 919542, **1999**.

371. Tohnishi, M.; Nakao, H.; Kohno, E.; Nishida, T.; Furuya, T.; Shimizu, T.; Seo, A.; Sakata, K.; Fujioka, S.; Kanno, H. Phthalamide Derivatives, or Salt Thereof Agrohorticultural Insecticide, and Method for Using the Same. EP 1006107, **2000**.

372. Kimura, M.; Morimoto, M.; Uehara, M.; Watanabe, M.; Yoshida, M. Substituted Aminoquinazolinone (thione) Derivatives or Salts Thereof, Intermediates Thereof, and Pest Controllers and a Method for Using the Same. EP 1097932 A1, **2001**.

373. Zhang, J.; Tang, X.; Ishaaya, I.; Cao, S.; Wu, J.; Yu, J.; Li, H.; Quain, X. Synthesis and Insecticidal Activity of Heptafluoroisopropyl-Containing Benzoylphenylurea Structures. *J. Agric. Food Chem.*, **2010**, *58*, 2736.

374. Zhou, S.; Meng, X.; Jin, R.; Ma, Y.; Xie, Y.; Zhao, Y.; Song, H.; Xiong, L.; Li, Z. Synthesis, Insecticidal Activities and Structure-Activity Relationship Study of Dual Chiral Sulfilimines. *Mol. Diversity*, **2017**, *21*, 915.

375. Prakash, G. K. S.; Hu, J.; Olah, G. A. Preparation of Tri- and Difluoromethylsilanes via an Unusual Magnesium Metal-Mediated Reductive Tri- and Difluoromethylation of Chlorosilanes Using Tri- and Difluoromethyl Sulfides, Sulfoxides, and Sulfones. *J. Org. Chem.*, **2003**, *68*, 4457.

376. Ishikawa, N.; Seiji, S.-N. The Preparation of Aryl Heptafluoroisopropyl Ketones from Aroyl Chlorides and Hexafluoropropene in the Presence of Fluoride Ions. *Bull. Chem. Soc. Jpn.*, **1975**, *48*, 1339

377. . Takechi, N.; Aït-Mohand, S.; Medebielle, M.; Dolbier,´ W. R., Jr. Nucleophilic Trifluoromethylation of Acyl Chlorides Using the Trifluoromethyl Iodide/TDAE Reagent. *Tetrahedron Lett.*, **2002**, *43*, 4317.

378. Naumann, D.; Finke, M.; Lange, H.; Dukat, W.; Tyrra, W. Die Reaktionen von Bis(perfluoroalkyl)cadmium-Komplexen mit Arylcarbonsäurechloriden: Synthese von Aryl-(perfluoroalkyl)ketonen, (Perfluoroalkyl-dihydropyridin)-arylcarbonsäureamiden, α,α-Bis(trifluoromethyl)benzyl-alkoholen und Benzoesäure-α,α-bis(trifluoromethyl)-benzylestern. *J. Fluorine Chem.*, **1992**, *56*, 215.

379. Chambers, R. D.; Musgrave, W. K. R.; Savory, J. Organometallic and Metalloid Compounds made from Heptafluoro-2-iodopropane, and their Properties. *J. Chem. Soc.*, **1962**, 1993.

380. Nair, H. K.; Burton, D. J. Perfluoroisopropylcadmium and Copper: Preparation, Stability and Reactivity. *J. Fluorine Chem.*, **1992**, *56*, 341.

381. Ishikawa, N.; OChiai, M. Heptafluoroisopropylation of Aromatic Ring by the Use of Copper. *Nippon Kagaku Kaishi*, **1973**, *1973*, 2351.

382. Mcloughlin, V. C. R.; Thrower, J. A Route to Fluoroalkyl-Substituted Aromatic Compounds Involving Fluoroalkylcopper Intermediates. *Tetrahedron*, **1969**, *25*, 5921.

383. Burch, R. R.; Calabrese, J. C. Transfer of Perfluoroalkyl Groups Between Metals: Preparation of the Anionic Perfluoroalkyl Metal Complex $Ag[CF(CF_3)_2]_2$. *J. Am. Chem. Soc.*, **1986**, *108*, 5359.

384. Bubot, C.; Mansuy, D.; Lecolier, S.; Normant, J. F. Action du Perfluoroisopropylargent sur les Halogénure d'Alcoyle et l'Anhydride Carbonique. *J. Organomet. Chem.*, **1972**, *42*, C105.

385. Sekiya, A.; Ishikawa, N.; Reaction of Heptafluoro-1-methylethylzinc Iodide with Halides and Anhydrides of Carboxylic Acids. *Chem. Lett.*, **1997**, *6*, 81.

386. Toscano, P. J.; Brand, H.; Geremia, S.; Randaccio, L.; Zangrando, E. Evidence for Steric Trans Influences and Effects in (Perfluoroisopropyl)cobaloximes. Molecular Structure of Trans-bis-(dimethylglyoximato)(triphenylphosphine)(perfluoroisopropyl) cobalt(III). *Organometallics*, **1991**, *10*, 713.

387. Jiang, D.-F.; Liu, C.; Guo, Y.; Xiao, J.-C.; Chen, Q.-Y. A General, Regiospecific Synthetic Route to Perfluoroalkylated Arenes via Arenediazonium Salts with $R_FCu(CH_3CN)$ Complexes. *Eur. J. Org. Chem.*, **2014**, *2014*, 6303.

388. Simon, C. M.; Kaminsky, W. Chemical Recycling of Polytetrafluoroethylene by Pyrolysis. *Polym. Degrad. Stab.*, **1998**, *62*, 1.

389. Van der Walt, I. J.; Grunenburg, A. T.; Nel, J. T.; Maluleke, G. G.; Bruinsma, S. L. The Continuous Depolymerization of Filled Polytetrafluoroethylene with a Continuous Process. *J. Appl. Polym. Sci.*, **2008**, *109*, 264.

390. Li, Y.; Wang, X.; Guo, Y.; Zhu, Z.; Wu, Y.; Gong, Y. Direct Heptafluoroisopropylation of Arylboronic Acids *via* Hexafluoropropene (HFP). *Chem. Commun.*, **2016**, *52*, 796.

391. Wang, X.; Li, Y.; Guo, Y.; Zhu, Z.; Wu, Y.; Cao, W. Direct Isoperfluoropropylation of Arenediazonium Salts with Hexafluoropropene. *Org. Chem. Front.*, **2016**, *3*, 304.

392. Liu, X.-H.; Leng, J.; Jia, S.-J.; Hao, J.-H.; Zhang, F.; Qin, H.-L.; Zhang, C. P. Copper-Mediated Aerobic Iodination and Perfluoroalkylation of Boronic Acids with $(CF_3)_2CFI$ at Room Temperature. *J. Fluorine Chem.*, **2016**, *189*, 59.

393. Zeng, Y.; Zhang, L.; Zhao, Y.; Ni, C.; Zhao, J.; Hu, J. Silver-Mediated Trifluoromethylation-Iodination of Arynes. *J. Am. Chem. Soc.*, **2013**, *135*, 2955.

394. Garratt, S. A.; Hughes, R. P.; Kovacik, I.; Ward, A. J.; Willemsen, S.; Zhang, D. Carbon-Fluorine Bond Activation

395. See Chapter 2

396. Gulliver, D. J.; Levason, W.;Webster, M. Coordination Stabilised Copper(I) Fluoride. Crystal and Molecular Structure of Fluorotris(triphenylphosphine)copper(I)·Ethanol (1/2), $Cu(PPh_3)_3F·EtOH$. *Inorg. Chim. Acta*, **1981**, *52*, 153.

397. Chaudhuri, M. K.; Dhar, S. S.; Vijayashree, N. Molecular Complexes of Copper(I): Easy Access to $CuF(PPh_3)_3·2ROH$ (R = Me or Et). *Transition Met. Chem.*, **2000**, *25*, 559.

398. Larsson, J. M.; Pathipati, S. R.; Szabó, K. J. Regio- and Stereoselective Allylic Trifluoromethylation and Fluorination Using $CuCF_3$ and CuF Reagents. *J. Org. Chem.*, **2013**, *78*, 7330.

399. Panferova, L. I.; Miloserdov, F. M.; Lishchynskyi, A.; Belmonte, M. M.; Benet-Buchholz, J.; Grushin, V. V. Well-Defined CuC_2F_5 Complexes and Pentafluoroethylation of Acid Chlroides. *Angew. Chem. Int. Ed.*, **2015**, *54*, 5218.

400. Lv, H.; Cai, Y.-B.; Zhang, J.-L. Copper-Catalyzed Hydrodefluorination of Fluoroarenes by Copper Hydride Intermediates. *Angew. Chem. Int. Ed.*, **2013**, *52*, 3203.

401. It should be noted that the scope of both referenced reactions was quite limited.

402. The vacuum transfer procedure was done for 4f and 4n

403. Note that 3b undergoes homolysis at room temperature only in the presence of an electrophile.

404. Curtiss, L. A.; Redfern, P. C.; Raghavachari, K.; Rassolov, V.; Pople, J. A. Assessment of Gaussian-2 and Density Functional Theories for the Computation of Enthalpies of Formation. *J. Chem. Phys.*, **1999**, *110*, 4703.

405. Dneprovskii, A. S.; Kasatochkin, A. N.; Kondakov, D. Y. Homolytic Substitution at Carbon in Reactions of Perfluoroisopropyl Iodide with Cobalt Benzyl Complexes. *Russ. J. Org. Chem.*, **1989**, *25*, 1984.

406. Ignatowska, J.; Wojciech, D. Sodium Dithionite Initiated Addition of CF_2Br_2, CF_3I and $(CF_3)_2CFI$ to Allylaromatics: Synthesis and the Reactivity of 4-aryl-1,1-difluorodienes and 4-aryl-1,1-bis(trifluoromethyl)dienes. *J. Fluorine Chem.*, **2007**, *128*, 997.

407. O' Reilly, N. J.; Maruta, M.; Ishikawa, N. Palladium and Nickel-Catalyzed Perfluoroalkylation of Aldehydes Using Zinc and Perfluoroalkyl Halides. *Chem. Lett.*, **1984**, *13*, 517.

408. Kitazume, T.; Ishikawa, N. Ultrasound-Promoted Selective Perfluoroalkylation on the Desired Position of Organic Molecules. *J. Am. Chem. Soc.*, **1985**, *107*, 5186.

409. Kitazume, T.; Ishikawa, N. Trifluoromethylation of Carbonyl Compounds with Trifluoromethylzinc Iodide Under Ultrasonic Irradiation. *Chem. Lett.*, **1981**, *10*, 1337.

410. Parr, R. G.; Yang, W. *Density-Functional Theory of Atoms and Molecules;* Oxford University Press: New York, 1989.

411. Becke, A. D. Densityfunctional Thermochemistry. III. The Role of Exact Exchange. *J. Chem. Phys.*, **1993**, *98*, 5648.

412. Lee, C.; Yang, W.; Parr, R. G. Development of the Colle-Salvetti Correlation-Energy Formula into a Functional of the Electron Density. *Phys. Rev. B: Condens. Matter Mater. Phys.*, **1988**, *37*, 785.

413. Godbout, N.; Salahub, D. R.; Andzelm, J.; Wimmer, E. Optimization of Gaussian-type Basis Sets for Local Spin Density Functional Calculations. Part I. Boron through Neon, Optimization Technique and Validation. *Can. J. Chem.*, **1992**, *70*, 560.

414. Peterson, K. A.; Puzzarini, C. Systematically Convergent Basis Sets for Transition Metals. II. Pseudopotential-Based Correlation Consistent Basis Sets for the Group 11 (Cu, Ag, Au) and 12 (Zn, Cd, Hg) Elements. *Theor. Chem. Acc.*, **2005**, *114*, 283.

415. Peterson, K. A.; Figgen, D.; Dolg, M.; Stoll, H. Energy-Consistent Relativistic Pseudopotentials and Correlations Consistent Basis Sets for the 4d Elements Y-Pd. *J. Chem. Phys.*, **2007**, *126*, 124101.

416. Frisch, M. J.; Trucks, G. W.; Schlegel, H. B.; Scuseria, G. E.; Robb, M. A.; Cheeseman, J. R.; Scalmani, G.; Barone, V.; Mennucci, B.; Petersson, G. A., et al. Gaussian 09, Revision A.2; Gaussian, Inc., Wallingford, CT, 2009.

417. te Velde, G.; Bickelhaupt, F. M.; van Gisbergen, S. J. A.; Fonseca Guerra, C.; Baerends, E. J.; Snijders, J. G.; Ziegler, T. Chemistry with ADF. *J. Comput. Chem.*, **2001**, *22*, 931.

418. ADF 2017, ADF Users Guide; SCM, Theoretical Chemistry, Vrije Universiteit: Amsterdam; http://www.scm.com, Accessed 6-15- 2017.

419. Becke, A. D. Density-Functional Exchange-Energy Approximation with Correct Asymptotic Behavior. *Phys. Rev. A: At., Mol., Opt. Phys.*, **1988**, *38*, 3098.

420. ADF 2008.01, ADF Users Guide; SCM, Theoretical Chemistry, Vrije Universiteit: Amsterdam, 2008; http://www.scm.com.

421. Wolff, S. K.; Ziegler, T.; van Lenthe, E.; Baerends, E. J. *J. Chem. Phys.* **1999**, *110*, 7689−7698.

422. van Lenthe, E.; Baerends, E. J.; Snijders, J. G. Relativistic Regular Two-Component Hamiltonian. *J. Chem. Phys*., **1993**, *99*, 4597−4610.

423. Autschbach, J.; Ziegler, T. In *Calculation of NMR and EPR Parameters: Theory and Application*, Kaupp, M., Buhl, M., Malkin, V. G., Eds.; Wiley-VCH: Weinheim, Germany, 2004; pp 249−264.

424. Tomasi, J.; Mennucci, B.; Cammi, R. Quantum Mechanical Continuum Solvation Models. *Chem. Rev.*, **2005**, *105*, 2999.

425. Klamt, A. *Quantum Chemistry to Fluid Phase Thermodynamics and Drug Design*; Elsevier: Amsterdam, 2005.

426. Klamt, A.; Schüürmann, G. COSMO: a New Approach to Dielectric Screening in Solvents with Explicit Expressions for the Screening Energy and its Gradient. *J. Chem. Soc., Perkin Trans. 2*, **1993**, *2*, 799.

427. Reed, A. E.; Curtiss, L. A.; Weinhold, F. Intermolecular Interactions from a Natural Bond Orbital, Donor-Acceptor Viewpoint. *Chem. Rev.*, **1988**, *88*, 899.

428. Weinhold, F.; Landis, C. R. *Valency and Bonding: A Natural Bond Orbital Donor-Acceptor Perspective*; University Press: Cambridge, U.K., 2005.

429. Glendening, E. D.; Badenhoop, J. K.; Reed, A. E.; Carpenter, J. E.; Bohmann, J. A.; Morales, C. M.; Landis, C. R.; Weinhold, F. *Natural Bond Order 6.0*; Theoretical Chemistry Institute, University of Wisconsin, Madison, WI, 2013; http://nbo6.chem.wisc.edu/, accessed 12−01-2013.

430. Glendening, E. D.; Landis, C. R.; Weinhold, F. NBO 6.0: Natural Bon Orbital Analysis Program. *J. Comput. Chem.*, **2013**, *34*, 1429.

431. Prepared by a modification of procedure for (2-methylpyridine)2NiBr2: Vallarino, L. M.; Hill, W. E.; Quagliano, J. V. Coordination Compounds of Nickel(II) Salts with Substituted Pyridines. Complexes of 2-, 3-, and 4-Methylpyridine. *Inorg. Chem.*, **1965**, *4*, 1598.

432. Zheng, J.; Lin, J.-H.; Yu, L.-Y.; Wei, Y.; Zheng, X.; Xiao, J.-C. Cross-Coupling between Difluorocarbene and Carbene-Derived Intermediates Generated from Diazocompounds for the Synthesis of *gem*-Difluoroolefins. *Org. Lett.* **2015**, *17*, 6150.

433. Zhang, W.; Wang, Y. Recent Advances in Carbon-Difluoroalkylation and -Difluoroolefination with Difluorocarbene. *Tetrahedron Lett.* **2018**, *59*, 1301.

434. Okoromoba, O. E.; Han, J.; Hammond, G. B., Xu, B. C. Designer HF-Based Fluorination Reagent: Highly Regioselective Synthesis of Fluoroalkenes and *gem*-Difluoromethylene Compounds from Alkynes. *J. Am. Chem. Soc.* **2014**, *136*, 14381.

435. Vandamme, M.; Paquin, J.-F. Eliminative Deoxofluorination Using XtalFluor-E: A One-Step Synthesis of Monofluoroalkenes from Cyclohexanone Derivatives. *Org. Lett.* **2017**, *19*, 3604.

436. Yang, M.-H.; Matikonda, S. S.; Altman, R. A. Preparation of Fluoroalkenes via the Shapiro Reaction: Direct Access to Fluorinated Peptidomimetics. *Org. Lett.* **2013**, *15*, 3894.

437. Leclerc, M. C.; Gorelsky, S. I.; Gabidullin, B. M.; Korobkov, I.; Baker, R. T. Selective Activation of Fluoroalkenes with N-Heterocyclic Carbenes: Synthesis of N-

Heterocyclic Fluoroalkenes and Polyfluoroalkenyl Imidazolium Salts. *Chem. Eur. J.* **2016**, *22*, 8063.

438. Ritter, S. K Tetrafluoroethylene Is Good for More Than Just Teflon. *C&EN* **2015**, *93*(22), 28

439. Ohashi, M.; Ogoshi, S. Transition Metal Mediated Transformations of Tetrafluoroethylene into Various Polyfluorinated Organic Compounds. *J. Synth. Org. Chem, Jpn.* **2016**, *74*, 1047.

440. Ritter, S. K. A new edition of fluoroalkyl additions. *C&EN* **2017**, *95*(30), 9.

441. Ritter, S. K. Fluorochemicals go short. *C&EN* **2010**, *88*(5), 12.

442. Ritter, S. K. The Shrinking Case for Fluorochemicals. *C&EN* **2015**, *93*(28), 27.

443. Buck, R.C. Toxicology Data for Alternative "Short-Chain" Fluorinated Substances. In Toxicological Effects of Perfluoroalkyl and Polyfluoroalkyl Substances. Molecular and Integrative Toxicology, DeWitt, J., Eds.; Humana Press, Switzerland, 2015; pp. 451.

444. Mudumbi, J. B. N.; Ntwampe, S. K. O.; Matsha, T.; Mekuto, L.; Itoba-Tombo, E. F. Recent Developments in Polyfluoroalkyl Compounds Research: A Focus on Human/Environmental Health Impact, Suggested Substitutes and Removal Strategies. *Environ. Monit. Assess.* **2017**, *189*, 402.

445. Takahira, Y.; Morizawa, Y. Ruthenium-Catalyzed Oelfin Cross-Metathesis with Tetrafluoroethylene and Analogous Fluoroolefins. *J. Am. Chem. Soc.* **2015**, *137*, 7031.

446. Myhre, G.; Shindell, D.; Bréon, F.-M.; Collins, W.; Fuglestvedt, J.; Huang, J.; Koch, D.; Lamarque, J.-F.; Lee, D.; Mendoza, B.; Nakajima, T.; Robock, A.; Stephens, G.; Takemura, T.; Zhang, H. Anthropogenic and Natural Radiative Forcing. In Climate

Change 2013: The Physical Science Basis. Contribution of Working Group I to the Fifth Assessment Report of the Intergovernmental Panel on Climate Change, Stocker, T.F.; Qin, D.; Plattner, G.-K.; Tignor, M.; Allen, S.K.; Boschung, J.; Nauels, A.; Xia, Y.; Bex, V.; Midgley, P.M., Eds.; Cambridge University Press, Cambridge, United Kingdom and New York, NY, USA, 2013.

447. Whittlesey, M. K.; Peris, E. Catalytic Hydrodefluorination with Late Transition Metal Complexes. *ACS Catal.* **2014**, *4*, 3152.

448. Cybulski, M. K.; McKay, D.; Macgregor, S. A.; Mahon, M. F.; Whittlesey, M. K. Room Temperature Regioselective Catalytic Hydrodefluorination of Fluoroarenes with *trans*-[Ru(NHC)$_4$H$_2$] through a Concerted Nucleophilic Ru-H Attack Pathway. *Angew. Chem. Int. Ed.* **2017**, *56*, 1515.

449. Kikushima, K.; Grellier, M.; Ohashi, M.; Ogoshi, S. Transition-Metal-Free Catalytic Hydrodefluorination of Polyfluoroarenes by Concerted Nucloephilic Aromatic Substitution with a Hydrosilicate. *Angew. Chem. Int. Ed.* **2017**, *56*, 16191.

450. Krüger, J.; Leppkes, J.; Ehm, C.; Lentz, D. Competition of Nucloephilic Aromatic Substitution, *σ*-bond Metathesis, and *syn* Hydrometalation in Titanium (III)-Catylzed Hydrodefluorination of Arenes. *Chem. Asian J.* **2016**, *11*, 3062.

451. Matsunami, A.; Kuwata, S.; Kayaki, Y. Hydrodefluorination of Fluoroarenes Using Hydrogen Transfer Catalysts with a Bifunctional Iridium/NH Moiety. *ACS Catal.* **2016**, *6*, 5181.

452. Krüger, J.; Ehm, C.; Lentz, D. Improving Selectivity in Catalytic Hydrodefluorination by Limiting S_NV Reactivity. *Dalton Trans.* **2016**, *45*, 16789.

453. Wu, J.; Xiao, J.; Dai, W.; Cao, S. Synthesis of Monofluoroalkenes Through Selective Hydrodefluorination of *gem*-Difluoroalkenes with Red-Al®. *RSC Adv.* **2015**, *5*, 34498.

454. Clot, E.; Mégret, C.; Kraft, B. M.; Eisenstein, O.; Jones, W. D. Defluorination of Perfluoropropene Using $Cp^*_2ZrH_2$ and Cp^*_2ZrHF: A Mechanism Investigation from a Joint Experimental-Theoretical Perspective. *J. Am Chem. Soc.* **2004**, *126*, 5647.

455. Kirkham, M. S.; Mahon, M. F.; Whittlesey, M. K. C-F Bond Activation of Perfluoroalkenes by Ruthenium Phosphine Hydride Complexes: X-ray Crystal Structures of *cis*-$Ru(dmpe)_2F(F\text{---}HF)$ and $[Ru(dcpe)_2H]^+$ $[(CF_3)_2C{=}C(O)CF_2CF_3]^-$. *Chem. Commun*, **2001**, *0*, 813-814. *Also see:* Noveski, D.; Braun. T.; Schulte, M.; Neumann, B.; Stammler, H.-G. C-F Activation and Hydrodefluorination of Fluorinated Alkenes at Rhodium. *Dalton Trans.* **2003**, *0*, 4075.

456. Vela, J.; Smith, M. J.; Yu, Y.; Ketterer, N. A.; Falschenriem, C. J.; Lachicotte, R. J.; Holland, P. L. Synthesis and Reactivity of Low-Coordinate Iron(II) Fluoride Complexes and Their Use in the Catalytic Hydrodefluorination of Fluorocarbons. *J. Am. Chem. Soc.* **2005**, *127*, 7857.

457. Kühnel, M. F.; Lentz, D. Titanium-Catalyzed C-F Activation of Fluoroalkenes. *Angew. Chem. Int. Ed.* **2010**, *49*, 2933.

458. Jaeger, A. D.; Ehm, C.; Lentz, D. Organocatalytic C-F Bond Activation with Alanes. *Chem. Eur. J.* **2018**, *24*, 6769-6777.

459. Schneider, H.; Hock, A.; Jaeger, A. D.; Lentz, D.; Radius, U. NHC Alane Adducts as Hydride Sources in the Hydrodefluorination of Fluoroaromatics and Fluoroolefins. *Eur. J. Inorg. Chem.* **2018**, *2018*, 4031.

460. Jaeger, A. D.; Walter, R.; Ehm, C.; Lentz, D., Gallium Hydrides and O/N-Donors as Tunable Systems in C−F Bond Activation. *Chem. Asian J.* **2018**, *13*, 2908.

461. Hu, J.; Han, X.; Yuan, Y.; Shi, Z. Stereoselective Synthesis of Z-fluoroalkenes Through Copper-Catalyzed Hydrodefluorination of *gem*-Difluoroalkenes with Water. *Angew. Chem. Int. Ed.* **2017**, *56*, 13342.

462. Kojima, R.; Kubota, K.; Ito, H. Stereodivergent Hydodefluorination of *gem*-Difluoroalkenes: Selective Synthesis of (*Z*)- and (*E*)-Monofluoroalkenes. *Chem. Commun.* **2017**, *53*, 10688.

463. See Chapter 3.

464. Baker, R. T., Andrella, N. O. Process for Preparation of Hydrofluoroalkenes by Selective Catalytic Consecutive Hydrodefluorination. WO2018039794, March 8, 2018.

465. Wilberg, K. B.; Murcko, M. A.; Laidig, K. E.; MacDougall, P. J. Origin of the Gauche Effect in Substituted Ethanes and Ethenes. *J. Phys. Chem.*, **1990**, *94*, 6956.

466. Burton, D. J. Fluorinated Ylides and Related Compounds. *Chem. Rev.*, **1996**, *96*, 1641.

467. Leclerc, M. C.; Da Gama, J. G.; Gabidullin, B. M.; Baker, R. T. A Closer Look at the Reactivity Between N-Heterocyclic Carbenes and Fluoroalkenes. *J. Fluorine Chem.*, **2017**, *203*, 81.

468. Jordan, A. J.; Wyss, C. M.; Bacsa, J.; Sadighi, J. P. Synthesis and Reactivity of New Copper(I) Hydride Dimers. *Organometallics*, **2016**, *35*, 613.

469. Frey, G. D.; Donnadieu, B.; Solelhavoup, M.; Bertrand, G. Synthesis of a Room-Temperature-Stable Dimeric Copper(I) Hydride. *Chem. Asian J.*, **2011**, *6*, 402.

470. Jordan, A. J.; Lalic, G.; Sadighi, J. P. Coinage Metal Hydrides: Synthesis, Characterization, and Reactivity. *Chem. Rev.*, **2016**, *116*, 8318.

471. Kuehnel, M. F.; Lentz, D.; Braun, T., Synthesis of Fluorinated Building Blocks by Transition-Metal-Mediated Hydrodefluorination Reactions. *Angew. Chem. Int. Ed.* **2013**, *52*, 3328.

472. Aizenberg, M.; Milstein, D., Homogeneous Rhodium Complex-Catalyzed Hydrogenolysis of C-F bonds. *J. Am. Chem. Soc.* **1995**, *117*, 8674.

473. Hintermann, S.; Pregosin, P. S.; Rüegger, H.; Clark, H. C., Electron Transfer Reactions Involving *trans*-[$PtH_2(PCy_3)_2$] and Fluorinated Benzonitriles. *J. Organomet. Chem.* **1992**, *435*, 225.

474. Kraft, B. M.; Lachicotte, R. J.; Jones, W. D., Aliphatic and Aromatic Carbon−Fluorine Bond Activation with $Cp^*_2ZrH_2$: Mechanisms of Hydrodefluorination. *J. Am. Chem. Soc.* **2001**, *123*, 10973.

475. Panetier, J. A.; Macgregor, S. A.; Whittlesey, M. K., Catalytic Hydrodefluorination of Pentafluorobenzene by [$Ru(NHC)(PPh_3)_2(CO)H_2$]: A Nucleophilic Attack by a Metal-Bound Hydride Ligand Explains an Unusual ortho-Regioselectivity. *Angew. Chem. Int. Ed.* **2011**, *50*, 2783.

476. Jaeger, A. D..; Ehm, C.; Lentz, D. Organocatalytic C−F Bond Activation with Alanes. *Chem. Eur. J.* **2018**, *24*, 6769.

477. Ehm, C.; Krüger, J.; Lentz, D., How a Thermally Unstable Metal Hydrido Complex Can Yield High Catalytic Activity Even at Elevated Temperatures. *Chem. Eur. J.* **2016**, *22*, 9305.

478. Luo, Y. R., *Comprehensive Handbook of Chemical Bond Energies*. CRC Press: Boca Rayton, FL, 2007.

479. Ehm, C.; Lentz, D., Partially Fluorinated Butatrienes: A Coupled Cluster Study. *J. Phys. Chem. A* **2010**, *114*, 3609.

480. Ehm, C.; Lentz, D., Cyclic Dimers of Tetrafluorobutatriene. *Theor. Chem. Acc.* **2011**, *129*, 507.

481. Wiberg, K. B., Application of the Pople-Santry-Segal CNDO Method to the Cyclopropylcarbinyl and Cyclobutyl Cation and to Bicyclobutane. *Tetrahedron* **1968**, *24*, 1083.

482. Glendening, E. D.; Badenhoop, J. K.; Reed, A. E.; Carpenter, J. E.; Bohmann, J. A.; Morales, C. M.; Weinhold, F. *NBO 5.0*, Theoretical Chemistry Institute, University of Wisconsin, Madison, WI, URL: http://www.chem.wisc.edu/~nbo5: 2001.

483. Minenkov, Y.; Occhipinti, G.; Jensen, V. R., Metal−Phosphine Bond Strengths of the Transition Metals: A Challenge for DFT†. *J. Phys. Chem. A* **2009**, *113*, 11833.

484. Tolman, C. A., Steric Effects of Phosphorus Ligands in Organometallic Chemistry and Homogeneous Catalysis. *Chem. Rev.* **1977**, *77*, 313.

485. See for example: Walther, D.; Liesicke, S.; Böttcher, L.; Fischer, R.; Görls, H.; Vaughan, G., Metal Complexes with 2,3-Bis(diphenylphosphino)-1,4-diazadiene Ligands: Synthesis, Structures, and an Intramolecular Metal-Mediated [4+2] Cycloaddtion Employing a Benzene Ring as a Dienophile. *Inorg. Chem.* **2003**, *42*, 625.

486. Craig, N. C.; Entemann, E. A., Thermodynamics of *cis-trans* Isomerizations. The 1,2-Difluoroethylenes. *J. Am. Chem. Soc.* **1961**, *83*, 3047.

487. Iwashita, A.; Chan, M. C. W.; Makio, H.; Fujita, T., Attractive Interactions in Olefin Polymerization Mediated by Post-Metallocene Catalysts with Fluorine-Containing Ancillary Ligands. *Catal. Sci. Technol.* **2014**, *4*, 599.

488. Talarico, G.; Busico, V.; Cavallo, L., "Living" Propene Polymerization with Bis(phenoxyimine) Group 4 Metal Catalysts: New Strategies and Old Concepts. *Organometallics* **2004**, *23*, 5989.

489. Falivene, L.; Credendino, R.; Poater, A.; Petta, A.; Serra, L.; Oliva, R.; Scarano, V.; Cavallo, L., SambVca 2. A Web Tool for Analyzing Catalytic Pockets with Topographic Steric Maps. *Organometallics* **2016**, *35*, 2286.

490. Banerjee, D.; Ghosh, A.; Chattopadhyay, S.; Ghosh, P.; Chaudhuri, R. K., Revisiting the '*Cis*-Effect' in 1,2-difluoro Derivatives of Ethylene and Diazene Using Ab Initio Multireference Methods. *Mol. Phys.* **2014**, *112*, 3206.

491. Bingham, R. C., The Stereochemical Consequences of Electron Delocalization in Extended π- Systems. An interpretation of the *Cis* Effect Exhibited by 1,2-Disubstituted Ethylenes and Related Phenomena. *J. Am. Chem. Soc.* **1976**, *98*, 535.

492. Wiberg, K. B.; Hadad, C. M.; Breneman, C. M.; Laidig, K. E.; Murcko, M. A.; Lepage, T. J., The Response of Electrons to Structural Changes. *Science* **1991**, *252*, 1266.

493. Wiberg, K. B.; Murcko, M. A.; Laidig, K. E.; MacDougall, P. J., Origin of the Gauche Effect in Substituted Ethanes and Ethenes. *J. Phys. Chem.* **1990**, *94*, 6956.

494. Ditchfield, R.; Ellis, P. D., ^{13}C NMR Chemical Shifts for Fluoroethylenes and Fluoroacetylene. *Chem. Phys. Lett.* **1972**, *17*, 342.

495. Yamamoto, T.; Tomoda, S., On the Origin of *cis*-Effect in 1,2-Difluoroethene. *Chem. Lett.* **1997**, *26*, 1069.

496. Cremer, D., The Role of Correlation in Calculations on 1,2-Difluoroethylenes. The *cis-trans* energy difference. *Chem. Phys. Lett.* **1981**, *81*, 481.

497. Feller, D.; Craig, N. C.; Groner, P.; McKean, D. C., Ab Initio Coupled Cluster Determination of the Equilibrium Structures of *cis*- and *trans*-1,2-Difluoroethylene and 1,1-Difluoroethylene. *J. Phys. Chem. A.* **2011**, *115*, 94.

498. Farcasiu, D., The Use and Misuse of the Hammond Postulate. *J. Chem. Educ.* **1975,** *52*, 76.

499. Hammond, G. S., A Correlation of Reaction Rates. *J. Am. Chem. Soc.* **1955**, *77*, 334.

500. IRC scans show that F-elimination proceeds first towards the electron poor P, then to the Cu. In the presence of silanes, an OR group could therefore be abstracted, which would lead to catalyst decomposition.

501. With the isolated complex preliminary reactivity was explored. Cross-coupling of the tetrafluoroethyl complex **7a** with iodobenzene (5 eq.) in the presence of 10 mol% of [(1,3-bis(2,4,6-trimethylphenyl)-4,5-dihydroimidazol-2-ylidene) copper(I) chloride] (80 % yield, determined by ^{19}F NMR) could be achieved. This represents a new route for the introduction of the CF_2CF_2H moiety to organic compounds. The use of **4.7b** under the same reaction conditions proved ineffective. Further investigation of this reaction is beyond the scope of this publication and will be reported in due course.

502. Bantreil, X.; Nolan, S. P. Synthesis of N-Heterocyclic Carbene Ligands and Derived Ruthenium Olefin Metathesis Catalysts. *Nat. Protoc.* 2011, 6, 69.

503. Lee, D.-W.; Yun, J. Direct Synthesis of Stryker's Reagent from a Cu(II) Salt. *Tetrahedron Lett.* **2005**, *46*, 2037.

504. Hunadi, R. J.; Baum, K. Tetrafluoroethylene: A Convenient Laboratory Preparation. *Synthesis* **1982**, *39*, 454.

505. Hercules, D. A.; Parrish, C. A.; Sayler, T. S.; Tice, T. K.; Williams, S. M.; Lowery, L. E.; Brady, M. E.; Coward, R. B.; Murphy, J. A.; Hey, T. A.; Scavuzzo, A. R.; Rummler, L. M.; Burns, E. G.; Matsnev, A. J.; Fernandez, R. E.; McMillen, C. D.; Thrasher, J. S. Preparation of Tetrafluoroethylene from the Pyrolysis of Pentafluoropropionate Salts. *J. Fluorine Chem.*, **2017**, *196*, 107.

506. Koroniak, H.; Palmer, K. W.; Dolbier, W. R.; Zhang, H.^{19}F NMR Properties of Some Trifluorovinyl- and Pentafluoropropenyl-Substituted Aromatics. *Magn. Reson. Chem.* **1993**, *31*, 748.

507. Burton, D. J.; Spawn, T. W.; Heinze, P. L.; Bailey, A. R.; Shin-Ya, S. Preparation of *E*-1,2,3,3,3-Pentafluoropropene, *Z*-1,2,3,3,3-Pentafluoropropene and *E*-1-Iodopentafluoropropene. *J. Fluorine Chem.* **1989**, *44*, 167.

508. Banks, R. E., Barlow, M. G., Nickkho-Amiry, M. Preparation of 2,3,3,3-Tetrafluoropropene from Trifluoroacetylacetone and Sulphur Tetrafluoride. *J. Fluorine Chem.* **1997**, *82*, 171.

509. Meißner, G., Kretschmar, K., Braun, T., Kemnitz, E. Consecutive Transformations of Tetrafluoropropenes: Hydrogermylation and Catalytic C-F Activation Steps at a Lewis Acidic Aluminium Fluoride. *Angew. Chem. Int. Ed.* **2017**, *56*, 16338.

510. Emsley, J. W., Phillips, L. Fluorine Chemical Shifts. *Prog. Nucl. Magn. Reson. Spectrosc.* **1971,** *7*, 1.

511. Brey, W. S. ^{19}F and ^{13}C Spectra of Fluorinated and Partially Fluorinated Vinyl Alkyl Ethers. *J. Fluorine Chem.* **2005**, *126*, 389.

512. Kučnirová, K.; Šimůnek, O.; Rybáčkoá, M.; Kvíčala, J. Structural Assignment of Fluorocyclobutenes by ^{19}F NMR Spectroscopy – Comparison of Calculated ^{19}F NMR Shielding Constants with Experimental ^{19}F NMR Shifts. *Eur. J. Org. Chem.* **2018**, *2018*, 3867.

513. Snegirev, V. F.; Makarov, K. N.; Zabolotskikh, V. F.; Sorokina, M. G.; Knunyants, I. L. Catalytic and Hydride Reduction of Hexafluoropropylene Dimers. *Russ. Chem. Bull.* **1983**, *32*, 2489.

514. Edwards, M. L.; Stemerick, D. M.; Jarvi, E. T.; Matthews, D. P.; McCarthy, J. R. Difluoromethyldiphenylphosphine Oxide. A New Reagent for Conversion of Carbonyl Compounds to 1,1-Difluoroolefins. *Tetrahedron Lett.* **1990**, *31*, 5571.

515. Tian, H.; Shimakoshi, H.; Imamura, K.; Shiota, Y.; Yoshizawa, K.; Hisaeda, Y. Photocatalytic Alkene Reduction by a B_{12}-TiO_2 Hybrid Catalyst Coupled with C-F Bond Cleavage for *gem*-Difluoroolefin Synthesis. *Chem. Commun*. **2017**, *53*, 9478.

516. J. Baker, 2.4 ed., Parallel Quantum Solutions, Fayetteville, AR, 2001

517. Baker, J., An Algorithm for the Location of Transition States. *J. Comput. Chem.* **1986**, *7*, 385.

518. Budzelaar, P. H. M., Geometry Optimization Using Generalized, Chemically Meaningful Constraints. *J. Comput. Chem.* **2007**, *28*, 2226.

519. Ehm, C.; Budzelaar, P. H. M.; Busico, V., Calculating Accurate Barriers for Olefin Insertion and Related Reactions. *J. Organomet. Chem.* **2015**, *775*, 39.

520. Tao, J.; Perdew, J. P.; Staroverov, V. N.; Scuseria, G. E., Climbing the Density Functional Ladder: Nonempirical Meta-Generalized Gradient Approximation Designed for Molecules and Solids. *Phys. Rev. Lett.* **2003**, *91*, 146401.

521. Balabanov, N. B.; Peterson, K. A., Systematically Convergent Basis Sets for Transition Metals. I. All-electron Correlation Consistent Basis Sets for the 3d Elements Sc–Zn. *J. Chem. Phys.* **2005**, *123*, 064107.

522. Balabanov, N. B.; Peterson, K. A., Basis Set Limit Electronic Excitation Energies, Ionization Potentials, and Electron Affinities for the 3d Transition Metal Atoms: Coupled Cluster and Multireference Methods. *J. Chem. Phys.* **2006**, *125*, 074110.

523. Schuchardt, K. L.; Didier, B. T.; Elsethagen, T.; Sun, L. S.; Gurumoorthi, V.; Chase, J.; Li, J.; Windus, T. L., Basis Set Exchange: A Community Database for Computational Sciences. *J. Chem. Inf. Model* **2007**, *47*, 1045.

524. Whitten, J. L., Coulombic Potential Energy Integrals and Approximations. *J. Chem. Phys.* **1973**, *58*, 4496.

525. Baerends, E. J.; Ellis, D. E.; Ros, P., Self-Consistent Molecular Hartree—Fock—Slater Calculations I. The Computational Procedure. *Chem. Phys.* **1973**, *2*, 41.

526. Feyereisen, M.; Fitzgerald, G.; Komornicki, A., Use of Approximate Integrals in *Ab Initio* Theory. An Application in MP2 Energy Calculations. *Chem. Phys. Lett.* **1993**, *208*, 359.

527. Vahtras, O.; Almlöf, J.; Feyereisen, M. W., Integral Approximations for LCAO-SCF Calculations. *Chem. Phys. Lett.* **1993**, *213*, 514.

528. Tomasi, J., Thirty Years of Continuum Solvation Chemistry: a Review, and Prospects for the Near Future. *Theor. Chem. Acc.* **2004**, *112*, 184.

529. The Berny algorithm was never fully published, see the Gaussian documentation for details.

530. Tao, J. M.; Perdew, J. P.; Staroverov, V. N.; Scuseria, G. E., Climbing the Density Functional Ladder: Nonempirical Meta-Generalized Gradient Approximation Designed for Molecules and Solids. *Phys. Rev. Lett.* **2003**, *91*, 146401.

531. Grimme, S., Density Functional Theory with London Dispersion Corrections. *Wiley Interdiscip. Rev. Comput. Mol. Sci.* **2011**, *1*, 211.

532. Grimme, S.; Ehrlich, S.; Goerigk, L., Effect of the Damping Function in Dispersion Corrected Density Functional Theory. *J. Comput. Chem.* **2011**, *32*, 1456.

533. Tobisch, S.; Ziegler, T., Catalytic Oligomerization of Ethylene to Higher Linear α-Olefins Promoted by the Cationic Group 4 $[(\eta^5\text{-Cp-}(CMe_2\text{-bridge})\text{-Ph})M^{II}(\text{ethylene})_2]^+$ (M = Ti, Zr, Hf) Active Catalysts: A Density Functional Investigation of the Influence of the Metal on the Catalytic Activity and Selectivity. *J. Am. Chem. Soc.* **2004**, *126*, 9059.

534. Dunlop-Brière, A. F.; Budzelaar, P. H. M.; Baird, M. C., α- and β-Agostic Alkyl–Titanocene Complexes. *Organometallics* **2012**, *31*, 1591.

535. Raucoules, R.; de Bruin, T.; Raybaud, P.; Adamo, C., Theoretical Unraveling of Selective 1-Butene Oligomerization Catalyzed by Iron−Bis(arylimino)pyridine. *Organometallics* **2009**, *28*, 5358.

536. Glendening, E. D.; Landis, C. R.; Weinhold, F., Natural bond orbital methods. *Wiley. Interdiscip. Rev. Comput. Mol. Sci.* **2012**, *2*, 1.

537. Miyawaki, J.; Sugawara, K.-I., ZEKE Photoelectron spectroscopy of the silver- and copper-ammonia complexes. *J. Chem. Phys.* 2003, 119, 6539.

538. Meyer, F.; Chen, Y.-M.; Armentrout, P. B., Sequential Bond Energies of $Cu(CO)_x^+$ and $Ag(CO)_x^+$ (x = 1-4). *J. Am. Chem. Soc.* **1995**, *117*, 4071.

539. Sievers, M. R.; Jarvis, L. M.; Armentrout, P. B., Transition-Metal Ethene Bonds: Thermochemistry of $M^+(C_2H_4)_n$ (M = Ti-Cu, n = 1 and 2) complexes. *J. Am. Chem. Soc.* **1998**, *120*, 1891.

540. Hertwig, R. H.; Koch, W.; Schröder, D.; Schwarz, H., A Comparative Computational Study of Cationic Coinage Metal-Ethylene Complexes $(C_2H_4)M^+$ (M = Cu, Ag, and Au). *J. Phys. Chem.* **1996**, *100*, 12253.

541. Vitale, G.; Valina, A. B.; Huang, H.; Amunugama, R.; Rodgeers, M. T., Solvation of Copper Ions by Acetonitrile. Structures and Sequential Binding Energies of $Cu^+(CH_3CN)_x$, x = 1-5, from Collision-Induced Dissociation and Theoretical Studies. *J. Phys. Chem.* **2001**, *105*, 11351.

542. Scheidt, F.; Neufeld, J.; Schaefer, M.; Thiehoff, C.; Gilmour, R. Catalytic Geminal Difluorination of Styrenes for the Construction of Fluorine-rich Bioisosters. *Org. Lett.*, **2018**, *20*, 8073.

543. Song, H.-X.; Han, Q.-Y.; Zhao, C.-L.; Zhang, C.-P. Fluoroalkylation Reactions in Aqueous Media: a Review. *Green Chem.*, **2018**, *90*, 617.

544. Scheidt, F.; Schaefer, M.; Sarie, J. C.; Daniliuc, C. G.; Molloy, J. J.; Gilmour, R. Enantioselective, Catalytic Vicinal Difluorination of Alkenes. *Angew. Chem. Int. Ed.*, **2018**, *57*, 16431.

545. Vaclavik, J.; Klimankova, I.; Budinska, A.; Beier, P. Advances in the Synthesis and Application of Tetrafluoroethylen- and 1,1,2,2-Tetrafluoroethyl-Containing Compounds. *Eur. J. Org. Chem.*, **2018**, 3554.

546. Singh, R. P.; Shreeve, J. M. Concentration-Dependent Reactions of Deoxofluor with Arylglyoxal Hydrates: A New Route to Polyfluoro Ethers. *Org. Lett.*, **2001**, *3*, 2713.

547. Sivaramakrishnan, H.; Upare, A. A.; Satagopan, D.; Chambers, O. R. The Preparation of Desflurane by the Vapor-Phase Fluorination of Isoflurane. *Org. Process Res. Dev.*, **2011**, *15*, 585.

548. Kaplan, P. T.; Lloyd, J. A.; Chin, M. T.; Vicic, D. A. Comparative Profiling of Well-Defined Copper Reagents and Precursors for the Trifluoromethylation of Aryl Iodides. *Beilstein J. Org. Chem.*, **2017**, *13*, 2297.

549. Sieglitz, A.; Herbert, B.; Rehn, K. Tetrafluoroethyl Aromatic Compounds from Tetrafluoroethylene. US 2862974 19581202, **1958**.

550. Zhou, Y.; Wang, J.; Gu, Z.; Wang, S.; Zhu, W.; Aceña, J. L.; Soloshonok, V.; Izawa, K.; Liu, H. Next Generation of Fluorine-Containing Pharmaceuticals, Compounds Currently in Phase II-III Clinical Trials of Major Pharmaceutical Companies: Structural Trends and Therapeutic Areas. *Chem. Rev.*, **2016**, *116*, 422.

551. Roth, B. D. The Discovery and Development of Atorvastatin, a Potent Novel Hypolipidemic agent. *Prog. Med. Chem.*, **2002**, *40*, 1.

552. Campbell, M. G.; Ritter, T. Late-Stage Fluorination: From Fundamentals to Application. *Org. Process Res. Dev.*, **2014**, *18*, 474.

553. Neumann, C. N.; Ritter, T. Late-Stage Fluorination: Fancy Novelty or Useful Tool? *Angew. Chem. Int. Ed.*, **2015**, *54*, 3216.

554. Yerien, D. E.; Bonesi, S.; Postigo, A. Fluorination Methods in Drug Discovery. *Org. Biomol. Chem.*, **2016**, *14*, 8392.

555. Ho. Y. A.; Leiendecker, M.; Liu, X.; Wang, C.; Alandini, N.; Rueping, M. Nickel-Catalyzed Csp^2-Csp^3 Bond Formation via C-F Bond Activation. *Org. Lett.*, **2018**, *20*, 5644.

556. Böhm, V. P. W.; Gstöttmayr, C. W. K.; Weskamp, T.; Herrmann, W. A. Catalytic C-C Bond Formation through Selective Activation of C-F Bonds. *Angew. Chem. Int. Ed.*, **2001**, *40*, 3387.

557. Mongin, F.; Mojovic, L.; Guillamet, B.; François, T.; Quéguiner. G. Cross-Coupling Reactions of Phenylmagnesium Halides with Fluoroazines and Fluorodiazines. *J. Org. Chem.*, **2002**, *67*, 8991.

558. Sun, A. D.; Love, J. A. Cross Coupling Reactions of Polyfluoroarenes via C-F Activation. *Dalton Trans.*, **2010**, *39*, 10362.

559. Johnson, S.; Hatnean, J. A.; Doster, M. Functionalization of Fluorinated Aromatics by Nickel-Mediated C-H and C-F Bond Oxidative Addition: Prospects for the Synthesis of Fluorine-Containing Pharmaceuticals. In *Progress in Inorganic Chemistry, Vol. 57*; Karlin, K. D., Eds; Wiley-VCH: Weinheim, Germany, **2002.**

560. Yoshikai, N.; Mashima, H.; Nakamura, E. Nickel-Catalyzed Cross-Coupling Reaction of Aryl Fluorides and Chlorides with Grignard Reagents under Nickel/Magnesium Bimetallic Cooperation. *J. Am. Chem. Soc.*, **2005**, *121*, 17978.

561. Hatnean, J. A.; Shoshani, M.; Johnson, S. A. Mechanistic Insight into Carbon-Fluorine Cleavage with a $(^{i}Pr_3P)_2Ni$ Source: Characterization of $(^{i}Pr_3P)_2Ni\text{-}C_6F_5$ as a Significant Ni(I) Byproduct in the Activation of C_6F_6. *Inorg. Chim. Acta.*, **2014**, *422*, 86.

562. Ohashi, M.; Ogoshi, S. Palladium-Catalyzed Cross-Coupling Reactions of Perfluoro Organic Compounds. *Catalysts*, **2014**, *4*, 321.

563. Ohashi, M.; Doi, R.; Ogoshi, S. Palladium-Catalyzed Coupling Reaction of Perfluoroarenes with Diarylzinc Compounds. *Chem. Eur. J.*, **2014**¸ *20*, 2040.

564. Ohashi, M.; Saijo, H.; Shibata, M.; Ogoshi, S. Palladium-Catalyzed Base-Free Suzuki-Miyaura Coupling Reactions of Fluorinated Alkenes and Arenes via a Palladium Fluoride Key Intermediate. *Eur. J. Org. Chem.*, **2013**, 443.

565. Doster, M.; Johnson, S. A. Selective C-F Bond Activation of Tetrafluorobenzenes by Nickel(0) with a Nitrogen Donor Analogous to N-Heterocyclic Carbenes. *Angew. Chem. Int. Ed.*, **2009**, *48*, 2185.

566. Catalytic C-C Bond Formation Accomplished by Selective C-F Activation of Perfluorinated Arenes. *J. Am. Chem. Soc*., **2006**, *128*, 15964.

567. Schaub, T.; Fischer, P.; Steffen, A.; Braun, T.; Radius, U.; Mix, A. C-F Activation of Fluorinated Arenes Using NHC-Stabilized Nickel(0) Complexes: Selectivity and Mechanistic Investigations. *J. Am. Chem. Soc.*, **2008**, *130*, 9304.

568. Cui, B.; Jia, S.; Tokunaga, E.; Shibata, N. Defluorosilylation of fluoroarenes and fluoroalkanes. *Nat. Commun.*, **2018**, *9*, 4393.

569. Baird, D. A.; Jamal, S.; Johnson, S. A. Influence of the Transmetalation Agent in Difficult Coupling Reactions: Control in the Selectivity of C-F Bond Activation by Ni(0) Complexes in the Presence of $AlMe_3$. *Organometallics* **2017**, *36*, 1436-1446.